

**Insulin-Mimetic Peroxovanadium Compounds:
Synthesis, Reactivity, and Mechanism of
Action.**

David A. Hall

*A thesis submitted to the Faculty of Graduate Studies and Research in partial
fulfillment of the requirements for the degree of Doctor of Philosophy*

June 1996
Department of Chemistry
McGill University
Montreal, Quebec
Canada

©David A. Hall



National Library
of Canada

Bibliothèque nationale
du Canada

Acquisitions and
Bibliographic Services Branch

Direction des acquisitions et
des services bibliographiques

395 Wellington Street
Ottawa, Ontario
K1A 0N4

395 rue Wellington
Ottawa (Ontario)
K1A 0N4

Author's name

Author's name

The author has granted an irrevocable non-exclusive licence allowing the National Library of Canada to reproduce, loan, distribute or sell copies of his/her thesis by any means and in any form or format, making this thesis available to interested persons.

L'auteur a accordé une licence irrévocable et non exclusive permettant à la Bibliothèque nationale du Canada de reproduire, prêter, distribuer ou vendre des copies de sa thèse de quelque manière et sous quelque forme que ce soit pour mettre des exemplaires de cette thèse à la disposition des personnes intéressées.

The author retains ownership of the copyright in his/her thesis. Neither the thesis nor substantial extracts from it may be printed or otherwise reproduced without his/her permission.

L'auteur conserve la propriété du droit d'auteur qui protège sa thèse. Ni la thèse ni des extraits substantiels de celle-ci ne doivent être imprimés ou autrement reproduits sans son autorisation.

ISBN 0-612-19727-1

Canada

For my parents

Abstract

The insulin mimetic bisperoxovanadium (bpV) complexes $K_2[VO(O_2)_2(OHpic)]$ (OHpic = 3-hydroxypicolinato) and $K_3[VO(O_2)_2(L-L')]$ have been prepared and characterized, where L-L' is a pyridinedicarboxylate (2,3-pdc, 2,4-pdc. and 2,5-pdc) or 3-acetatoxypicolinato (acetpic). The single crystal X-ray structures of three of the compounds have been determined: bpV(OHpic), bpV(2,4-pdc) and bpV(acetpic). These complexes, with the addition of one other previously reported unsubstituted bpV(pic) complex, comprise two series of insulin mimetic bpV complexes varying in the structure of their ancillary ligands. Structure activity relationships are reported for these compounds.

The stability of peroxovanadium (pV) compounds in HEPES (4-(2-hydroxyethyl)-1-piperazineethanesulfonic acid, MOPS (4-morpholinepropanesulfonic acid), and phosphate buffer at pH 7.4 is determined as well as their stability at pH 4, 5, 6 and 7. The use of HEPES with pV complexes is not recommended, but phosphate and MOPS buffer provide alternative buffers at physiological pH. The reactivity of pV compounds with EDTA (ethylenediaminetetraacetic acid), DTT (dithiothreitol), bovine liver catalase and potassium ferrocyanide is discussed.

The oxidation of tris(3-sulfonatophenyl)phosphine to the corresponding oxide, the oxidation of cysteine to the disulfide cystine and to cysteinesulfinic acid by bpV compounds are described. The oxidations are models of the mechanism of inhibition of the enzyme protein tyrosine phosphatase (PTP) by pV complexes. The mechanism for the insulin mimetic activity of pV compounds *in vivo* is discussed

Résumé

Les complexes bisperoxovanadium (bpV) $K_2[VO(O_2)_2(OHpic)]$ (OHpic = 3-hydroxypicolinato) et $K_3[VO(O_2)_2(L-L')]$, "imitateurs" de l'insuline, ont été préparés et caractérisés, dans le cas où L-L' est un ligand pyridinedicarboxylate (2,3-pdc, 2,4-pdc, et 2,5-pdc) ou 3-acetatoxypicolinate (acetpic). Les structures aux rayons X de trois des complexes ont été déterminées: bpV(OHpic), bpV(2,4-pdc) et bpV(acetpic). Ces complexes, plus un autre complexe non-substitué bpV(pic) précédemment étudié, forme deux séries de bp complexes, "imitateurs" de l'insuline, variant par la structure des ligands organiques. Les relations existantes entre la structure des complexes et leur activité sont reportées pour ces complexes.

La stabilité des composés peroxovanadium (pV) dans les solutions tampons d'HEPES (acide 4-(2-hydroxyethyl)-1-piperazineethanesulfonique), de MOPS (acide 4-morpholinepropanesulfonique), et de phosphate à pH 7.4 est déterminée ainsi que leur stabilité à pH 4, 5, 6 et 7. L'utilisation du tampon HEPES avec les complexes pV n'est pas recommandée, mais les tampons phosphate et MOPS procurent des bons alternatifs du pH physiologique. Les reactivités des composés pV avec l'EDTA (acide ethylenediaminetetraacétique), le DTT (dithiothreitol), l'enzyme catalase du foie de bovin et le ferrocyanure de potassium sont discutées.

L'oxydation de tris(3-sulfonatophenyl)phosphine en oxyde correspondant, l'oxydation de la cystéine en cystine (disulfure) et en acide cystéinesulfinique par les composés bpV sont décrites. Les réactions d'oxydation sont des modèles du mécanisme d'inhibition de l'enzyme "protein tyrosine phosphatase (PTP)" par les complexes pV. Le mécanisme de l'activité *in vivo* des composés pV "imitateurs" de l'insuline est discuté

Acknowledgments

I owe a great debt to a number of people who have helped, guided, encouraged and inspired me throughout my time at McGill. I must acknowledge my supervisor Dr. Alan Shaver for his support and understanding and an astonishing ability to get to the heart of matters. I have always been able to count on Dr. Shaver to come through in the “crunch”.

I would like to gratefully acknowledge Dr. Barry Posner for his guidance and all he has taught me about the finer points of kinases and phosphatases. Dr. Posner and the members of his lab, especially Gerry Baquiran, Dr. Chang-Ren Yang, and Dr. Paul Bevan are acknowledged for their biological testing of my compounds. Mrs. Sheryl Jackson is also thanked for her help and patience.

Many of the compounds I used in my studies were synthesized by Dr. Jesse Ng. Jesse is one of the finest teachers I have ever encountered and it was through his help that I was able to carry out this project to its completion. From helping me run my first NMR to proofreading my thesis Jesse has always been there to offer support and share his knowledge of chemistry.

Crystal structures were solved by Dr. Rosemary Hynes and Dr. Anne-Marie Lebuis. Dr. Lebuis is gratefully acknowledged for her patience and for helping me tidy up the odd mess. Dr. Bruce Lennox and Dr. David Harpp are thanked for their instructive conversations on electrochemistry and sulfur chemistry respectively.

My colleagues in lab 435 provided support, education and understanding. Dr. John Harrod is thanked for his instructive conversations and for not letting me lose sight of the basics. I would like to thank Dr. Marie-Laurence Abasq for translating my abstract into

French and Dr. Kamyar Rahimian for his help and guidance. Dr. Darlene Trojansek, Dr. H  l  ne Boily, Dr. Mohammed El-Khateeb, Vladimir Dioumaev, Ronghua Shu, Dr. Leijun Hao, Dr. Shixuan Xin, and Dr. Jiliang He are thanked for making the lab a pleasant place to work.

The occupants of lab 230 are also thanked for their advice, loans of equipment, and for being pleasant lunch companions. Dr. John Finkenbine, Grace, and the students of Chem 392 provided me with no end of challenges but made for many pleasant afternoons.

Finally, but most of all, I must thank my wife Mary Jane. It was her support, understanding and helpful insights that made all this possible.

Abbreviations

2,6-pdc	2,6-pyridinedicarboxylato
3,4,7,8-Me ₄ phen	3,4,7,8-tetramethyl-1,10-phenanthroline
3-acetpic	3-acetatoxypyridine-2-carboxylato
3-NH ₂ pzc	3-aminopyrazine-2-carboxylato
3-OHpic	3-hydroxypyridine-2-carboxylato
4,4'-Me ₂ bipy	4,4'-dimethyl-2,2'-bipyridine
4,7-dim ₂ phen	4,7-dimethyl-1,10-phenanthroline
4OH-2,6pdc	4-hydroxy-2,6-pyridinedicarboxylato
5-CH ₃ phen	5-methyl-1,10-phenanthroline
5-NH ₂ phen	5-amino-1,10-phenanthroline
5-NO ₂ phen	5-nitro-1,10-phenanthroline
acetpic	3-acetatoxypyridine-2-carboxylato
ada	N-(2-amidomethyl)iminodiacetato
Bicine	<i>N,N</i> -bis(2-hydroxyethyl)glycine
bipy	2,2'-bipyridine
bipy-4,4'-(COO) ₂	2,2'-bipyridine-4,4'-dicarboxylato
bipyH	2,2'-bipyridinium
BMOV	bis(maltolato)oxovanadium(IV)
bpg	<i>N,N</i> -bis(2-pyridylmethyl)glycine
bpV	bisperoxovanadium
BSA	bovine serum albumin
cit	citrato
cystH	cysteine
DM	diabetes mellitus
DTT	dithiothreitol
EDTA	ethylenediaminetetraacetic acid
EPR	electron paramagnetic resonance
EXAFS	extended X-ray absorption fine structure
Fmoc	9-fluorenylmethyl chloroformate
GlyGly	glycylglycine
glyH	glycine
HEDTA	ethylenediaminetetraacetic acid
HEPES	4-(2-hydroxyethyl)-1-piperazineethanesulfonic acid

Hheida	<i>N</i> -(2-hydroxyethyl)iminodiacetato
Hz	hertz
IDA	iminodiacetato
IDDM	insulin dependent diabetes mellitus
IGF-II	insulin-like growth factor receptor II
IRK	insulin receptor kinase
isoquin	isoquinoline-2-carboxylato
m,n-pdc	pyridine-m,n-dicarboxylato
MES	4-morpholineethanesulfonic acid
MOPS	4-morpholinepropanesulfonic acid
mpV	monoperoxovanadium
NADP	nicotinamide adenine dinucleotide phosphate
NADV	nicotinamide adenine dinucleotide vanadate
nicH	nicotinic acid
NIDDM	non-insulin dependent diabetes mellitus
NMR	nuclear magnetic resonance
NTA	nitrilotriacetato
OHpic	3-hydroxypyridine-2-carboxylato
ox	oxalato
phen	1,10-phenanthroline
pic	pyridine-2-carboxylato
PIPES	1,4-piperazinebis(ethanesulfonic acid)
PTP	protein tyrosine phosphatase
pV	peroxovanadate
pzc	pyrazine-2-carboxylato
quin	quinolato
TAPS	3-[[tris(hydroxymethyl)methyl]amino]-1-propanesulfonic acid
tpa	<i>N,N,N</i> -tris(2-pyridylmethyl)amine
Tricine	<i>N</i> -[tris(hydroxymethyl)methyl]glycine
TRIS	tris(hydroxymethyl)aminomethane
UV	ultraviolet
UV-Vis	ultraviolet-visible
V(2,6-pdc)	NH ₄ [VO ₂ (2,6-pdc)(H ₂ O)]

Table of Contents

Abstract.....	i
Résumé.....	ii
Acknowledgments.....	iii
Abbreviations.....	v
Chapter 1. Introduction.....	1
1.1. Diabetes.....	1
1.2. Insulin Action.....	1
1.3. Treatment of Diabetes Mellitus.....	6
1.4. Insulin Mimetic Metal Ions.....	10
1.5. The Chemistry of Vanadium.....	11
1.6. Insulin Mimetic Vanadium Compounds.....	19
1.6.1. Vanadate.....	19
1.6.2. Vanadyl and Vanadyl Complexes.....	20
1.6.3 Peroxovanadium and Peroxovanadium Complexes.....	23
1.7. Plan of Study.....	28
1.8. References.....	30
Chapter 2. Synthesis and Characterization of Insulin-Mimetic Peroxovanadium Compounds.....	34
2.1. Introduction.....	34
2.2. Results and Discussion.....	40
2.2.1. Syntheses.....	40
2.2.2. Structural Features.....	42
2.2.2.a. bpV Complexes.....	42
2.2.2.b. Gmpv(2,6-pdc).....	49
2.2.3 Biological Activity.....	51
2.3. Experimental.....	
2.3.1. General.....	58
2.3.2. Chemicals.....	
2.3.3. bpV(OHpic).....	59
2.3.3.a. Synthesis.....	
K ₂ [VO(O ₂) ₂ (OHpic)]•3H ₂ O.....	59
2.3.3.b. Structure Determination.....	60
2.3.4. bpV(2,3-pdc).....	61

2.3.4.a. Synthesis	
$K_3[VO(O_2)_2(2,3\text{-pyridinedicarboxylato})]\cdot 2H_2O$	61
2.3.5. bpV(2,4-pdc)	61
2.3.5.a. Synthesis	
$K_3[VO(O_2)_2(2,4\text{-pyridinedicarboxylato})]\cdot 3.25H_2O$	61
2.3.5.b. Structure Determination	
$K_3[VO(O_2)_2(2,4\text{-pdc})]\cdot 3.25 H_2O$	62
2.3.6. bpV(2,5-pdc)	63
2.3.6.a. Synthesis	
$K_3[VO(O_2)_2(2,5\text{-pyridinedicarboxylato})]\cdot 2H_2O$	63
2.3.7. bpV(acetpic).....	64
2.3.7.a. Synthesis	
Potassium 3-acetatoxypicolinate.....	64
2.3.7.b. Synthesis	
$K_3[VO(O_2)_2(3\text{-acetatoxypicolinato})]\cdot 2H_2O$	64
2.3.7.c. Structure Determination	
$K_3[VO(O_2)_2(3\text{-acetpic})]\cdot 2H_2O$	65
2.3.8. GmpV(2,6-pdc)	66
2.3.8.a. Synthesis	
$C(NH_2)_3[VO(O_2)_2(2,6\text{-pdc})(H_2O)]\cdot H_2O$	66
2.3.8.b. Structure Determination	66
2.3.9. KmpV(2,6-pdc)	67
2.3.9.a. Synthesis	
$K[VO(O_2)_2(2,6\text{-pdc})(H_2O)]\cdot 2H_2O$	67

Chapter 3. The Stability and Reactivity of Insulin-mimetic Peroxovanadium Complexes.....

3.1. Introduction	72
3.2. Results and Discussion	76
3.2.1. Stability Studies	76
3.2.1.a. mpV(2,6-pdc)	76
3.2.1.b. bpV(pic)	81
3.2.1.c. bpV(OHpic)	86
3.2.2. Stability of bpV(phen) in the Absence of Light.....	89
3.2.3. The Interaction of Vanadate, V(2,6-pdc), and bpV(phen) with EDTA	91

3.2.4. The Interaction of Vanadate, bpV(phen), and bpV(OHpic) with DTT	95
3.2.5. The Interaction of bpV(OHpic) with HEPES, MOPS and Phosphate Buffers.....	99
3.2.6. The Interaction of bpV(pic) and bpV(OHpic) with HEPES and MOPS at Varying Ratios of pV buffer	99
3.2.6.a. bpV(OHpic)	100
3.2.6.b. bpV(pic)	101
3.2.7. The Interaction of bpV's with Catalase.....	104
3.2.8. The reaction of bpV(OHpic) with potassium ferrocyanide	
3.2.9. Effect of UV light on bpV complexes	119
3.3. Conclusions	120
3.4. Experimental	122
3.4.1. General	122
3.4.2. Chemicals	122
3.4.3. Stability Studies	123
3.4.4. Stability of bpV(phen) in the Absence of Light.....	124
3.4.4. The Interaction of Vanadate, V(2,6-pdc), and bpV(phen) with EDTA	124
3.4.5. The Interaction of Vanadate, bpV(phen), and bpV(OHpic) with DTT	126
3.4.6. The Interaction of bpV(OH-pic) with HEPES, MOPS and Phosphate Buffers.....	127
3.4.7. The interaction of bpV(pic)and bpV(OHpic) with HEPES and MOPS at varying ratios of pVbuffer	127
3.4.8. The Interaction of bpV's with Catalase.....	128
3.4.8. Effect of UV light on bpV Complexes.....	130
3.4.9. The Reaction of bpV(OHpic) with Potassium Ferrocyanide.....	130
3.5. References.....	132
Chapter 4. The Mechanism of the Inhibition of PTP by Bisperoxovanadium Compounds.....	134
4.1. Introduction	134
4.2. Results	136
4.2.1. Phosphine Oxidations.....	136
4.2.2. Cysteine Oxidations, Water Insoluble Products	136

4.2.2. Cysteine Oxidations, Water Soluble Products	138
4.3. Discussion.....	140
4.4. Conclusions	144
4.5. Experimental.....	145
4.5.1. General	145
4.5.2. Chemicals	146
4.5.3. Phosphine Oxidation.....	146
4.5.4. Oxidation of cysteine to cystine with bpV(OHpic), bpV(pic), KVO ₃ , and H ₂ O ₂	147
4.5.5. HPLC analysis of the reaction of cysteine with bpV(OHpic).....	147
4.5.6. N-FMOC-cysteinesulfinic acid.....	149
4.5.7. Potassium N-FMOC-cysteinesulfonate monohydrate.....	150
4.6. References.....	151
Appendices.....	154
A.1. Crystallographic Tables and Figures for bpV(OHpic).....	154
A.2. Crystallographic Tables and Figures for bpV(2,4pdc).....	159
A.3. Crystallographic Tables and Figures for bpV(acetpic).....	172
A.4. Crystallographic Tables and Figures for GmpV(2,6-pdc).....	178
A.5. Kinetic Data for the Reaction of Potassium Ferrocyanide with bpV(OHpic).....	183

Chapter 1. Introduction

1.1. Diabetes

Diabetes mellitus (DM) is a serious metabolic disease that affects an estimated 15 million people in the United States alone.¹ The cost of DM to society is staggering, an estimated 1 in 7 health care dollars in the United States is spent on patients with diabetes mellitus.² The cost to society as a whole is much greater when the loss of productivity due to increased morbidity and absenteeism in the work place are factored in. Yet despite the tremendous economic costs, the greatest cost is that to the quality of life of diabetes sufferers.

There are two types of DM; Type I and Type II. Type I, insulin dependent diabetes mellitus (IDDM), often affects young children and is also known as juvenile onset diabetes. In Type I DM the pancreas does not produce sufficient insulin, a polypeptide hormone with a molecular weight of approximately 6000, to control blood glucose levels. Type II DM, non-insulin dependent diabetes mellitus (NIDDM), also known as late onset diabetes, is characterized by a lack of response by the tissues of the body to insulin. Type II diabetics generally have normal or above normal insulin levels but their bodies no longer respond properly to it.

1.2. Insulin Action

Insulin is a polypeptide hormone produced by the beta cells of the islets of Langerhans in the pancreas. It was isolated by Banting and Best in 1922 at the University

of Toronto.³ Insulin is initially secreted as a zymogen* that is later modified through removal of a polypeptide sequence to yield an active hormone. Insulin consists of two chains linked by disulfide bonds as is shown in Figure 1.2.1.³ Insulin exerts a number of metabolic effects, all of which serve to lower blood glucose levels.³ These are summarized below:

1. Stimulates the uptake of glucose by muscle and adipose cells.
2. Promotes oxidation of glucose and incorporation of glucose into glycogen in liver and muscle cells.
3. Inhibits the metabolic breakdown of glycogen in muscle and liver cells.
4. Promotes the synthesis of fats and inhibits their breakdown by adipose tissues.
5. Increases amino acid uptake and promotes protein synthesis while inhibiting protein breakdown.

The mechanisms by which insulin exerts its action are still not fully understood however the insulin receptor is well characterized.⁴ The insulin receptor is a transmembrane protein consisting of 2α and 2β subunits.⁵ A schematic representation of the insulin receptor is given in Figure 1.2.2. The extracellular portion of the insulin receptor contains a site to recognize and bind insulin, the intracellular (cytosolic) portion of the receptor contains a kinase domain**. Kinases act to form phosphate esters on target molecules. The binding of insulin extracellularly is thought to bring about an allosteric change in the receptor that is transmitted through the plasma membrane activating the kinase domain. The kinase has been identified as a tyrosine kinase. Tyrosine kinases are relatively rare accounting for less than 0.05% of all protein phosphorylation in cells.⁶ Of

*A zymogen is the inactive form of an enzyme or hormone that is initially secreted but later modified to give the active species. This is seen in digestive enzymes (as a safeguard against potential digestion of the cell producing the enzyme) as well as with insulin.

** Kinases are enzymes that catalyze the formation of phosphate esters. Tyrosine kinases act to phosphorylate tyrosine residues on target substrates.

particular interest is the fact that the insulin receptor kinase (IRK) is autophosphorylating.⁵ The receptor is phosphorylated at 13 tyrosine residues in the β subunit in three clusters.⁴ The consequence of this autophosphorylation is a continued activity of IRK independent of insulin binding. Phosphorylation of other tyrosine residues on target proteins allow IRK to initiate the biochemical cascade responsible for insulin's metabolic effects. Regulation of the IRK is presumed to be due to a protein tyrosine phosphatase (PTP) that acts to hydrolyze the tyrosine phosphate esters of IRK thus rendering it inactive.⁷ Inhibition of the PTP associated with IRK might thus potentiate the metabolic effect of insulin.

The single crystal X-ray structures of a number of PTPs have recently been reported.⁸⁻¹¹ A striking homology in active site structure among PTPs have been observed. Of particular interest is a catalytically essential cysteine residue. In *Yersinia* PTP the pKa of the catalytically essential cysteine thiol is approximately 4.7, and similar pKa's would be expected for other PTPs.¹⁰ Thus at physiological pH the cysteine exists as a thiolate anion. The crystal structure of PTP1B with the tungstate ion (WO_4^{2-}), a phosphate analog, in the active site indicates that the active site cysteine (Cys²¹⁵) is well positioned to act as a nucleophile on a bound phosphotyrosine substrate.¹⁰ A putative mechanism is given in Figure 1.2.3.

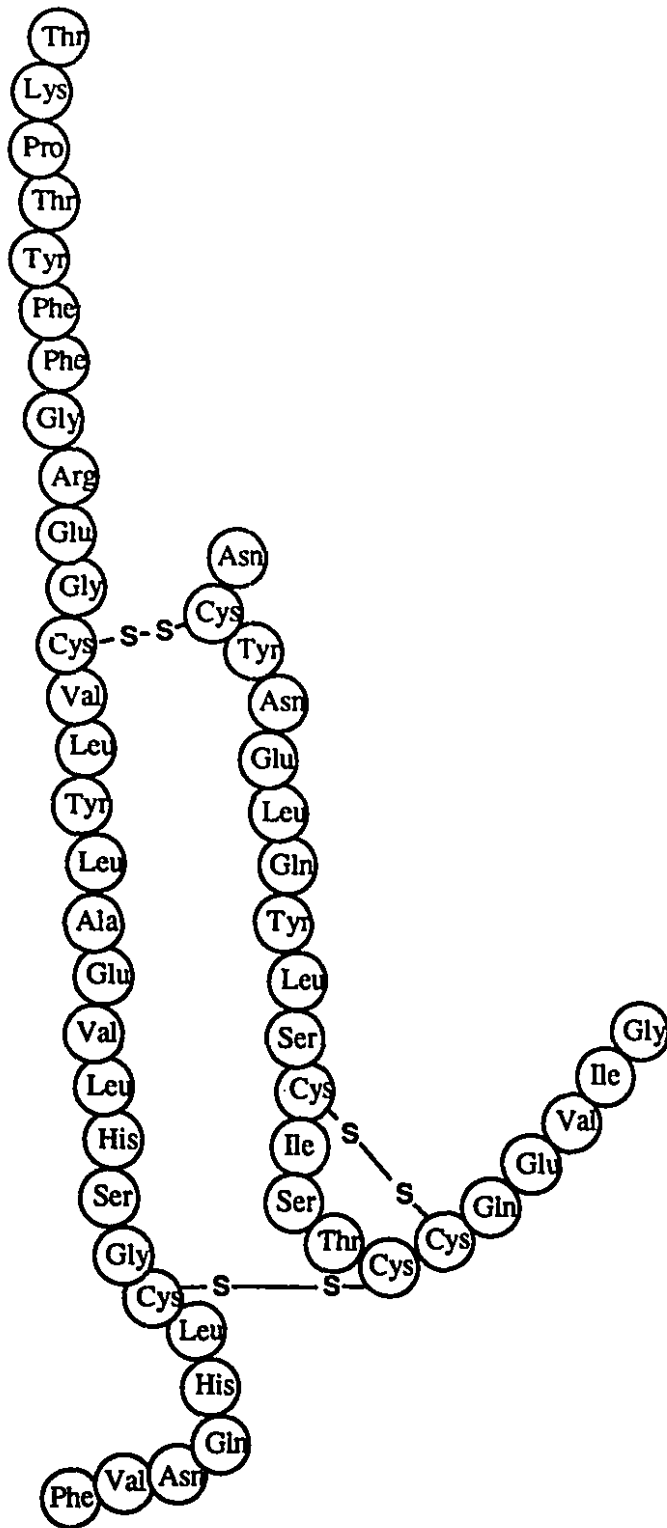


Figure. 1.2.1. The Structure of Human Insulin

Adapted from: Keeton, W. T. and Gould, J. L. (1986). *Biological Science*. New York, W. W. Norton and Co. Inc. p.411

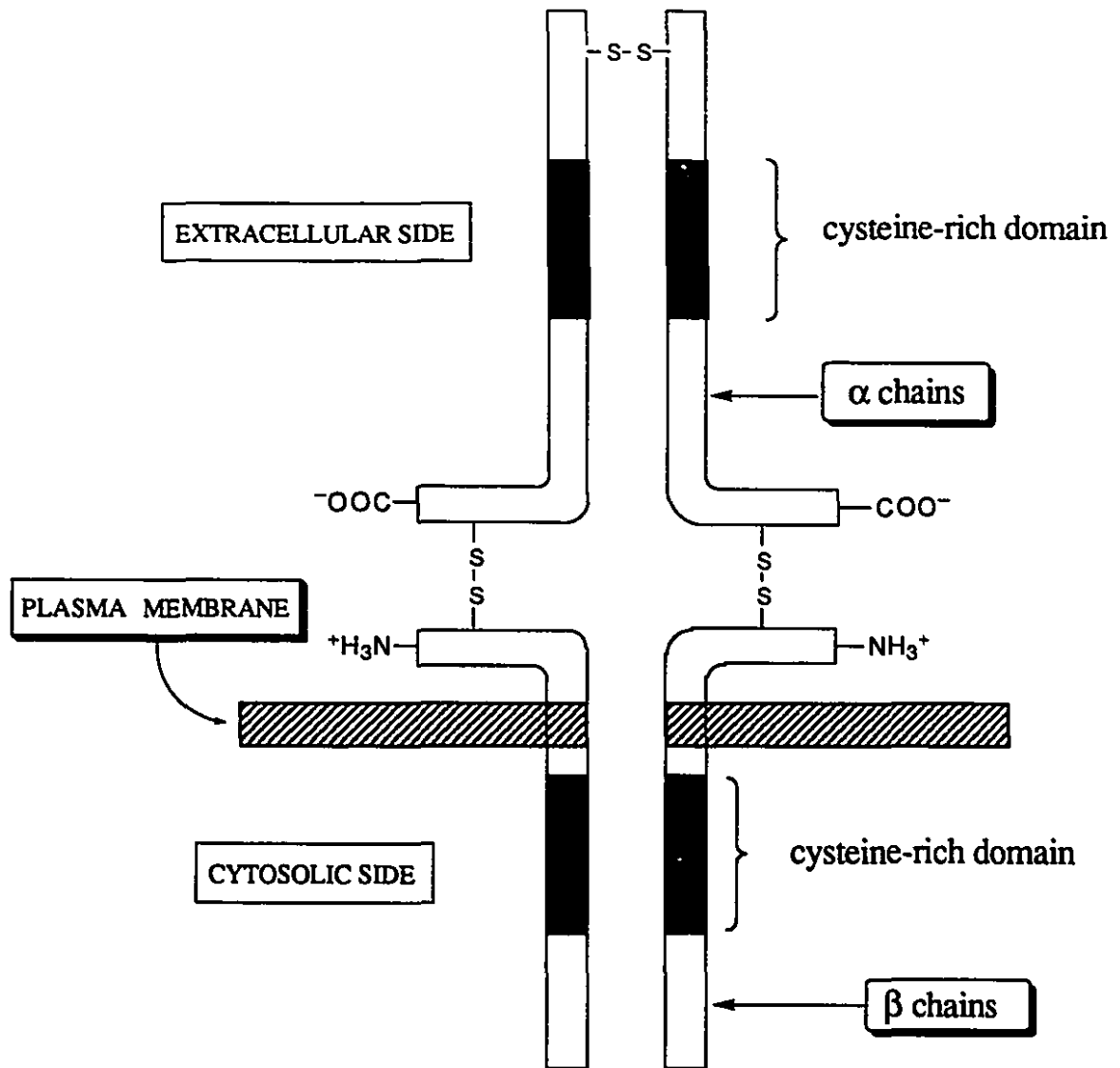


Figure 1.2.2. Schematic representation of the insulin receptor.

Adapted from Keeton, W. T.; Gould, J. L. *Biological Science*; 4 ed.; W. W. Norton and Co. Inc.: New York, 1986.

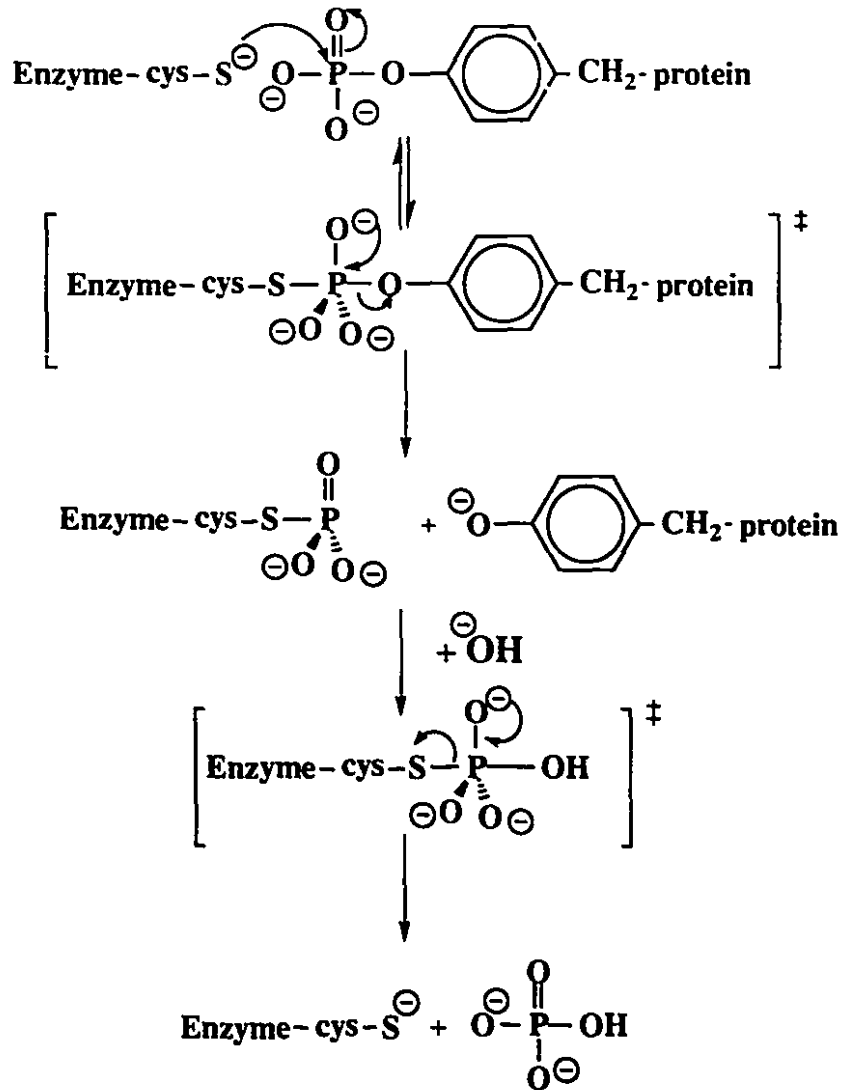


Figure 1.2.3. Putative mechanism for the hydrolysis of phosphotyrosine by PTP¹⁰

1.3. Treatment of Diabetes Mellitus

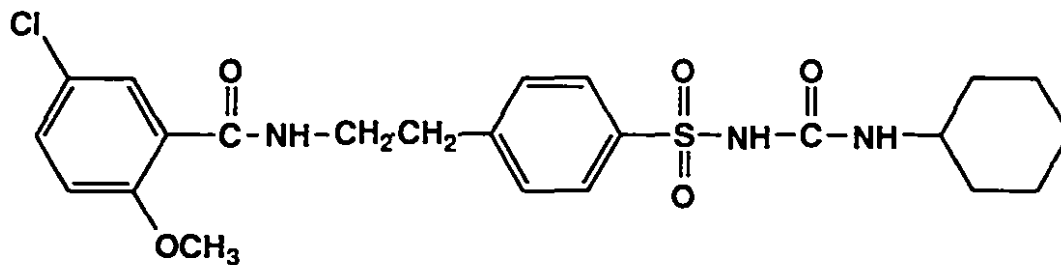
Although the symptoms may be similar the different underlying causes of type I and type II DM necessitate different strategies be used in their treatment. Type II DM is generally treated by controlling the patient's diet or through the use of oral antidiabetic drugs.¹² There are three main types of oral antidiabetic drugs used in the treatment of

Type II DM: sulfonylureas, biguanides¹³ and alpha glucosidase inhibitors.¹² The structures of representative compounds are given in Figure 1.3.1.

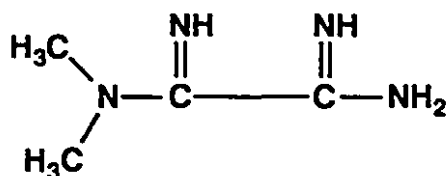
Sulfonylureas are thought to act by stimulating the pancreas to produce more insulin.¹³ Recent studies indicate they may do so as a result of two mechanisms.¹⁴ Sulfonylureas are presumed to cause a depolarization of the beta cell membrane by blocking potassium channels sensitive to adenosine triphosphate, this depolarization results in an influx of calcium that leads to the secretion of insulin.¹⁴ Additionally sulfonylureas may interact directly with a protein kinase that promotes insulin exocytosis.*¹⁴ Chronic administration of sulfonylureas however results in improved glucose tolerance without increased insulin levels.¹³ A possible explanation for this increased sensitivity to insulin may be a modification of the insulin receptor.¹³

Biguanides are another class of oral antidiabetic agents that are thought to exert their action extrapancreatically.¹³ A number of mechanisms have been proposed but it is not clear which, if any, mechanism is predominantly responsible for their antidiabetic action. Proposed mechanisms include: reduction in the absorption of glucose through the gastrointestinal tract, the stimulation of anaerobic glycolysis and glucose uptake by cells, the inhibition of gluconeogenesis, and the inhibition of fatty acid degradation.¹³

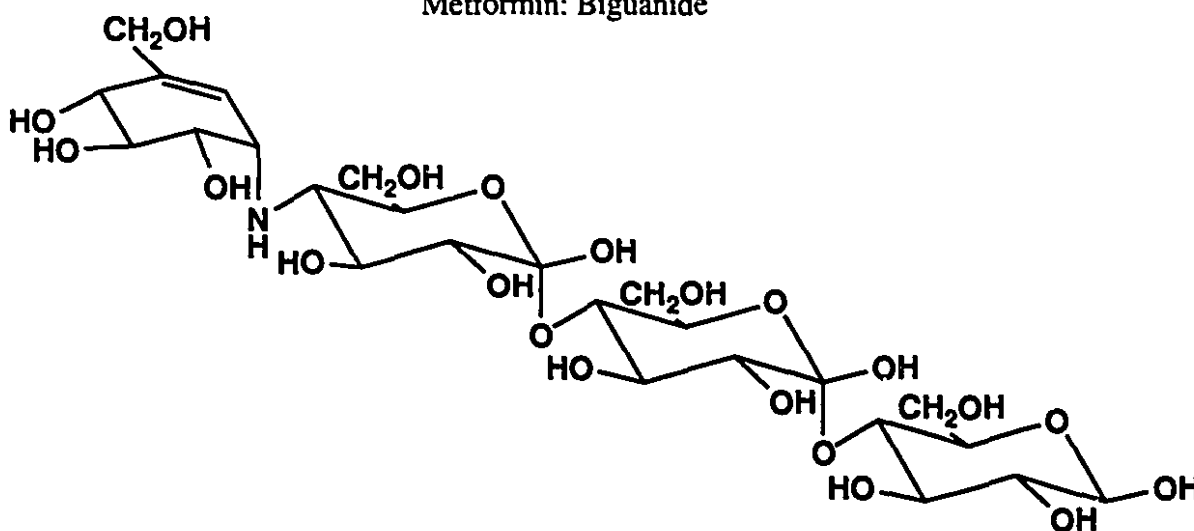
* Exocytosis is a process by which cells release substances (as secretory products) contained in vesicles to the exterior of the cell. This is accomplished by fusing the vesicular membrane with the cell membrane subsequently releasing the contents.



Glyburide: Sulfonylurea



Metformin: Biguanide



Acarbose: Alpha glucosidase inhibitor

Figure 1.3.1. Three representative oral antidiabetic drugs. Ref. Merck Index 10th Ed., Merck & Co., Rahway N.J., USA, 1985

Alpha glucosidase inhibitors are a newer treatment for NIDDM.¹² These compounds are thought to exert their antidiabetic effect by retarding the digestion of

complex carbohydrates in the gut. These compounds like all drug treatments of NIDDM must be used with care to avoid potential hypoglycemia.

Type I diabetics require, depending on the severity of their disease, intramuscular insulin injections on a chronic basis. Insulin, being a polypeptide hormone, must be administered by injection because if given orally it would be digested by the body thus rendering it inactive. The availability of inexpensive portable blood glucose monitors has improved the patients control over their glucose levels through tailoring their insulin dosage.¹⁵ Although advances have been made in the details of diagnosis and treatment of DM the fundamentals have not changed significantly since the discovery and isolation of insulin by Banting and Best over 70 years ago. Currently much attention is being paid to the implantation of insulin producing cells into diabetic patients.¹⁶ Diabetic dogs have been weaned from insulin following transplant of encapsulated insulin producing cells.¹⁶ This form of treatment has the benefit of being a reasonably natural method for controlling blood glucose as the cells are able to respond to the body's changing blood glucose levels. There are, however, shortcomings to this treatment including finding a suitable technique for the encapsulation of the cells that allows passage of nutrients into the cells and insulin from them.¹⁷ Also the encapsulating material must not elicit an immune response or be so bulky as to require a large volume be injected to give the sufficient number of cells.¹⁷ The cost of such implants would also be quite high and would probably not be an option in developing countries where even life sustaining insulin injections are a luxury that are often not affordable.¹⁸ For now the principle treatment for IDDM remains intra-muscular insulin injection. Insulin injections are only a treatment for IDDM and are not a cure. The prognosis for IDDM sufferers includes a number of potential serious complications including blindness and a shortened life-expectancy. For these reasons there has been considerable effort directed at alternative treatments, prevention, and cures for DM.

1.4. Insulin Mimetic Metal Ions

Insulin mimics are compounds that *in vitro* or *in vivo* elicit some or all of the effects of insulin. In trying to design or identify a compound as a potential treatment for DM, especially for type I, a compound that mimics the metabolic effects of insulin as closely as possible is desirable. A number of metal ions have been observed to have insulin like activity. These insulin mimetic ions include manganese¹⁹, zinc^{19,20}, cadmium and mercury²¹ and more significantly vanadate.²² Chromium, administered orally as chromium (III) tripicolinate, is not a true insulin mimic but rather, in individuals with chromium deficiencies, it acts to stimulate glucose uptake by the cells.²³ Chromium(III) tripicolinate has also been observed in clinical trials in humans to lower serum cholesterol levels.²⁴ Chromium picolinate is available as an over-the-counter dietary supplement in the United States and is marketed as an anabolic agent.

Recently a great deal of interest has been focused on the insulin mimetic effects of vanadium. In 1980 there were two reports of increased rates of glucose oxidation, one of the effects of insulin, in isolated rat adipocytes that had been incubated in vanadate solutions.^{25,26} The insulin mimetic effects of vanadate *in vivo* were demonstrated with its administration to rats in their drinking water.²⁷ Insulin mimetic effects of vanadyl compounds have also been demonstrated both *in vitro*²⁵ and *in vivo*.²⁸ More recently discrete vanadyl complexes have been designed to increase their absorption through the gut thus increasing their usefulness as an oral treatment for diabetes.²⁹ In 1987 Posner et al. discovered that peroxovanadium (pV) compounds were potent insulin mimics *in vitro*^{30,31} and later studies have confirmed their insulin mimetic effects *in vivo*.³² The interest in vanadium (as vanadium(IV), vanadium(V) and pV compounds) as insulin mimics warrants a discussion of the diverse chemistry of vanadium before a more in depth discussion of insulin mimetic vanadium compounds.

1.5. The Chemistry of Vanadium

The aqueous chemistry of vanadium is noted for both its complexity and the beautiful colours of its solutions. Vanadium was first reported in 1801 by Del Rio at the University of Mexico although this claim was later retracted and dismissed as impure chromium. Del Rio had tentatively called this new element erythronium owing to the intensely red coloured solutions it formed in acid media. It was the Swede Sefström who finally identified and named vanadium in 1830. Vanadium's name is derived from Vanadis, a Norse goddess of beauty and love. Indeed the vast array of colours produced by vanadate solutions makes it an aesthetically pleasing metal to work with.

The diverse colour and chemistry of vanadium can be largely attributed to its range of oxidation states. Vanadium has the electronic structure $3d^34s^2$ and exists in the -1, 0, 1+, 2+, 3+, 4+, and 5+ oxidation states.³³ Pure vanadium is rare due to its reactivity towards oxygen, nitrogen, and carbon at the high temperatures used in thermometallurgical processes.³³ Vanadium is most commonly found in nature in the 3+ and 4+ oxidation states.³³ Vanadium is widely distributed in the earth's crust at an estimated abundance of 0.01-0.05%³⁴, relatively common when compared to Co (0.003%), Ni (0.008%) or Cu (0.006%).³⁵ Some important vanadium containing minerals include patronite, vanadinite, and carnotite.³³ The latter is predominantly mined for its uranium content but the vanadium is often recovered as well.³³ Another source of vanadium is from fossil fuels, most notably those from Venezuela.³³

The wide range of oxidation states of vanadium has given rise to a diverse chemistry ranging from low valent organometallic compounds such as vanadocene to highly oxidized water soluble pV complexes. Vanadium may act as a powerful reducing

agent in its 2⁺ oxidation state, indeed vanadium(II) hydroxide is among the most powerful reducing agents known in inorganic chemistry.³⁶ However in its 5⁺ oxidation state vanadium may act as a powerful oxidant.³⁷ In aqueous solutions however only the 3⁺, 4⁺ and 5⁺ oxidation states are of importance as the 2⁺ state reduces water to dihydrogen.²²

Vanadium-51 has a nuclear spin of 7/2 and a natural abundance of nearly 100% making it an NMR active nucleus in its 5⁺ oxidation state.³⁸ The ⁵¹V nucleus has a relatively large nuclear moment (5.1392β_N) and consequently has a sensitivity of approximately 0.38 that of the proton.³⁸ Due to its electric quadrupole moment ⁵¹V NMR line widths vary from 60-800 Hz depending on the symmetry of the vanadium complex.³⁸ The range of chemical shifts observed for vanadate complexes is about 600 ppm³⁸ thus even though lines may be quite broad they are usually separated and well defined. The chemical shifts observed for monoperoxovanadium (mpv) compounds ranges from approximately -505 to -769 ppm but at neutral pH most are found in the -590 to -640 ppm range³⁹. The chemical shift range for bisperoxovanadium* (bpV) compounds is approximately -700 to -770 ppm.³⁹ ⁵¹V NMR spectroscopy has been used in the characterization of metal binding sites in human transferrin and has the potential to be used in the characterization of vanadium(V) binding to other macromolecules.⁴⁰ An excellent review of ⁵¹V NMR was recently published by Howarth.³⁹

Free vanadium in biological systems generally exists as either vanadate(V) or vanadyl(IV), with vanadate predominating in oxygenated solutions at pH > 4.⁷ At neutral pH vanadyl readily undergoes aerial oxidation to vanadate(V) possibly according to the equation below²²:

* Although the proper terminology is diperoxovanadium, the term bisperoxovanadium has gained a foothold in the literature and will be used in this thesis.



In aqueous solution vanadate exists in a complex equilibrium dependent on both concentration and pH. Many oligomerization equilibria exist simultaneously with the monomer, dimer, tetramer and pentamer exchanging on the millisecond timescale.⁴¹ These pathways have recently been elucidated through the use of two dimensional EXSY NMR.⁴² A typical ⁵¹V NMR of the vanadate region is shown in Figure 1.5.1. The vanadate decamer ($\text{V}_{10}\text{O}_{28}^{6-} / \text{HV}_{10}\text{O}_{28}^{5-}$) may be present although its formation is only favoured under high concentration and low pH conditions; a hexamer may also be observed at high ionic strength.²² The monomer differs in hydration states depending on pH in aqueous solution (H_2VO_4^- at pH 5-9, HVO_4^{2-} at pH 9-12 and VO_4^{3-} at pH > 13).⁷

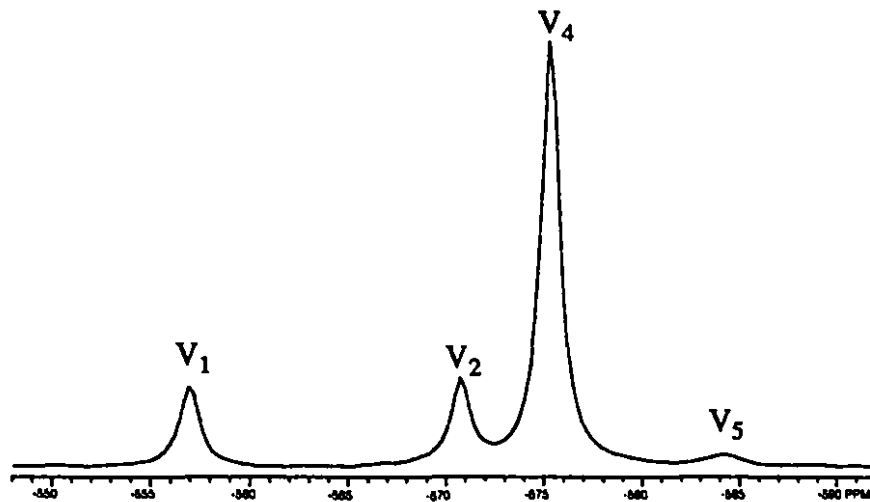


Figure 1.5.1. Vanadium-51 NMR of NaVO_3 in D_2O . $\text{V}_1 = \text{H}_2\text{VO}_4^-$, $\text{V}_2 = \text{V}_2\text{O}_7^{4-}$, $\text{V}_4 = \text{V}_4\text{O}_{12}^{4-}$, and $\text{V}_5 = \text{V}_5\text{O}_{15}^{5-}$

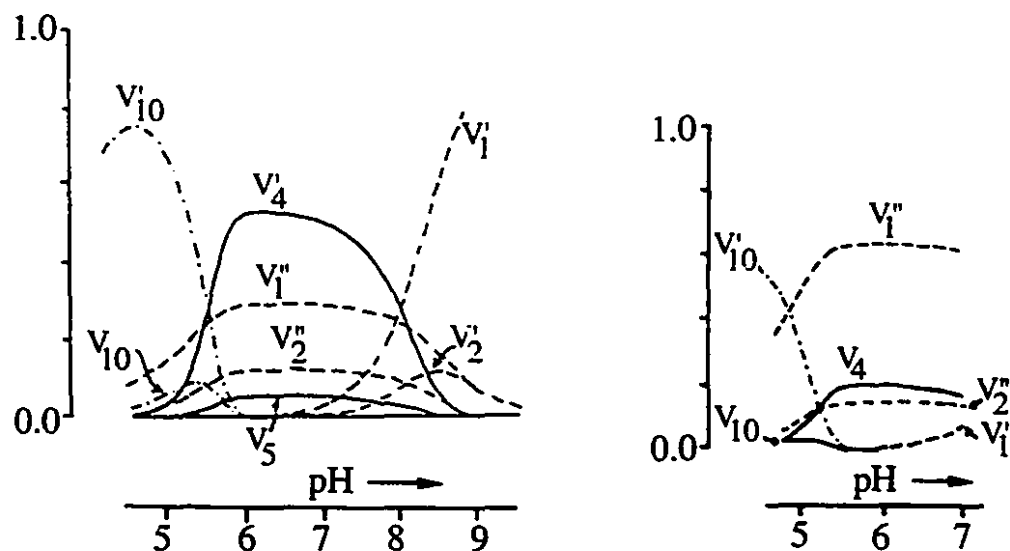


Figure 1.5.2. The distribution of vanadates at various pHs²² $V_1' = HVO_4^{2-}$, $V_1'' = H_2VO_4^-$, $V_2' = HV_2O_7^{3-}$, $V_2'' = H_2V_2O_7^{2-}$, $V_4 = V_4O_{12}^{4-}$, $V_5 = V_5O_{15}^{5-}$, $V_{10} = V_{10}O_{28}^{6-}$, $V_{10}' = HV_{10}O_{28}^{5-}$

The vanadium-51 nucleus is also EPR active in its 4+ oxidation state.³⁸ The unpaired electron is strongly coupled to the spin 7/2 vanadium centre and produces a characteristic 8-line signal.³⁸ This technique is extremely sensitive and reasonable spectra of samples containing vanadium at a concentration as low as 20 μ M can be obtained.³⁸ Vanadyl has seen use as a probe of protein structure owing to its EPR sensitivity.⁴³ EPR has also been employed to study the interaction of vanadyl with various biomolecules including amino acids⁴⁴, glutathione^{45,46}, and nucleotides.⁴⁷

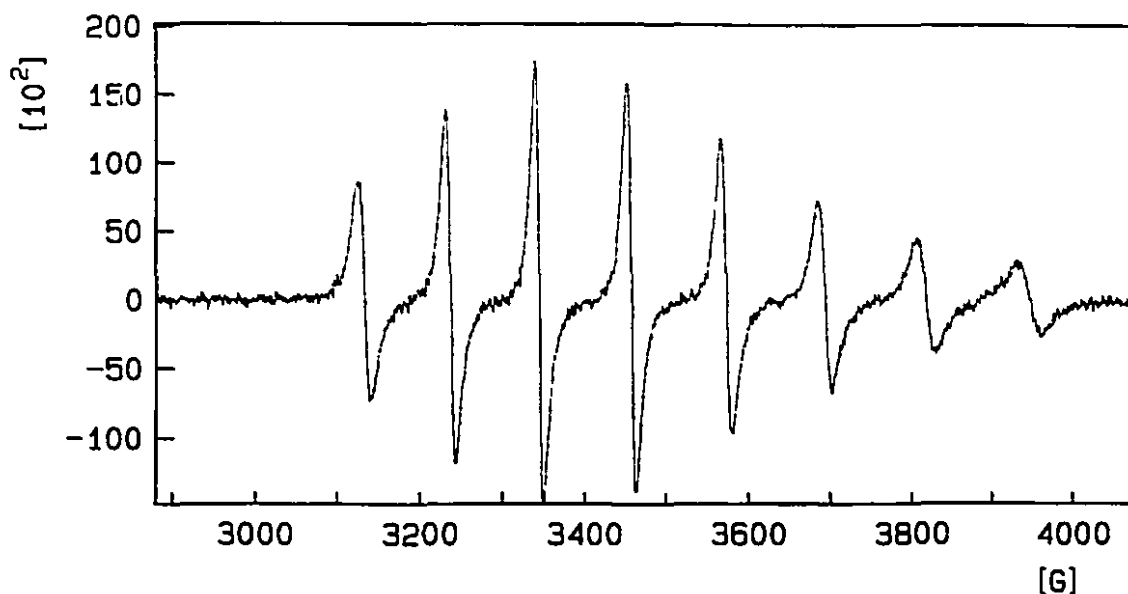


Figure 1.5.3. A typical ^{51}V EPR spectrum. VOSO_4 in H_2O .⁴⁸

Vanadium is an essential trace element that is widely distributed throughout the biosphere.³⁸ Vanadium is present in sea water at a concentration of approximately 50 nM^{22} as the pentavalent monomeric anion $(\text{H}_2\text{VO}_4^-)^{49}$ and some sea creatures have evolved the ability to concentrate this vanadium. Ascidiaceans (sea squirts) concentrate vanadium in specialized blood cells at concentrations as high as 0.15M . Some terrestrial organisms concentrate vanadium⁴⁹, *Amanita muscaria* concentrates vanadium in the $4+$ oxidation state.⁴⁹ There has been some debate about the structure of this vanadium compound but the currently accepted structure is given below in Figure 1.5.4.⁴⁹

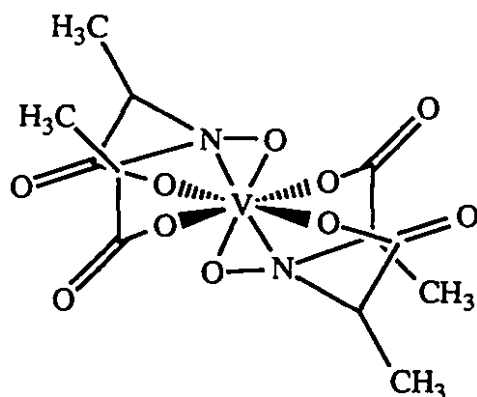


Figure 1.5.4. Postulated structure of amavadin, as found in the vanadium accumulating fungus *Amanita muscaria*.⁴⁹

Vanadium has long been recognized as an essential trace element in the higher animals.⁵⁰ In rats a deficiency of vanadium results in a general retardation of growth.⁵⁰ Interestingly the level of vanadium in mammalian plasma is homeostatically maintained.⁷ Serious interest in the bioinorganic chemistry of vanadium came about as a result of the identification of enzymes containing vanadium in their active sites.²² One such class of enzyme are the vanadium haloperoxidases³⁷, found primarily in marine organisms such as sea algae and also in terrestrial lichens.²² The haloperoxidases catalyze the chlorination, bromination, and iodination of organic substrates by peroxide according to the equation below²²:



The nomenclature of haloperoxidases is based on the most electronegative halide that the enzyme oxidizes with hydrogen peroxide.⁵¹ Using this system a chloroperoxidase would be expected to oxidize chloride, bromide and iodide whereas a bromoperoxidase would be expected to oxidize bromide and iodide and so on.⁵¹ All vanadium bromoperoxidases thus far elucidated are similar in amino acid composition, molecular weight, charge and

vanadium content.⁵¹ In the resting state the vanadium exists in the +5 oxidation state.⁵¹ EXAFS studies indicate the vanadium is probably coordinated in a distorted octahedral geometry with a vanadyl oxygen ligand, two nitrogen donor ligands and three unknown light atom donors.⁵¹ The mechanism by which vanadium bromoperoxidases act has not yet been fully elucidated however it is thought that vanadium remains in the +5 oxidation state, is the catalytically important species, and that bromine oxidation occurs after the coordination of hydrogen peroxide.⁵¹ An excellent review of marine haloperoxidases has recently been published by Butler and Walker.⁵¹

A functional model for vanadium haloperoxidase has recently been reported by Colpas et al.⁵² The mpV compound, K(18-crown-6)[VO(O₂)N-(2-hydroxyethyl)iminodiacetato)] ([VO(O₂)(Hheida)]⁻), and one equivalent of triflic acid reacted with excess tetra-*n*-butylammonium bromide or tetra-*n*-butylammonium iodide to form the tribromide or triiodide anions.⁵² The bromination of Phenol Red to Bromophenol Blue is also observed. The addition of excess peroxide, Phenol Red, triflic acid, and tetra-*n*-butylammonium bromide to the solution demonstrated that the reaction was catalytic in the vanadium complex and multiple turnovers were observed.⁵² The observations of Colpas et al. suggest that the active site of the vanadium haloperoxidase enzyme may be hydrophobic and that an acid or base catalyst is readily accessible.⁵² Very recently Colpas et al. extended their study to include four additional functional models of vanadium haloperoxidase.⁵³ Details of the catalytic cycle and the rate constants for bromide and iodide oxidation are reported.⁵³

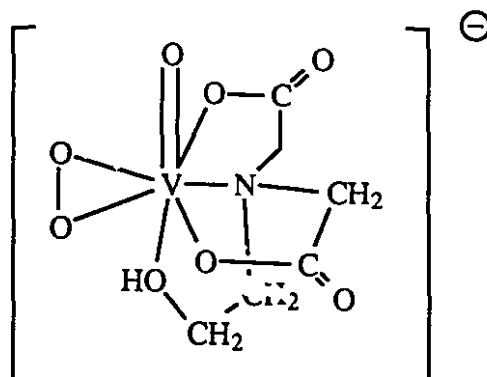


Figure 1.5.6. The structure of [VO(O₂)(Hheida)]⁻, a functional model for vanadium haloperoxidase⁵²

The oxidation of organic compounds by pV compounds has been reviewed recently by Butler et al.³⁷ These oxidations include; the epoxidation and hydroxylation of alkenes and allylic alcohols, the oxidation of sulfides to sulfoxides and sulfones, the hydroxylation of alkenes and arenes, and the oxidation of primary and secondary alcohols to aldehydes and ketones.³⁷ Other interesting oxidations include the oxidation of 2,2'-bipyridine to picolinic acid in aqueous solution⁵⁴, and the catalytic hydroxylation of benzene to phenol.^{55,56}

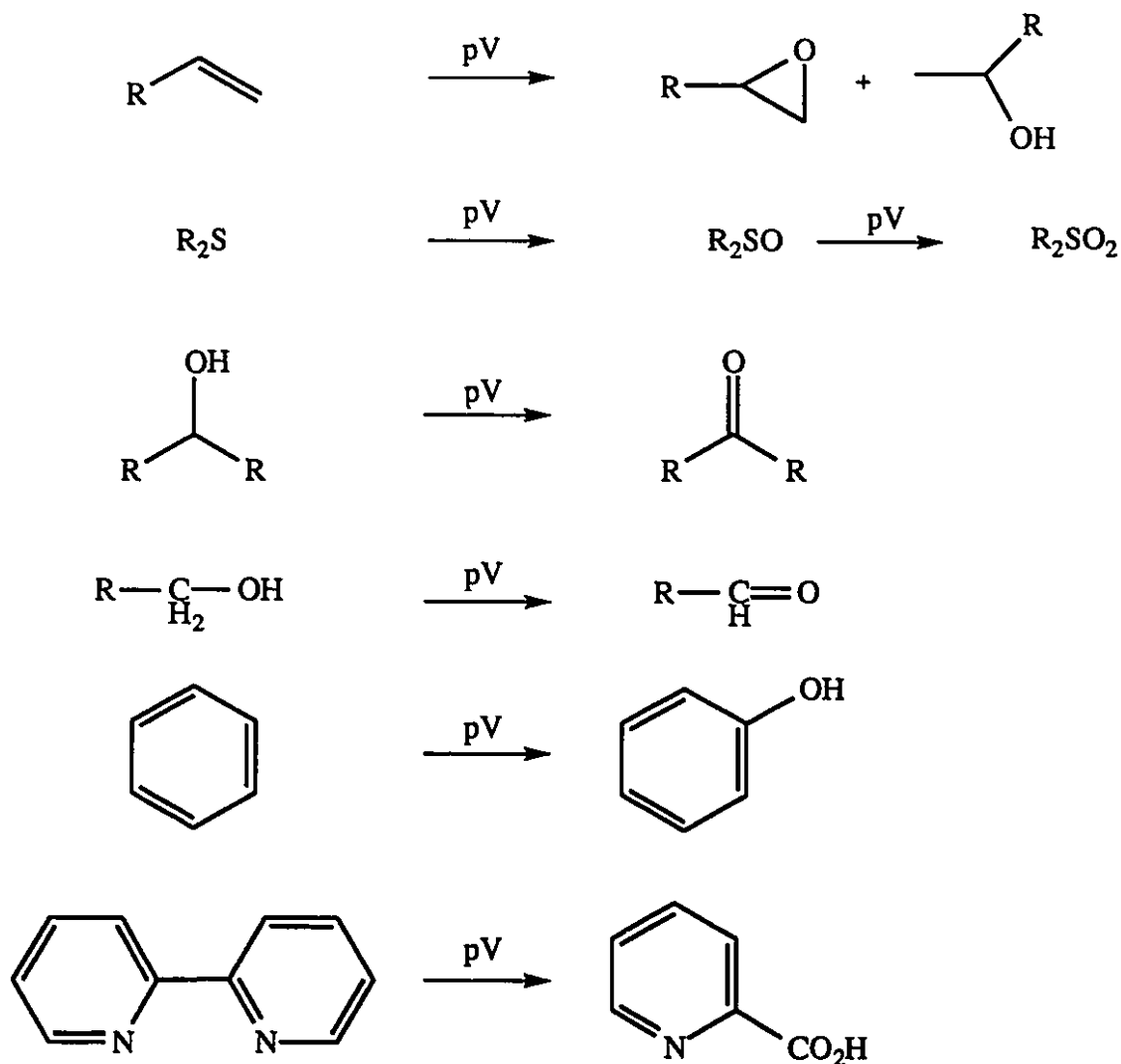


Figure 1.5.7. The oxidation of organic molecules by pV compounds³⁷.

1.6. Insulin Mimetic Vanadium Compounds.

1.6.1. Vanadate

In 1980 there were two reports of the insulin mimetic effect of vanadate by stimulating glucose oxidation *in vitro*.^{25,26} In both reports the effects were observed in isolated rat adipocytes.^{25,26} Shechter and Karlsh suggested that vanadate was reduced to vanadyl upon entering the cell and that this was the species that was responsible for insulin mimesis.²⁵ Incubation of the adipocytes with vandyll however showed it to be a less potent

insulin mimic than vanadate.²⁵ Indeed maximal stimulation of glucose oxidation was not observed with vanadyl sulfate although this was attributed to solubility problems with the vanadyl sulfate.²⁵

In 1985 it was observed that diabetic rats that were fed vanadate (V^{5+}) in their drinking water showed a normalization of blood glucose levels.²⁷ Further studies of vanadate have shown that it mimics many but not all of the actions of insulin.⁷ Vanadate has not been observed to increase protein synthesis in adipocytes or skeletal muscle.⁷ It is suggested that the differences in the effects of vanadate versus insulin may be due to a less specific action of vanadate on protein phosphorylation.⁷

1.6.2. Vanadyl and Vanadyl Complexes

The use of vanadyl(IV) ions for the treatment of diabetes *in vivo* has been reported by McNeil et al.²⁸ The use of vanadyl as opposed to vanadate was based on the lower toxicity of vanadyl when given orally and the assumption that the active species *in vivo* is vanadyl(IV).²⁹ Sakurai et al. reported that vanadate(V) was reduced to vanadyl(IV) *in vivo* after detecting vanadyl(IV) in subcellular fractions of rat liver from rats that had been injected with vanadate(V).⁵⁷ The conclusions of Sakurai et al.⁵⁷ as reported by others²⁹ are more far reaching than their data might suggest. Sakurai et al. observed EPR resonances consistent with vanadyl but no attempt was made to determine the presence of vanadate.⁵⁷ The high sensitivity of vanadium(IV) EPR allows detection of vanadium(IV) at micromolar concentrations.³⁸ Indeed from the observations of Sakurai et al. all that can be said is that some vanadate is reduced to vanadyl(IV) in subcellular rat liver fractions and the presence or absence of vanadate(V) can not be confirmed.⁵⁷ Indeed it has been suggested that an equilibrium between vanadyl and vanadate may exist *in vivo* with the equilibrium varying with different tissues or organs depending on their environment.⁵⁸

Vanadyl sulfate is poorly absorbed when given orally.²⁹ Orvig et al. have proposed the use of bis(maltolato)oxovanadium(IV) (BMOV) as an oral hypoglycemic agent.²⁹ The bismaltolato ligand was chosen because of its hydrophobicity, low toxicity, and its documented ability to mobilize other metal ions.^{29,59} BMOV has been shown to lower the plasma glucose and lipid levels when given orally to streptozocin-diabetic* rats.⁶⁰ Orally administered (p.o.) BMOV is roughly twice as potent as vanadyl sulfate, when given intra-peritoneally (i.p.) BMOV was roughly three times as potent as vanadyl sulfate, and whereas an intravenous (i.v.) infusion of BMOV was effective in reducing plasma glucose levels, vanadyl sulfate was not.⁶⁰

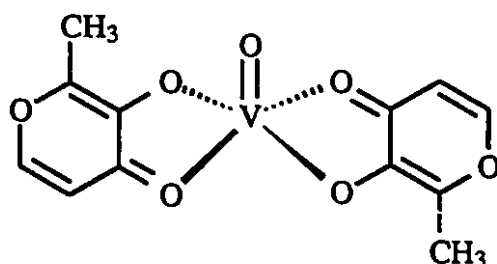


Figure 1.6.1. The structure of bis(maltolato)oxovanadium(IV)

Similar strategies to improve the absorption of vanadyl have been proposed by Shechter et al.⁶¹ and Watanabe et al..⁶² Shechter et al. proposed the use of an ionophore to increase the hydrophobicity of vanadyl, an example of such a complex is shown in Figure 1.6.2. They have related the insulin mimetic effect of the vanadyl ionophore complex to the ability of the ionophore to extract vanadyl from water into methylene chloride. The implication is that hydrophobic vanadyl complexes are more readily able to pass through the plasma membrane into the cell. Watanabe et al. have reported a bis(pyrrolidine-n-

* Diabetes can be induced in rats through the administration of the drug streptozocin. Administration of streptozocin results in death of pancreatic beta cells, the cells that produce insulin.

carbodithioato) complex that has shown insulin mimetic activity when given orally to rats, this compound is shown in Figure 1.6.2.⁶²

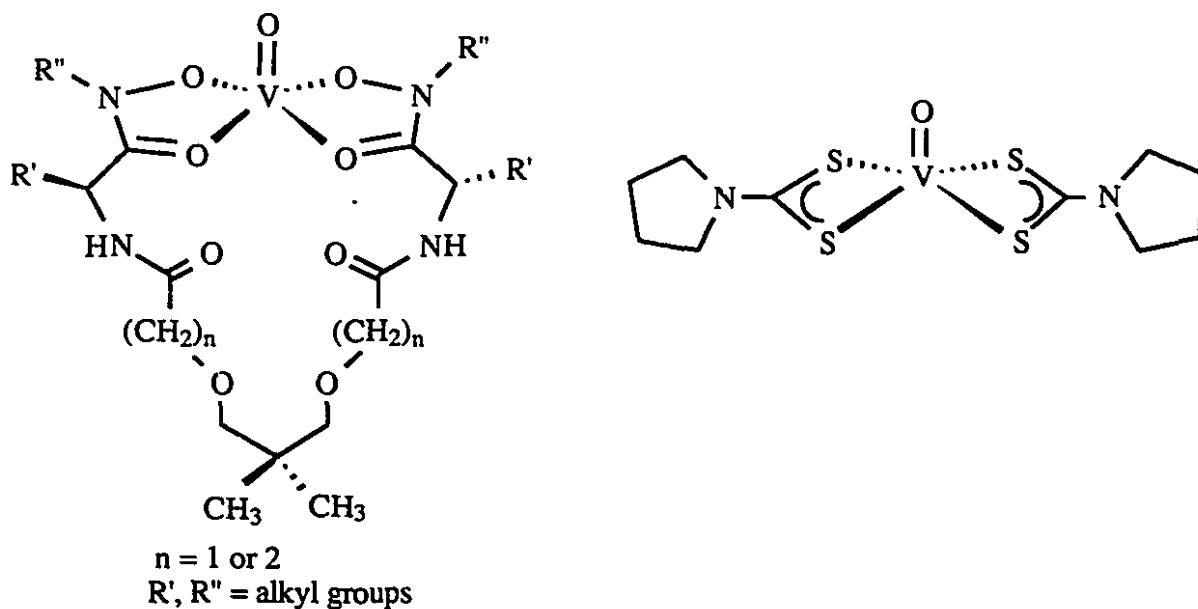


Figure 1.6.2. Insulin mimetic vanadyl complexes with hydrophobic ligands. A dipodal chelator with amino acid bridges⁶¹ (left) and a bis(pyrrolidine-n-carbodithioato) complex⁶² (right).

Ideally a vanadium based treatment for DM would be delivered orally and be sufficiently potent to allow for a dosage significantly below the toxic level. The vanadyl compound BMOV is well tolerated orally⁶⁰ but *in vitro* testing has shown it to be a much poorer inhibitor of PTP than pV compounds.⁶³

Recently the interaction of vanadium(IV) with a peptide fragment from the active site of PTP1B has been probed through the use of EPR.⁶⁴ Cornman et al. used the fragment VHCSAG-NH₂* (single letter amino acid nomenclature) from the active site of PTP1B.⁶⁴ The histidine and cysteine residues are conserved across the entire family of

* Single letter amino acid nomenclature. V=valine, H=histidine, C=cysteine, S=serine, A=alanine, G=glycine, F=phenylalanine, M=methionine

PTPs and the cysteine is necessary for enzymatic activity.⁶⁴ EPR studies with the natural fragment VHCSAG-NH₂ at pH's ranging from 5-9 and with the mutant peptide fragments VHCGAG-NH₂, VHMSAG-NH₂, and VFCSAG-NH₂ at physiological pH indicate that two vanadyl peptide complexes are being formed.⁶⁴ The first complex which is predominant at lower pH is consistent with coordination of the vanadyl with the histidine of the natural fragment and the second which is predominant at higher pH is consistent with coordination to the cysteine thiolate.⁶⁴ The observation is consistent with a PTP inhibitory mechanism in which the active site cysteine coordinates to the vanadium atom.⁶⁴ Indeed the observed pK_a of cysteine in *Yersinia* PTP is 4.7¹⁰ thus, at physiological pH, it would be deprotonated making a vanadyl-thiolato species very likely.

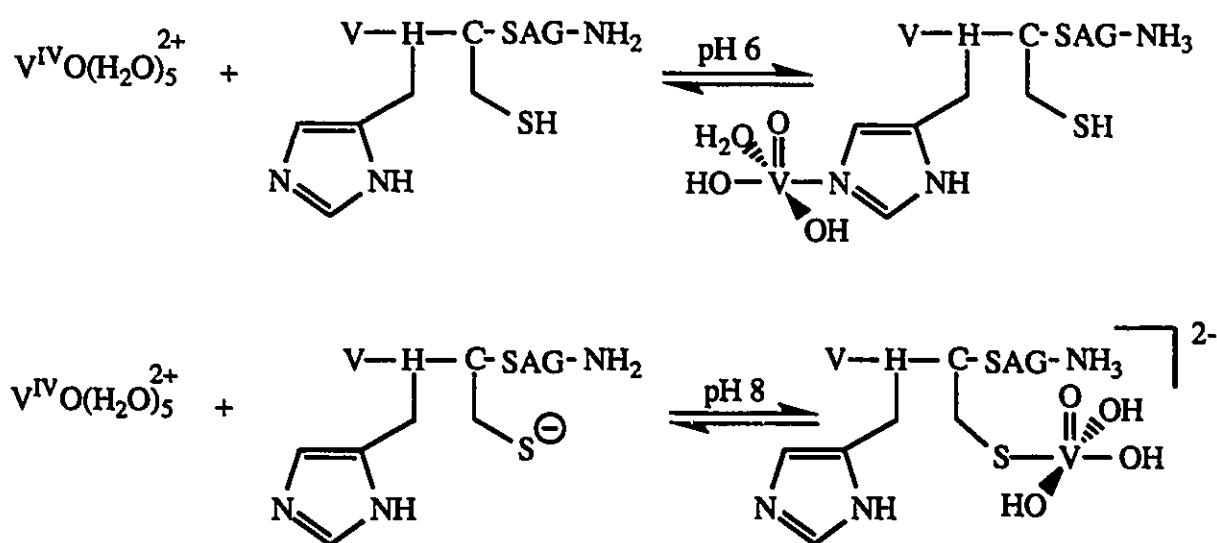


Figure 1.6.3. Vanadyl peptide complexes with a peptide fragment from PTP1B⁶⁴

1.6.3 Peroxovanadium and Peroxovanadium Complexes

Posner and co-workers carried out experiments to compare the effects of vanadate and hydrogen peroxide, also a known insulin mimic, on insulin-like growth factor receptor II (IGF-II) binding and IRK activity.³⁰ Insulin induces a translocation of IGF-II receptors from an intracellular compartment to the plasma membrane in a manner analogous to the

insulin induced translocation of the glucose transporter from an intracellular compartment to the plasma membrane.³⁰ For this reason assays of ¹²⁵I-IGF-II binding provide a measure of insulin mimesis. Posner et al. observed that both vanadate and hydrogen peroxide when tested separately resulted in modest insulin mimetic effects.³⁰ However when vanadate and hydrogen peroxide were combined a synergistic effect was observed that resulted in substantial insulin mimetic effects.³⁰ Figure 1.6.4 summarizes the effects of vanadate, hydrogen peroxide, insulin and combinations thereof on ¹²⁵I-IGF-II binding.³⁰ Posner et al. also showed that pre-incubation of the vanadate with hydrogen peroxide was necessary for their synergistic activity.³¹ If vanadate (10⁻³M), hydrogen peroxide (10⁻³M), and catalase (200µg/mL) (catalase is an enzyme which rapidly catalyzes the disproportionation of H₂O₂ to H₂O and O₂) were mixed simultaneously the insulin mimetic activity was that of vanadate alone.³¹ If, however, vanadate and hydrogen peroxide were allowed to react 10 minutes before the addition of catalase the full synergism of the combination was maintained.³¹ Posner et al. correctly reasoned that the vanadate was reacting with the hydrogen peroxide to form peroxovanadate (pV) species.³¹

Mixtures of peroxide and vanadate can give a mixture of mono, di, tri or even tetra peroxides in solution depending on pH and concentration.³⁷ One of the active species generated by Posner et al. was probably [VO(O₂)₂(H₂O)₂]⁻ among others. These aquo species cannot however be isolated and must be prepared *in situ*. The compounds are also unstable in solution and decompose to vanadate within hours. However peroxovanadium compounds with stabilizing ligands are well known and a number of peroxovanadium complexes both new and previously reported were prepared for testing.⁶⁵ Some representative examples of bpV and mpV compounds are shown in Figure 1.6.5. These compounds are powerful insulin mimics both *in vitro* and *in vivo*.⁶⁵ Indeed pV compounds are the first compounds other than insulin that acutely and markedly decrease

plasma glucose levels in hypoinsulinemic BB rats (BB rats are genetically type 1 diabetic).³²

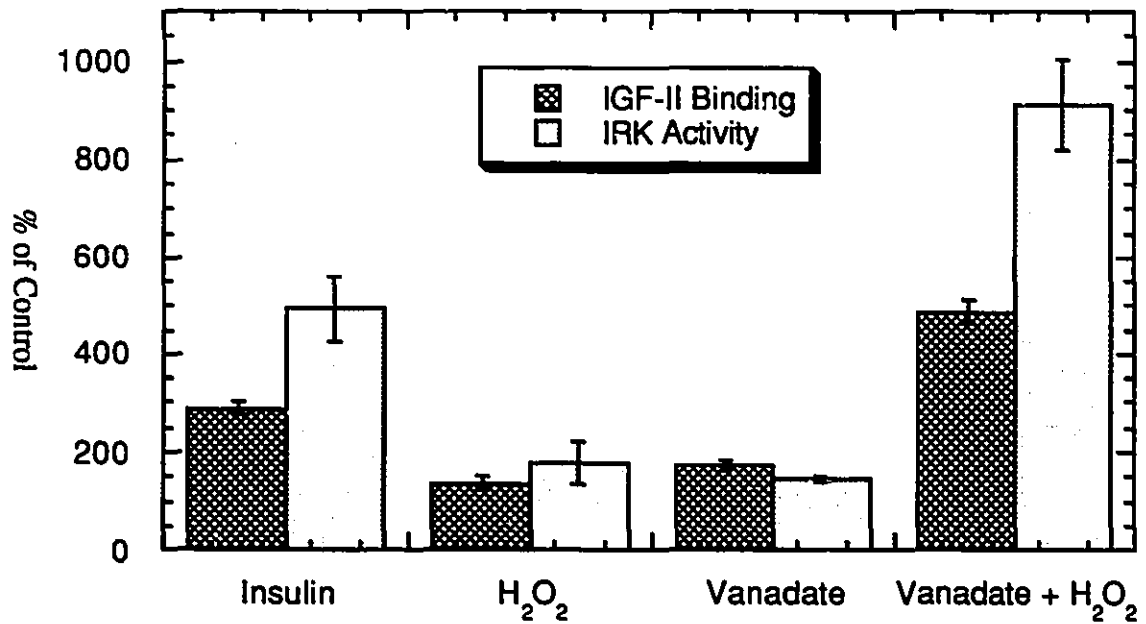
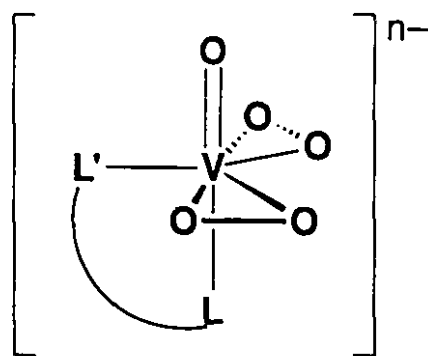


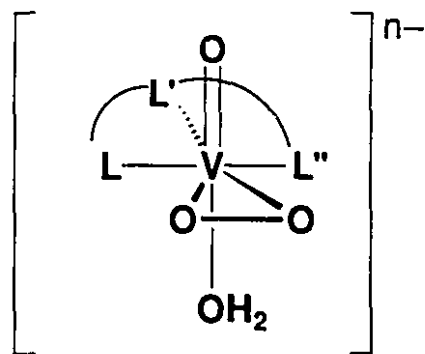
Figure 1.6.4. The effect of insulin, vanadate, and H₂O₂ on basal tyrosine kinase activity and ¹²⁵I-IGF-II binding of rat adipocytes³⁰.

Adipocytes were incubated with insulin, vanadate, H₂O₂, or a mixture of H₂O₂ and vanadate for 15 min. at 37°C. One aliquot of cells was used for determining tyrosine kinase activity and a second for determining ¹²⁵I-IGF-II binding. Each value is the mean +/- S.E. of three separate experiments. Insulin was present at 10 ng/mL, vanadate at 1 mM, and H₂O₂ at 1mM. Abbreviations used IRK=insulin receptor kinase, IGF-II=insulin like growth factor receptor II.



bisperoxovanadium compound

L-L'=1,10-phenanthroline
 =picolinato ion
 =bipyridine



monoperoxovanadium compound

L-L'-L''=2,6-pyridinedicarboxylato ion

Figure 1.6.5. Representative structures of peroxovanadium compounds with stabilizing ancillary ligands.

In order to determine the relationship of various structural features of peroxovanadium compounds to their insulin mimetic activity, a number of complexes have been tested. Figure 1.6.6 shows a series of nearly isostructural oxalato (ox) pV compounds with 2, 1 or 0 peroxide ligands and their relative IRK activities.⁶⁵ This demonstrated the relationship between the peroxide ligand and insulin mimetic activity. As shown the bpV compound is roughly twice as potent an IRK activator as a structurally similar monoperoxo compound and ten times as potent as the complex that contains no peroxo group.

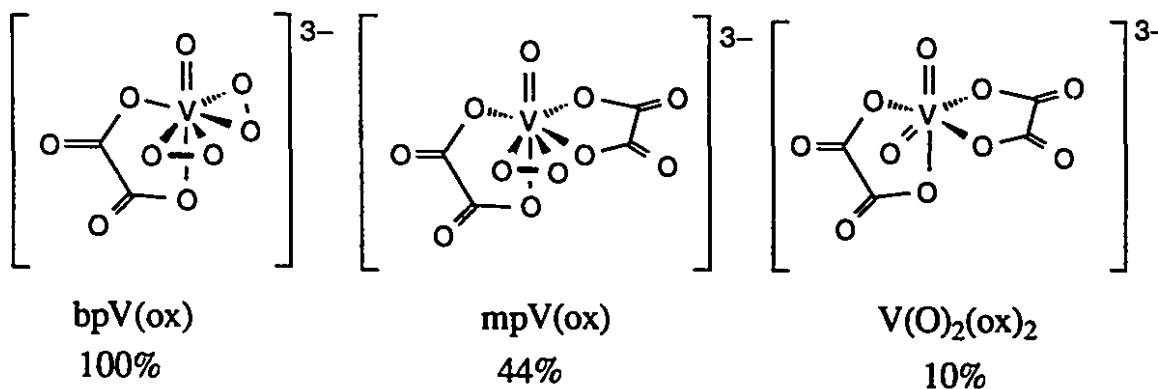


Figure 1.6.6. A series of approximately isostructural vanadium complexes with 2, 1, and 0 peroxide ligands and their relative IRK activities⁶⁵

The metal centres have also been varied to determine their effect on insulin mimetic activity. The series consisting of a peroxovanadate, peroxotungstate and peroxomolybdate is shown in Figure 1.6.7. All of the compounds have been shown to be potent PTP inhibitors but only the peroxovanadium compound is an IRK activator.⁶⁶ PTP inhibition assays are carried out on purified PTP enzyme whereas IRK assays are carried out on whole cells. This suggests that peroxovanadate compounds may enjoy a greater bioavailability than their corresponding molybdate and tungstate compounds.⁶⁶

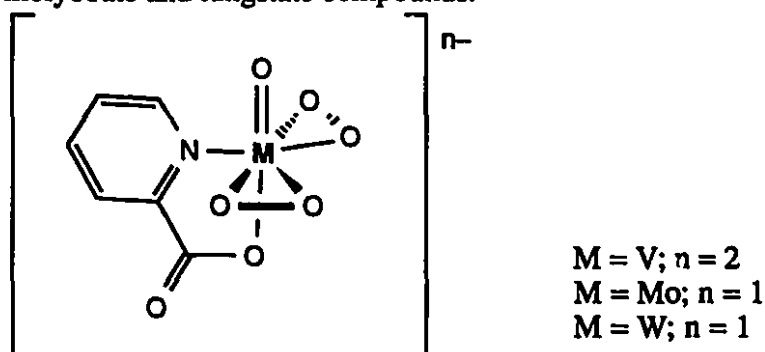


Figure 1.6.7. A series of isostructural peroxo complexes differing only in their metal centres⁶⁶.

The activity of monoperoxovanadium complexes of the 2,6-pyridinedicarboxylato (2,6-pdc) ligand and containing either peroxide or tert-butyl peroxide was also assessed.⁶⁵

The t-butyl-peroxide complex activates IRK roughly one sixth as strongly as does the peroxide analog.⁶⁵ The complexes are isostructural with the exception of the obvious difference in the steric bulk of the peroxide ligands and the difference in overall charge. It is tempting to speculate that the difference in the observed activity is a result of the added steric bulk on the peroxide ligand, however the situation is somewhat confounded by the differing charges on the complexes and the potential difference in oxidation chemistry between the two ligands.

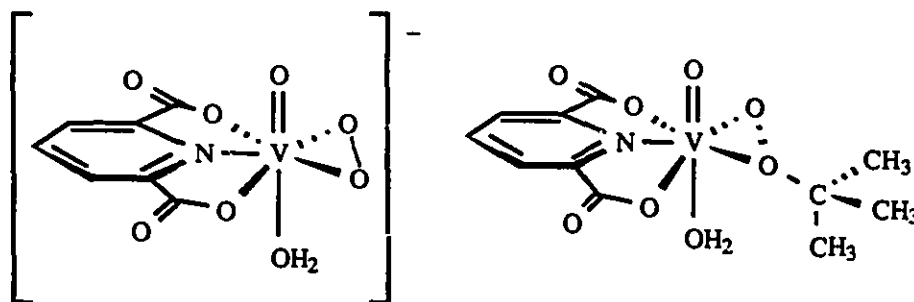


Figure 1.6.8. Two monoperoxovanadium complexes $\text{NH}_4[\text{VO}(\text{O}_2)(2,6\text{-pyridinedicarboxylato})\text{H}_2\text{O}]\cdot\text{H}_2\text{O}$ and its t-butyl-peroxide analog $[\text{VO}(\text{O}_2\text{-t-butyl})(2,6\text{-pyridinedicarboxylato})(\text{H}_2\text{O})]$.

1.7. Plan of Study

The principal goal of this research is to extend the understanding of the insulin-mimetic properties of pV compounds. A better understanding of the chemistry of pV compounds directed towards obtaining greater insight into their mechanism of action may yield compounds that could act as oral therapeutics for the treatment of DM. Investigations of the synthesis of series of pV compounds that contain substituted ancillary ligands of related structures are reported. The effect of slight variations in the ancillary ligand structure on insulin mimetic activity was determined. These kinds of structure activity relationships provide key information for future drug design.

The stability and reactivity of pV compounds was also assessed to determine the appropriate conditions for biological assays. Stability studies also help to determine the fate of pV compounds *in vivo*. These studies also provide insight into the route by which compounds may be administered. If a compound is to be given orally it must be able to withstand the acid environment of the stomach and be absorbed in the intestine.

The reactivity of pV compounds was also investigated in order to understand how they may be exerting their insulin mimetic effect. Reactions of pVs with cysteine and a water soluble triphenylphosphine analog were investigated as models for the reaction of pV with the enzyme PTP. Reactions with cysteine, a key residue in the active site of PTP, provided insight into the mechanism whereby pV compounds exert their insulin mimetic effect.

1.8. References

- (1) Plourde, R.; d'Alarcao, M.; Saltiel, A. R. *J. Org. Chem.* **1992**, *57*, 2606-2610.
- (2) Rubin, R. J.; Altman, W. M.; Mendelson, D. N. *J. of Clin. Endocrin. Metab.* **1994**, *78*, 809A-809F.
- (3) Keeton, W. T.; Gould, J. L. *Biological Science*; 4th Ed. ed.; W. W. Norton and Co. Inc.: New York, 1986.
- (4) Espinal, J. *Nature* **1987**, *328*, 574-575.
- (5) Stryer, L. *Biochemistry*; 3rd ed.; W.H. Freeman and Co.: New York, 1988.
- (6) Espinal, J. *Understanding Insulin Action*; Ellis Horwood Ltd.: Great Britain, 1989.
- (7) Posner, B. I.; Shaver, A.; Fantus, G. In *New Antidiabetic Drugs*; C. J. Bailey and P. R. Flatt, Ed.; Smith Gordon: London, 1990; pp 107-117.
- (8) Su, X.-D.; Taddei, N.; Stefani, M.; Giampietro, R.; Norlund, P. *Nature* **1994**, *370*, 575-578.
- (9) Stuckey, J. A.; Schubert, H. L.; Fauman, E. B.; Zhang, Z.-Y.; Dixon, J. E.; Saper, M. A. *Nature* **1994**, *370*, 571-575.
- (10) Barford, D.; Flint, A. J.; Tonks, N. K. *Science* **1994**, *263*, 1397-1404.
- (11) Zongchao, J.; Barford, D.; Flint, A. J.; Tonks, N. K. *Science* **1995**, *268*, 1754-1758.
- (12) Rachman, J.; Turner, R. C. *Diabetic Medicine* **1995**, *12*, 467-478.
- (13) De Pirro, R.; Pezzino, V. In *Receptor Biochemistry and Methodology*; J. C. Venter and L. C. Harrison, Ed.; Alan R. Liss Inc.: New York, 1988; Vol. 12B; pp 107-120.
- (14) Eliason, L.; Renström, E.; Ämmälä, C.; Beggren, P.-O.; Bertorello, A. M.; Bokvist, K.; Chibalin, A.; Deeney, J. T.; Flatt, P. R.; Gäbel, J.; Gromada, J.; Larsson, O.; Lindström, P.; Rhodes, C. J.; Rorsman, P. *Science* **1996**, *271*, 813-815.
- (15) Reach, G.; Wilson, G. S. *Anal. Chem.* **1992**, *64*, 381-386.
- (16) Ross, P. E. *Sci. Am.* **1993**, *268*, 18-22.

- (17) Lacy, P. E. *Sci. Am.* **1995**, 50-58.
- (18) Chale, S. S.; Swai, A. B. M.; Phare, G. M. M.; McLarty, D. G. *BMJ* **1992**, *304*, 1215.
- (19) Shisheva, A.; Shechter, Y. *Biochemistry* **1992**, *31*, 8059-8063.
- (20) Shisheva, A.; Gefel, D.; Shechter, Y. *Diabetes* **1992**, *41*, 982-988.
- (21) Ezaki, O. *J. Biol. Chem.* **1989**, *264*, 16118-16122.
- (22) Rehder, D. *Angew. Chem. Int. Ed. Engl.* **1991**, *30*, 148-167.
- (23) Mertz, W. *Science* **1981**, *213*, 1332-1338.
- (24) Press, R. I.; Geller, J.; Evans, G. W. *West. J. Med.* **1990**, *152*, 41-45.
- (25) Shechter, Y.; Karlish, S. J. D. *Nature* **1980**, *284*, 556-558.
- (26) Dubyak, G. R.; Kleinzeller, A. *J. Biol. Chem.* **1980**, *255*, 5306-5312.
- (27) Heyliger, C. E.; Tahiliani, A. G.; McNeill, J. H. *Science* **1985**, *227*, 1474-1477.
- (28) Pederson, R.; Ramanadham, S.; Bacham, A.; McNeill, J. *Diabetes* **1989**, *38*, 1390-1395.
- (29) McNeill, J.; Yuen, V. G.; Hoveyda, H.; Orvig, C. *J. Med. Chem.* **1992**, *35*, 1489-1491.
- (30) Kadota, S.; Fantus, I. G.; Deragon, G.; Guyda, H. J.; Posner, B. I. *J. Biol. Chem.* **1987**, *262*, 8252-8256.
- (31) Kadota, S.; Fantus, I. G.; Deragon, G.; Guyda, H. J.; Hersh, B.; Posner, B. I. *Biochem. Biophys. Res. Comm.* **1987**, 259-266.
- (32) Yale, J.-F.; Lachance, D.; Bevan, A. P.; Vigeant, C.; Shaver, A.; Posner, B. I. *Diabetes* **1995**, *44*, 1274-1279.
- (33) Cotton, F. A.; Wilkinson, G. *Advanced Inorganic Chemistry*; 4th Ed. ed.; John Wiley & Sons: Toronto, 1980, pp 1396.
- (34) Clark, R. J. H. *The Chemistry of Titanium and Vanadium. An Introduction to the Chemistry of the Early Transition Elements.*; Elsevier: New York, 1968, pp 329.

- (35) Butler, I. S.; Harrod, J. F. *Inorganic Chemistry. Principles and Applications*; Benjamin/Cummings Publishing Company Inc.: Redwood City, 1989, pp 721.
- (36) Kranz, M. In *Inorganic Syntheses*; J. Kleinberg, Ed.; McGraw-Hill Book Company, Inc.: Toronto, 1963; Vol. 7; pp 97-99.
- (37) Butler, A.; Clague, M. J.; Meister, G. E. *Chem. Rev.* **1994**, *94*, 625-638.
- (38) Chasteen, N. *Structure and Bonding* **1983**, *53*, 105-138.
- (39) Howarth, O. *Prog. NMR Spectrosc.* **1990**, *22*, 453-485.
- (40) Butler, A.; Eckert, H. *J. Am. Chem. Soc.* **1989**, *111*, 2802-2809.
- (41) Crans, D. C. *Comments Inorg. Chem.* **1994**, *16*, 1-33.
- (42) Crans, D. C.; Rithner, C. D.; Thiesen, L. A. *J. Am. Chem. Soc.* **1990**, *112*, 2901-2908.
- (43) Chasteen, N. D.; DeKoch, R. J.; Rogers, B. L.; Hanna, M. W. *J. Am. Chem. Soc.* **1973**, *95*, 1301-1309.
- (44) Pessoa, J. C.; Vilas Boas, L. F.; Gillard, R. D. *Polyhedron* **1990**, *9*, 2101-2125.
- (45) Dessi, A.; Micera, G.; Sanna, D. *J. Inorg. Biochem.* **1993**, *52*, 275-286.
- (46) Ferrer, E. G.; Williams, P. A. M.; Baran, E. J. *J. Inorg. Biochem.* **1993**, *50*, 253-262.
- (47) Williams, P. A. M.; Baran, E. J. *J. Inorg. Biochem.* **1992**, *48*, 15-19.
- (48) Laura Deakin is thanked for obtaining the EPR spectrum of this sample.
- (49) Butler, A.; Carrano, C. J. *Coordination Chemistry Reviews* **1991**, *109*, 61-105.
- (50) Macara, I. G. *Trends in Biochem. Sci.* **1980**, 92-94.
- (51) Butler, A.; Walker, J. V. *Chem. Rev.* **1993**, *93*, 1937-1944.
- (52) Colpas, G. J.; Hamstra, B. J.; Kampf, J. W.; Pecoraro, V. L. *J. Am. Chem. Soc.* **1994**, *116*, 3627-3628.
- (53) Colpas, G. J.; Hamstra, B. J.; Kampf, J. W.; Pecoraro, V. L. *J. Am. Chem. Soc.* **1996**, *118*, 3469-3478.
- (54) Szentivanyi, H.; Stomberg, R. *Acta Chem. Scand.* **1983**, *A37*, 709-714.

- (55) Bianchi, M.; Bonchio, M.; Conte, V.; Coppa, F.; Di Furia, F.; Modena, G.; Moro, S.; Standen, S. *J. Mol. Catal.* **1993**, *116*, 107-116.
- (56) Bonchio, M.; Conte, V.; Di Furia, F.; Modena, G. *J. Org. Chem.* **1989**, *54*, 4368-4371.
- (57) Sakurai, H.; Shimomura, S.; Fukuzawa, K.; Ishizu, K. *Biochem. Biophys. Res. Comm.* **1980**, *96*, 293-298.
- (58) Ramanadham, S.; Heyliger, C.; Gresser, M. J.; Tracey, A. S.; McNeill, J. H. *Biol. Trace Elem. Res.* **1991**, *30*, 119-124.
- (59) Caravan, P.; Gelmini, L.; Glover, N.; Herring, F. G.; Li, H. L.; McNeill, J. H.; Rettig, S. J.; Setyawati, I. A.; Shuter, E.; Sun, Y.; Tracey, A. S.; Yuen, V. G.; Orvig, C. *J. Am. Chem. Soc.* **1995**, *117*, 12759-12770.
- (60) McNeill, J. H.; Yuen, V. G.; Dai, S.; Orvig, C. *Mol. Cell. Biochem.* **1995**, *153*, 175-180.
- (61) Shechter, Y.; Shisheva, A.; Lazar, R.; Libman, J.; Shanzer, A. *Biochemistry* **1992**, *31*, 2063-2068.
- (62) Watanabe, H.; Masami, N.; Komazawa, K.; Sakurai, H. *J. Med. Chem.* **1994**, *37*, 876-877.
- (63) Unpublished results; Gerry Baquiran and Barry Posner.
- (64) Cornman, C. R.; Zovinka, E. P.; Meixner, M. H. *Inorg. Chem.* **1995**, *34*, 5099-5100.
- (65) Posner, B. I.; Faure, R.; Burgess, J. W.; Bevan, A. P.; Lachance, D.; Zhang-Sun, G.; Fantus, I. G.; Ng, J. B.; Hall, D. A.; Soo Lum, B.; Shaver, A. *J. Biol. Chem.* **1994**, *269*, 4596-4604.
- (66) Shaver, A.; Ng, J. B.; Hall, D. A.; Posner, B. I. *Mol. Cell. Biochem.* **1995**, *153*, 5-15.

Chapter 2. Synthesis and Characterization of Insulin-Mimetic Peroxovanadium Compounds.

2.1. Introduction

Peroxovanadium (pV) complexes have been reported as early as 1959¹ but the insulin-mimetic properties of pV compounds were not discovered until 1987.^{2,3} The synthesis of pV compounds is accomplished by a general procedure although modifications may be made to optimize specific reactions. Bisperoxovanadium compounds are prepared by addition of hydrogen peroxide to a basic aqueous solution of vanadium pentoxide forming a mixture of aquo pV complexes (i.e. $[\text{VO}(\text{O}_2)_2(\text{OH})_2]^{3-}$, $[\text{VO}(\text{O}_2)_2(\text{H}_2\text{O})(\text{OH})]^{2-}$; etc.). The appropriate bidentate ligand is then added to the mixture⁴ and alternately combinations of vanadium pentoxide and ancillary ligand have, in some cases, been dissolved in dilute peroxide followed by addition of base^{5,6} to give near neutral or slightly basic conditions.

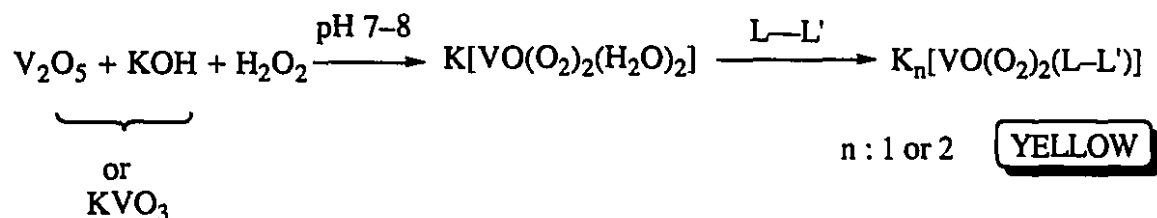
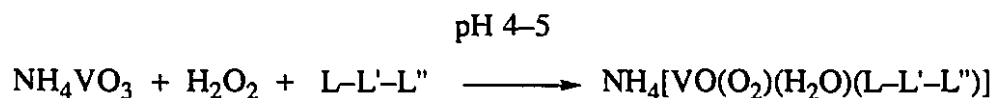


Figure 2.1.1. General synthetic scheme for the synthesis of bisperoxovanadium complexes. L-L' is a bidentate ligand such as bipyridine, phenanthroline, or picolinic acid and derivatives.

Monoperoxovanadium (mpV) complexes are usually synthesized from weakly acidic aqueous mixtures of ammonium metavanadate, hydrogen peroxide and the ancillary

ligand.⁷ Alternately mixtures of vanadium pentoxide and base have been used to generate the vanadate to which was added the ancillary ligand and hydrogen peroxide.⁸



RED

Figure 2.1.2. General synthetic scheme for the synthesis of monoperoxovanadium complexes. L-L'-L'' is a tridentate ligand such as 2,6-pyridinedicarboxylic acid.

Peroxovanadium compounds tend to decompose when recrystallization attempted. Generally high purity crystalline solids are collected by filtration of the reaction mixture after crystallization is induced by result of cooling, addition of alcohol, or evaporation. The difficulty in recrystallizing peroxovanadium compounds requires that reasonable yields of contaminant free compounds be obtained directly from the reaction.

Table 2.1.1 – A list of peroxovanadium compounds with their abbreviations, selected ⁵¹V NMR data and references to their preparation and X-ray structural determination, where available*

Abbrevn.	COMPLEX	δ (⁵¹ V) ^a	References (X-Ray)
bpV(phen)	K[VO(O ₂) ₂ (phen)]·3H ₂ O	-746	4
bpV(bipy)	K[VO(O ₂) ₂ (bipy)]·5H ₂ O	-747	4, (9)b
bpV(ox)	K ₃ [VO(O ₂) ₂ (ox)]·2H ₂ O	-739	4, 10, (11)
bpV(NH ₃)	NH ₄ [VO(O ₂) ₂ (NH ₃)]	-711, -748, -753	12, (13)
mpV(2,6-pdc)	NH ₄ [VO(O ₂)(2,6-pdc)(H ₂ O)]·H ₂ O	-598	1, (7)

* Updated version of table appearing in: *Cell. Biochem.* 1995, 153, 5-15.

Shaver, A.; Ng, J. B.; Hall, D. A.; Posner, B. I. *Mol. and*

mpV(pic)	$\text{VO}(\text{O}_2)(\text{pic})(\text{H}_2\text{O})_2$	-600	(14)
bpV(pic)	$\text{K}_2[\text{VO}(\text{O}_2)_2(\text{pic})] \cdot 2\text{H}_2\text{O}$	-744	15, (16)
bpV(Me ₂ phen)	$\text{K}[\text{VO}(\text{O}_2)_2(4,7\text{-Me}_2\text{phen})] \cdot 0.5\text{H}_2\text{O}$	-748	
mp(but)V(2,6-pdc)	$\text{VO}(\text{OO-Bu}^t)(\text{H}_2\text{O})(2,6\text{-pdc})$	-597	(17)
mpV(ox)	$\text{K}_3[\text{VO}(\text{O}_2)(\text{ox})_2] \cdot 0.5\text{H}_2\text{O}$	-592	(18)
mpV(picbipy)	$\text{VO}(\text{O}_2)(\text{pic})(\text{bipy}) \cdot \text{H}_2\text{O}$	-579	(19)
mpV(picphen)	$\text{VO}(\text{O}_2)(\text{pic})(\text{phen}) \cdot \text{H}_2\text{O}$	-581	
bpV(OHpic)	$\text{K}_2[\text{VO}(\text{O}_2)_2(3\text{-OHpic})] \cdot \text{H}_2\text{O}$	-741	(16)
bpV(Me ₄ phen)	$\text{K}[\text{VO}(\text{O}_2)_2(3,4,7,8\text{-Me}_4\text{phen})] \cdot 5\text{H}_2\text{O}$	-745	15
bpV[bipy(CO ₂ ⁻)]	$\text{K}_3[\text{VO}(\text{O}_2)_2\{\text{bipy-4,4'-(COO)}_2\}]$	-747	
bpV(CO ₃)	$\text{K}_3[\text{VO}(\text{O}_2)_2(\text{CO}_3)] \cdot 3\text{H}_2\text{O}$	-762	10, 5, (20)
bpV(2,3-pdc)	$\text{K}_3[\text{VO}(\text{O}_2)_2(2,3\text{-pdc})] \cdot 2\text{H}_2\text{O}$	-743	21
bpV(2,4-pdc)	$\text{K}_3[\text{VO}(\text{O}_2)_2(2,4\text{-pdc})] \cdot 3.25\text{H}_2\text{O}$	-743	(21)
bpV(2,5-pdc)	$\text{K}_3[\text{VO}(\text{O}_2)_2(2,5\text{-pdc})] \cdot 2\text{H}_2\text{O}$	-742	21
bpV(Mephen)	$\text{K}[\text{VO}(\text{O}_2)_2(5\text{-Mephen})] \cdot 2\text{H}_2\text{O}$	-743	
bpV(NH ₂ phen)	$\text{K}[\text{VO}(\text{O}_2)_2(5\text{-NH}_2\text{phen})] \cdot 0.5\text{H}_2\text{O}$	-744	
bpV(NO ₂ phen)	$\text{K}[\text{VO}(\text{O}_2)_2(5\text{-NO}_2\text{phen})] \cdot 2\text{H}_2\text{O}$	-739	(22)
mpV(OHpdcc)	$\text{NH}_4[\text{VO}(\text{O}_2)(\text{H}_2\text{O})(4\text{-OH-2,6-pdc})] \cdot \text{H}_2\text{O}$	-599	
bpV(acetpic)	$\text{K}_3[\text{VO}(\text{O}_2)_2(3\text{-acetpic})] \cdot 2\text{H}_2\text{O}$	-745	(21)
mpV(quin)	$\text{NH}_4[\text{VO}(\text{O}_2)(\text{isoquin})] \cdot 5\text{H}_2\text{O}$	-746	15
bpV(pzc)	$\text{K}_2[\text{VO}(\text{O}_2)_2(\text{pzc})] \cdot x\text{H}_2\text{O}$	-732	14
bpV(3-NH ₂ pzc)	$\text{K}_2[\text{VO}(\text{O}_2)_2(3\text{-NH}_2\text{pzc})] \cdot x\text{H}_2\text{O}$	-739	
mpV(ida)	$\text{M}[\text{VO}(\text{O}_2)(\text{IDA})] \cdot 0.5\text{H}_2\text{O}$; M: K, NH ₄		(23)
mpV(cit)	$\text{K}_2[\text{VO}(\text{O}_2)(\text{cit})_2] \cdot 2\text{H}_2\text{O}$	-541, -548	24
bpV(F)	$\text{M}_2[\text{VO}(\text{O}_2)_2\text{F}]$ (M: Na, K, Rb, Cs, NH ₄)		6, (25)
bpV(F ₂)	$(\text{NH}_4)_3[\text{VO}(\text{O}_2)_2\text{F}_2]$		26
mpV(EDTA)	$\text{M}_3[\text{VO}(\text{O}_2)(\text{EDTA})] \cdot 2\text{H}_2\text{O}$; M: Na, NH ₄		27
	$\text{H}[\text{VO}(\text{O}_2)(\text{H}_2\text{O})(2,6\text{-pdc})] \cdot \text{H}_2\text{O}$		28
mpV(HEDTA)	$\text{M}_2[\text{VO}(\text{O}_2)(\text{HEDTA})] \cdot 4\text{H}_2\text{O}$		29
bpV(acetate)	$\text{M}_2[\text{VO}(\text{O}_2)_2(\text{CH}_3\text{COO})]$	-705	30
	$\text{NH}_4[\text{VO}(\text{O}_2)_2(\text{bipy})] \cdot 4\text{H}_2\text{O}$		31
	$(\text{bipyH})[\{\text{VO}(\text{O}_2)_2(\text{bipy})\}_2] \cdot x\text{H}_2\text{O}_2 \cdot (6-x)\text{H}_2\text{O}$ (x:0.5)		(32)
	$(\text{bipyH})[\text{VO}(\text{O}_2)_2(\text{bipy})] \cdot (3+x)\text{H}_2\text{O}_2 \cdot (2-x)\text{H}_2\text{O}$ (x:0.4)		(33)
	$\text{PPh}_4[\text{VO}(\text{O}_2)(\text{pic})_2] \cdot \text{H}_2\text{O}$	-596 ^c	

	VO(O ₂)(quin)L (L: EtOH, DMF, DMSO, THF)		34
	M ₃ [VO(O ₂) ₂ (HPO ₄)]·2H ₂ O (M: K, NH ₄)		34
	K ₂ [V ₂ O ₂ (O ₂) ₃ (cystH) ₂]·H ₂ O		35
	M ₂ [V(O ₂) ₃ F] (M: Na, K, NH ₄)		36
	M[V(O ₂) ₃] (M: Na, K)		37
	Na ₃ [V(O ₂) ₄]·H ₂ O ₂ ·10.5H ₂ O *		(38)
	Na ₃ [V(O ₂) ₄]·14H ₂ O *		(38)
	NH ₄ [VO(O ₂)(malato)]·H ₂ O		27
	M[VO(O ₂)(malato)]·H ₂ O, M=Na, K, NH ₄ , Cs		(39)d
mpV(NTA)	Na ₂ [VO(O ₂)(NTA)]·5H ₂ O	-549	40
	K ₂ [VO(O ₂)(NTA)]		27, (8)
	K ₂ [VO(O ₂)(NTA)]·2H ₂ O		(41)
	Ba[VO(O ₂)(NTA)]·3H ₂ O		42
	M ₂ [VO(O ₂) ₂ Cl] (M: Na, K, NH ₄)		43
	M ₂ [V(O ₂) ₃ Cl] (M: Na, K, NH ₄)		43
	M[VO(O ₂) ₂ (glyH)]·H ₂ O (M: K, NH ₄)		44
bpV(H ₂ O)	K[VO(O ₂) ₂ (H ₂ O) _x] (x: 1 or 2)	-688 to -695	10, 45, 46
	(NH ₄) ₄ [VO(O ₂) ₂]·2O		47
	(NH ₄) ₃ [VO(O ₂) ₂]·2OH]·H ₂ O		48
	K ₂ [VO(O ₂) ₂]·2(μ-nicH)]·H ₂ O		49
	V ₂ O ₂ (O ₂) ₃ (glyH) ₂ (H ₂ O) ₂		44
	(NH ₄) ₅ [V ₂ O ₂ (O ₂) ₄ PO ₄]·H ₂ O		(50)
	K[VO(O ₂)(Hheida)]		(51)
	NE ₄ [VO(O ₂)(GlyGly)]·1.58H ₂ O		(52)
	K[VO(O ₂)ada]		(53)
	[VO(O ₂)tpa]ClO ₄		53
	[VO(O ₂)bpg]		(53)
	H[VO(O ₂)bpg] ₂ (ClO ₄)		(53)

* This report questions the claims made by Chaudhuri et al.^{36,37}. Won et al.³⁸ report being unable to reproduce the elemental analysis of compounds synthesized exactly as reported by Chaudhuri et al.^{36,37} and suggest they may be impure samples of a tetraperoxovanadate species.

^a All ⁵¹V NMR spectra were obtained on aqueous solutions on a Varian XL-300 NMR spectrometer operating at 78.891 MHz. Chemical shifts are in parts per million (ppm) with respect to VOCl₃ as external reference at 0.00 ppm, with negative shifts being upfield.

^b X-ray of NH₄⁺ salt.

^c In CD₃OD.

^d X-ray of dimer, NH₄⁺ salt

Abbreviations

phen	1,10-phenanthroline
4,7-Me ₂ phen	4,7-dimethyl-1,10-phenanthroline
3,4,7,8-Me ₄ phen	3,4,7,8-tetramethyl-1,10-phenanthroline
5-CH ₃ phen	5-methyl-1,10-phenanthroline
5-NO ₂ phen	5-nitro-1,10-phenanthroline
5-NH ₂ phen	5-amino-1,10-phenanthroline
bipy	2,2'-bipyridine
bipyH	2,2'-bipyridinium
4,4'-Me ₂ bipy	4,4'-dimethyl-2,2'-bipyridine
bipy-4,4'-(COO) ₂	2,2'-bipyridine-4,4'-dicarboxylato
pic	pyridine-2-carboxylato
3-OHpic	3-hydroxypyridine-2-carboxylato
3-acetpic	3-acetoxypyridine-2-carboxylato
m,n-pdc	pyridine-m,n-dicarboxylato
ox	oxalato
pzc	pyrazine-2-carboxylato
3-NH ₂ pzc	3-aminopyrazine-2-carboxylato
4OH-2,6pdc	4-hydroxy-2,6-pyridinedicarboxylato
IDA	iminodiacetato
cit	citrato
EDTA	ethylenediaminetetraacetato
HEDTA	ethylenediaminetetraacetic acid
isoquin	isoquinoline-2-carboxylato
quin	quinolato
NTA	nitrilotriacetato
glyH	glycine
cystH	cysteine
nicH	nicotinic acid
Hheida	N-(2-hydroxyethyl)iminodiacetato

GlyGly	glycylglycine
ada	<i>N</i> -(2-amidomethyl)iminodiacetato
tpa	<i>N,N,N</i> -tris(2-pyridylmethyl)amine
bpg	<i>N,N</i> -bis(2-pyridylmethyl)glycine

There have been reports of pV compounds having antitumor activity against L1210 murine leukemia in mice.²⁷ The tests also served to determine the toxicity of these compounds.²⁷ The mechanism by which these compounds exert their antitumor activities has not been elucidated. Djordjevic et al. have speculated that the pV compounds could undergo a one electron intramolecular reduction (V(V) to V(IV)) and oxidize a peroxide to superoxide.²⁷ This might be related to the antitumor activity of pV compounds by altering the free radical character within the cell.²⁷ The catalytic oxidative, epoxidative, and hydroxylative abilities of pV complexes are also noted as properties that may be responsible for their antitumor activities.²⁷

Djordjevic and Wampler tested the antitumor activity of 11 peroxovanadium compounds and three vanadate compounds.²⁷ The structures varied in the number of peroxo ligands, the ancillary ligand, and counter ion.²⁷ The antitumor activity and toxicity of the peroxovanadium compounds was dependent on the type of ancillary ligand.²⁷ Differences in activity related to the type of counter ion present were also observed (potassium versus ammonium salts) in four pairs of complexes.²⁷ Therefore it was reasonable to assume that the insulin-mimetic properties of pV compounds might also be dependent on the nature of the complex.

The large number of pV compounds previously reported served as starting point for studies of the insulin mimetic properties of pV and other peroxometal compounds.⁵⁴ In order to extend these studies the synthesis of peroxovanadium compounds comprising two series of compounds differing only in the structure of their ancillary ligand was planned. In this way the effects of ancillary ligand structure on insulin mimetic activity could be

better probed. The ligand chosen was picolinic acid as the bpV(pic) compound had been shown to be a potent insulin mimic.⁵⁴

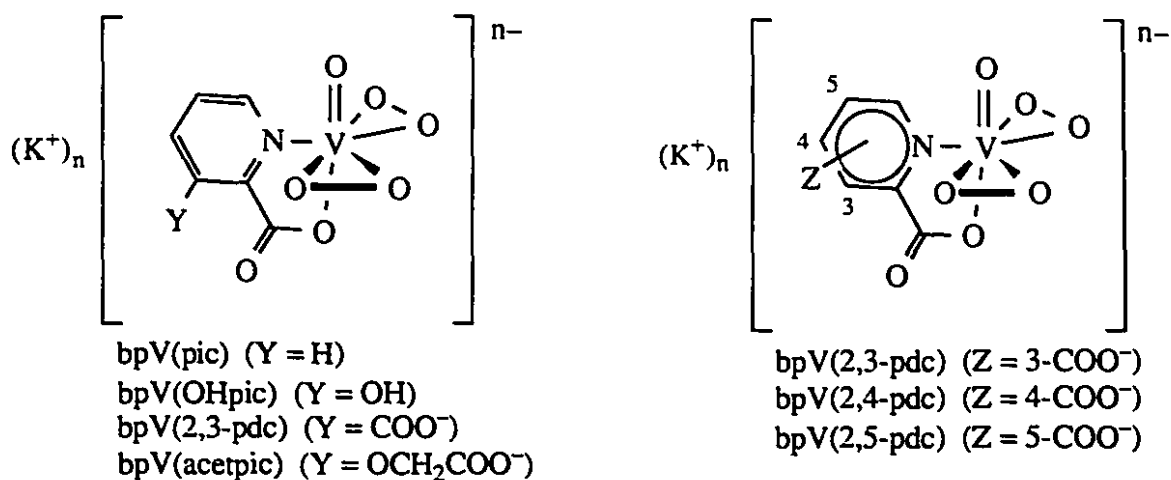


Figure 2.1.3. Two series of pV compounds with substituted picolinic acid ligands.

A monoperoxovanadium complex, mpV(2,6-pdc), whose crystal structure as a ammonium salt had been determined⁷ was recrystallized as the guanidinium salt and also as the potassium salt. The antitumor activities of the complexes reported by Wampler et al. varied with differing counter ions.²⁷ The guanidinium salt of mpV(2,6-pdc) was prepared and characterized crystallographically in hopes that if an assay of the PTPase activity of mpV(2,6-pdc) complexes with different counter ions showed differing reactivity that this could be related to differences in solid state structure.

2.2. Results and Discussion

2.2.1. Syntheses

The syntheses of the bpV complexes were accomplished with varying yields as shown in Table 2.2.1 although all syntheses gave pure products. The yields of the

bpV(acetpic) and bpV(2,4-pdc) were low, probably due to loss of product discarded with insoluble vanadates that were precipitated initially. The precipitation of insoluble vanadates rather than the desired product is often a problem in these syntheses. The amount of insoluble vanadates produced can sometimes be minimized by control of pH and optimization of the amount of ethanol added to induce precipitation. All products were collected as yellow powders or crystals. A strong singlet was observed in the ^{51}V NMR spectra of these compounds. An additional much weaker peak was observed at approximately -700 ppm which was attributed to an aquo bpV anion formed by dissociation of the ancillary ligand.⁵⁵ The ^1H NMR were consistent with this showing roughly the same proportions of bound and unbound ligand.

Table 2.2.1. Yields of the syntheses of bpV complexes.

Complex	Yield (%)
bpV(OHpic)	81
bpV(2,3-pdc)	67
bpV(2,4-pdc)	57
bpV(2,5-pdc)	93
bpV(acetpic)	34

Although the pV compounds described above have shown no tendency to decompose rapidly or explode even upon grinding (for KBr IR samples) or ignition (flame tests) it must be kept in mind that these compounds contain an intimate mixture of oxidant (peroxo ligands) and "fuel" (organic ligands) and there is potential for an explosive reaction. Attempts to synthesize the neutral monoperoxovanadium compound $\text{VO}(\text{O}_2)(\text{OHpic})(\text{H}_2\text{O})_2$ were unsuccessful as a result of a sudden, unpredictable and violent decomposition of the reaction mixture. A similar compound, $\text{VO}(\text{O}_2)(\text{pic})(\text{H}_2\text{O})_2$, has been reported to decompose excess hydrogen peroxide in acidic aqueous solution

through a radical chain mechanism after a brief induction period.⁵⁶ It is likely that a similar mechanism was responsible for the violent decomposition of $\text{VO}(\text{O}_2)(\text{OHpic})(\text{H}_2\text{O})_2$. Rotary evaporation of the reaction mixtures for the synthesis of pV compounds should be carried out with extreme care and never allowed to proceed to dryness due to the presence of hydrogen peroxide.

2.2.2. Structural Features

2.2.2.a. bpV Complexes

Single crystal X-ray structures of three representative members of the two series of bpV picolinato based compounds, bpV(OHpic) (Figure 2.2.1), bpV(2,4-pdc) (Figure 2.2.2) and bpV(acetpic) (Figure 2.2.3) were obtained. All three compounds crystallized as yellow solids. The X-ray structures showed similar coordination about the vanadium centre with six oxygen atoms and one nitrogen atom in the inner coordination sphere in the three compounds. The bpV(2,4-pdc) structure contained 4 molecules in the asymmetric unit and consequently the bond lengths and angles reported in tables 2.2.2 and 2.2.3 are averages of these four molecules. There were some slight variations in some of the lengths and angles from one molecule to the other that presumably were the result of crystal packing forces. Full tables of bond lengths and angles, crystallographic parameters, atomic parameters, thermal factors and least squares planes (where appropriate) are included in the appendices.

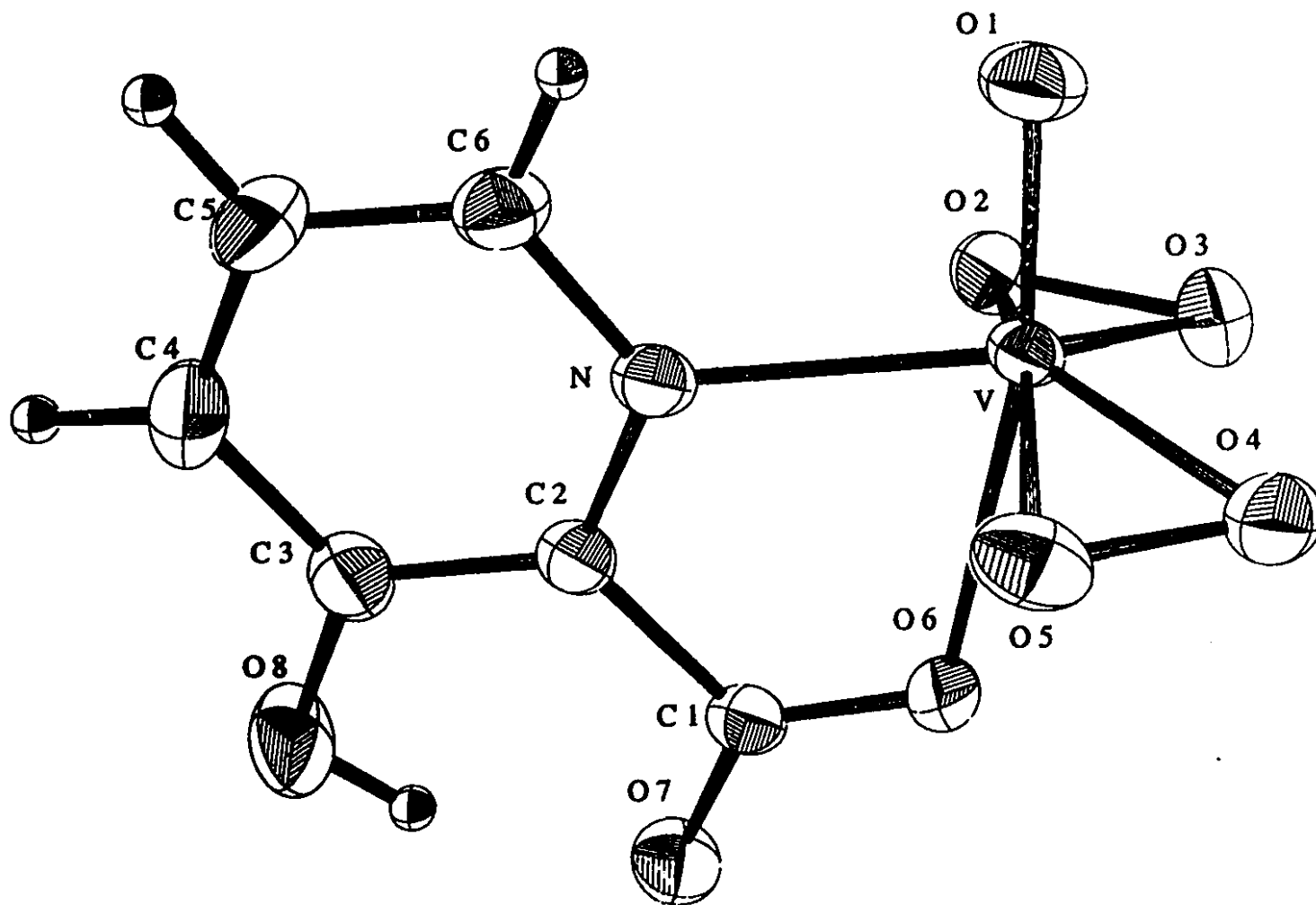


Figure 2.2.1. ORTEP diagram of $K_2[VO(O_2)_2(OHpic)] \cdot 2H_2O$, $R=2.3\%$, $R_w=2.8\%$

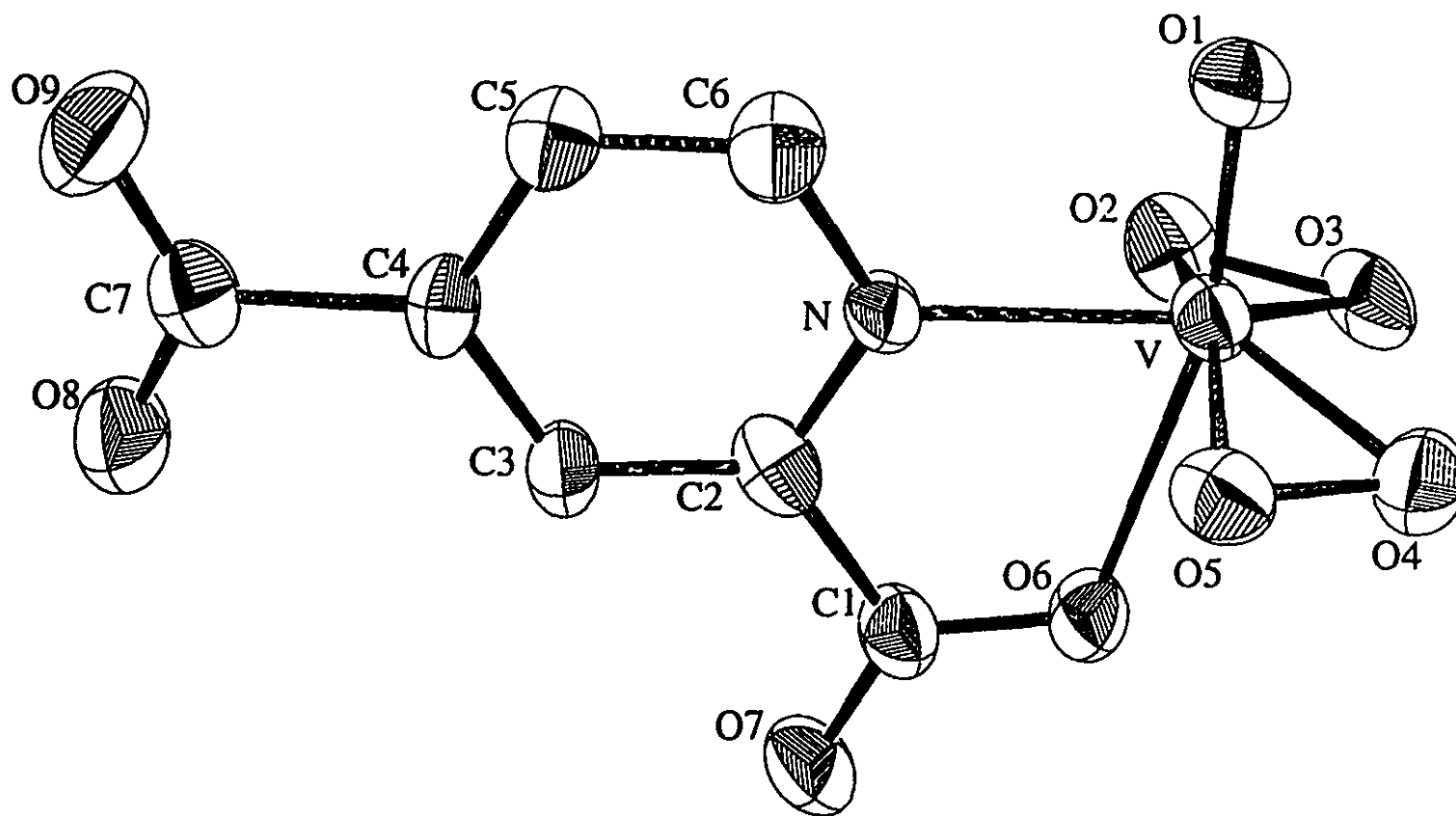


Figure 2.2.2. ORTEP diagram of $K_3[VO(O_2)_2(2,4\text{-pdc})] \cdot 3.25 H_2O$, $R=4.9\%$, $R_w=5.5\%$

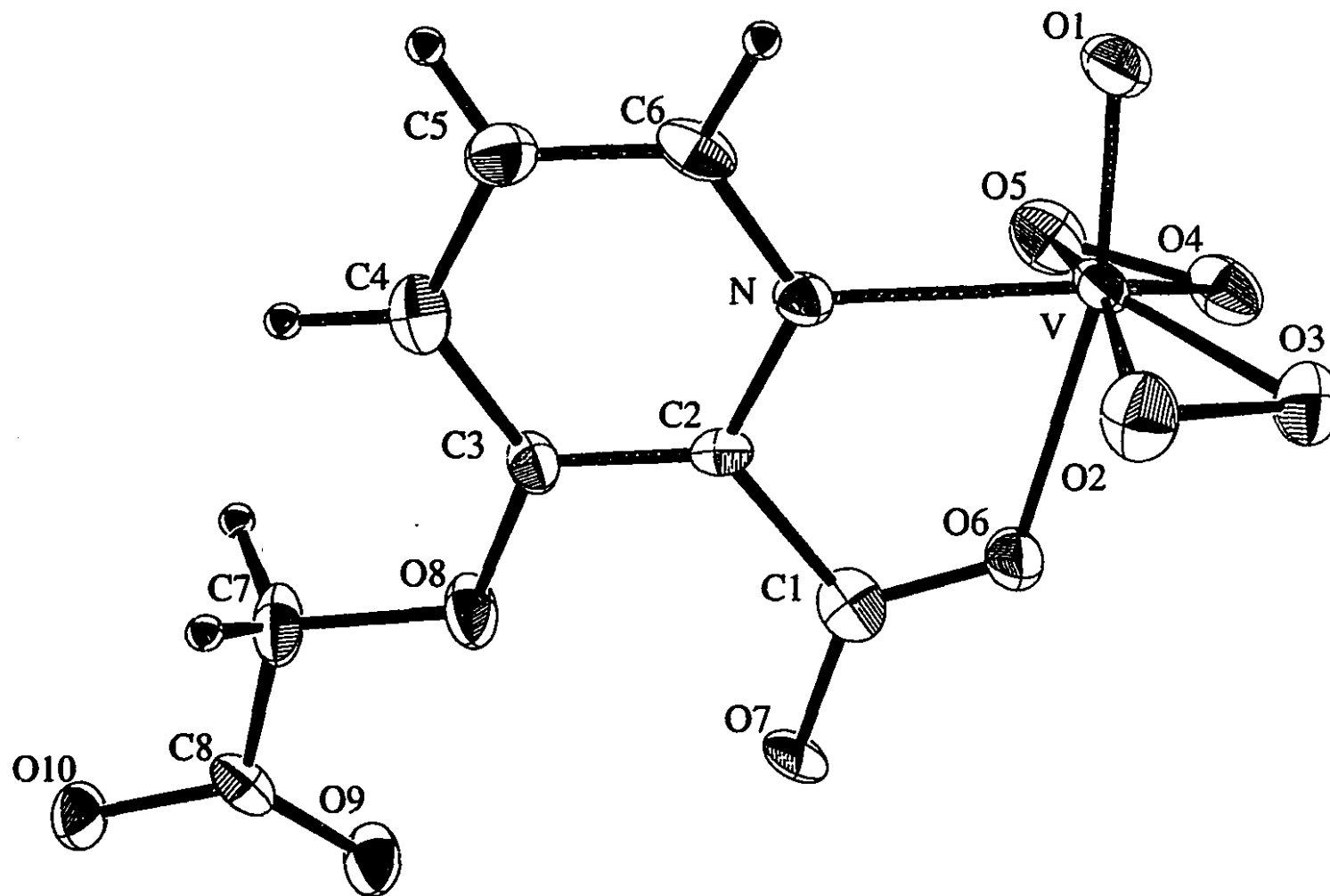


Figure 2.2.3. ORTEP diagram of $K_3[VO(O_2)_2(\text{acetpic})] \cdot 2H_2O$, $R=3.6\%$, $R_w=2.6\%$

Table 2.2.2. Selected bond lengths for bpV(OHpic), bpV(2,4-pdc), and bpV(acetpic).

	bpV(OHpic)	bpV(2,4-pdc) (average)	bpV(acetpic)
Atoms	Distance (Å)	Distance (Å)	Distance (Å)
V-O(1)	1.606(2)	1.622(9)	1.621(3)
V-O(2)	1.924(2)	1.913(10)	1.917(4)
V-O(3)	1.902(2)	1.875(9)	1.866(4)
V-O(4)	1.877(2)	1.862(10)	1.878(4)
V-O(5)	1.908(2)	1.909(10)	1.941(4)
V-O(6)	2.314(2)	2.300(9)	2.190(3)
V-N	2.137(2)	2.144(11)	2.179(4)
O(2)-O(3)	1.463(2)	1.460(14)	1.461(5)
O(4)-O(5)	1.461(2)	1.452(13)	1.480(5)
O(6)-C(1)	1.247(3)	1.279(17)	1.264(6)
O(7)-C(1)	1.268(2)	1.243(17)	1.233(6)
C(1)-C(2)	1.497(3)	1.509(20)	1.516(7)

Table 2.2.3. Selected bond angles for bpV(OHpic), bpV(2,4-pdc), and bpV(acetpic).

	bpV(OHpic)	bpV(2,4-pdc) (average)	bpV(acetpic)
Atoms	Angle (°)	Angle (°)	Angle (°)
O(1)-V-O(2)	98.76(8)	100.2(5)	98.32(17)
O(1)-V-O(3)	101.56(8)	102.3(5)	103.39(17)
O(1)-V-O(4)	103.17(7)	102.4(5)	104.84(17)
O(1)-V-O(5)	101.43(8)	99.2(5)	97.78(17)
O(1)-V-O(6)	168.73(7)	166.3(4)	166.04(15)
O(1)-V-N	94.92(7)	93.1(4)	93.39(16)
O(2)-V-N	84.76(6)	87.8(4)	89.97(15)
O(2)-V-O(3)	44.95(7)	45.3(4)	45.41(15)
O(3)-V-O(4)	90.14(7)	89.1(5)	88.04(16)
O(4)-V-O(5)	45.40(7)	45.3(4)	45.56(15)
O(5)-V-N	88.59(7)	87.2(4)	85.59(15)

The crystal structures of bpV(OHpic) (Figure 2.2.1), bpV(2,4-pdc) (Figure 2.2.2) and bpV(acetpic) (Figure 2.2.3) all show similar coordination about the vanadium centre. If each peroxide ligand is considered to occupy two coordination sites then the complexes can be described as distorted pentagonal bipyramids (or trigonal bipyramids if the peroxo ligands are considered to occupy 1 coordination sites each). In all three structures the oxo group (O1) and a carboxylato oxygen (O6) occupy the axial positions*. The pentagonal

* Refer to ORTEP diagrams (figure 2.2.1, 2.2.2, or 2.2.3) for numbering scheme.

plane is defined by the two peroxo ligands and the nitrogen atom. In all three structures the V-O distances for cis-peroxo atoms (O2 and O5) is on average less than for the trans-peroxo atoms (O3 and O4) (see Figure 2.2.4 for a diagram identifying the cis and trans peroxo oxygen atoms) consistent with a survey of structures by Butler et al.⁵⁷

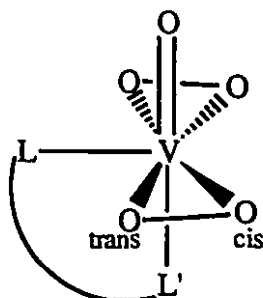


Figure 2.2.4. Diagram identifying cis and trans peroxo atoms in a bpV complex⁵⁷.

In the bpV(OHpic) structure there is an intramolecular hydrogen bond between the hydroxyl hydrogen HO(8) and carboxylate oxygen O(7) (Figure 2.2.1). In the bpV(2,4-pdc) structure (Figure 2.2.2), the 2,4-pdc ligand is planar, with O(8) being on average the farthest away from the plane of the pyridine ring (range 0.14(2)-0.33(2) Å). As can be seen in Figure 2.2.3 the acetpic ligand also exhibits a high degree of planarity. The plane formed by the acetatoxy moiety (C(7), C(8), and O(8)) is tilted only 10.0° from the plane formed by the rest of the ligand and the vanadium atom. These observations are for the compounds in the solid state and some of the bond lengths and angles are no doubt influenced by crystal packing forces. In solution, free rotation and flexibility of conformation about the pendant acetpic moiety and the 4-carboxylate of the 2,4-pdc ligand would be expected.

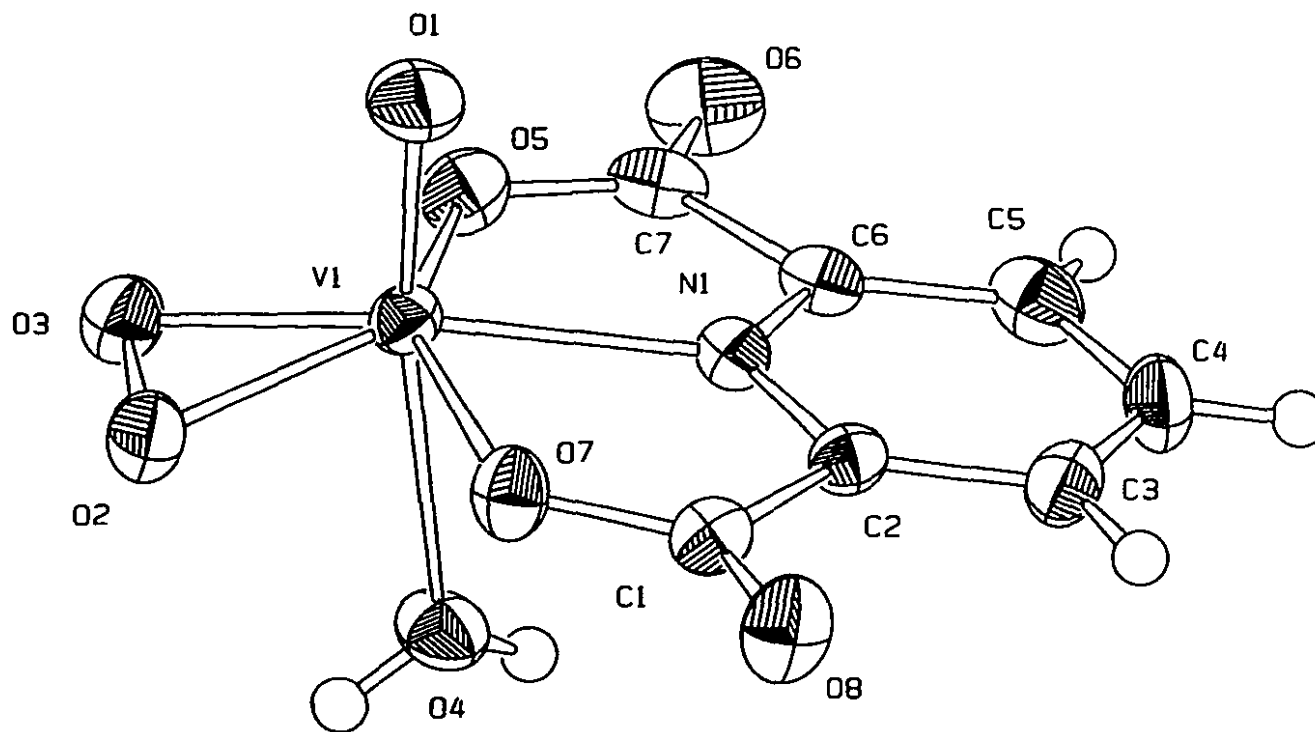


Figure 2.2.4. ORTEP diagram of $C(NH_2)_3[VO(O_2)(2,6-pdc)(H_2O)] \cdot H_2O$; $R=3.4\%$ $R_w=4.3\%$

2.2.2.b GmpV(2,6-pdc).

The structure of GmpV(2,6-pdc) (Figure 2.2.4) showed a seven coordinate trigonal bipyramidal geometry⁷ with the inner coordination sphere comprised of 6 oxygen atoms and one nitrogen atom. Selected bond lengths and angles are given in tables 2.2.4 and 2.2.5.

The structure of the GmpV(2,6-pdc) is similar to that of the mpV(2,6-pdc) with only slight differences. The 2,6-pdc ligand in the GmpV(2,6-pdc) structure is angled away from the vanadyl oxygen atom (O(1)). The O(1)-V-N(1) angle is 4.7° greater than in the mpV(2,6-pdc) structure and the O(4)-V-N(1) angle 4.8° less.⁷ This shift in the 2,6-pdc ligand may be due to crystal packing forces exerted on the ligand by the guanidinium counterion which is positioned above the 2,6-pdc ligand on the vanadyl oxygen atom (O(1)) side of the molecule. There is also a lengthening of one of the peroxo bonds (V-O(3)) in the GmpV(2,6-pdc) structure. This is unusual as most monoperoxo compounds have symmetrical peroxo bond lengths.⁵⁷ The lengthening may be due in part to the hydrogen bonds to the O(3) atom.

Table 2.2.4. Selected bond lengths for GmpV(2,6-pdc) and the analogous bond lengths for mpV(2,6-pdc)⁷

	GmpV(2,6-pdc)	mpV(2,6-pdc)
Atoms	Distance (Å)	Distance (Å)
V-O(1)	1.590(2)	1.579(2)
V-O(2)	1.871(2)	1.870(2)
V-O(3)	1.901(2)	1.872(2)
V-O(4)	2.289(2)	2.211(2)
V-O(5)	2.045(2)	2.053(2)
V-O(7)	2.042(2)	2.064(2)
V-N(1)	2.069(2)	2.088(2)
O(2)-O(3)	1.445(3)	1.441(3)
O(5)-C(7)	1.294(4)	1.280(4)
O(6)-C(7)	1.217(4)	1.233(4)
O(7)-C(1)	1.285(3)	1.288(4)
O(8)-C(1)	1.228(4)	1.223(4)
C(1)-C(2)	1.501(4)	1.505(4)
C(6)-C(7)	1.504(4)	1.498(4)

Table 2.2.5. Selected bond angles for GmpV(2,6-pdc) and the analogous bond angles for mpV(2,6-pdc)⁷

	GmpV(2,6-pdc)	mpV(2,6-pdc)
Atoms	Angle (°)	Angle (°)
O(1)-V-O(2)	103.5(1)	102.3(1)
O(1)-V-O(3)	102.1(1)	101.9(1)
O(1)-V-O(4)	172.0(1)	172.1(1)
O(1)-V-O(5)	94.5(1)	94.9(1)
O(1)-V-O(7)	94.3(1)	96.2(1)
O(1)-V-N(1)	96.9(1)	92.2(1)
O(2)-V-O(3)	45.05(9)	45.3(1)
O(2)-V-O(4)	84.13(9)	85.4(1)
O(2)-V-N(1)	149.03(9)	152.8(1)
O(3)-V-O(4)	84.91(9)	84.8(1)
O(3)-V-N(1)	149.03(9)	153.(1)
O(4)-V-N(1)	75.17(9)	80.0(1)
O(5)-V-N(1)	74.91(9)	74.3(1)
O(7)-V-N(1)	74.86(8)	74.5(1)

The GmpV(2,6-pdc) structure showed a number of hydrogen bonding interactions. The peroxo ligand (atoms O(2) and O(3)) is involved in hydrogen bonding interactions with both the guanidinium counter ion and the coordinated water molecule of another GmpV(2,6-pdc) unit. Other hydrogen bond interactions and close contacts are given in Table 2.2.6 and illustrated in Figure 2.2.5.

Table 2.2.6. Hydrogen bonding interactions for GmpV(2,6-pdc)

Atom	Atom	Distance (Å)	Symmetry Operation ^a
O(4)	O(8)	2.804(3)	$1/2-x, y-1/2, 1/2-z$
O(2)	N(4)	2.912(4)	$x-1/2, 1/2-y, z-1/2$
O(6)	N(4)	3.051(4)	$-1/2+x, -1/2-y, -1/2+z$
O(6)	N(2)	2.959(5)	$-1/2+x, -1/2-y, -1/2+z$
O(4)	O(W)	3.061(4)	$-x+1, -y, -z+1$
O(3)	N(3)	3.050(4)	$x-1/2, 1/2-y, z-1/2$
O(3)	O(4)	2.869(3)	$-x, -y, -z$
O(1)	O(W)	3.207(4)	$x-1/2, 1/2-y, z-1/2$
O(6)	O(W)	2.985(4)	$3/2-x, -1/2+y, 1/2-z$

^aSymmetry operations refer to the second atom listed

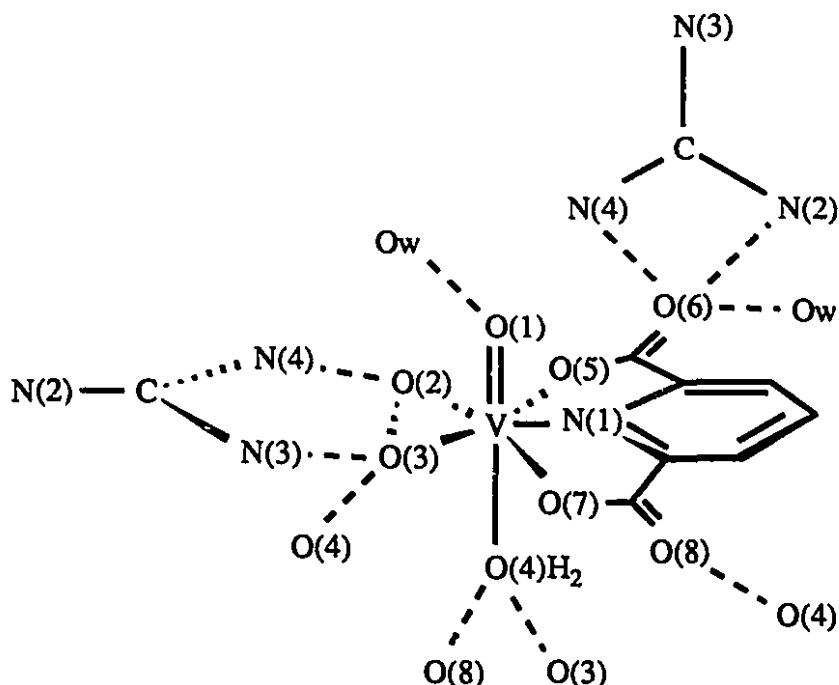


Figure 2.2.5. Hydrogen bonding interaction in the solid state structure of GmpV(2,6-pdc). Refer to Table 2.2.6 for symmetry transformations.

2.2.3 Biological Activity

Assays of the PTP inhibition activity of the two picolinate based series of pV compounds were carried out and the results are summarized in Table 2.2.7.

Table 2.2.7. The percent inhibition of PTP by various pV compounds. Errors correspond to the standard deviation.⁵⁸

Series #1		Series #2	
Complex	PTP inhibition at 10 ⁻⁷ M (%)	Complex	PTP inhibition at 10 ⁻⁷ M (%)
bpV(pic)	89.4 ± 4.2	bpV(2,3-pdc)	83.7 ± 4.5
bpV(OHpic)	91 ± 22	bpV(2,4-pdc)	81.7 ± 9.1
bpV(2,3-pdc)	83.7 ± 4.5	bpV(2,5-pdc)	82 ± 23
bpV(acetpic)	66 ± 13		

Two distinct series of pV compounds can be defined when the compounds whose syntheses are reported above are combined with the parent compound bpV(pic).^{15,16} As was discussed in the introduction, insulin exerts its metabolic effect by binding to the IRK. Once activated by insulin the IRK is thought to remain catalytically active until a PTP dephosphorylates key catalytic tyrosine residues. Inhibition of PTP would thus result in a much enhanced IRK activity. It is through the inhibition of PTP that pV compounds are thought to exert their insulin mimetic effect.⁵⁹ Assays of PTP inhibition are carried out by labeling the insulin receptor of rat liver endosomes with ³²P and, after incubation with or without inhibitors, measuring the loss of radioactivity from the insulin receptor.⁵⁴ Thus PTP inhibition assays provide a means by which the insulin mimetic properties of pV compounds can be quantified. Assays of PTP inhibition by the compounds comprising the two series are summarized in Table 2.2.7.

The PTP inhibition data for the picolinate derivatives indicate that there is little difference within or between the two series of peroxovanadium compounds. When

comparing substitution at the 3 position the bpV(acetpic) complex shows a slight decrease in activity relative to the bpV(pic) complex and bpV(2,3-pdc) complex. The large error on the determination of activity of the bpV(OHpic) complex makes a comparison of activity difficult, although the activity of the bpV(acetpic) and bpV(OHpic) agree within errors they barely do so. Similarly the series comprised of bpV(2,3-pdc), bpV(2,4-pdc), and bpV(2,5-pdc) shows no difference in activity as a result of the substitution of a carboxylate group around the pyridine ring. The complex of the 2,6-pdc ligand is not included in the series as the tridentate chelation of the ligand results in a monoperoxo complex.⁷

There are however differences in reactivity within other series of pV compounds. A similar study was carried out on a series of pV compounds with phen based ancillary ligands (Figure 2.2.6). In these studies the effect of the addition of methyl groups to the phen ring was investigated. A significant reduction in PTP inhibition was observed depending on the number and location of methyl groups. The 4,7-Me₂phen derivative was approximately one half as active as the phen complex and the 3,4,7,8-Me₄phen roughly one fifth as active.⁵⁴ A second study of the phen system in which various substituents were substituted at the 5 position was also carried out.⁶⁰ The compounds in this series show roughly the same level of PTP inhibition as the phen complex (Table 2.2.8). Also studied were the bpV(bipy) and bpV(4,4'-bipy(CO₂⁻)₂) complexes.⁵⁴ Assays of PTP inhibition by the two compounds show that the pV complex of the bipy carboxylated at the 4 and 4' positions is roughly 1/3 as potent as the bipy complex.⁵⁴

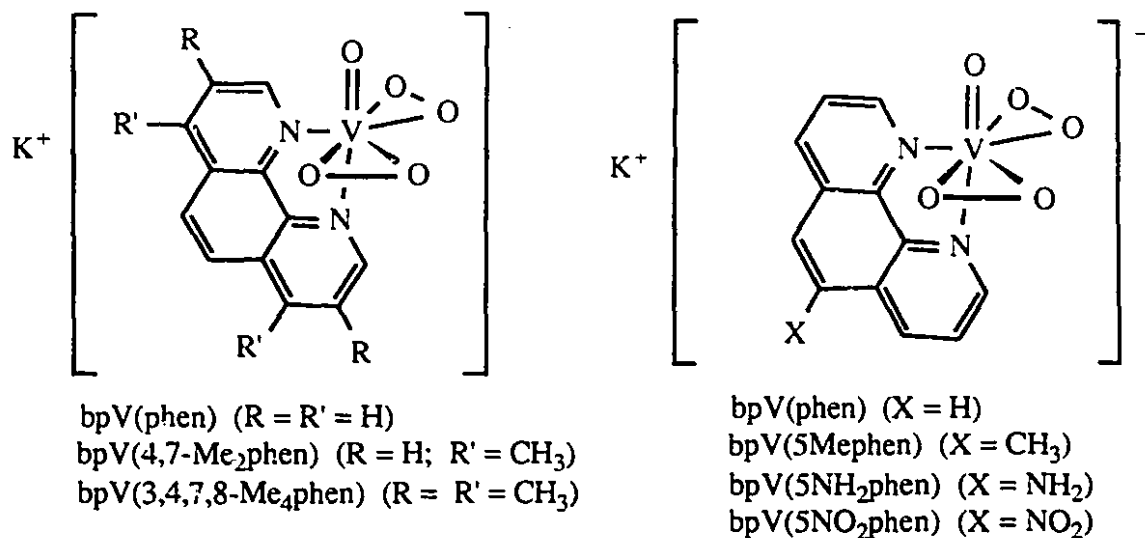


Figure 2.2.6. Two series of phenanthroline based pV complexes.

Table 2.2.8. The percent inhibition of PTP by various pV compounds. Errors correspond to the standard deviation.⁵⁸

Series #1		Series #2	
Complex	PTP inhibition at 10 ⁻⁷ M (%)	Complex	PTP inhibition at 10 ⁻⁷ M (%)
bpV(phen)	74 ± 12	bpV(phen)	74 ± 12
bpV(4,7-Me ₂ phen)	33.2 ± 4.7	bpV(5-Mephen)	81 ± 23
bpV(3,4,7,8-Me ₄ phen)	20.9 ± 3.5	bpV(5-NH ₂ phen)	73 ± 32
		bpV(5-NO ₂ phen)	79 ± 46

The natural substrate for PTPs is a phosphotyrosine containing peptide.

Phosphotyrosine and pV complexes are structurally similar. Taking as an example a picolinate pV complex we can compare the structures of phosphotyrosine and pV: 1. both have a hydrophobic aromatic ring, 2. the phosphotyrosine has a phosphorus atom in the 5+ oxidation state that is highly oxygenated and the pV compound has a vanadium atom in the

5+ state that is also highly oxygenated. Trigonal bipyramidal vanadium complexes have been identified as potentially acting as transition state analogs for the hydrolysis of phosphate esters.⁶¹ The structural similarities between pV's and phosphotyrosine makes pV compounds a likely substrate analog for PTP.

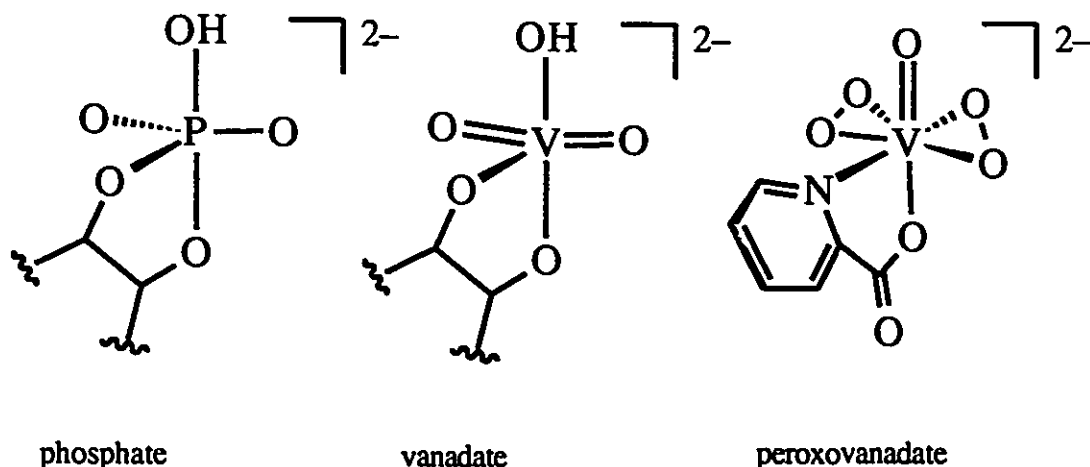


Figure 2.2.7. Structural similarity between phosphate and vanadate esters and a peroxovanadium complex.^{62,63}

Recent crystallographic studies have shown that the binding of phosphotyrosine occurs in a deep recognition pocket.⁶⁴ Presumably a peroxovanadium compound that is excessively bulky would be a poor substrate for PTP as it would not be able to fit into the binding pocket. The phenanthroline series of pV complexes is very sensitive to the addition of methyl groups at the 3,4,7 and 8 positions while substitutions at the 5 position seem to have little effect on activity. A possible explanation for these differences in activity is an increase in steric bulk on the ligand resulting in poorer binding to the enzyme. The phen ligand is more sterically demanding than is the pic ligand and the addition of methyl groups in the 3,4,7 or 8 positions may introduce sufficient bulk to interfere with binding to PTP. pV complexes of phen derivatives functionalized at the 5 position are sterically less demanding as the substituent would be pointing away from the binding pocket. The natural

substrate for PTP is a phospho-tyrosine polypeptide. The phospho-tyrosine is thought to point into the active site recognition pocket with the polypeptide pointing away from the active site. Thus a substituent in the 5 position of phen would be positioned similarly to the polypeptide chain of the natural substrate and accordingly its steric bulk would be of no consequence. Further, the electronic nature of the substituent at the 5 position appears to have no effect on the activity. Substitution with either polar (5-NH₂phen, 5-NO₂phen) or nonpolar (5-Mephen) substituents appears to be irrelevant to activity. The PTP activities of two bipy complexes (bpV(bipy) and bpV((4,4'-bipy(CO₂⁻)₂)) indicate that the addition of bulky substituents in these positions, polar or nonpolar can lead to loss in activity. The increase in the charge on anion from -1 to -3 is unlikely to be the cause of this effect as other trivalent anionic pV compounds such as bpV(ox) show high levels of PTP inhibition.⁵⁴ Likewise there is no significant difference in activity between bpV(pic) which is dianionic and bpV complexes of 2,3-, 2,4- and 2,5-pdc which are trianionic.

The smaller picolinate ligand appears to be less sensitive to substitution, although the bpV(acetpic) was marginally less active than other picolinate complexes. This may be due to the pendant acetatoxy moiety being bulky enough to interfere with binding to PTP. Substitutions at the 4 position of the picolinate ring would presumably have less effect than at other positions as the substituents would be pointing out of the binding pocket of the enzyme. The relative insensitivity of the picolinate system to substitution and the insensitivity of the phenanthroline system to substitutions at the 5 position provides a possible route for the modification of ligands with large biogenic groups that could act to facilitate uptake or bioavailability.

The specificity of PTP1B is thought to be dependent on binding not to the phosphotyrosine alone but also as a result of binding of the phosphotyrosine side chain.⁶⁴ Binding of a phosphotyrosine substrate results in conformational changes in PTP1B (this

also occurs in *Yersinia* PTP upon binding (ungstate).⁶⁴ In the unliganded native conformation the active site of the enzyme is essentially closed but upon binding of phosphotyrosine or a phosphopeptide the active site opens as a result of a shift in the surface loop⁶⁴ consisting of residues Trp¹⁷⁹-Ser¹⁸⁷. The additional specificity and binding affinity that is conferred through interactions between the PTP and side chain amino acids may potentially be exploited in the design of pV compounds. The modification of phenanthroline ligands at the 5 position or picolinate ligands at the 4 position may provide a route by which this specificity and increased binding affinity may be accomplished. It has yet to be determined however if this structural change in the PTP may be induced by the binding of pV compounds.

2.4. Conclusions

The synthesis and characterization of 5 new pV complexes has been accomplished including the single crystal X-ray structures of three representative complexes. All of the complexes show a high level of insulin mimetic activity when tested *in vitro*. The compounds can be grouped to define two different series of complexes varying in the structure of the picolinate based ancillary ligand. The first series consisted of complexes in which different functional groups were substituted at the 3 position of the picolinate ligand. The second series was comprised of a series of picolinate based pV complexes in which carboxylate groups were substituted at the 3, 4, and 5 positions. Despite the differences in the structure of the ligands their pV complexes all showed very similar insulin mimetic activity as quantified by PTP inhibition assays. This was in contrast to previous studies of complexes based on the phenanthroline ligand and to a lesser degree to studies on the bipyridine ligand. The phenanthroline system was found to be sensitive to the substitution of methyl groups at the 3, 4, 7 and 8 positions but not to substitutions at the 5 position regardless of the nature of the substituent. The bipyridine was shown to be sensitive to substitutions at the 4 and 4' position also. The fact that PTP inhibition was independent of

changes in the structure of the picolinate was rationalized on the basis of steric considerations. The phenanthroline and bipyridine ligands would seem to be more sterically demanding than the picolinate ligand, resulting in decreased binding affinity for PTP when substituents increase the "width" of the ligands. The Substitutions on the 5 position of the phenanthroline system had no significant effect on PTP inhibition and this was attributed to these substituents facing away from the binding site of the PTP in a manner analogous to the peptide chain of a natural phosphotyrosine peptide substrate.

The relative insensitivity of the picolinate pV complexes to substitution makes them a useful starting point for the synthesis of a second generation of pV compounds. The various functional groups at the 3 position and the carboxylate groups at the 4 and 5 positions provide a tether to which larger groups may be attached. In this way enhanced activity and specificity might be accomplished with the rational design of new groups designed to bind to recognition sites on the surface of PTP.⁶⁴

2.3. Experimental:

2.3.1. General

Infrared spectra were measured on an Analect Instruments AQS-18 FTIR spectrometer with the samples as KBr pellets. Typical abbreviations for the infrared bands are: vs, very strong; s, strong; m, medium; w, weak. ⁵¹V NMR spectra of solutions of the complexes in D₂O (98% D purity, MSD Isotopes) were obtained at ambient temperature on a Varian XL-300 NMR spectrometer operating at 78.891 MHz. Vanadium-51 chemical shifts were measured in parts per million (± 1 ppm) using VOCl₃ as an external standard at 0.00 ppm, upfield shifts are considered negative. ¹H NMR spectra of samples in D₂O (99.9% D, Isotec Inc.) were obtained with a Varian Gemini 200 MHz NMR spectrometer using HOD at 4.63 ppm as a reference. ¹³C NMR spectra of samples in D₂O (99.9% D,

Isotec Inc.), using added 1,4-dioxane as a reference at 67.4 ppm, or CD₃OD referenced to 49.0 ppm, were obtained with a Varian Gemini 200 MHz NMR spectrometer operating at 50.289 MHz. Abbreviations for nmr spectra are: s, singlet; m, multiplet; d, doublet; br, broad. Elemental analyses were performed by Guelph Chemical Laboratories, Guelph, Ontario, Canada.

2.3.2. Chemicals:

The compounds V₂O₅ (99.99%), pyridine-2-carboxylic acid (picolinic acid), 3-hydroxypyridine-2-carboxylic acid (3-hydroxypicolinic acid), ethyl bromoacetate (98%), 2,5-pyridinedicarboxylic acid (98%), 2,4-pyridinedicarboxylic acid monohydrate (98%), and 2,3-pyridinedicarboxylic acid (99%) were supplied by Aldrich Chemical Co. and used as received. Guanidine hydrochloride (99%) was purchased from Sigma and used as received. Solutions of H₂O₂ (30% by volume) were purchased from ACP Chemicals Inc. Distilled water was used in all preparations. All other solvents were ACS reagent grade, from various suppliers.

2.3.3. bpV(OHpic)

2.3.3.a. Synthesis: K₂[VO(O₂)₂(OHpic)]•3H₂O

A mixture of V₂O₅ (1.30 g, 7.1 mmol) and KOH (1.84 g, 33.0 mmol) in H₂O (15 mL) in a 125-mL Erlenmeyer flask was heated and stirred for 20 min to give a light green solution. To the cooled solution, 30% H₂O₂ (1 mL, 8.8 mmol) was added, immediately turning it yellow, and after it was stirred for 20 min the solution was filtered through a medium-porosity frit. Additional H₂O₂ (12 mL, 20.8 mmol) was added to the filtrate and the resulting yellow solution was stirred for 30 min. Any yellow solid precipitated during that time was filtered and redissolved with H₂O₂ (6 mL, 8.8 mmol). The solution was then

cooled to 0°C and a slurry of 3-hydroxypicolinic acid (2.01 g, 14.0 mmol) in abs. ethanol (30 mL) was slowly added resulting in a bright yellow suspension after stirring for 30 min at room temperature. A yellow powder was filtered, washed with cold ethanol and dried *in vacuo*. The washings were added to the mother liquor and stored at 5°C for 48 h to give a second crop similarly washed and dried. Total yield: 4.29 g (81%). Elemental analysis consistent with loss of two water molecules upon prolonged drying.

Anal. Calcd. for $C_6H_4K_2NO_8V \cdot H_2O$ (fw: 365.25): C, 19.73; H, 1.66; N, 3.83. Found: C, 19.48; H, 1.82; N, 3.79. ^{51}V nmr (D_2O , ppm): -740.8. 1H nmr (D_2O , ppm): 8.78 (br s, 1 H), 7.63 (s, 2 H); IR (KBr, cm^{-1}): ν (O-H), 2792 (m), ν (C=O), 1630 (s), ν (V=O), 927 (s), ν (O-O), 862 (s), 868 (m).

2.3.3.b.: Structure Determination: $K_2[VO(O_2)_2(OHpic)] \cdot 3H_2O$ *

Yellow square prism crystals of bpV(OHpic) (0.33 X 0.30 X 0.30 mm) were obtained by cooling a hydrogen peroxide ethanol solution of the complex at 5°C and were sealed in a capillary tube. Standard intensities monitored over 24 h showed no change for the first 20 h and then decayed 5%. Following data collection, the crystal decayed rapidly and no absorption correction was performed. Cell dimensions were obtained from 20 reflections with $10.00^\circ \leq 2\theta \leq 24.00^\circ$. A total of 2594 reflections having $2\theta \leq 49.9^\circ$ were collected on a Rigaku AFC6S diffractometer using the ω scan mode with graphite monochromated Mo $K\alpha$ radiation ($-8 \leq h \leq 8$; $0 \leq k \leq 32$; $0 \leq l \leq 8$); of these 2392 were unique and 2102 having $I \geq 2.5\sigma(I)$ were employed in the final refinement of the structure using the NRCVAX system of crystallographic software.⁶⁵ Merging R for 202 pairs of symmetry-related reflections was 2%. The structure was solved by direct methods, which gave the positions of all non-hydrogen atoms. Hydrogen atoms were located in a difference map and were refined isotropically; all other atoms were refined anisotropically.

* Structure Determined by Dr. Rosemary Hynes.

2.3.4. bpV(2,3-pdc)

2.3.4.a. Synthesis: $K_3[VO(O_2)_2(2,3\text{-pyridinedicarboxylato})]\cdot 2H_2O$

The compound V_2O_5 (0.9g, 5 mmol) was added to a solution of KOH (0.9g, 16 mmol) in water (15 mL). The mixture was stirred with gentle heating until a clear, nearly colourless solution was obtained. To the cooled solution was added approximately 1 mL H_2O_2 (30%) which resulted in a change of colour to yellow and a small amount of precipitate. After stirring for 5 min, the solution was filtered through a medium porosity glass frit and the precipitate left on the frit was dissolved in H_2O_2 (approx. 9 mL, 30%). The combined filtrates were then slowly added to a solution of 2,3-pyridinedicarboxylic acid (2.0g, 12 mmol) and KOH (1.0g, 18 mmol) in water (15 mL). After stirring for approximately 2 hr the solution was adjusted to pH 8 by addition of 6 M HCl. Ethanol was then added until a persistent precipitate was observed and the solution was maintained at 5°C for 20 hr. The solution was filtered and the white, water insoluble precipitate left on the frit was discarded. The filtrate was kept at 5°C for an additional 18 hr and a fluffy yellow precipitate was collected by vacuum filtration and dried *in vacuo* (1.1g, 2.4 mmol). Two additional crops of yellow precipitate were collected from the filtrate upon further addition of ethanol and standing at 5°C. The total yield was 3.05 g (67%). IR(KBr): $\nu(CO)$ 1635 (s), $\nu(CO)$ 1397 (s); $\nu(VO)$ 940 (m), $\nu(OO)$ 867 (s), 838 (m) cm^{-1} . ^{51}V NMR (D_2O): δ -742. 1H NMR (D_2O): δ 9.1 (br, 1H), 7.9 (br, 1H), 7.7 (br, 1H). Anal. Calcd for $C_7H_7NO_{11}K_3V$: C, 18.71; H, 1.57; N, 3.12. Found: C, 18.69; H, 1.55; N, 3.12.

2.3.5. bpV(2,4-pdc)

2.3.5.a. Synthesis: $K_3[VO(O_2)_2(2,4\text{-pyridinedicarboxylato})]\cdot 3.25H_2O$

The compound V_2O_5 (2.3g, 13 mmol) was added to a solution of KOH (2.8g, 50 mmol) in water (20 mL). The mixture was stirred and heated gently until a clear, nearly colourless

solution was obtained (approx. 15 min). To the cooled solution (cold water bath, 8°C) was added 4 mL of H₂O₂ (30%) resulting in the formation of a yellow slurry. The mixture was stirred for approximately 5 min and filtered through a medium porosity glass frit. The precipitate left on the frit was dissolved in H₂O₂ (approx. 25 mL). The combined filtrates were stirred for 5 min and the formation of additional precipitate was noted. More KOH (0.2g, 3.6 mmol) was added to the reaction mixture prior to its slow addition to a solution of 2,4-pyridinedicarboxylic acid monohydrate (5.0g, 27 mmol) and KOH (3.0g, 53 mmol) in water (25 mL). After stirring for 30 min the solution was filtered and ethanol (30 mL, absolute) was added. The solution was maintained at 5°C for 12 hr and filtered again. The insoluble precipitate was dissolved on the frit in H₂O₂ (20 mL, 30%) and all the filtrates combined. Ethanol (150 mL, absolute) was added and the solution kept at 5°C for 3 hr. The solution was then filtered and the residue discarded. Additional ethanol (50 mL, absolute) was added to the filtrate and the solution was maintained at 5°C for 12 hr to give yellow crystals which were collected on a frit and dried *in vacuo* (2.5g, 5.3 mmol). Prolonged cooling of the mother liquor at 5°C gave a second crop of yellow crystals. The total yield was 3.5g (57%). IR(KBr): $\nu(\text{CO})$ 1669 (br,s); $\nu(\text{CO})$ 1373 (s); $\nu(\text{VO})$ 940 (s); $\nu(\text{OO})$ 865 (s), 852 (s) cm^{-1} . ^{51}V NMR (D₂O): δ -743. ^1H NMR (D₂O): δ 9.15 (br, 1H), 8.21 (s,1H), 7.93 (br, 1H). Anal. Calcd. for C₇H_{9.5}NO_{12.25}K₃V: C, 17.82; H, 1.79; N, 2.97. Found: C, 18.18; H, 1.79; N, 2.96.

2.3.5.b. Structure Determination: K₃[VO(O₂)₂(2,4-pdc)]·3.25 H₂O*

Yellow thin plate crystals of bpV(2,4-pdc) (0.4 x 0.17 x 0.1 mm), obtained by cooling a hydrogen peroxide-ethanol solution of the complex at 5°C, were mounted on a glass fibre and coated with epoxy. Cell dimensions were obtained from 25 reflections with $80.00^\circ \leq 2\theta \leq 100.00^\circ$. A total of 4355 reflections having $2\theta \leq 110^\circ$ were collected on a Rigaku AFC6S diffractometer using the $\theta/2\theta$ scan mode with graphite-monochromated Cu

* Structure Determined by Dr. Rosemary Hynes and Dr. Anne-Marie Lebuis.

K α radiation ($-7 \leq h \leq 7$; $0 \leq k \leq 40$; $0 \leq l \leq 12$); of these 3978 were unique and 3389 having $I \geq 2.5\sigma(I)$ were employed in the solution and refinement of the structure using the NRCVAX system of crystallographic software.⁶⁵ Merging R for 377 pairs of symmetry-related reflections was 3.0%. The data were corrected for absorption (psi scans). The structure was solved by direct methods which gave the positions of all non-hydrogen atoms. The hydrogen atom positions for the 2,4-pdc ligand were calculated. Refinement was carried out in blocks of 2 molecules at a time.

2.3.6. bpV(2,5-pdc)

2.3.6.a. Synthesis: $K_3[VO(O_2)_2(2,5\text{-pyridinedicarboxylato})] \cdot 2H_2O$

The compound V_2O_5 (2.3g, 13 mmol) was added to a solution of KOH (2.8g, 50 mmol) in water (20 mL). The mixture was stirred for 15 min until a clear, almost colourless solution was obtained. The solution was cooled to 0°C and filtered. To the filtrate was added 6.5 mL of H_2O_2 (30%) which gave a change of colour to yellow and the formation of precipitate. The mixture was stirred 10 min and filtered through a medium porosity glass frit. The precipitate left on the frit was dissolved in H_2O_2 (30%, 18.5 mL). The combined filtrates were added over a period of 10 min to a slurry of 2,5-pyridinedicarboxylic acid (5.0g, 30 mmol) in a solution of KOH (3.5g, 62 mmol) and water (22 mL). The yellow solution was stirred for 1 hr and filtered. Absolute ethanol (45 mL) was then added to the solution until a persistent precipitate was observed. The mixture was cooled at 5°C for 18 hr and filtered. The precipitate was collected on a frit and washed with a small volume of H_2O and the insoluble residue discarded. An additional 200 mL of absolute ethanol was then added to the filtrates and the mixture cooled at 5°C for 48 hr. The title compound was collected as a yellow precipitate which was washed with 5 mL of absolute ethanol, and dried *in vacuo*. Total yield 5.28g (93%). IR(KBr): $\nu(CO)$ 1617 (s); $\nu(CO)$ 1362 (s); $\nu(VO)$ 932 (s); $\nu(OO)$ 890 (s), 860 (s) cm^{-1} . ^{51}V NMR (D_2O): δ -742

ppm. ^1H NMR (D_2O): δ 9.46 (br, 1H), 8.44 (br, d, 1H), 8.01 (br, d, 1H). Anal Calcd for $\text{C}_7\text{H}_7\text{NO}_{11}\text{K}_3\text{V}$: C, 18.71; H, 1.57; N, 3.12. Found: C, 18.60; H, 1.29; N, 2.98.

2.3.7. bpV(acetpic)

2.3.7.a. Synthesis: Potassium 3-acetatoxypicolinate

The compound ethyl-2-(2-ethoxycarbonyl-3-pyridyloxy)acetate (11g, 43 mmol), prepared by literature method⁶⁶, was added to a solution of KOH (5.1g, 91 mmol) in H_2O (100 mL) and the mixture refluxed for 3 hr. The solution was washed with CH_2Cl_2 (2X25 mL) and reduced to approximately half volume by rotary evaporation. The solution was cooled to 5°C and ethanol added to give a sand coloured precipitate which was collected by filtration. Total yield (not optimized) 6.8g (58%). The compound (5.1g, 19 mmol) was purified by dissolution in a mixture of hot CH_3OH (75 mL) and H_2O (13 mL) and filtered. The filtrate was cooled to 5°C and absolute ethanol added (2 mL). The resulting crystals were collected by vacuum filtration and dried *in vacuo*. Total yield (not optimized) 3.3g (65%). ^1H NMR (D_2O): δ 7.88 (d, 1H), 7.18 (m, 2H), 4.38 (s, 2H).

2.3.7.b. Synthesis: $\text{K}_3[\text{VO}(\text{O}_2)_2(3\text{-acetatoxypicolinato})]\cdot 2\text{H}_2\text{O}$

The compound V_2O_5 (0.80g, 4.4 mmol) was added to a solution of KOH (1.0g, 18 mmol) in H_2O (20mL). The mixture was stirred for 10 min until a clear, almost colourless solution was obtained. The filtrate was then cooled to approximately 8°C and 2 mL of H_2O_2 (30%) was added which gave a change of colour to yellow and the formation of precipitate. After stirring for approximately 20 min the mixture was filtered through a medium porosity glass frit. The precipitate left on the frit was dissolved in H_2O_2 (30%, 6 mL). The potassium 3-acetatoxypicolinate (2.2g, 8.0 mmol) was added to the filtrate and the pH of the solution adjusted to 7 with KOH. The solution was stirred for approximately 1.5 hr and then filtered. Absolute ethanol (4 mL) was added to the filtrate and the solution

cooled at 5°C for 3 hours. The solution was then filtered and the pale yellow water-insoluble precipitate discarded. This was repeated after a further 20 hr cooling at 5°C and the solution was allowed to stand at 5°C for a further 8 days. The resulting yellow/orange crystals (1.1g, 2.3 mmol) were collected by filtration and dried *in vacuo*. A second crop of precipitate (0.20g, 0.42mmol) was collected upon addition of absolute ethanol and cooling at 5°C. Total yield 1.3g (34%). IR(KBr): $\nu(\text{CO})$ 1619 (s); $\nu(\text{CO})$ 1401 (s); $\nu(\text{VO})$ 912 (s); $\nu(\text{OO})$ 860 (s), 875 (s) cm^{-1} . ^{51}V NMR (D_2O): δ -745 ppm ^1H NMR (D_2O): δ 8.8 (br, 1H), 7.5 (br, 2H), 4.5 (s, 1H). Anal Calcd for $\text{C}_8\text{H}_9\text{NO}_{12}\text{K}_3\text{V}$: C, 20.04; H, 1.89; N, 2.92. Found: C, 20.28; H, 2.00; N, 2.80.

2.3.7.c. Structure Determination: $\text{K}_3[\text{VO}(\text{O}_2)_2(3\text{-acetpic})]\cdot 2\text{H}_2\text{O}^*$

Yellow needles of bpV(3-acetpic) (0.33 x 0.1 x 0.1 mm), obtained by cooling a hydrogen peroxide-ethanol solution of the complex at 5°C, were mounted on a glass fibre and coated with epoxy. Cell dimensions were obtained from 25 reflections with $30.00^\circ \leq 2\theta \leq 35.00^\circ$. A total of 2251 reflections having $2\theta \leq 45^\circ$ were collected on a Rigaku AFC6S diffractometer using the $\theta/2\theta$ scan mode with graphite-monochromated $\text{Mo K}\alpha$ radiation ($-7 \leq h \leq 7$; $0 \leq k \leq 11$; $-11 \leq l \leq 11$); of these 2060 were unique and 1537 having $I \geq 2.5\sigma(I)$ were employed in the solution and refinement of the structure using the NRCVAX system of crystallographic software⁶⁵. Merging R for 191 pairs of symmetry-related reflections was 1.9%. The structure was solved by direct methods which gave the positions of all non-hydrogen atoms. All the hydrogen atom positions were found by difference map. All non hydrogen atom positions were refined anisotropically. The hydrogen atom positions were refined isotropically.

* Structure Determined by Dr. Rosemary Hynes.

2.3.8. GmpV(2,6-pdc)

2.3.8.a. Synthesis: $C(NH_2)_3[VO(O_2)(2,6-pdc)(H_2O)] \cdot H_2O$

The ammonium salt of mpV(2,6-pdc), (prepared by the literature method⁷ by Jesse B. Ng) (0.11 g, 0.34 mmol) was dissolved in distilled water (20 mL). This solution was slowly added to a solution of guanidine hydrochloride (0.70 g, 7.3 mmol) in distilled water (20 mL). The mixture was cooled at 5°C and two crops of crystals unsuitable for crystallographic analysis were collected. The mixture was then concentrated to approximately half volume by bubbling N₂ through the solution and then cooled at 5°C. A final crop of crystalline material was collected and a crystal suitable for X-ray crystallographic analysis was selected. ⁵¹V NMR (D₂O): δ -595 ppm. Anal Calcd for C₈H₁₃N₄O₁₂V: C, 26.68; H, 3.64; N, 15.56. Found: C, 26.76; H, 3.64; N, 15.59.

2.3.8.b.: Structure Determination: $C(NH_2)_3[VO(O_2)(2,6-pdc)(H_2O)] \cdot H_2O^*$

An orange block crystal of the guanidinium salt of mpV(2,6-pdc) (0.45 x 0.45 x 0.40 mm) was sealed in a capillary tube with a small amount of mother liquor. Cell dimensions were obtained from 25 reflections with $34 < 2\theta < 35^\circ$. A total of 4896 reflections having $2\theta \leq 50.0^\circ$ were collected on a Rigaku AFC6S diffractometer using the ω - 2θ scan mode with graphite-monochromated Mo K α radiation ($0 \leq h \leq 13$; $-12 \leq k \leq 12$; $-15 \leq l \leq 15$); of these 2465 were unique (R_{int} 0.069) and 1788 having $I \geq 2.5\sigma(I)$ were employed in the solution and refinement of the structure using the TEXSAN system of crystallographic software.⁶⁷ The structure was solved by Patterson method and expanded by a difference map.** All the hydrogen atom positions were found by in the

* Structure Determined by Dr. Anne-Marie Lehuis.

** Structure Solution Methods:

PHASE: Calbrese, J. C.; PHASE - Patterson Heavy Atom Solution Extractor. University of Wisconsin-Madison, Ph. D. Thesis (1972)

DIRDIF: Beurskens, P. T.; DIRDIF: Direct Methods for Difference Structures - an automatic procedure for phase extension and refinement of difference structure factors. Technical Report 1984/1 Crystallography Laboratory, Toernooiveld, 6525 Ed Nijmegen, Netherlands.

difference map position, all other hydrogens were refined isotropically. The data were corrected for absorption (psi scans, transmission range 0.95-1.00).

2.3.9. **KmpV(2,6-pdc)**

2.3.9.a. **Synthesis: $K[VO(O_2)(2,6-pdc)(H_2O)] \cdot 2H_2O$**

The ammonium salt of mpV(2,6-pdc), (prepared by the literature method⁷ by Jesse B. Ng) (0.50 g, 1.6 mmol) was dissolved in distilled water (50 mL). The pH of the solution was raised from 4.7 to 6.4 through the addition of KOH(aq). The solution was concentrated to approximately 1/4 volume by rotary evaporation after addition of KCl (2g, 27 mmol). The mixture was then cooled at 0°C for 1.5 h and the red precipitate collected by filtration and washed with cold water. ⁵¹V NMR (D₂O): δ -595 ppm. Anal Calcd for C₇H₉NO₁₀VK: C, 23.54; H, 2.54; N, 3.92. Found: C, 23.25; H, 2.19; N, 3.81.

2.4. References

- (1) Hartkamp, H. *Angew. Chem.* **1959**, *71*, 553.
- (2) Kadota, S.; Fantus, I. G.; Deragon, G.; Guyda, H. J.; Posner, B. I. *J. Biol. Chem.* **1987**, *262*, 8252-8256.
- (3) Kadota, S.; Fantus, I. G.; Deragon, G.; Guyda, H. J.; Hersh, B.; Posner, B. I. *Biochem. Biophys. Res. Comm.* **1987**, 259-266.
- (4) Vuletic, N.; Djordjevic, C. *J. Chem. Soc. Dalton Trans.* **1973**, 1137-114.
- (5) Basumatary, J. K.; Chaudhuri, M. K.; Dutta Purkayastha, R. N.; Hiese, Z. *J. Chem. Soc. Dalton Trans.* **1986**, 709-711.
- (6) Chaudhuri, M. K.; Ghosh, S. K. *Polyhedron* **1982**, *1*, 553-555.
- (7) Drew, R. E.; Einstein, F. W. B. *Inorg. Chem.* **1973**, *12*, 829-835.
- (8) Wei, Y. G.; Zhang, S. W.; Huang, C. Q.; Shao, M. C. *Polyhedron* **1994**, *13*, 1587-1591.
- (9) Szentivanyi, H.; Stomberg, R. *Acta Chem. Scand.* **1983**, *A37*, 553-559.
- (10) Schwendt, P.; Petrovic, P.; Uskert, D. *Z. Anorg. Allg. Chem.* **1980**, *466*, 232-236.
- (11) Begin, D.; Einstein, F. W. D.; Field, J. *Inorg. Chem.* **1975**, *14*, 1785-1790.
- (12) Schwendt, P.; Pisárcik, M. *Coll. Czech. Chem. Commun.* **1982**, *47*, 1549-1555.
- (13) Drew, R. E.; Einstein, F. W. B. *Inorg. Chem.* **1972**, *11*, 1079-1083.
- (14) Mimoun, H.; Saussine, L.; Daire, E.; Postel, M.; Fischer, J.; Weiss, R. *J. Am. Chem. Soc.* **1983**, *105*, 3101-3110.
- (15) Quilitzsch, U.; Wieghardt, K. *Inorg. chem.* **1979**, *18*, 869-871.
- (16) Shaver, A.; Ng, J. B.; Hall, D. A.; Soo Lum, B.; Posner, B. I. *Inorg. Chem.* **1993**, *32*, 3109-3113.
- (17) Mimoun, H.; Chaumette, P.; Mignard, M.; Saussine, L.; Fischer, J.; Weiss, R. *Nouv. J. Chim.* **1983**, *7*, 467-475.

- (18) Stomberg, R. *Acta Chem. Scand.* **1986**, A40, 168-176.
- (19) Szentivanyi, H.; Stomberg, R. *Acta Chem. Scand.* **1983**, A37, 709-714.
- (20) Stomberg, R. *Acta Chem. Scand.* **1985**, A39, 725-731.
- (21) Shaver, A.; Hall, D. A.; Ng, J. B.; Lebuis, A.-M.; Hynes, R. C.; Posner, B. I. *Inorg. Chim. Acta* **1995**, 229, 253-260.
- (22) Shaver, A.; Ng, J. B.; Hynes, R. C.; Posner, B. I. *Acta Cryst.* **1994**, C50, 1044-1046.
- (23) Djordjevic, C.; Craig, S. A.; Sinn, E. *Inorg. Chem.* **1985**, 24, 1281-1283.
- (24) Djordjevic, C.; Lee, M.; Sinn, E. *Inorg. Chem.* **1989**, 28, 719-723.
- (25) Stomberg, R. *Acta Chem. Scand.* **1984**, A38, 223-228.
- (26) Stomberg, R. *Acta Chem. Scand.* **1984**, A37, 541-545.
- (27) Djordjevic, C.; Wampler, G. J. *Inorg. Biochem.* **1985**, 25, 51-55.
- (28) Wiegardt, K. *Inorg. Chem.* **1978**, 17, 57-64.
- (29) Schwendt, P.; Sivak, M.; Lapshin, A. E.; Smolin, Y. I.; Shepelev, Y. F.; Gyepesova, D. *Trans. Metal Chem.* **1994**, 19, 34-36.
- (30) Vitler, H.; Rehder, D. *Inorg. Chim. Acta* **1987**, 136, L7-L10.
- (31) Campbell, N. J.; Capparelli, M. V.; Griffith, W. P.; Skapski, A. C. *Inorg. Chim. Acta* **1983**, 77, L215-L216.
- (32) Szentivanyi, H.; Stomberg, R. *Acta Chem. Scand.* **1984**, A38, 101-107.
- (33) Stomberg, R.; Szentivanyi, H. *Acta Chem. Scand.* **1984**, A38, 121-128.
- (34) Bhattacharjee, M.; Chaudhuri, M. K.; Paul, P. C. *Can. J. Chem.* **1992**, 70, 2245-2248.
- (35) Chaudhuri, M. K.; Paul, P. C. *Ind. J. Chem.* **1992**, 31A, 466-468.
- (36) Chaudhuri, M. K.; Ghosh, S. K. *Inorg. Chem.* **1982**, 21, 4020-4022.
- (37) Chaudhuri, M.; Ghosh, S.; Islam, N. *Inorg. Chem.* **1985**, 24, 2706 - 2707.
- (38) Won, T.-J.; Barnes, C. L.; Schlempler, E. O.; Thompson, R. C. *Inorg. Chem.* **1995**, 34, 4499-4503.

- (39) Djordjevic, C.; Lee-Renslo, M.; Sinn, E. *Inorg. Chim. Acta* **1995**, *233*, 97-102.
- (40) Wu, D.; Lei, X.; Cao, R.; Hong, M. *Jigeou Huaxue* **1992**, *11*, 65-67.
- (41) Djordjevic, C.; Wilkins, P. L.; Sinn, E.; Butcher, R. J. *Inorg. Chim. Acta* **1995**, *230*, 241-244.
- (42) Kuchta, L.; Sivak, M.; Pavelik, F. *J. Chem. Res.* **1993**, 393.
- (43) Chaudhuri, M. K.; Ghosh, S. K. *Inorg. Chem.* **1984**, *23*, 534-537.
- (44) Bhattacharjee, M.; Chaudhuri, M. K.; Islam, N. S.; Paul, P. C. *Inorg. Chim. Acta* **1990**, *169*, 97-100.
- (45) Bhattacharjee, M.; Chaudhuri, M.; Islam, N. *Inorg. Chem.* **1989**, *28*, 2420-2423.
- (46) Jaswal, J. S.; Tracey, A. S. *Inorg. Chem.* **1991**, *30*, 3718-3722.
- (47) Stomberg, R.; Olson, S.; Svensson, I. B. *Acta Chem. Scand.* **1984**, *A38*, 653-656.
- (48) Campbell, N. J.; Flanagan, J.; Griffith, W. P.; Skapski, A. C. *Trans. Met. Chem.* **1985**, *10*, 353-354.
- (49) Djordjevic, C.; Puryear, B. C.; Vuletic, N.; Abelt, C. J.; Sheffield, S. J. *Inorg. Chem.* **1988**, *27*, 2926-2932.
- (50) Schwendt, P.; Tyrselová, J.; Pavelcik, F. *Inorg. chem.* **1995**, *34*, 1964-1966.
- (51) Colpas, G. J.; Hamstra, B. J.; Kampf, J. W.; Pecoraro, V. L. *J. Am. Chem. Soc.* **1994**, *116*, 3627-3628.
- (52) Einstein, F. W. B.; Batchelor, R. J.; Angus-Dunne, S. J.; Tracey, A. S. **1996**,
- (53) Colpas, G. J.; Hamstra, B. J.; Kampf, J. W.; Pecoraro, V. L. *J. Am. Chem. Soc.* **1996**, *118*, 3469-3478.
- (54) Posner, B. I.; Faure, R.; Burgess, J. W.; Bevan, A. P.; Lachance, D.; Zhang-Sun, G.; Fantus, I. G.; Ng, J. B.; Hall, D. A.; Soo Lum, B.; Shaver, A. *J. Biol. Chem.* **1994**, *269*, 4596-4604.
- (55) Tracey, A.; Jaswal, J. *J. Am. Chem. Soc.* **1992**, *114*, 3835-3840.

- (56) Borchio, M.; Conte, V.; Di Furio, F.; Modena, G.; Moro, S.; Edwards, J. O. *Inorg. Chem.* **1994**, *33*, 1631-1637.
- (57) Butler, A.; Clague, M. J.; Meister, G. E. *Chem. Rev.* **1994**, *94*, 625-638.
- (58) Unpublished results; Gerry Baquiran and Barry Posner.
- (59) Posner, B. I.; Shaver, A.; Fantus, G. In *New Antidiabetic Drugs*; ; C. J. Bailey and P. R. Flatt, Ed.; Smith Gordon: London, 1990, pp 107-117.
- (60) Unpublished results; Jesse B. Ng, Alan Shaver and Barry Posner.
- (61) Richter, J.; Rehder, D. *Z. Naturforsch.* **1991**, *46 b*, 1613-1620.
- (62) Gresser, M. J.; Tracey, A. S. In *Vanadium in Biological Systems*; ; N. D. Chasteen, Ed.; Kluwer Academic Publishers: Boston, 1990, pp 63-79.
- (63) Shaver, A.; Ng, J. B.; Hall, D. A.; Posner, B. I. *Mol. and Cell. Biochem.* **1995**, *153*, 5-15.
- (64) Zongchao, J.; Barford, D.; Flint, A. J.; Tonks, N. K. *Science* **1995**, *268*, 1754-1758.
- (65) Gabe, E. J.; Le Page, Y.; Charland, J. P.; Lee, F. L.; White, P. S. *J. Appl. Cryst.* **1989**, *22*, 384-387.
- (66) Shiotani, S.; Morita, H. *J. Heterocyclic Chem.* **1986**, *23*, 665-668.
- (67) Texsan - Texray Structure Analysis Package, Molecular Structure Corporation (1985).

Chapter 3. The Stability and Reactivity of Insulin-mimetic Peroxovanadium Complexes

3.1. Introduction

The growing interest in pV complexes in the fields of biochemistry and medicine, has generated the need for information regarding the stability and reactivity of pV compounds. Among the most striking features of pV compounds is their potential as oxidants. The vanadium exists in its d^0 state and is coordinated to between 1 and 4 (usually 1 or 2) peroxo ligands. Indeed there has been much interest in pV compounds as catalytic oxidants.¹ Biological assays of the activity of pV compounds pose particular complications. Typically the buffer solutions used in biological assays of enzyme inhibition or activation contain a large number substances that may react with pV compounds. Often included in the buffer systems are reducing agents such as dithiothreitol (DTT) or β -mercaptoethanol to protect against aerial oxidation of the enzyme. These agents may reduce pV compounds. Recently Crans reviewed the interaction of vanadates with common biological buffers and additives.² The chemistries of vanadates and pV complexes are very different and an understanding of the chemistry of pV complexes with biological media is necessary in determining the conditions for drug formulation or biological assays.

Crans recommends the use of HEPES buffer for vanadate solutions as it has been shown to have little effect on the rate of the exchange between vanadate oligomers and forms no stable complex that is identifiable by ^{51}V NMR.² Imidazole is also recommended as it does not form any complexes identifiable by ^{51}V NMR but it does change the relative amounts of oligovanadates slightly and as a result must be assumed to be interacting with vanadate in some way.² Other buffers that interact weakly with vanadate and may be suitable if not used in large excess or under conditions that favor

complex formation are TRIS, TAPS, MES, PIPES, and acetate (see Figure 3.1.1 for structures).² TRIS and vanadate form a well-defined complex; a solution of 20mM TRIS and 1 mM vanadate at neutral pH gives rise to approximately 0.01mM of a vanadate-TRIS complex.² Some strongly interacting buffers that are not recommended are triethanolamine, Tricine, Bicine or any diethanol amine derivative.² These form stable complexes with vanadate with respect to the time scale of oligovanadate exchange.² Inorganic buffers may also interact with vanadate.² Phosphate and presumably carbonate and borate form anhydride like complexes with vanadate.² The phosphate complex is much less stable than the complexes of some of the amine type buffers but there still exists significant interaction.² The structural and chemical similarities between vanadate and phosphate compound this problem.² The determination of the active species in some assays may be difficult if both phosphate and vanadate are present, for example a vanadate phosphate complex may compete with a vanadate dimer.² Vanadate has been known to replace phosphate in some instances such as with the co-factor NADP which can be replaced under certain circumstances with NADV.³

Crans et al. have also remarked on the interaction of vanadate with some of the more common additives to biological buffer systems.² EDTA reacts with vanadate to form a stable 1:1 complex easily identified by ⁵¹V NMR. Vanadate also reacts with commonly added reducing agents designed to retain the reduced form of proteins in solution, among them DTT and β -mercaptoethanol. These agents reduce vanadate to vanadyl and severely interfere with biological assays. Some slight interactions are also noted with bovine serum albumin (BSA), ethylene glycol and glycerine. These additives are not strictly contraindicated but should be used with caution.

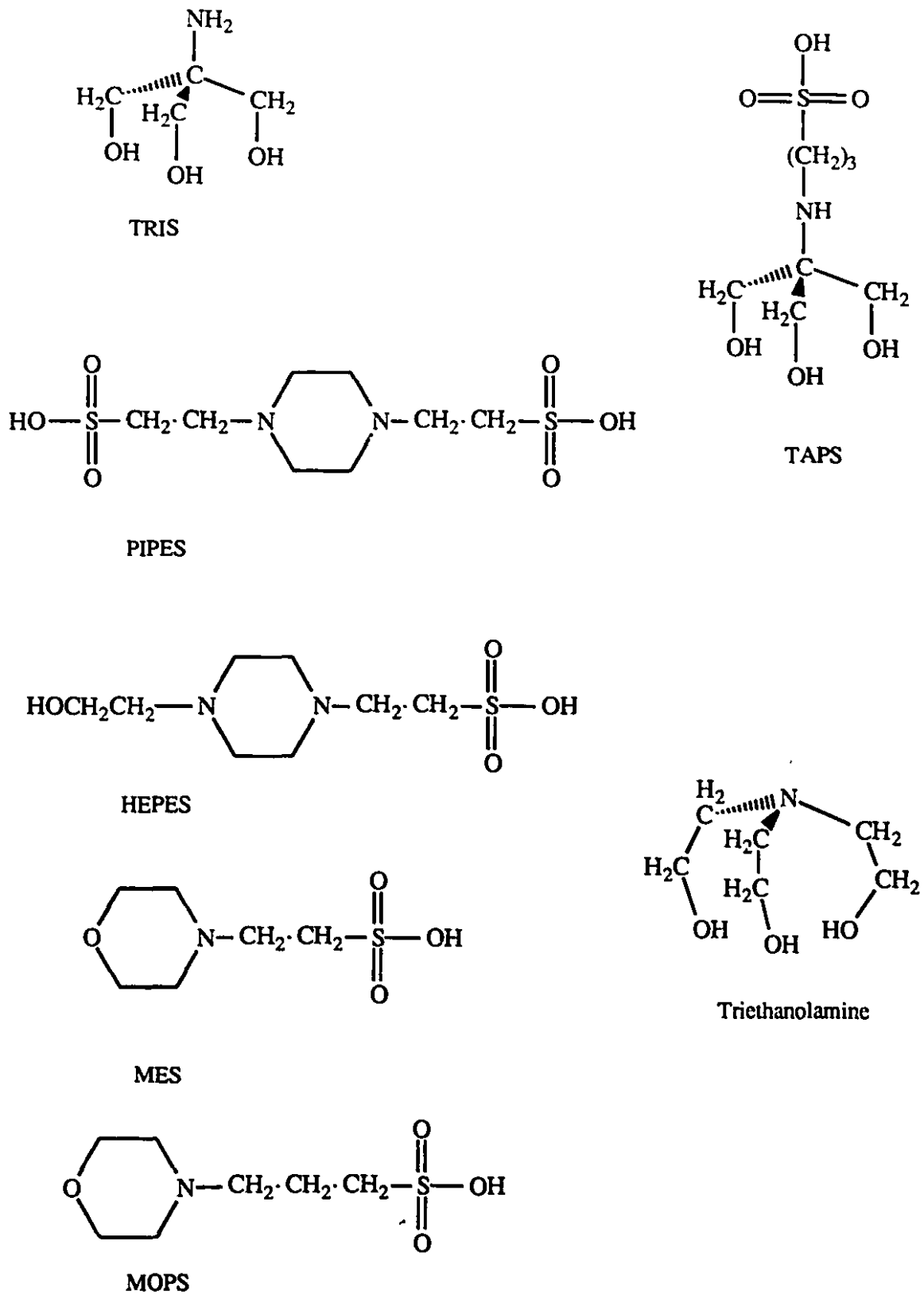
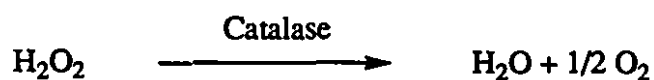


Figure 3.1.1. The structure of some common biological buffers.

The stability of pV compounds is of particular interest. The stability of pVs at various pH's tends to determine their biological availability and the appropriateness of various routes of administration. If a pV complex is to be given orally it must be able to withstand the acid environment of the stomach or be suitably encapsulated and absorbed in the more basic environment of the small or large intestine. It is also important to determine stability if pV complexes are to be administered orally in the drinking water of animals. The stability of pV compounds with regards to light is also of concern as it determines the protocols that must be employed in handling solutions of the compounds. Crans et al. have investigated the stability of some vanadate, vanadyl, and some pV compounds in unbuffered water, buffered water, and in buffered water containing β -mercaptoethanol.⁴ Stabilities were monitored by ^{51}V NMR, UV-vis spectroscopy, and EPR.⁴

Early studies on the insulin mimetic activity of pV compounds made use of mixtures of vanadate and hydrogen peroxide to generate the active species.⁵ In the preparations the enzyme catalase was used to remove excess peroxide.⁵ Catalase is a metalloenzyme that catalyzes the disproportionation of hydrogen peroxide to oxygen and water.⁶ Catalase is an extremely efficient enzyme and it is estimated that a single molecule can catalyze more than 10^6 reactions per second.⁷ It is ubiquitous *in vivo*, where it prevents oxidative damage by hydrogen peroxide.⁸ Hydrogen peroxide may be produced *in vivo* by superoxide dismutase which scavenges superoxide radicals converting them to the less reactive hydrogen peroxide or through the spontaneous reaction of two hydroperoxyl radicals.⁸ The effect of catalase on peroxovanadium compounds has not however been investigated.



To further the understanding of the reactivity of pV complexes in biological media the stability of pV compounds was determined at pHs ranging from 4-7 and in various buffers at physiological pH. The effect of light on the stability of pV compounds was also investigated. The interaction of pV and vanadate compounds with DTT, a common addition to biological buffer systems, and EDTA was also investigated. The reaction of various pV compounds with catalase was probed by ^{51}V NMR and the rate of reaction with bpV(pic) and bpV(OHpic) determined. Electron transfer reactions between bpV(OHpic) and potassium ferrocyanide were investigated both under continuous UV-Vis irradiation and with light exposure minimized.

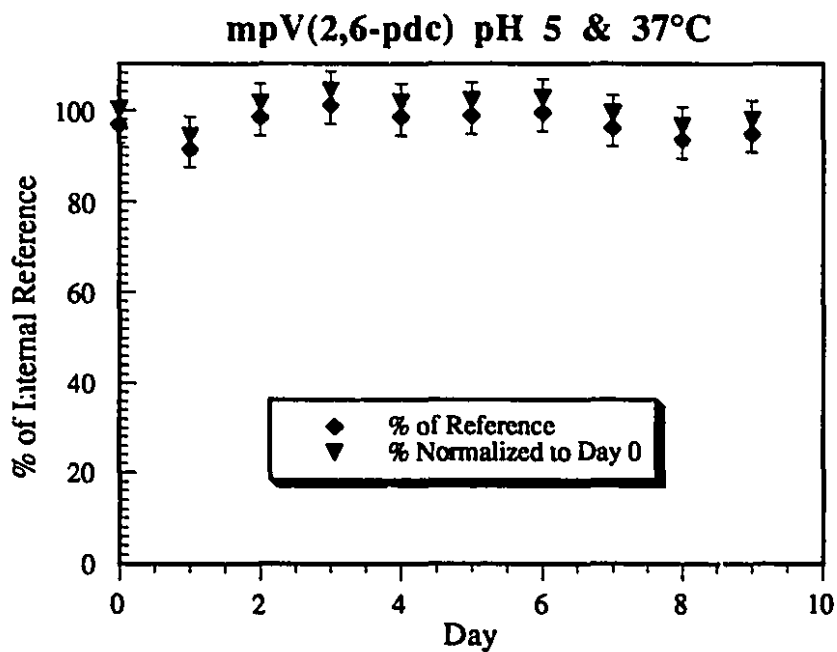
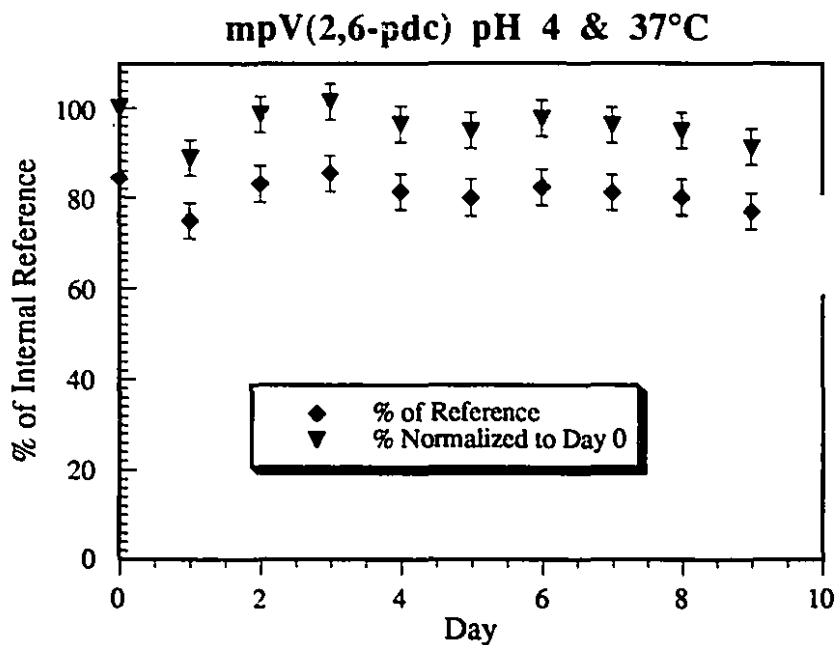
3.2. Results and Discussion

3.2.1. Stability Studies

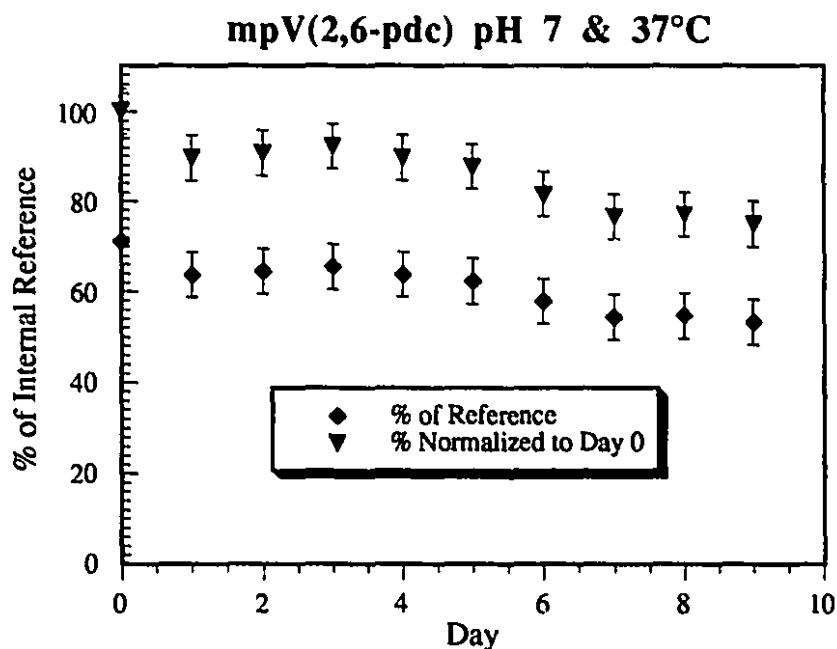
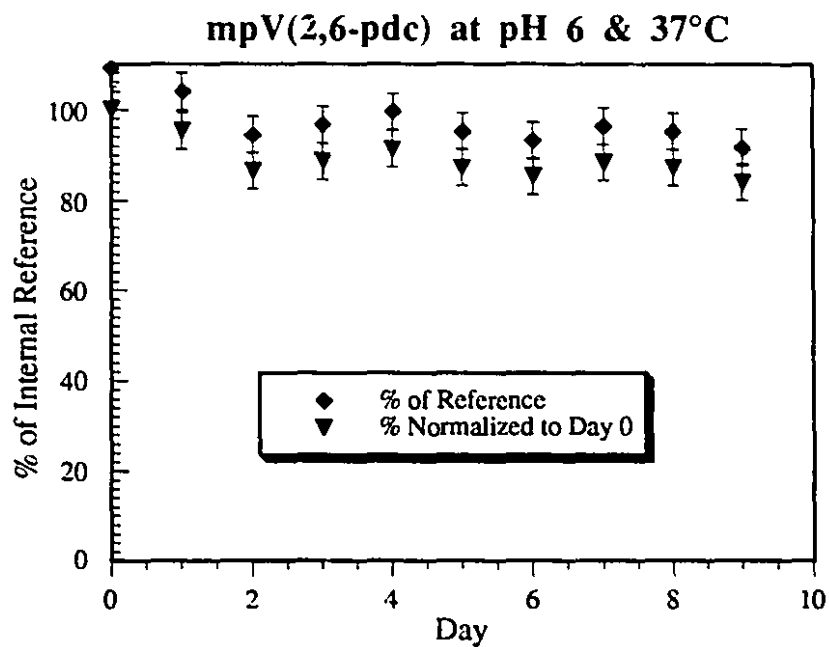
The stabilities of mpV(2,6-pdc), bpV(pic) and bpV(OHpic) at pH 4, 5, 6, and 7 at 37°C were monitored by ^{51}V NMR over the course of 9 days. Integration of the peak due to the pV compound was compared to that of an internal reference. Plots of the data showing the absolute percentage of the area of the pV peak relative to the internal reference as well as a plot of the percent normalized to 100% at day zero are given. The samples were prepared in NMR tubes which were flame sealed. No special precautions to protect the samples from light were taken.

3.2.1.a. mpV(2,6-pdc):

The mpV(2,6-pdc) complex showed a very high level of stability at all pH's tested. At both pH 4 and 5 mpV(2,6-pdc) showed no significant decomposition after 9 days at 37°C as is shown in graphs 3.2.1 and 3.2.2. No new peaks appeared in the ^{51}V NMR spectra.



Graph 3.2.1 and Graph 3.2.2. Graphs showing the stability of mpV(2,6-pdc) relative to an internal reference as determined by ^{51}V NMR at pH 4 and 5 and 37°C. Graphs show both the percentage of the integration of the mpV(2,6-pdc) relative to the reference (◆) and also the percent of the initial concentration of mpV(2,6-pdc) normalized to day zero (▼).



Graph 3.2.3 and Graph 3.2.4. Graphs showing the stability of mpV(2,6-pdc) relative to an internal reference as determined by ^{51}V NMR at pH 6 and 7 and 37°C. Graphs show both the percentage of the integration of the mpV(2,6-pdc) relative to the reference (◆) and also the percent of the initial concentration of mpV(2,6-pdc) normalized to day zero (▼).

At pH 6 and 7 mpV(2,6-pdc) proved to be less stable than at the lower pH's. At pH 6 after 9 days the mpV(2,6-pdc) had decomposed approximately 15%. A small peak appeared in the spectrum on day 1 at -557 ppm and persisted throughout the experiment with no change in intensity, this peak is consistent with a monomeric vanadate species. At pH 7 mpV(2,6-pdc) decomposed approximately 25% after 9 days. A small peak was barely apparent at day zero at -563 ppm which continued to grow throughout the study with new peaks also appearing at -570 (divanadate) and -575 ppm (tetravanadate).

The monoperoxo compound mpV(2,6-pdc) is stable at acidic pH. This is perhaps not surprising since it is synthesized under mildly acidic conditions.⁹ At higher pH's some decomposition was observed mostly to vanadates. Of note was the presence of a vanadate peak in the ⁵¹V NMR spectra at pH 7. Since the concentration was normalized to day zero the percent decomposition is not strictly correct since it is clear from the presence of the vanadate peak that at day zero some decomposition had already occurred. The decreasing stability with increasing pH for mpV(2,6-pdc) is interesting and not readily explainable. The mechanism of decomposition is not clear but one possibility may involve the deprotonation of the water molecule coordinated to the vanadium atom resulting, somehow, in a less stable compound. Further studies would be required to determine the actual mechanism of decomposition.

Titration of mpV(2,6-pdc) with NaOH from pH 3.5 to 10 showed a significant consumption of base at a pH of approximately 7.5. At approximately pH 8 the solution went from red to colourless and remained so throughout the remainder of the titration. After titration the pH of the solution was lowered to approximately pH 3.5 again giving a red solution. The solution was then re-titrated giving an identical curve.

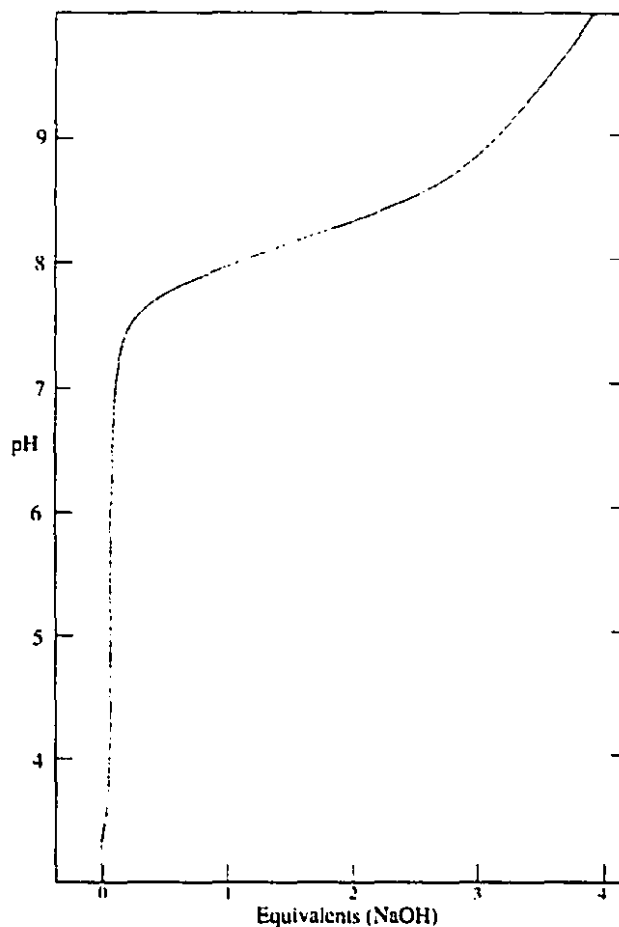


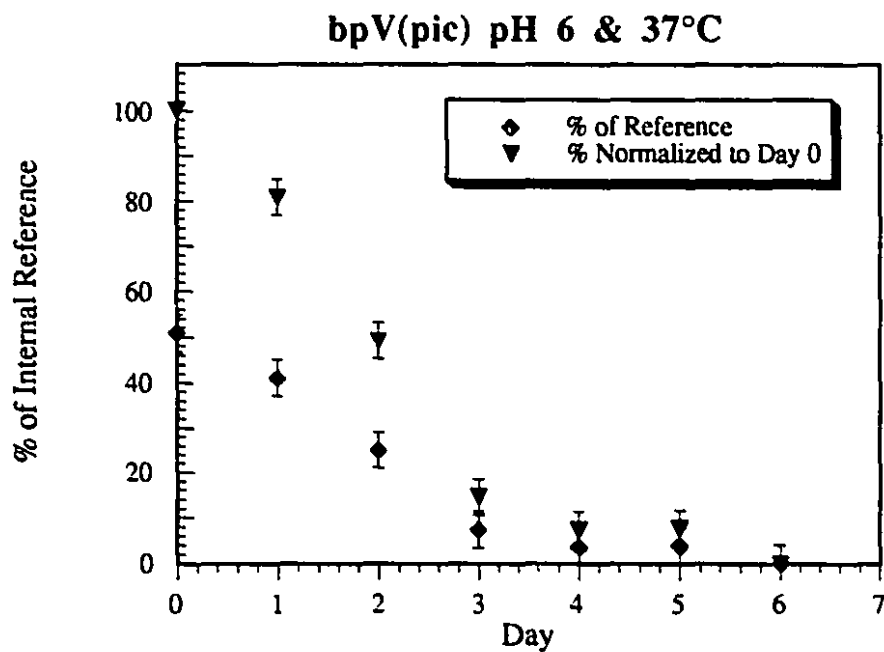
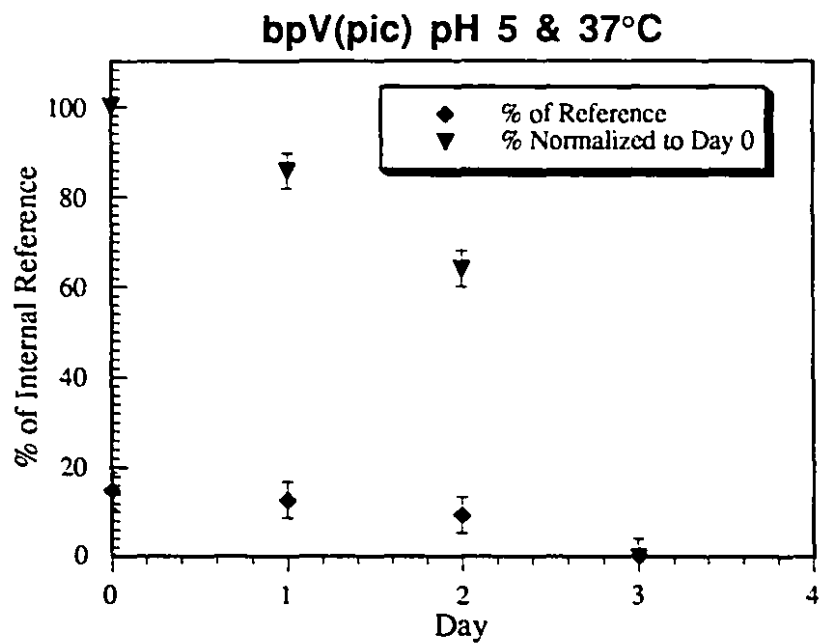
Figure 3.2.1. Figure showing the curve for the titration of mpV(2,6-pdc) (12 mM) with NaOH (0.10 M). Gradations on the abscissa correspond to 0.10 mL titrant.

Titration mpV(2,6-pdc) with NaOH (aq) showed that, to a rough approximation, four equivalents of base were consumed in going from pH 3.5 to 10. The red colour that returned upon re-acidification of the solution to a pH of 3.5 could be attributed to either the reformation of the mpV(2,6-pdc) species or the formation of the red VO_2^+ species. Upon re-titrating the solution however an essentially identical curve was obtained. If the red species had been VO_2^+ the titration curve would have shown evidence of the free ligand. The compound $\text{NH}_4[\text{VO}_2(2,6\text{-pdc})(\text{H}_2\text{O})]^{10}$ (V(2,6-pdc)) is colourless and shows a different titration curve (Figure 3.2.2) with base consumption at a lower pH therefore this would not be the predominant species in the re-acidified solution. Thus the decomposition

of mpV(2,6-pdc) in basic solutions occurs with the consumption of base and is reversible if the pH is promptly lowered. The results of the titration are consistent with the decreased stability of mpV(2,6-pdc) at higher pH.

3.2.1.b. bpV(pic):

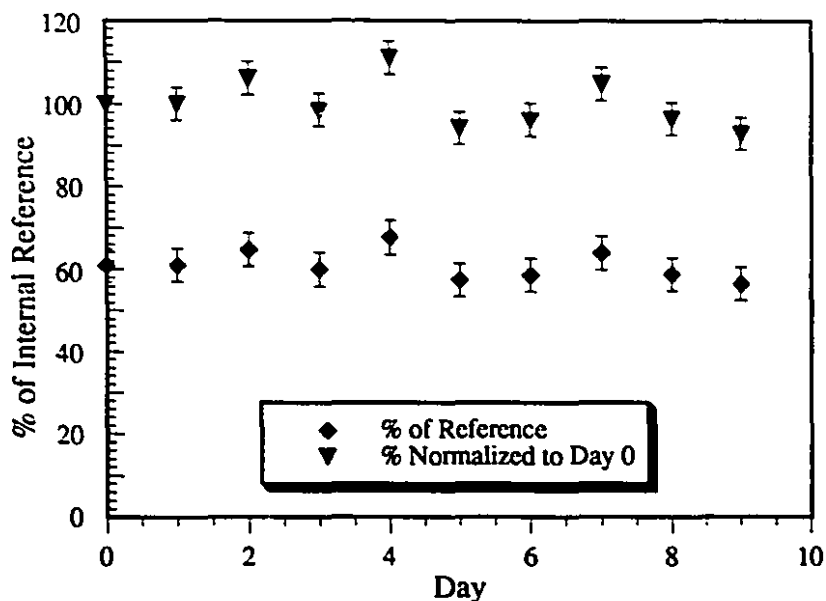
The signal for bpV(pic) appeared at -744 ppm in the ^{51}V NMR spectrum. An additional peak at either -700 ppm or -717 ppm depending on pH is generally observed in the ^{51}V spectrum of bpV(pic). The relative areas of the peak at -700 ppm or -717 ppm and the peak at -740 ppm vary with concentration and pH. The peaks at -700 ppm and -717 ppm have been assigned to pV species in which the ligand has dissociated from the bpV(pic), most likely an aquo species ^{11,12}



Graph 3.2.5 and Graph 3.2.6. Graphs showing the stability of bpV(pic) relative to an internal reference as determined by ^{51}V NMR at pH 5 and 6 and 37°C. Graphs show both the percentage of the integration of the bpV(pic) relative to the reference (◆) and also the percent of the initial concentration of bpV(pic) normalized to day zero (▼).

At pH 4 no signal for bpV(pic) was observed in the ^{51}V NMR spectrum within 2 hours of the addition of the complex. At pH 5 signals at -717, -690, and -631 ppm were observed in addition to the peak at -743 ppm corresponding to bpV(pic). The bpV(pic) signal decreased with time while the other peaks grew, with the peak at -631 ppm growing at the greatest rate. By day 3 no signal was observed for bpV(pic) and a new peak had appeared at -597 ppm. On day 4 two new peaks at -514 and -543 ppm appeared and grew in area throughout the course of the study until by day 9 only these two peaks and a small peak at -631 ppm remained. At pH 6 the ^{51}V NMR spectrum at day zero showed peaks at -717, -691, and -631 ppm in addition to the peak corresponding to bpV(pic). With time the peak at -631 ppm grew while the peak corresponding to bpV(pic) decreased in area. By day 3 a new peak began to appear at -656 ppm and also at -557 ppm. On day 4 a new peak also appeared at -574 ppm. The peaks at -574 and -557 ppm continued to grow throughout the course of the study with concomitant decrease of all other peaks. The area of the peak at -631 ppm decreased the slowest throughout the study. On day 9 a new peak was observed at -547 ppm.

bpV(pic) pH 7 & 37°C



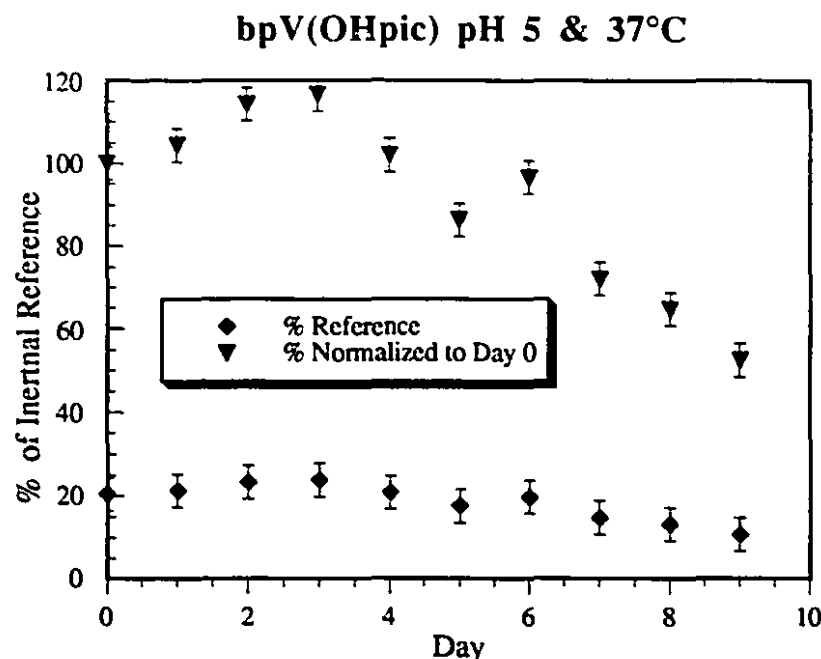
Graph 3.2.7. Graph showing the stability of bpV(pic) relative to an internal reference as determined by ^{51}V NMR at pH 7 and 37°C. Graphs show both the percentage of the integration of the bpV(pic) relative to the reference (◆) and also the percent of the initial concentration of bpV(pic) normalized to day zero (▼).

At pH 7 bpV(pic) showed essentially no decomposition. Two peaks were observed throughout the study, that for the bpV(pic) at -743 ppm and that of the diaquo pV species at -700 ppm. Near the end of the study a very small peak at -631 ppm was observed. No peaks corresponding to vanadates were observed.

Obviously bpV(pic) is very sensitive to pH. At pH 4 the bpV had completely decomposed in less than 2 h. At pH 5 there was very little bpV(pic) at day zero but there were peaks corresponding to an aquo pV species and also peaks around -631 ppm probably corresponding to a monoperoxovanadium compound.¹³ Decomposition of the bpV(pic) continued with 60% remaining by day 2 and with no bpV(pic) remaining by day 3. The decay as shown in graph 3.2.5 when normalized to 100% at day zero is somewhat misleading as the amount of bpV(pic) at day zero is certainly not 100% of the dissolved

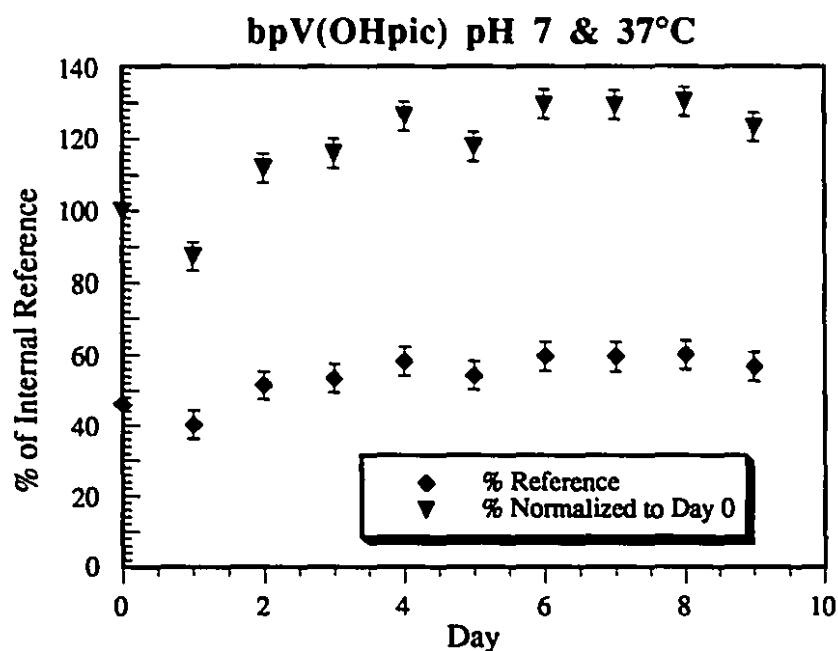
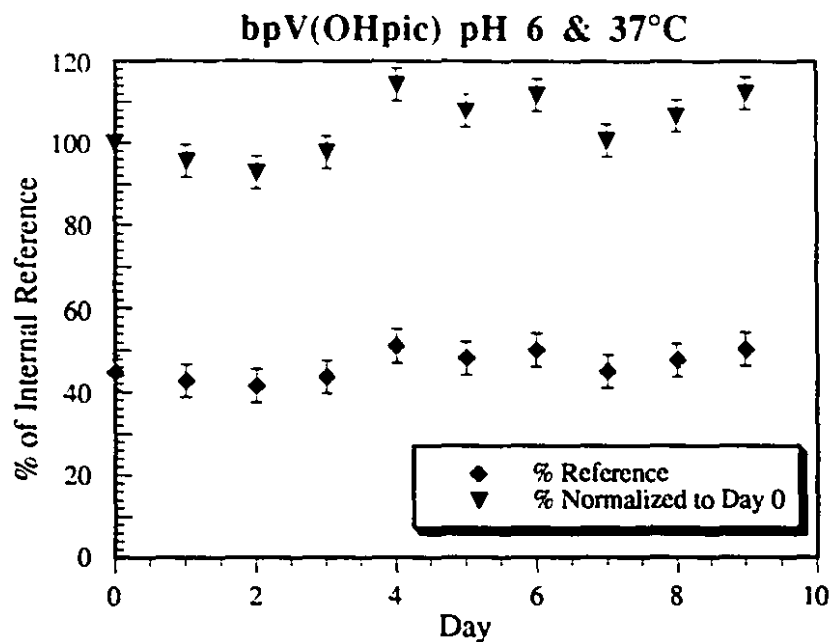
concentration. At pH 6 similar results were observed. At day zero there was a larger concentration of bpV(pic) relative to the internal reference than was observed at pH 5 but peaks of decomposition products were still observed. The bpV(pic) persisted until day 6 at pH 6. A peak in the monoperoxo region ¹³ persisted throughout the study and peaks in the vanadate region appeared and grew as the study progressed. With both the pH 6 and pH 5 samples, observations suggest that the first step in decomposition is a quick equilibrium or decomposition followed by a second, slower decomposition leading to vanadate products. This may be as a result of partial dissociation of the pic ligand resulting in some of the less stable aquo peroxovanadate species which then decomposes. At lower pH the pyridine nitrogen of any free pic ligand may be protonated resulting in a decreased binding affinity of the aquo bpV for it. This would shift any equilibrium that exists between the bpV(pic) and the ligand free aquo pV towards the less stable ligand free aquo species. The pKa of the pic ligand is 5.52¹⁴ therefore at pH 5 a significant amount of any free pic in solution would be protonated.

3.2.1.c. bpV(OHpic):



Graph 3.2.8. Graph showing the stability of bpV(OHpic) relative to an internal reference as determined by ^{51}V NMR at pH 5 and 37°C. Graphs show both the percentage of the integration of the bpV(OHpic) relative to the reference (◆) and also the percent of the initial concentration of bpV(OHpic) normalized to day zero (▼).

At pH 4 no signal for bpV(OH-pic) was observed in the ^{51}V NMR spectrum within 2 hours of the dissolution of the complex. At pH 5 the ^{51}V NMR spectrum at day zero showed peaks at -717, -689, and -624 ppm in addition to the peak corresponding to bpV(OHpic). The integration of the peak corresponding to bpV(OHpic) was quite low relative to the internal reference. For the first 3 days of the study the areas of these peaks remained relatively constant and after that the area of the bpV(OHpic) signal decreased and the area of the -717, -689, and -624 ppm peaks increased. No signals indicating the presence of vanadates were observed.



Graph 3.2.9 and Graph 3.2.10. Graphs showing the stability of bpV(OHpic) relative to an internal reference as determined by ^{51}V NMR at pH 6 and 7 and 37°C. Graphs show both the percentage of the integration of the bpV(OHpic) relative to the reference (◆) and also the percent of the initial concentration of bpV(OHpic) normalized to day zero (▼).

At pH 6 the ^{51}V NMR spectrum of bpV(OHpic) showed, in addition to the peak for bpV(OHpic), peaks at -691 and -717 ppm. Throughout the course of the study the spectra remained largely unchanged with no new peaks appearing and no significant changes in the relative areas of any of the signals. At pH 7 only two peaks are observed in the ^{51}V NMR spectrum, that from the bpV(OHpic) and a peak at -700 ppm. The spectra remained unchanged throughout the study and no new peaks are observed.

At low pH bpV(OHpic) is unstable and it immediately decomposes. At pH 5 the spectrum on day zero showed some bpV(OHpic). The amount of bpV(OHpic) remained relatively constant throughout the first 3 days and then decayed to approximately 50% of its initial concentration by day 9. No vanadate signals were observed by ^{51}V NMR throughout the course of the study, instead signals for other bpV and mpV species were present, although not positively identified, these species were probably aquo bis- and monoperoxovanadate species and possibly a monoperoxo OHpic species. A continuation of the study beyond 9 days would have likely shown the development of vanadates as the mpV species decomposed. At pH 6 the spectrum of bpV(OHpic) showed two peaks attributed to bpV species as well as the peak corresponding to bpV(OHpic). At pH 7 only the bpV(OHpic) signal and one other in the bpV region were observed. Both the pH 6 and pH 7 bpV(OHpic) samples showed essentially no change over the course of 9 days. As was the case with the bpV(pic) samples at pH 5 and 6, the bpV(OHpic) sample appeared to have undergone a rapid decomposition or rapidly established a new equilibrium, presumably for the same reasons as bpV(pic). The greater stability of bpV(OH-pic) at lower pH may be due to the lower pKa (~5.1) of the OHpic ligand.

Light is known to decompose pV compounds and it is possible that exposure to light may have resulted in shortened life spans of the complexes.¹⁵

3.2.2. Stability of bpV(phen) in the Absence of Light:

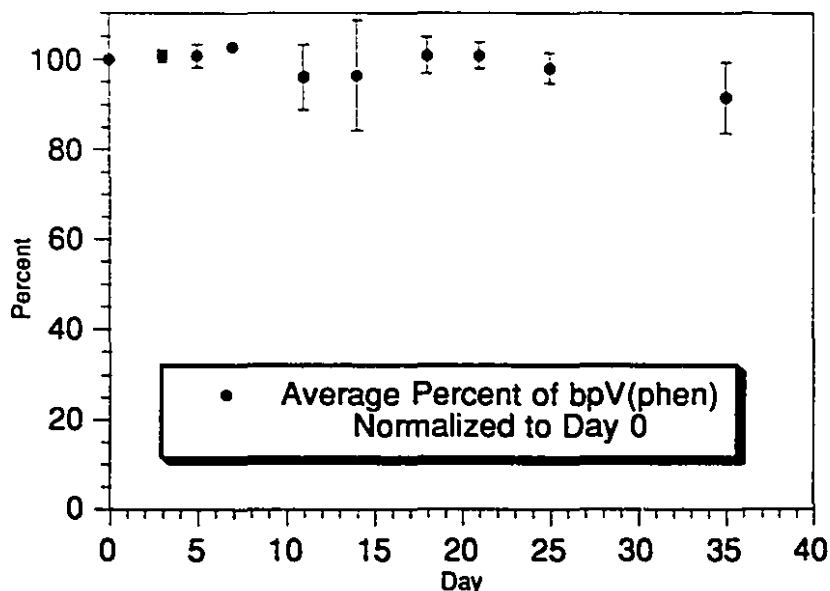
Samples of bpV(phen) at pH 7.4 (phosphate buffer) and room temperature were prepared and shielded from light. The stability of these samples was monitored by ^{51}V NMR.

Table 3.2.1 The stability of bpV(phen) relative to an internal reference as determined by ^{51}V NMR at pH 7.4 shielded from light. The data is for four samples each normalized to their concentration at day zero.

Day	Sample 1	Sample 2	Sample 3	Sample 4
0	100	100	100	100
3	99	101	102	100
5	104	99	101	99
7	103	103	103	102
11	103	89	101	90
14	108	80	102	95
18	105	75	100	98
21	104	71	100	98
25	97	66	102	95
35	84	41	100	91

The samples of bpV(phen) showed a very high degree of stability when shielded from light with almost no breakdown after 35 days except in the case of sample 2. The variation is not readily explained, applying Student's t-test at the 95% level of confidence allows for the exclusion of the sample 2 data from day 18 onward from analysis.

**Stability of bpV(phen) at pH 7.4
at room temperature (light shielded)**



Graph 3.2.11. Graph showing the stability of light shielded bpV(phen) relative to an internal reference as determined by ^{51}V NMR at room temperature and pH 7.4. Graphs show the average percent of the initial concentration of bpV(phen) normalized to day zero. Errors correspond to ± 1 standard deviation.

The study of bpV(phen) at pH 7.4 and shielded from light served not only to show the long life of these compounds but also showed the potential for variability for seeming unexplainable reasons. One of the four samples had decayed by 60% after 35 days while the other samples had on average decayed by only 8%. Crans et al. noted that studies of the stability of bpV(pic) showed some variability also although she reported the complete decomposition of the bpV(pic) in water in less than 1 day.⁴ Although these compounds do have a long life in aqueous solution particularly when shielded from light the potential for variability should be noted when preparing solutions for *in vivo* testing especially when given in the drinking water of test animals. Preparation of fresh solutions daily is advisable although it is clear from the data that if reasonable precautions are taken solutions may survive much longer.

3.2.3. The Interaction of Vanadate, V(2,6-pdc), and bpV(phen) with EDTA:

The interaction of EDTA, an additive to some biological buffer systems, with bpV(phen), V(2,6-pdc), and vanadate was investigated. Solutions of vanadate, V(2,6-pdc) and bpV(phen) with equimolar amounts of EDTA were prepared in phosphate buffered solutions (approximately pH 7.4) and their ^{51}V NMR spectra compared to that of EDTA free controls.

The ^{51}V NMR spectrum of the sample containing only vanadate displayed a major peak at -574 ppm and a minor peak at -582 ppm corresponding to the tetra- and penta-vanadate species. The region from -550 to -570 ppm was broadened and ill defined, and a very small peak was observed at -510 ppm. The spectra obtained from the sample containing vanadate and EDTA showed a large broad peak at -517 ppm and peaks at -564, -574, and a small peak at -582 ppm. The peak at -517 ppm was approximately 1200 Hz wide at half peak height. The integration of the peak at -517 ppm was roughly three times that of the combined vanadate peaks .

The ^{51}V NMR spectra of samples containing only bpV(phen) and the sample containing bpV(phen) and EDTA were almost identical, both displayed a large peak at -745 ppm but the sample containing only bpV(phen) showed a very small peak at -714 ppm that peak was shifted to -704 ppm in the bpV(phen) EDTA mixture. The peak was however, almost insignificant in area relative to the peak at -745 ppm. No other peaks were observed.

The sample containing V(2,6-pdc) showed ^{51}V NMR signals indicating that it had partially decomposed to vanadate in the buffer solution (almost 50% decomposition).

Peaks in the ^{51}V NMR spectra appeared at -529 ppm and at -574 and -582 ppm. The sample containing the mixture of V(2,6-pdc) and EDTA however showed a large, broad peak at -517 ppm with a small shoulder at approximately -530 ppm and a very small peak at -562 ppm. Repetition of the experiment in the absence of buffer showed no decomposition of the V(2,6-pdc) in the absence of EDTA. The sample containing EDTA and V(2,6-pdc) showed a broad peak at -517 ppm, a well defined but somewhat weak shoulder at -529 ppm and 3 very small peaks at approximately -557, -571 and -574 ppm.

Titration of V(2,6-pdc) with NaOH from pH 3.5 to 10 showed a significant consumption of base at a pH of approximately 6 (Figure 3.2.2). After titration the pH of the solution was lowered to approximately pH 3.5 and re-titrated giving an identical curve. From this titration it is clear that V(2,6-pdc) reacts with a significant amount of base beginning at a pH of approximately 6 and is therefore not stable at elevated pHs.

The bpV(OHpic) only sample showed a major peak at -741 ppm as well as a peak at -715 ppm and a very small peak at -730 ppm. The spectrum of the sample containing the mixture of bpV(OHpic) and EDTA was similar to the spectrum of the EDTA free sample with the addition of 2 small peaks at -514 ppm (approx. 10% of the bpV(OHpic) peak) and a peak at -547 ppm (approx. 3% of the bpV(OHpic) peak).

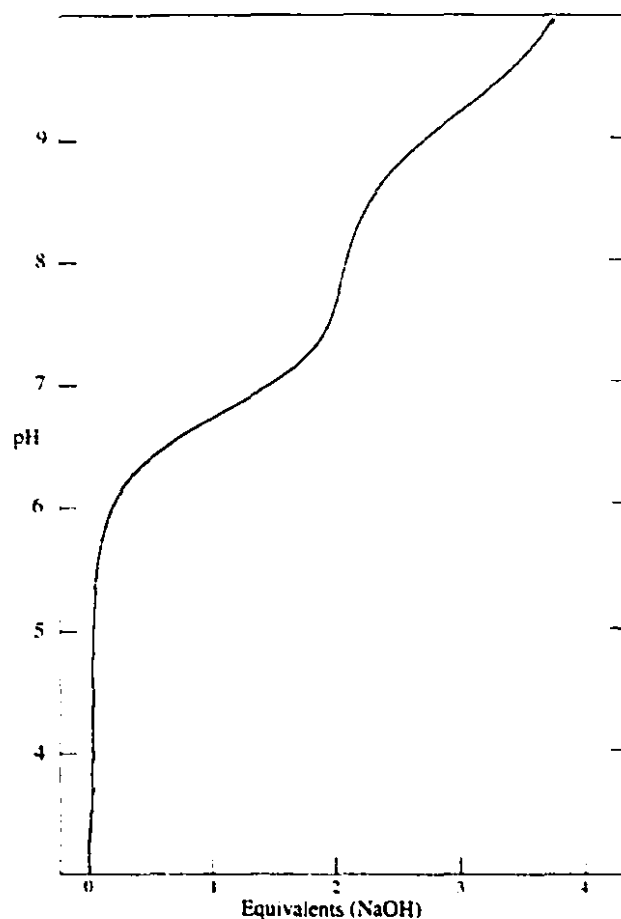


Figure 3.2.2. Figure showing the curve for the titration of V(2,6-pdc) (12 mM) with NaOH (0.10 M). Gradations on the abscissa correspond to 0.10 mL titrant.

The sample containing only bpV(pic) showed a major peak in the ^{51}V NMR at -743 ppm and two smaller peaks at -715 and -728 ppm. The spectrum of the mixture containing both bpV(pic) and EDTA was similar to that of the bpV(pic) only sample with the addition of 2 small peaks at -514 ppm (approx. 15% of the bpV(pic) peak) and a peak at -547 ppm (approx. 7% of the bpV(pic) peak).

The reaction of vanadate with EDTA is well known to give a 1:1 vanadate EDTA complex whose structure is shown in Figure 3.2.3.^{2,4,16} Indeed this was observed in this experiment when phosphate buffer was used.¹⁶ The vanadate complex V(2,6-pdc) also

reacted with EDTA. At neutral pH this compound partially decomposed to vanadates before the addition of EDTA. Addition of EDTA resulted in the formation of a new peak consistent with a vanadate EDTA complex.¹⁶ The V(2,6-pdc) contains the tridentate 2,6-pdc ligand which is displaced by the tetradentate EDTA ligand. The complex contains a water ligand that is easily lost. In contrast bpV(phen) is inert and showed no reaction with EDTA. Although the tetradentate binding of the EDTA may be thermodynamically favoured over the bidentate phenanthroline or picolinate ligands the substitutionally inert pV complex makes this process kinetically unfavourable. The reaction of bpV(pic) and bpV(OHpic) with EDTA led to the appearance of two relatively small peaks at -514 and -547 ppm. The compounds responsible of these peaks have not been identified but likely arise from the interaction of vanadate and EDTA. Although fairly inert both bpV(OHpic) and bpV(pic) exist in equilibrium with small amounts of aquo bisperoxovanadium species resulting from the dissociation of the heteroligand. These aquo complexes are labile and consequently some reaction with EDTA was observed.

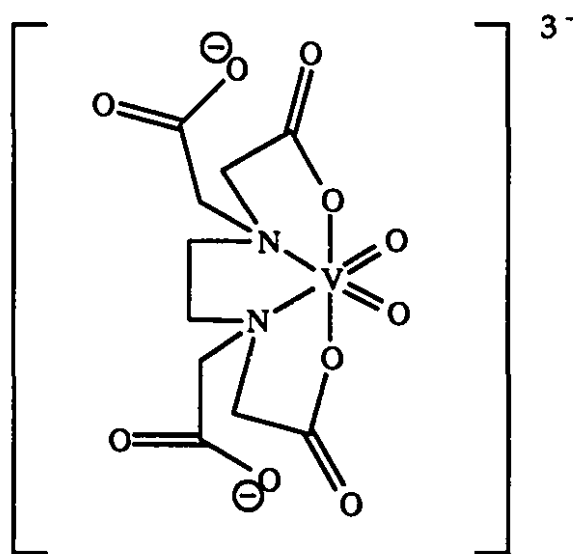


Figure 3.2.3. 1:1 vanadate EDTA complex¹⁶

3.2.4. The Interaction of Vanadate, bpV(phen), and bpV(OHpic) with DTT.

Reducing agents such as DTT or β -mercaptoethanol are common additives to biological buffer systems. These reducing agents protect against aerial oxidation and retain the reduced state of cysteine thiols, the reaction of cystine disulfides with DTT is shown in Figure 3.2.4. In order to determine the compatibility of these additives with pV compounds the effect of DTT on bpV(phen), bpV(OHpic) and vanadate at ratios of vanadium to DTT of 1:1, 1:2, 1:4, 2:1 and 4:1 was investigated. Samples were prepared at these ratios and then analyzed by ^{51}V NMR spectroscopy. The predominant features of the ^{51}V NMR spectra of the mixtures are summarized in Table 3.2.2. Spectra of the vanadium compounds were also run in the absence of DTT, the major peaks are as follows with the integrations (where appropriate) given in parenthesis: KVO_3 -582ppm (1.7), -575ppm, -570ppm (87.4, both peaks), -557ppm (16.5), bpV(OHpic) -741ppm (99.8), -695ppm (25.4), bpV(phen) -746ppm.

Table 3.2.2. Table summarizing the ^{51}V NMR spectra of mixtures of bpV(phen), bpV(OHpic) and KVO_3 with DTT.

Ratio PV (or KVO_3):DTT	bpV(phen) (integration)	bpV(OHpic) (integration)	KVO_3 (integration)
4:1	Major peak at -746ppm (70.4) and vanadate peaks (29.5)	Major peak at -741ppm (47.1), peak at -702ppm (14.9) corresponding to the diaquodiperoxovanadate species, vanadate peaks (20.3), and a peak at -625 ppm (12.8)	Vanadate peaks (48.6) a peak at -522ppm (6.1) and peaks at -346ppm and -357ppm (21.5) and a peak at -396ppm (7.1)

2:1	Major peak at -746ppm (60.6) and vanadate peaks (44.0)	Predominantly vanadate peaks with a broad peak centered at -535ppm (62.0 all peaks), peak at -741ppm (17.9), and a peak at -625ppm (13.8)	Vanadate peaks (38.4) a peak at -522ppm (14.4) and peaks at -346ppm and -357ppm (47.6) and a peak at -396ppm (17.8)
1:1	Peak at -746ppm (39.6) and vanadate peaks (61.3)	Predominantly vanadate peaks with a broad peak centered at -535ppm (79.4 all peaks), a peak at -741ppm (10.5), and a small peak at -625ppm (11.1)	Vanadate peaks (7.6) a peak at -522ppm (16.1) and peaks at -346ppm and -357ppm (49.8) and a peak at -396ppm (17.3)
1:2	Many peaks in the vanadate region: -575ppm, -567ppm, -544ppm, -532ppm, -520ppm (72.9 for all peaks) and peaks at -394ppm (6.9) and -350ppm (12.2)	Sharp peaks at -521ppm and -557ppm and a broad peak in the vanadate region (55.8 all peaks), peaks at -347ppm and -357ppm (55.0) and a peak at -395ppm (20.9)	Peak at -522ppm (10.8) and peaks at -346ppm and -357ppm (35.7) and a peak at -396ppm (10.5)
1:4	no signal observed	no signal observed	no signal observed

The reaction observed for vanadates and DTT was consistent with the observations of Crans et al. for the reaction of vanadates with β -mercaptoethanol, another thiol based biological reducing agent.⁴ At the ratio of 4:1 DTT to vanadate no signals were observed by ^{51}V NMR after 40 min reaction. This is consistent with reduction to an NMR silent vanadyl species. As the ratio of DTT to vanadate was increased from 1:4 to 2:1 the

vanadate peaks decreased and new peaks were observed at -522, -396, -357, and -346 ppm. Crans et al. reported a peak at -356 ppm for the reaction of vanadate with β -mercaptoethanol, the peak we observe at -357 ppm is consistent with the formation of a similar vanadate sulfur compound.⁴

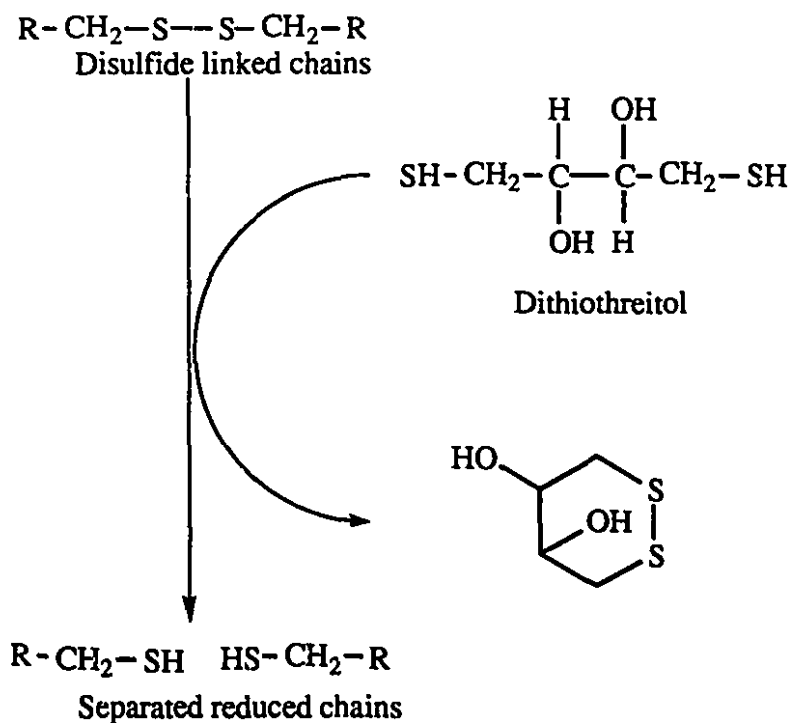


Figure 3.2.4. The reaction of DTT with cysteine.

The two bisperoxovanadium complexes, bpV(phen) and bpV(OHpic), both reacted with DTT. At a ratio of 4:1 DTT to bpV complex both showed no signals, presumably having been reduced to a vanadyl species. The complex bpV(phen) appeared to be less sensitive to reduction by DTT than bpV(OHpic). At a ratio of 2:1 DTT to bpV the ^{51}V NMR spectrum of the bpV(phen) complex showed mostly peaks in the vanadate region with two additional peaks at -394 and -350 ppm. At the same ratio of DTT to bpV the ^{51}V NMR of the bpV(OHpic) complex showed a greater proportion of peaks at -346, -357 and -395 ppm relative to the vanadate peaks than the bpV(phen) complex. At 2:1 DTT to bpV neither the phen or OHpic complex showed any ^{51}V NMR signals in the bpV region. This

is consistent with the observations by Crans et al. with bpV(pic) and β -mercaptoethanol at this ratio. At a concentration of 1:1 DTT to bpV the ^{51}V NMR of the bpV(phen) sample showed both vanadate peaks and the bpV(phen) peak at a ratio of roughly 2:1. At the same ratio of DTT to bpV the ^{51}V NMR of the bpV(OHpic) solution showed only a weak signal for the bpV(pic) species but did show peaks in the vanadate region and also a peak at -625 ppm consistent with a monoperoxovanadate species.¹³ At a ratio of 1:2 DTT to bpV(phen) only peaks due to bpV(phen) and vanadates were observed in the ^{51}V NMR spectrum of this sample whose integrations were at a ratio of 3:2. Similarly at 1:4 DTT to bpV(phen) only peaks for bpV(phen) and vanadates were observed in the ^{51}V NMR spectrum whose integrations were at a ratio of 2:1. At 1:2 and 1:4 ratios of DTT to bpV(OHpic) peaks not only for vanadates and bpV(OHpic) were observed but also a peak at -625 ppm consistent with a mpV species.¹³ At the 1:4 ratio of DTT to bpV(OHpic) a signal in the ^{51}V NMR consistent with an aquo bpV species was observed that was not present in the ^{51}V NMR spectra at the 1:2 DTT to bpV(OHpic) sample. Clearly pV compounds are not compatible with reducing agents such as DTT. In biological assays that require proteins be protected from aerial oxidation the use of deoxygenated solvents and inert gas is recommended.

The enhanced stability of bpV(phen) relative to bpV(OHpic) may be in part due to an equilibrium existing between the bpV(OHpic) and the ligand-free aquo bpV species. The labile aquo species may be more reactive towards DTT than the ligand bound species. The absence of a peak for a monoperoxo species in the ^{51}V NMR spectra of any of the bpV(phen) samples may indicate that the monoperoxo species is more reactive than the bpV(phen) and that upon its formation reacts with any DTT remaining in solution. In the reaction of bpV(OHpic) with DTT, particularly when the bpV(OHpic) is in excess relative to DTT, reaction may be occurring rapidly with an aquo bisperoxovanadate species giving a monoperoxo species. The monoperoxovanadium species would then compete with the

aquo species for reaction with DTT giving the observed mixture of monoperoxo and bisperoxo peaks in the ^{51}V NMR spectra.

3.2.5. The Interaction of bpV(OHpic) with HEPES, MOPS and Phosphate Buffers.

Solutions of bpV(OHpic) (0.05 M) were prepared in pH 7.4 HEPES, MOPS and phosphate buffers (0.1 M) as well as a control solution in distilled water. After 1 day the solutions were analyzed by ^{51}V NMR in order to determine the stability of bpV(OHpic) in the buffer solutions. The phosphate buffered solution showed a peak at -740 ppm corresponding to the bpV(OHpic) as well as peaks at -728 and -717 ppm corresponding to aquo bpV species.^{11,12} The proportion of aquo bpV species to bpV(OHpic) was approximately 1:1.5. The MOPS sample showed two peaks in the ^{51}V NMR at -740 ppm and at -711 ppm consistent with bpV(OHpic) and an aquo bpV species. The relative concentrations of the bpV(OHpic) to aquo bpV species was approximately 1:2.5. The sample containing bpV(OHpic) in HEPES buffer showed peaks in the ^{51}V NMR corresponding only to mono-, di-, tetra-, and pentavanadates at -556, -570, -574, and -584 ppm respectively, the bpV(OHpic) having completely decomposed.

3.2.6. The Interaction of bpV(pic) and bpV(OHpic) with HEPES and MOPS at Varying Ratios of pV:buffer.

Solutions of bpV(pic) and bpV(OHpic) were prepared in pH 7.4 HEPES and MOPS buffers at varying ratios. Control samples in distilled water were also prepared. After 1 h and 6.5 h the ^{51}V NMR spectra of the samples were compared to the controls to determine the effects of buffer concentration on pV stability. ^{51}V NMR spectra obtained approximately 1 h after addition of the bpV compounds to the buffer solutions showed only

slight differences from the spectra of the control solutions. There was no observable decomposition of any of the samples but some differences in the chemical shifts of certain peaks were evident.

3.2.6.a. bpV(OHpic):

HEPES Buffer

The control samples (one sample at the vanadium concentration in the 50:1 sample and one at the vanadium concentration in the 10:1 and 2:1 samples) showed peaks at -741 ppm in the ^{51}V NMR spectrum corresponding to bpV(OHpic). The 50:1 control showed a broad peak corresponding to the aquo bpV species at -701 ppm whereas the aquo bpV peak appeared as a broad peak at -706 ppm in the spectrum of 10:1 and 2:1 controls. In the 50:1, 10:1, and 2:1 HEPES:bpV(OHpic) samples the aquo bpV peak sharpened and was observed at -709, -707 and -706 ppm respectively. No decomposition to vanadates was observed.

Approximately 6.5 h later some decomposition of bpV(OHpic) was observed in the HEPES buffer solutions that was not observed in the control solutions. In the 50:1 HEPES:bpV(OHpic) sample, a new peak at -556 ppm was observed whose integration corresponded to approximately 15% of the total integration for the aquo bpV peak and bpV(OHpic) peaks combined. The 10:1 HEPES:bpV(OHpic) sample showed a very small vanadate peak at -556 ppm corresponding to less than 1% of the total integration for the aquo bpV peak and bpV(OHpic) peaks combined. The 2:1 HEPES:bpV(OHpic) sample, showed no decomposition to vanadate.

MOPS Buffer

In the ^{51}V spectra of the 50:1, 10:1, and 2:1 MOPS:bpV(OHpic) samples the aquo bpV peak sharpened relative to the controls and was observed at -714, -711 and -708 ppm respectively. No decomposition to vanadates was observed.

After approximately 6.5 h some decomposition of bpV(OHpic) was observed in MOPS buffer solutions that was not observed in the control solutions. In the 50:1 MOPS:bpV(OHpic) sample a new peak at -556 ppm was observed whose integration corresponded to approximately 4% of the total integration for the aquo bpV peak and bpV(OHpic) peaks combined. Neither the 10:1 MOPS:bpV(OHpic) sample nor the 2:1 MOPS:bpV(OHpic) sample showed any significant decomposition to vanadate.

3.2.6.b. bpV(pic):

HEPES Buffer

The results for bpV(pic) dissolved in HEPES and MOPS buffer were very similar to the corresponding bpV(OHpic) results. ^{51}V NMR spectra obtained approximately 1 h after addition of the bpV(pic) to the buffer solutions showed only slight differences from the spectra of the control solutions. There was no observable decomposition of any of the samples but some differences in the chemical shifts of certain peaks was evident. The control samples (50:1, 10:1 and 2:1) showed peaks at -743 ppm in the ^{51}V NMR spectrum corresponding to bpV(pic). The 50:1 control showed a broad peak corresponding to the aquo bpV species at -702 ppm whereas the aquo bpV peak appeared as a broad peak at -711 ppm in the spectrum of the 10:1 and 2:1 control. The 10:1 and 2:1 control showed a very small peak at -630 ppm consistent with a monoperoxo species. In the 50:1, 10:1, and 2:1 HEPES:bpV(pic) samples the aquo bpV peak sharpened and was observed at -709,

-707 and -707 ppm respectively. Peaks were observed at -630 ppm in the 10:1 and 2:1 sample spectra but these were observed at a similar intensity in the control sample. No decomposition to vanadates was observed in any of these samples.

Approximately 6.5 h after addition of bpV(pic) to the buffer and control solutions some decomposition of bpV(pic) was observed in the buffer solutions that was not observed in the control solutions. The 50:1 HEPES:bpV(pic) sample showed a new peak at -556 ppm was observed whose integration corresponded to approximately 16% of the total integration for the aquo bpV peak and bpV(OHpic) peaks combined. The 10:1 HEPES:bpV(pic) sample and the 2:1 HEPES:bpV(pic) sample showed no significant decomposition to vanadate.

MOPS Buffer

In the ^{51}V spectra of the 50:1, 10:1, and 2:1 MOPS:bpV(pic) obtained after 1 h, the aquo bpV peak sharpened relative to the controls and was observed at -713, -711 and -708 ppm respectively. Small peaks were observed at -630 ppm in the 10:1 and 2:1 samples but these were observed at a similar intensity in the control sample. No decomposition to vanadates was observed.

Approximately 6.5 h after addition of bpV(pic) to the buffer and control solutions no significant decomposition of bpV(pic) was observed in the MOPS buffer solutions that was not observed in the control solutions.

The stability of bpV compounds in biological buffer systems is of importance for the design of experiments involving bpV compounds. The use of HEPES buffer with vanadate has been recommended by Crans.⁴ In ^{51}V NMR studies of the interaction of bpV(pic) and bpV(OHpic) with HEPES and MOPS at physiological pH it was observed

that as the relative concentration of HEPES to bpV was increased so too did the rate of decomposition of the bpV.

Crans et al. reported an enhanced stability of bpV(pic) in HEPES buffer relative to an unbuffered solution of bpV(pic).⁴ The concentrations of HEPES and bpV(pic) were 15-20mM and 10 mM respectively corresponding to a ratio of approximately 2:1 buffer to bpV(pic). At such a ratio of buffer to reagent the buffer would be relatively ineffective in controlling pH. In assays of PTP inhibition by pV compounds concentrations of pV are on the order of 10^{-6} or 10^{-7} M.¹⁷ Under these conditions the buffer would be in great excess of the pV. Stability testing at higher ratios of buffer to bpV therefore provide information more applicable to use in the design of biological assays.

There seems to be little decomposition of bpV compounds in phosphate buffer although phosphate is known to interact with vanadate.⁴ The ^{51}V NMR of bpV compounds that show equilibrium mixtures of both the ligand free and ligand bound bpV complexes shows additional peaks in the aquo bpV region when dissolved in phosphate buffer solutions. This may be as a result of interactions between aquo bpV complexes and phosphate but this has not been confirmed.

The reason for the decreased stability of bpV compounds in HEPES relative to MOPS may be as a result of the pendant hydroxyl group on HEPES. It has been observed that catechols readily reduce bpV complexes to give vanadates¹⁸ and the oxidation of primary and secondary alcohols by pV complexes has also been reported.¹ The pendant hydroxyl of HEPES may act as a reducing agent being oxidized to an aldehyde by pV compounds giving vanadate. MOPS however does not have a alcohol group and thus is not prone to such an oxidation.

The use of phosphate or MOPS buffer is indicated for use at physiological pH. At other pH's the use of buffers containing alcohol groups that could act as reductants or secondary amines that could coordinate to the vanadium atom is not recommended. An example of a reasonable buffer is MES (pKa=6.1), whose structure is given in Figure 3.1.1.

3.2.7. The Interaction of bpV's with Catalase:

Catalase is an enzyme that catalyzes the disproportionation of hydrogen peroxide to oxygen and water. The reaction of the compounds bpV(OHpic), bpV(pic), and bpV(phen) with bovine liver catalase in pH 7.4 phosphate buffered solutions was investigated by ^{51}V NMR. The integration for all bpV species was compared to that of an internal reference. Since the reaction is enzymatic only the concentration of the bpV is changing. Therefore the reactions can be treated as pseudo first order and pseudo first order rate constants (k_1) can be calculated independently of the initial concentration of the bpV.¹⁹ Second order rate constants (k_2) can be calculated from the pseudo first order rate constants using the concentration of catalase (units L^{-1})^{*}. The data were fitted to the equation $C=C_0 \times e^{-kt}$ for approximately 3 half lives ($t=0$ values not included) and the value of k used in the determination of rate constants. Plots of the natural logarithm of the relative area of the bpV peaks against time are also shown. A typical series of NMR spectra are shown in figure 3.2.5.

* The activity of catalase is reported by Sigma in units/mg of protein where one unit decomposes one micromole of H_2O_2 /min at pH 7 and 25°C from a concentration of H_2O_2 of 10.3-9.2 mM.

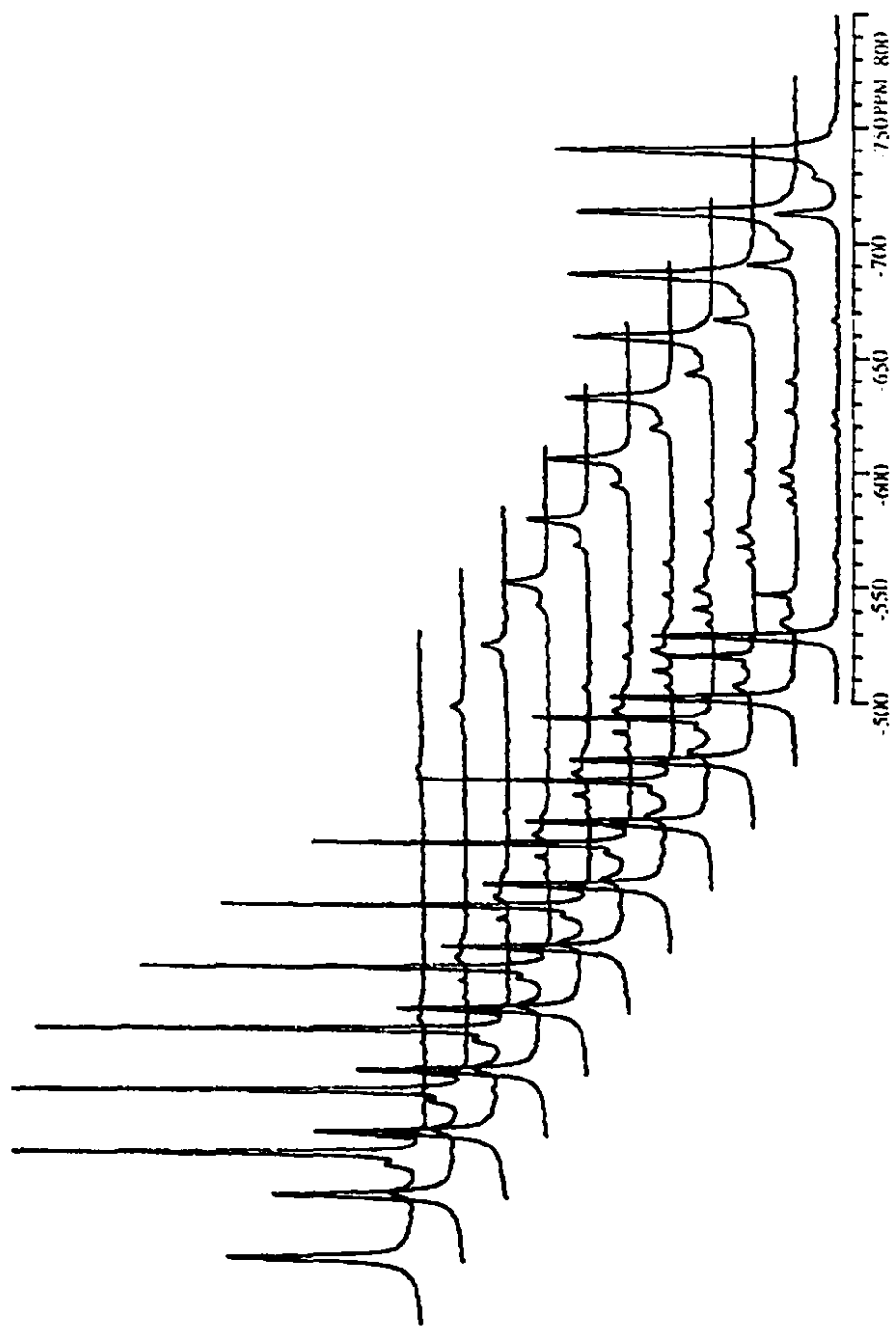
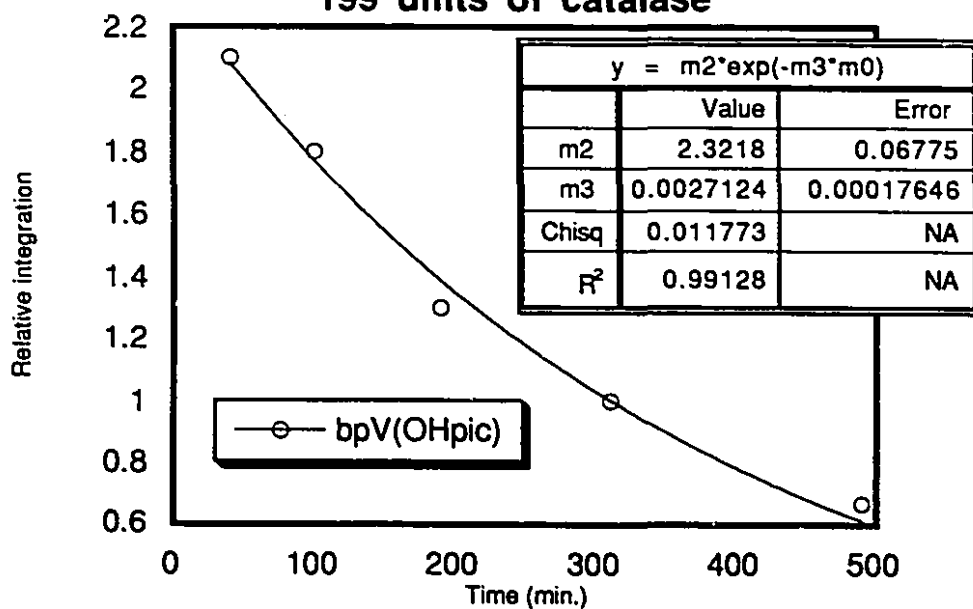
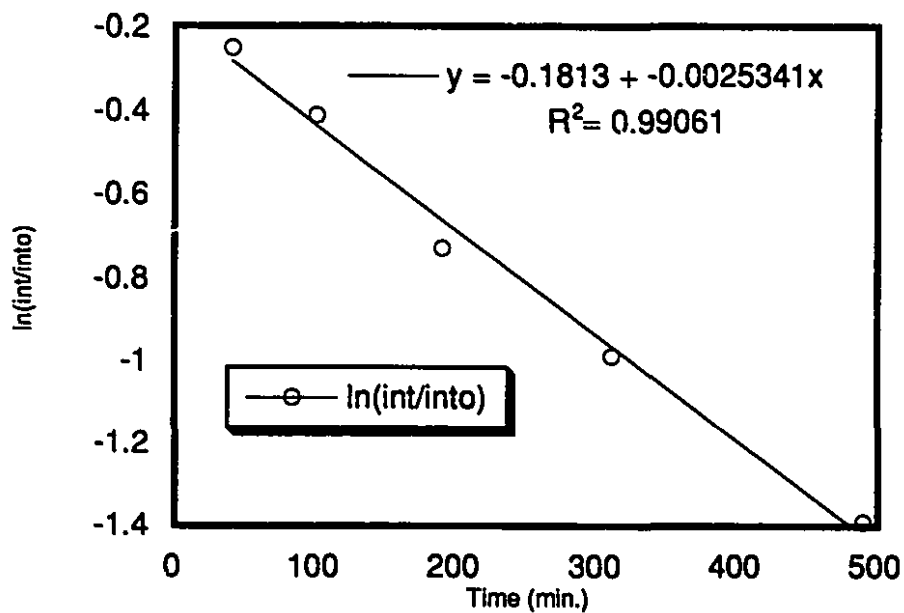


Figure 3.2.5. Typical stacked plot of a the kinetic analysis of the reaction of bpV(OHpic) with catalase by 51V NMR.

Sample #1 The reaction of bpV(OHpic) with 199 units of catalase

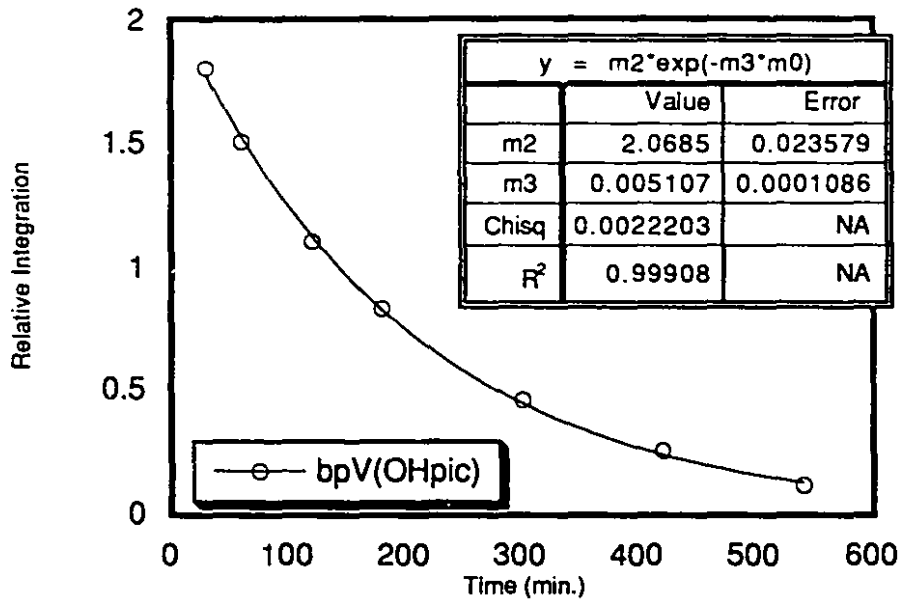


Sample #1 The reaction of bpV(OHpic) with 199 units of catalase. log plot

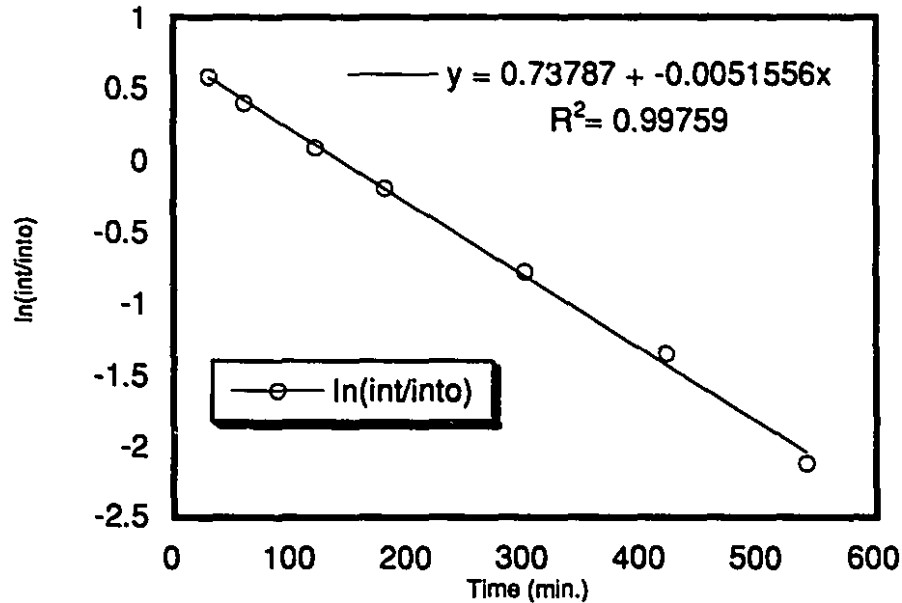


Graphs 3.2.12 and 3.2.13. Graphs of the relative integration of the bpV peaks of a bpV(OHpic) solution with 199 units of catalase fitted to the first order rate equation and a log plot of the same data.

Sample #2 The reaction of bpV(OHpic) with 410 units of catalase.

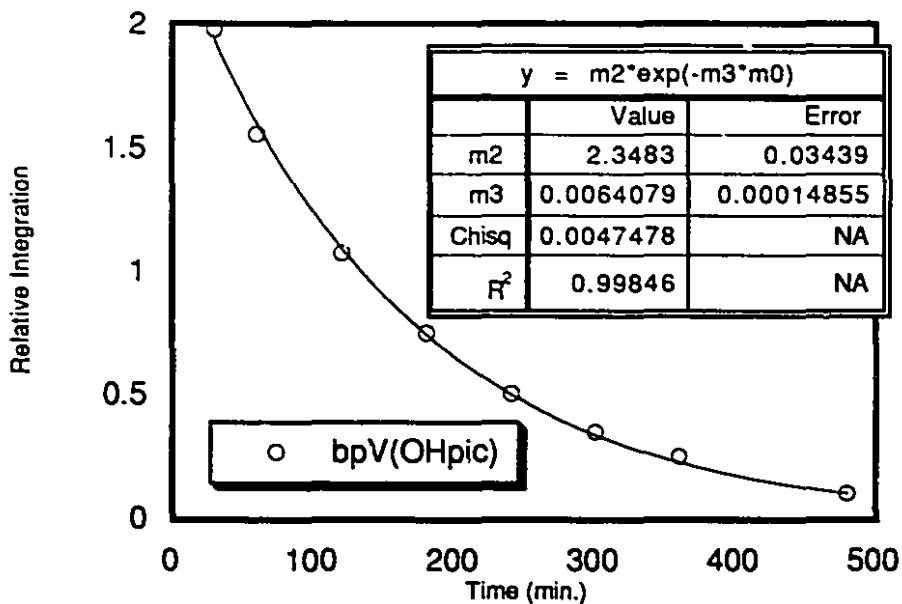


Sample #2 The reaction of bpV(OHpic) with 410 units of catalase. log plot

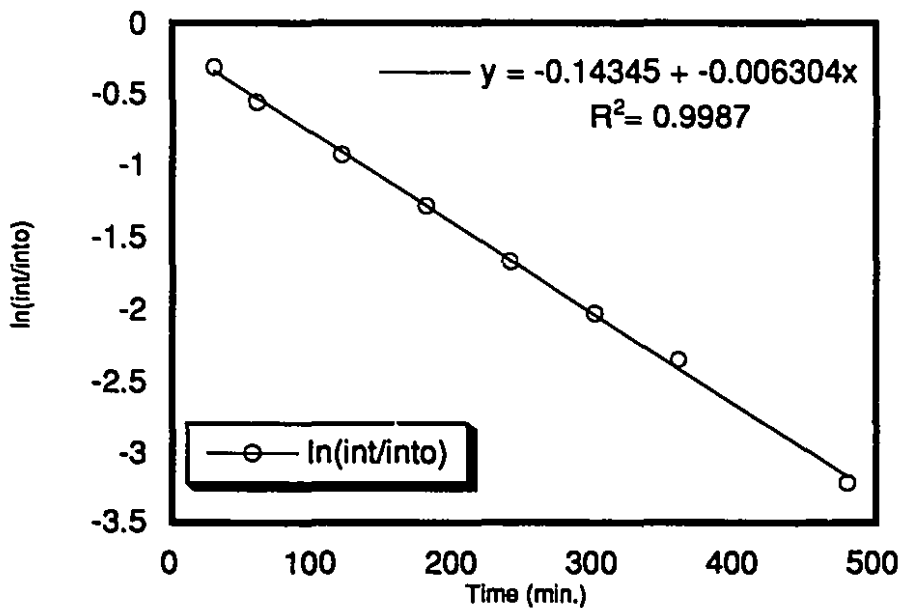


Graphs 3.2.14 and 3.2.15 Graphs of the relative integration of the bpV peaks of a bpV(OHpic) solution with 410 units of catalase fitted to the first order rate equation and a log plot of the same data.

Sample #3 The reaction of bpV(OHpic) with 450 units of catalase.

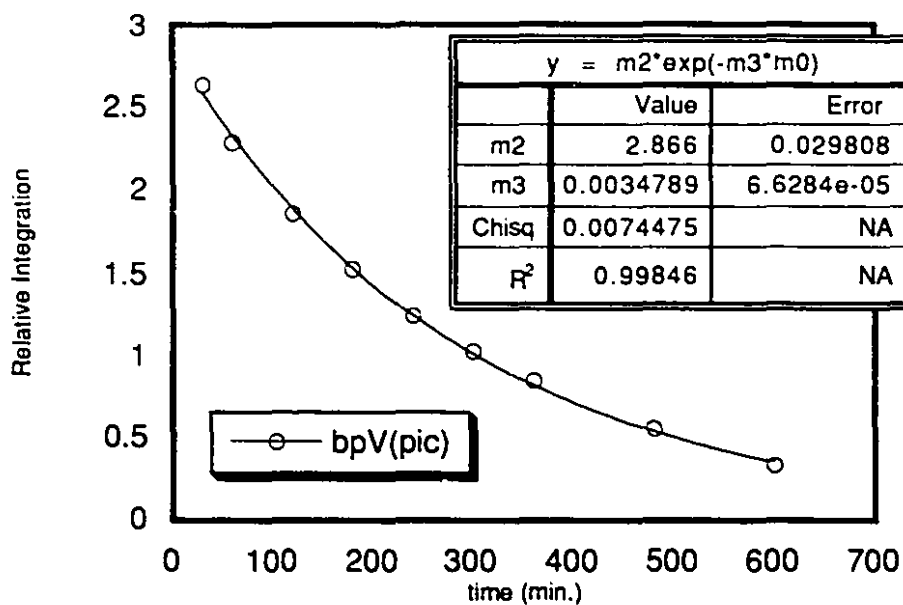


Sample #3 The reaction of bpV(OHpic) with 450 units of catalase. log plot

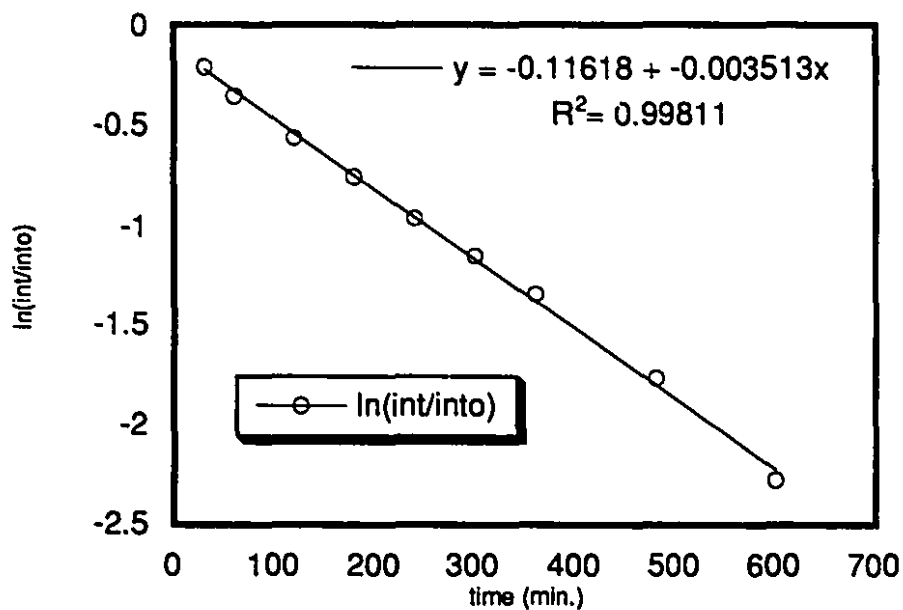


Graphs 3.2.16 and 3.2.17. Graphs of the relative integration of the bpV peaks of a bpV(OHpic) solution with 450 units of catalase fitted to the first order rate equation and a log plot of the same data.

Sample #4 The reaction of bpV(pic) with 394 units of catalase.

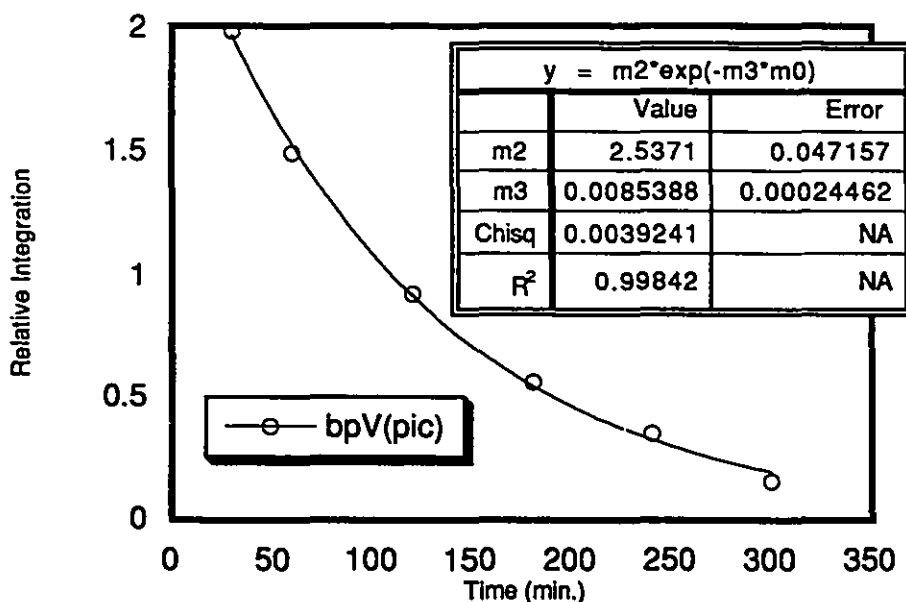


Sample #4 The reaction of bpV(pic) with 394 units of catalase. log plot

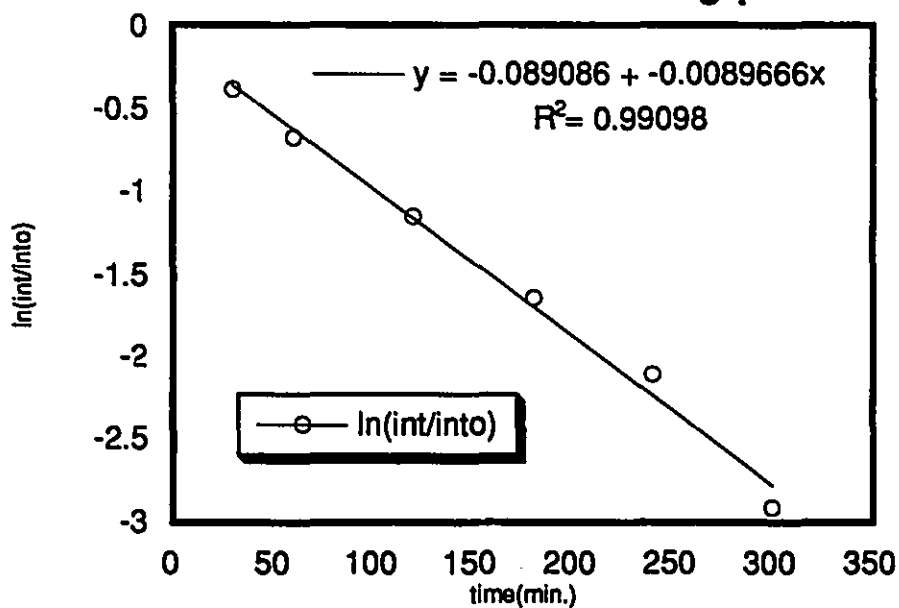


Graphs 3.2.18 and 3.1.19. Graphs of the relative integration of the bpV peaks of a bpV(pic) solution with 394 units of catalase fitted to the first order rate equation and a log plot of the same data.

Sample #5 The reaction of bpV(pic) with 884 units of catalase.

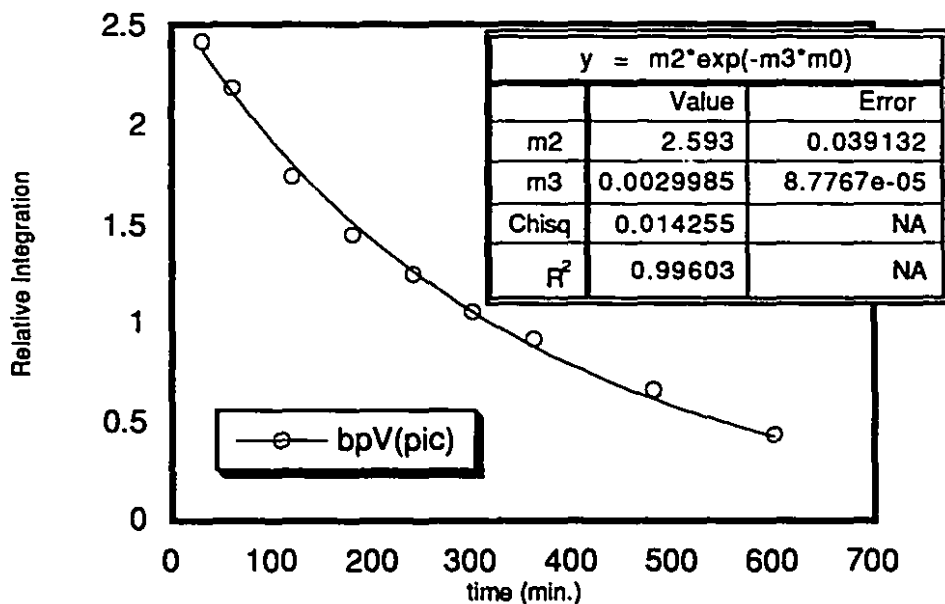


Sample #5 The reaction of bpV(pic) with 884 units of catalase. log plot

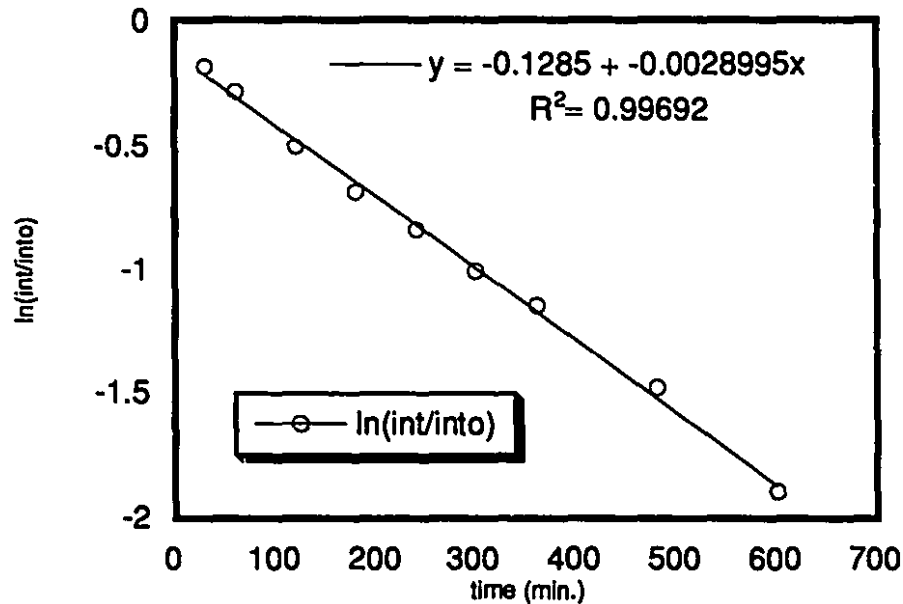


Graphs 3.2.20 and 3.2.21. Graphs of the relative integration of the bpV peaks of a bpV(pic) solution with 884 units of catalase fitted to the first order rate equation and a log plot of the same data.

Sample #6 The reaction of bpV(pic) with 426 units of catalase and 0.1 wt% BSA.



Sample #6 The reaction of bpV(pic) with 426 units of catalase and 0.1 wt% BSA. log plot



Graphs 3.2.22 and 3.2.23. Graphs of the relative integration of the bpV peaks of a bpV(pic) solution with 426 units of catalase in 0.1wt% BSA fitted to the first order rate equation and a log plot of the same data.

The rate constants derived from the plots above are summarized in Table 3.2.3.

Table 3.2.3. Rate constants for the reaction of bpV(OHpic) and bpV(pic) with bovine liver catalase. Errors are estimated at $\pm 10\%$ of the rate constant.

Sample # (bpV, total units of catalase in the sample)	k_1 (min^{-1})	k_2 ($\text{units}^{-1} \text{ L min}^{-1}$)
#1 (bpV(OHpic), 199 units)	2.7×10^{-3}	9.7×10^{-9}
#2 (bpV(OHpic), 410 units)	5.1×10^{-3}	8.8×10^{-9}
#3 (bpV(OHpic), 450 units)	6.4×10^{-3}	1.0×10^{-8}
#4 (bpV(pic), 394 units)	3.5×10^{-3}	6.3×10^{-9}
#5 (bpV(pic), 884 units)	8.5×10^{-3}	6.9×10^{-9}
#6 (bpV(pic), 426 units) 0.1wt% BSA added	3.0×10^{-3}	5.0×10^{-9}

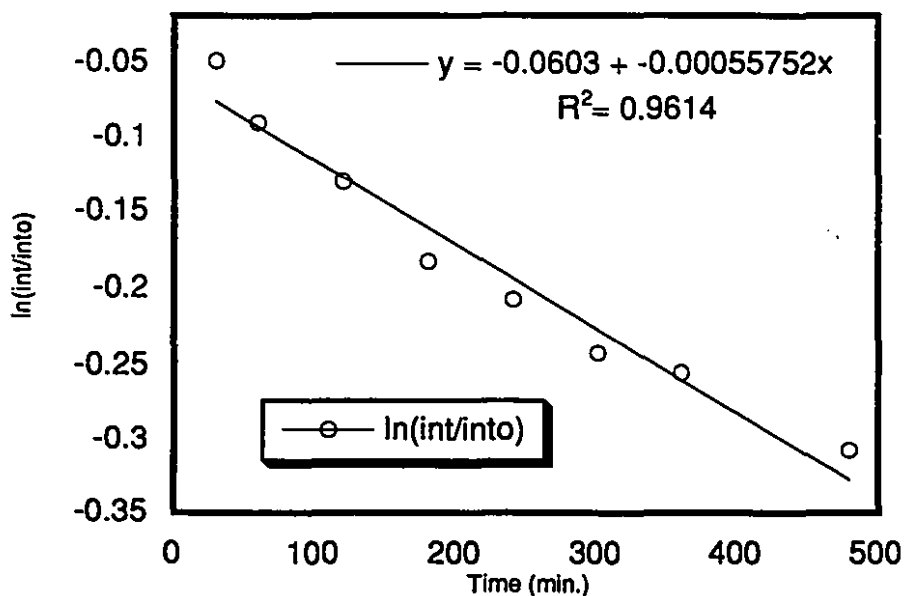
The reactions using bpV(phen) were not amenable to kinetic analysis. The reactions were markedly slower than the reactions with bpV(pic) and bpV(OHpic). Half lives for samples #7 (896 units of catalase) and #8 (1719 units of catalase) were both approximately 8 hours. Sample #9 (197 units of catalase) only showed 25% reaction after 8 hours.

Catalase reacted with peroxovanadium compounds to produce vanadates. The average second order rate constant for the reaction of catalase with bpV(OHpic) based on three determinations was found to be $9.6 \times 10^{-9} \text{ units}^{-1} \text{ L min}^{-1}$. This is slightly faster but not significantly different than the second order rate constant determined for the reaction of bpV(pic) and catalase which averaged $6.6 \times 10^{-9} \text{ units}^{-1} \text{ L min}^{-1}$ for two determinations. Errors on the rate constants are estimated at approximately $\pm 10\%$ based on the pipetting error for the addition of catalase. The rate for the reaction of bpV(pic) with catalase in 0.1

wt% BSA was somewhat slower with a second order rate constant of $5.0 \times 10^{-9} \text{ units}^{-1} \text{ L min}^{-1}$ but agreed with the bpV(pic) rate constant within experimental error. BSA is often added to biological buffer systems to prevent enzymes adhering to surfaces and thus reducing their effective concentration. The reduced rate of reaction in the presence of BSA indicates that such a loss of enzyme is probably not a factor in these assays. The decrease in rate may be due to interaction or association of the pV with the BSA leading to a lowering of its effective concentration. Indeed albumin is known to bind and transport metal ions *in vivo*.²⁰

The reaction of bpV(phen) with catalase was much slower than with either the bpV(pic) or bpV(OHpic). The half life of both samples #7 (796 units of catalase) and #8 (1719 units of catalase) was 8 h even though sample #8 had twice the concentration of catalase as in sample #7, in a pseudo first order system the rate of reaction of sample #8 would be expected to be double that of sample #7. This is not consistent with the reaction being first order in catalase unless the system was saturated in bpV(phen). Sample #9 (197 units of catalase) showed only 25% reaction after 8 hours and a plot of the natural logarithm of the relative integration of bpV(phen) versus time was not linear indicating the reaction was not first order. It is possible that the decomposition of catalase may be in part responsible for the deviation of the log plot from linearity. A number of factors could be responsible for the non pseudo first order behavior of the reaction. In such a slow reaction the decomposition of catalase under near saturation conditions would result in a slowing of the reaction thus resulting in a deviation from the expected linear log plot. Alternately product inhibition could be a factor with the free phenanthroline ligand somehow interacting with the metal centres of the catalase, again this scenario would explain the deviation from linearity of the log plot. This was not, however investigated.

Sample #9 The reaction of bpV(phen) with 197 units of catalase. log plot



Graph 3.2.24. Graph of the natural logarithm of the relative integration of the bpV peaks of a bpV(phen) solution with 197 units of catalase

3.2.8. The reaction of bpV(OHpic) with potassium ferrocyanide:

Attempts to investigate the electrochemistry of pV complexes in water through the use of cyclic voltammetry were unsuccessful. The electrochemical reduction of VO_2^+ (aq) to VO^{2+} (aq) in 1.0 M H_2SO_4 occurs irreversibly but at a very slow rate, a diffusion limited peak not being observed until the potential was almost 1 V more negative than the standard potential of the redox couple (1.00 V vs. NHE).²¹ The reduction potential observed for $\text{VO}(\text{O}_2)(\text{pic})(\text{H}_2\text{O})_2$ in DMF was -1.26 V vs. SCE.²² Unfortunately this potential is outside the potential range of neutral aqueous solutions using platinum or glassy carbon electrodes²³ and water is the only suitable solvent for anionic bpV complexes. Since cyclic voltammetry is essentially an outer sphere electron transfer process²⁴ the

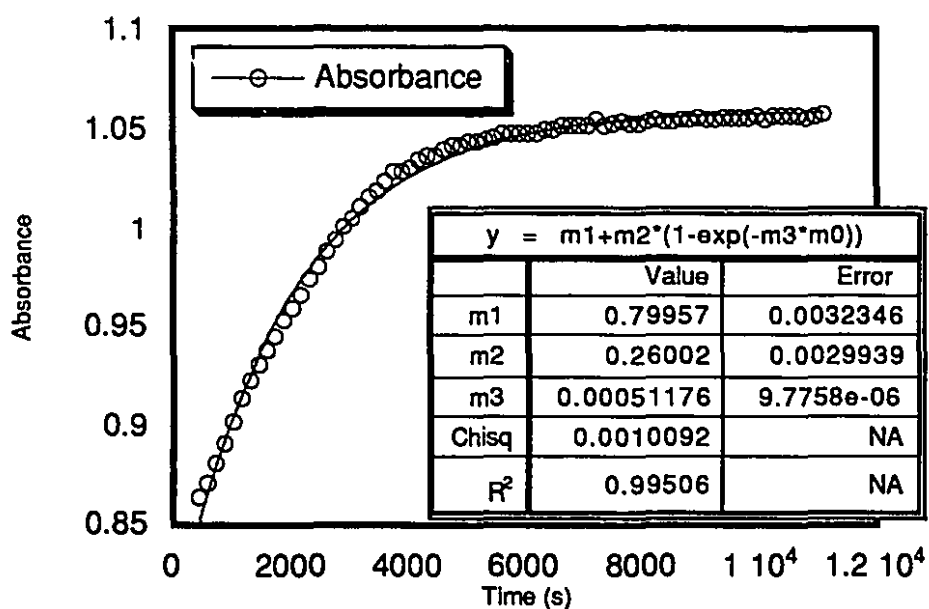
reaction of bpV(OHpic) with potassium ferrocyanide, a classic outer sphere electron transfer agent²⁵, was carried out.

The kinetics of the reaction of bpV(OHpic) with potassium ferrocyanide in pH 7.4 phosphate buffered solutions under continuous UV irradiation was investigated. The reaction was carried out under pseudo first order conditions with a 25 fold excess of bpV(OHpic). The rates derived from the UV-Vis data are given in Table 3.2.4.

Table 3.2.4. Rate constants for the reaction of bpV(OHpic) and potassium ferrocyanide under UV-visible irradiation.

Sample#	bpV(OHpic) (mole L ⁻¹)	K ₄ [Fe(CN) ₆] (mole L ⁻¹)	K _{obs} (s ⁻¹)	K ₂ (M ⁻¹ s ⁻¹)
#1	5.0 X 10 ⁻³	2.0 X 10 ⁻⁴	5.1 X 10 ⁻⁴	0.10
#2	5.0 X 10 ⁻³	2.0 X 10 ⁻⁴	5.0 X 10 ⁻⁴	0.10
#3	2.5 X 10 ⁻³	1.0 X 10 ⁻⁴	1.7 X 10 ⁻⁴	0.068

bpV(OHpic) (5.0×10^{-3} M) and potassium ferrocyanide (2.0×10^{-4} M).



Graph 3.2.24. Graph showing the absorbance data for sample #1, the reaction of bpV(OHpic) with potassium ferrocyanide.

Graphs showing the data for sample for #2 and #3 can be found in appendix A.5.

Reaction mixtures that were not continuously irradiated gave poorly reproducible results that could not be fitted to first order kinetics. Overall the reaction was much slower.

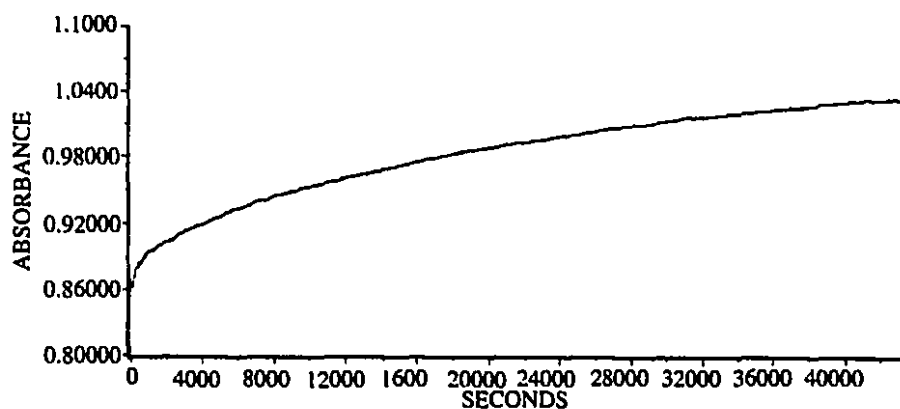
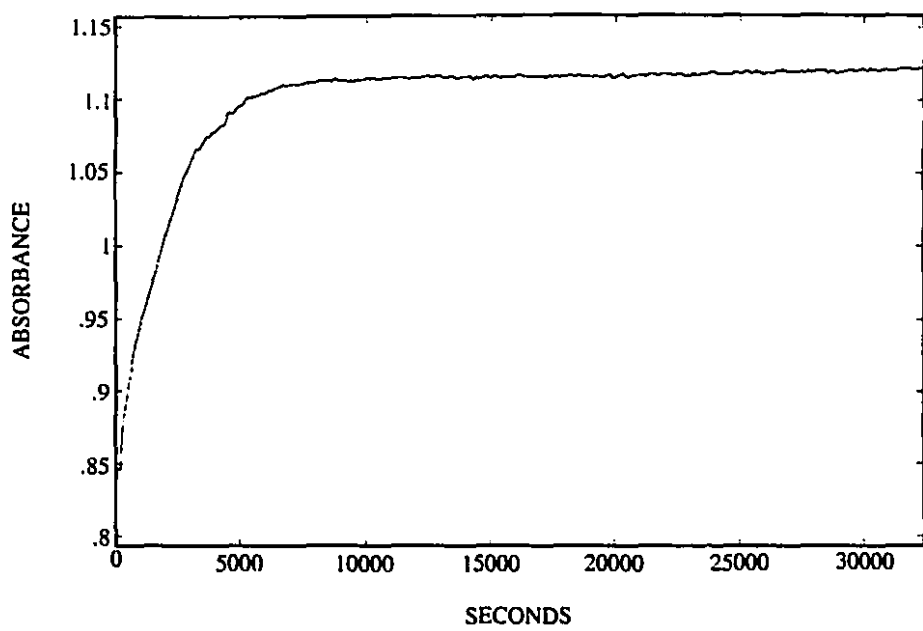


Figure 3.2.6. Figure showing the UV-vis spectra of the reaction of bpV(OHpic) ($5 \times 10^{-3} \text{ M}$) and potassium ferrocyanide ($2 \times 10^{-4} \text{ M}$) under continuous UV irradiation (top) and with irradiation for 1.0 s every 144 s. Absorbance monitored at 420 nm.

A UV-Vis spectrometer that had malfunctioned by continuously irradiating the sample provided an interesting result. When continuously irradiated bpV(OHpic) reacted with potassium ferrocyanide with a first order rate constant of $0.10 \text{ M}^{-1} \text{ s}^{-1}$ for reactions with $5.0 \times 10^{-3} \text{ M}$ bpV(OHpic) and $2.0 \times 10^{-4} \text{ M}$ potassium ferrocyanide (two determinations) and $0.068 \text{ M}^{-1} \text{ s}^{-1}$ for reactions with $2.5 \times 10^{-3} \text{ M}$ bpV(OHpic) and $1.0 \times$

10⁻⁴ M potassium ferrocyanide (one determination) at 25°C. The error for the kinetic determinations with the lower concentration of reactants was greater as the absorbance change in the UV-Vis spectra was relatively small. The average of the observed rate constants was 0.089 M⁻¹ s⁻¹. In samples that were not continuously irradiated the results were less reproducible and did not behave as pseudo first order reactions, the reaction being slower than in the irradiated samples. Oxidations of cyclohexane and benzene by the pV compound VO(O₂)(pic)(H₂O)₂ have been reported to occur at greater rates under UV and visible irradiation.¹⁵ The slow reactivity of the sample that was not irradiated provides some explanation for why the complexes were not amenable for study by cyclic voltammetry. Cyclic voltammetry is a rate dependent process that measures outer sphere electron transfer. The slow rate of reaction of bpV(OHPic) with potassium ferrocyanide and the non pseudo first order behavior of the system is indicative of a system that does not react by an outer sphere mechanism or a system in which reaction with ferrocyanide is occurring with a species other than the bpV. The reactivity that is observed may result from either a decomposition product or from a transient reactive species. It is possible that the reaction that is occurring is not with the peroxovanadium compound *per se* but rather with a species in which the peroxide ligand has been activated by cleavage of the peroxide oxygen-oxygen bond, possibly to form a radical cation.^{1,26} Alternately a homolytic or heterolytic cleavage of one of the peroxo-vanadium bonds could also be responsible for the observed reactivity. Homolytic V-O_{peroxo} bond cleavage has been proposed for oxidation reactions involving VO(O₂)(pic)LL' and A⁺[VO(O₂)(pic)₂]^{*} with olefins, arenes and alkenes.²⁷ The peroxometal complex then behaves essentially as a 1,3-dipolar reagent

$$\overset{\oplus}{\text{M}}-\text{O}-\overset{\ominus}{\text{O}} \quad 28.$$

The effect of UV-Vis light on potassium ferrocyanide cannot be neglected. It is possible that irradiation of the ferrocyanide could result in changes in reactivity also.

* L, L'=H₂O or basic ligands, A⁺=H⁺ or PPh₄⁺

Aquated electrons are produced both by steady illumination and laser flash photolysis by UV light in aqueous solutions of ferrocyanide.²⁹⁻³¹ An aquated electron could then react with a pV compound to give a reactive radical cation species.²⁶ The intensity of UV light required to eject an electron from ferrocyanide is, however, probably greater than that supplied by the lamp of a UV spectrophotometer.

3.2.9. Effect of UV light on bpV complexes:

Irradiation of bpV(OHpic), bpV(phen) and bpV(pic) by a UV-visible light source in the absence of potassium ferrocyanide was also investigated. The ⁵¹V NMR spectra of the bpV(pic), bpV(OHpic) and bpV(phen) that had been irradiated for 1 h by the UV lamp in a HP8452A UV-Vis spectrophotometer showed no differences from the spectra of the light shielded control solutions. Thus in the absence of a reducing agent pV compounds are relatively stable when irradiated by UV-visible light. Light induced cleavage of O-O or V-O_{peroxo} peroxide bonds would be expected to be readily reversible, thus in the absence of a reducing agent to compete with the back reaction very little decomposition was observed. In biological media however there are generally many reducing reagents with which the pV could react.

The observation of the accelerated reaction of bpV(OHpic) with potassium ferrocyanide upon irradiation with UV-visible light points out an important consideration in following reactions of pV compounds by UV-Vis spectroscopy. The act of observing may perturb the system in such a way that unreliable results are obtained. In order to minimize the impact of light on reactions the integration time (exposure to the UV lamp) should be minimized and the time between measurements maximized.

3.3. Conclusions

The stabilities of the bpV compounds bpV(OHpic), bpV(pic) and mpV(2,6-pdc) were determined at pH 4, 5, 6, and 7 at 37°C. The mpV compound was very stable, showing only limited decomposition at pH 7. At lower pH's no decomposition was observed over the course of 9 days. The bpV compounds showed their greatest stability at neutral pH with decreased stability at lower pHs. The bpV complexes appeared to undergo a rapid decomposition at lower pHs (< 2 h) followed by slow decomposition. The decomposition of bpV(pic) proceeded faster than that of bpV(OHpic).

Light shielded samples of bpV(phen) at pH 7.4 and room temperature showed no significant decomposition after 35 days although there was some variability among the samples.

The interaction of EDTA and DTT, two common additives to biological buffer systems, with pV compounds and vanadate was also investigated. Vanadate and V(2,6-pdc) reacted readily with EDTA but no interaction with bpV(phen) was observed and very little interaction was noted with bpV(pic) and bpV(OHpic). Thus although EDTA is not compatible with vanadates or coordinatively unsaturated vanadate complexes, it is suitable for use with coordinatively saturated bpV complexes although its long term use is not recommended. The reaction of DTT with bpV(phen), bpV(OHpic) and vanadate showed this reducing agent to be incompatible with both pV compounds and vanadate. When in excess, the DTT was able to reduce both the bpV compounds and the vanadate leaving no vanadium(V) species detectable by ^{51}V NMR.

Studies with the biological buffers HEPES, MOPS and phosphate showed bpV compounds to be most stable in MOPS and phosphate at physiological pH. There may be

some interaction between phosphate and aquo bpV species and this should be considered if phosphate buffers are to be employed. With increasing ratios of HEPES relative to bpV compound the stability of bpV compounds decreased. MOPS appears less prone to decompose bpV compounds and its structural similarity to HEPES makes it an unlikely candidate to interact with vanadates.

Catalase, an enzyme that catalyzes the disproportionation of hydrogen peroxide, reacts with bpV compounds. Catalase has seen use in the *in situ* preparation of aquo pV compounds for biological testing.⁵ Caution must be used in exercising this procedure as the concentration of pV will decrease as it reacts with catalase. Rate constants for the reaction of bpV(OHpic) (9.6×10^{-9} units⁻¹ L min⁻¹) and bpV(pic) (6.6×10^{-9} units⁻¹ L min⁻¹) were determined.

Attempts to investigate the electrochemistry of bpV complexes by cyclic voltammetry were unsuccessful. The rate of outer sphere electron transfer by potassium ferrocyanide to bpV(OHpic) was investigated. Under continuous irradiation the reaction occurred with a second order rate constant of $0.089 \text{ M}^{-1} \text{ s}^{-1}$. Samples that were not irradiated showed very slow, poorly reproducible reactions that were not second order. In the absence of potassium ferrocyanide irradiation of bpV samples for 1h in phosphate buffer had no significant effect on the short term stability of the compounds.

3.4. Experimental

3.4.1. General

^{51}V NMR spectra of solutions of the complexes in D_2O (98% D purity, MSD Isotopes) were obtained at ambient temperature on a Varian XL-300 NMR spectrometer operating at 78.891 MHz. Vanadium-51 chemical shifts were measured in parts per million (± 1 ppm) using VOCl_3 as an external standard at 0.00 ppm, upfield shifts are considered negative. Measurements of pH were made on an Orion 5202A pH meter using either a Orion Ross 8102 combination electrode or an NMR combination electrode (Aldrich).

3.4.2. Chemicals

HEPES (free acid 99.5%), MOPS (free acid 99.5% and Na Salt 99%), phosphate buffer (pH 7.4, 0.1 M), Bovine Albumin (96-99%), and bovine liver catalase (thymol free) were purchased from Sigma and used without further purification. Potassium ferrocyanide trihydrate (99.9%) was purchased from Baker and used without further purification. pH 7 phosphate buffer (0.1 M) was purchased from Fluka and used as received. EDTA tetrasodium salt hydrate (98%) and L-cysteine were purchased from Aldrich and used as received. Dibasic potassium phosphate (ACS reagent grade) was purchased from ACP and used without further purification. All pV compounds were prepared by the method described in Chapter 2 or were prepared by the literature method^{10,32,33} by either the author or Jesse B. Ng. Distilled water was used in all preparations. All other solvents were ACS reagent grade, from various suppliers.

3.4.3. Stability Studies

Solutions (1.0×10^{-2} M) of bpV(pic), bpV(OHpic), and mpV(2,6-pdc) were prepared from pH 4, 5, 6 and 7 buffers. The pH 4, 5, and 6 buffers were prepared by adding KOH to acetic acid until the desired pH was obtained, the buffers were 0.5 M in acetate. The pH 7 buffer employed was a phosphate buffer obtained from Fluka and was used without modification. Aliquots of 0.50 mL were taken from the stock solutions and placed in an NMR tube to which was added 0.50 mL of D₂O. The final concentration of the samples was 5.0×10^{-3} M. Sealed melting point capillaries containing 50 μ l of a solution of V(2,6-pdc) (0.1330g in 10 ml H₂O) were placed in the NMR tubes to act as an internal reference*. NMR spectra for day zero were obtained at less than 2 hours after preparation of the samples. The NMR tubes were flame sealed to protect against evaporation of solvent during the course of the study. The samples were then incubated at 37°C and spectra recorded at 24 h intervals for 9 days or until the loss of signal for the pV species.

Titration of mpV(2,6-pdc), the 2,6-pdc ligand, the OHpic ligand and V(2,6-pdc) were carried out using a Radiometer PHM63 pH meter equipped with a TTT80 titration controller, ABU80 automatic burette and a REC80 chart recorder with a REA160 titration module. The pH was measured with a Radiometer K-4040 calomel reference electrode and a G-2040C glass electrode (Dr. J. Chin is thanked for the loan of this equipment). An aqueous NaOH solution (0.10 M, volumetric standard, Aldrich) was used as the titrant. The compounds mpV(2,6-pdc) (0.0391 g), 2,6-pdc (0.0207 g), OHpic (0.0174 g), and V(2,6-pdc) (0.0317g) were dissolved in water (10.0 mL) and a 3.00 mL aliquot of the solution transferred to the titration vessel and its pH adjusted to approx. 3.5 using an HClO₄ solution or, in the case of the 2,6-pdc ligand, an NaOH solution. After titration to a

* Solutions of this compound have been found to be very stable, >1 yr.

pH of 10 the pH of the solution was lowered to approx. 3.5 with HClO₄ (aq) and again titrated to pH 10.

3.4.4. Stability of bpV(phen) in the Absence of Light

Five solutions of bpV(phen) (10 mM) were prepared in separate volumetric flasks in phosphate buffer (pH 7.4, 0.1M, Sigma). Aliquots of the solutions (0.35 mL) were added to equal amounts of D₂O in NMR tubes. Sealed melting point capillaries containing 50 µl of a solution of V(2,6-pdc) (0.1330g in 10 ml H₂O) were placed in the NMR tubes to act as an internal reference. The samples were kept wrapped in two layers of aluminum foil when not being analyzed by NMR. ⁵¹V NMR spectra were obtained within 0.5 h of preparation of the samples and at intervals thereafter. The NMR tube containing sample #4 broke midway through the study and was therefore not included in the analysis of the results.

3.4.4. The Interaction of Vanadate, V(2,6-pdc), and bpV(phen) with EDTA

Solutions of bpV(phen) (25mM), Na₃VO₄ (25mM), V(2,6-pdc) (25mM), and EDTA tetrasodium salt hydrate (25 mM) were prepared in phosphate buffer (0.1 M, pH 7.4). Samples were prepared in NMR tubes containing D₂O (0.50 mL) as shown in Table 3.4.1. and analyzed by ⁵¹V NMR 0.5 h after their preparation.

Table 3.4.1. The preparation of samples for ^{51}V NMR analysis of the interaction of EDTA with vanadate, bpV(phen), V(2,6-pdc), bpV(OHpic), and bpV(pic). (buffer=pH 7.4, 0.1M phosphate)

Sample	Na_3VO_4 (mL)	bpV(phen) (mL)	V(2,6-pdc) (mL)	bpV(OHpic) (mL)	bpV(pic) (mL)	EDTA (mL)	Buffer (mL)
#1	0.25	-	-	-	-	-	0.25
#2	0.25	-	-	-	-	0.25	-
#3	-	0.25	-	-	-	-	0.25
#4	-	0.25	-	-	-	0.25	-
#5	-	-	0.25	-	-	-	0.25
#6	-	-	0.25	-	-	0.25	-
#7	-	-	-	0.25	-	-	0.25
#8	-	-	-	0.25	-	0.25	-
#9	-	-	-	-	0.25	-	0.25
#10	-	-	-	-	0.25	0.25	-

The pH's of the solutions were checked before NMR analysis and the pH of some solutions lowered to physiological pH (± 0.2) through the addition of DCl (37% in D_2O) as is shown in Table 3.4.2.

Table 3.4.2. The pH of samples before and after adjustment with DCl (37% in D_2O) for ^{51}V NMR analysis of the interaction of EDTA with vanadate, bpV(phen), V(2,6-pdc), bpV(OHpic), and bpV(pic).

Sample	pH	pH after adjustment with DCl (37% in D_2O)
#1	8.70	7.22
#2	9.90	7.41
#3	7.55	
#4	7.94	7.19
#5	6.69	
#6	7.44	
#7	7.50	

Sample	pH	pH after adjustment with DCl (37% in D ₂ O)
#8	7.77	7.54
#9	7.50	
#10	7.84	7.59

The analysis of V(2,6-pdc) was also carried out identically to the procedure given above but with the buffer being replaced by distilled water.

3.4.5. The Interaction of Vanadate, bpV(phen), and bpV(OHpic) with DTT.

Solutions of KVO₃ (40mM), bpV(phen) (40mM), bpV(OHpic) (40 mM) , and DTT (40 mM) were prepared in D₂O. Samples were prepared as shown in Table 3.4.3 and analyzed by ⁵¹V NMR 40 min after their preparation.

Table 3.4.3. The preparation of samples for ⁵¹V NMR analysis of the interaction of DTT with vanadate, and bpV(phen), and bpV(OHpic).

PV (or KVO ₃) :DTT	PV (or KVO ₃) Volume (mL)	DTT Volume (mL)	D ₂ O Volume (mL)
1:1	0.20	0.20	0.80
1:2	0.20	0.40	0.40
1:4	0.20	0.80	0
2:1	0.20	0.10	0.70
4:1	0.20	0.05	0.75

3.4.6. The Interaction of bpV(OH-pic) with HEPES, MOPS and Phosphate Buffers.

Solutions of HEPES (free acid, 200mM), MOPS (free acid, 200mM) and dibasic potassium phosphate (200mM) were prepared in distilled water. The pH of the HEPES and MOPS solutions were adjusted to pH 7.4 using KOH (1 M) and the pH of the phosphate solution adjusted to 7.4 using HCl (6 M). Aliquots (0.35 mL) of a solution of bpV(OHpic) (10mM) in D₂O were added to an equal amount of the buffer solution in 3 NMR tubes. The tubes were wrapped in aluminum foil to shield them from light and their ⁵¹V NMR spectra was obtained after 24 h. A sample of bpV(OHpic) (5 mM) containing no buffer (pH 7.3, not adjusted) was also prepared and this sample was compared to a sample of bpV(OHpic) in MOPS, prepared as described above, by ⁵¹V NMR after 22 h.

3.4.7. The interaction of bpV(pic)and bpV(OHpic) with HEPES and MOPS at varying ratios of pV:buffer.

Solutions of HEPES (free acid, 200mM, Sigma) and MOPS (Na salt, 200 mM, Sigma) were prepared in distilled water. The pH of the HEPES and MOPS solutions were adjusted to pH 7.4 using NaOH (1 M) and HCl (6 M) respectively. Solutions of bpV(pic) (10 mM) and bpV(OHpic) (10 mM) were prepared in D₂O. Samples were prepared in NMR tubes at ratios of buffer:bpV of 50:1, 10:1, and 2:1 as well as control samples containing no buffer. The samples were prepared as described in the table below. ⁵¹V NMR spectra were obtained at approximately 1 h and 6.5 h after sample preparation.

Table 3.4.4. The preparation of NMR samples for the study of the interaction of bpV(pic) and bpV(OHpic) with HEPES and MOPS buffers.

Sample #	HEPES (mL)	MOPS (mL)	bpV(pic) (mL)	bpV(OHpic) (mL)	D ₂ O (mL)	H ₂ O (mL)
#1	0.50	-	-	0.20	0.30	-
#2	0.25	-	-	0.50	-	0.25
#3	0.050	-	-	0.50	-	0.45
#4	-	0.50	-	0.20	0.30	-
#5	-	0.25	-	0.50	-	0.25
#6	-	0.050	-	0.50	-	0.45
#7	-	-	-	0.20	0.30	0.50
#8	-	-	-	0.50	-	0.50
#9	0.50	-	0.20	-	0.30	-
#10	0.25	-	0.50	-	-	0.25
#11	0.050	-	0.50	-	-	0.45
#12	-	0.50	0.20	-	0.30	-
#13	-	0.25	0.50	-	-	0.25
#14	-	0.050	0.50	-	-	0.45
#15	-	-	0.20	-	0.30	0.50
#16	-	-	0.50	-	-	0.50

3.4.8. The Interaction of bpV's with Catalase:

Solutions of bpV(pic) (35 mM) and bpV(OHpic) (35 mM) were freshly prepared in phosphate buffer (0.1 M, pH 7.4, Sigma) for each kinetic run. Catalase (bovine liver, 19,900 units* /mg of protein) solutions at various concentrations were prepared in phosphate buffer (0.1 M, pH 7.4, Sigma). In a typical kinetic run 0.35 mL of bpV solution, 0.35 mL of D₂O and 0.010 mL catalase solution were added to an NMR tube containing a sealed melting point capillary containing 50 µl of a solution of V(2,6-pdc) (0.1330g in 10 ml H₂O) to act as an internal reference. The sample was mixed and fitted

* The activity of catalase is reported by Sigma in units/mg of protein where one unit decomposes one micromole of H₂O₂/min at pH 7 and 25°C from a concentration of H₂O₂ of 10.3-9.2 mM.

with a vented cap to release oxygen (paramagnetic) from the tube. ^{51}V NMR spectra were obtained at time 0, 0.5 h, 1.0 h, 2 h, 3 h, and at 2 h intervals thereafter for 13 h. The spectra were analyzed by comparing the integration of the internal reference with the integration of all bisperoxovanadium species and the rate of disappearance of the bpV species was determined.

Samples of bpV(pic) and bpV(OHpic) were prepared as shown in the 3.4.5:

Table 3.4.5. Table showing the amounts of bpV(pic), bpV(OHpic), bpV(phen), and catalase used in the kinetic determinations of the rate of reaction of bpV species with catalase.

Sample #	pV Species	Concentration of pV in sample	Mass of catalase, volume of water, number of units.
#1	bpV(OHpic)	16.9 mM	0.0100 g 10.00 mL 199 units
#2	bpV(OHpic)	17.3 mM	0.0103 g 5.00 mL 410 units
#3	bpV(OHpic)	17.7 mM	0.0113 g 5.00 mL 450 units
#4	bpV(pic)	18.5 mM	0.0099 g 5.00 mL 394 units
#5	bpV(pic)	16.5 mM	0.0111 g 2.50 mL 884 units
#6 ^a	bpV(pic)	17.5 mM	0.0107 g 5.00 mL 426 units
#7	bpV(phen)	16.9 mM	0.0100 g 2.50 mL 796 units
#8	bpV(phen)	18.0 mM	0.0216 g 2.50 mL 1719 units
#9	bpV(phen)	17.1 mM	0.0099 g 10.00 mL 197 ¹ units

^a Sample #6 was prepared with the addition of 0.1 wt% BSA

3.4.8. Effect of UV light on bpV Complexes:

Solutions of bpV(OHpic) (20 mM), bpV(pic) (20 mM) and bpV(phen) were prepared in phosphate buffer (0.1 M, pH 7.4, Sigma). Aliquots (3 mL) of each solution were placed in a quartz UV cell and irradiated for 1 h by the UV lamp of a HP8452A UV-Vis spectrophotometer, the remainder of the solution was stored shielded from light in aluminum foil. Aliquots (0.35 mL) of the irradiated and light shielded solutions were added to equal amounts of D₂O and analyzed by ⁵¹V NMR.

3.4.9. The Reaction of bpV(OHpic) with Potassium Ferrocyanide:

Stock solutions of bpV(OHpic) and potassium ferrocyanide trihydrate were prepared in deoxygenated distilled water. Aliquots (1.00 mL) of each of the solutions were added to a quartz cuvette. The increase in absorbance at 420 nm corresponding to the formation of ferricyanide was monitored by UV-Vis spectroscopy on a Hewlett Packard HP8451A UV-Vis spectrometer that continuously irradiated the samples with UV-Vis light. The samples were maintained at 25°C throughout the course of the experiment. Three samples were prepared. Pseudo first order rate constants were determined by fitting the absorbance data to the equation $y = A_0 - A \times (1 - e^{-kt})$. Second order rate constants were determined by dividing the pseudo first order rate constant by the concentration of bpV(OHpic).

Similar kinetic runs were carried out on a HP8452A UV-Vis spectrophotometer, in which the samples were irradiated for only 1.0 s every 144 s.

Table 3.4.6. The preparation of samples for the kinetic analysis of the reaction of bpV(OHpic) and potassium ferrocyanide.

Sample#	bpV(OHpic) (mole L ⁻¹)	K ₄ [Fe(CN) ₆] (mole L ⁻¹)
#1	5.0 X 10 ⁻³	2.0 X 10 ⁻⁴
#2	5.0 X 10 ⁻³	2.0 X 10 ⁻⁴
#3	2.5 X 10 ⁻³	1.0 X 10 ⁻⁴

Uv-Vis spectra of potassium ferrocyanide and potassium ferricyanide are given in Figure 3.4.1.

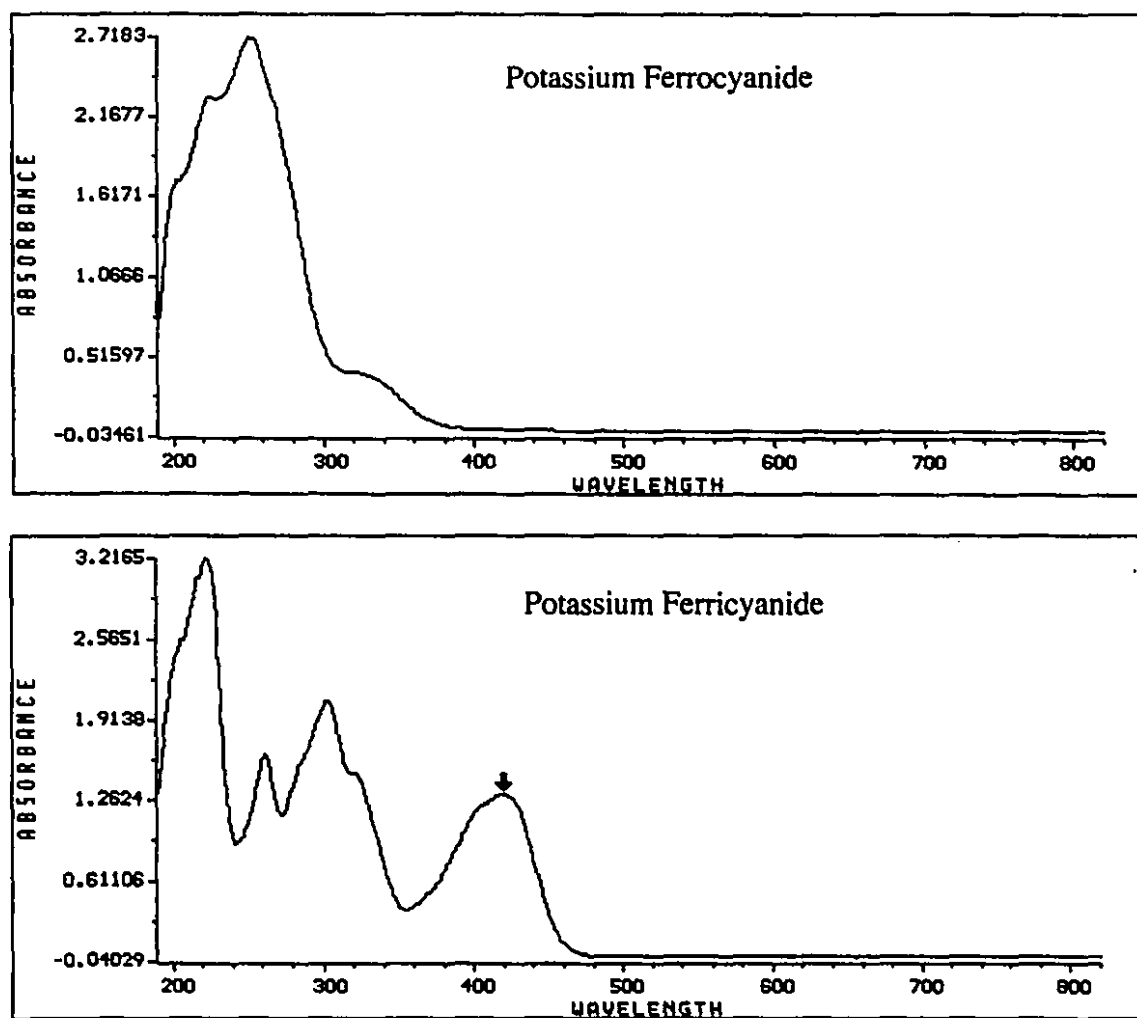


Figure 3.4.1. Figure showing the UV-Vis spectra of potassium ferrocyanide, K₄[Fe(CN)₆], and potassium ferricyanide, K₃[Fe(CN)₆].

3.5. References

- (1) Butler, A.; Clague, M. J.; Meister, G. E. *Chem. Rev.* **1994**, *94*, 625-638.
- (2) Crans, D. C. *Comments Inorg. Chem.* **1994**, *16*, 1-33.
- (3) Crans, D. C.; Marshman, R. W.; Nielsen, R.; Felty, I. *J. Org. Chem.* **1993**, *58*, 2244-2252.
- (4) Crans, D. C.; Mahroof-Tahir, M.; Keramidas, A. D. *Mol. Cell. Biochem.* **1995**, *153*, 17-24.
- (5) Kadota, S.; Fantus, I. G.; Deragon, G.; Guyda, H. J.; Hersh, B.; Posner, B. I. *Biochem. Biophys. Res. Comm.* **1987**, 259-266.
- (6) Lippard, S. J.; Berg, J. M. *Principles of Bioinorganic Chemistry*; University Science Books: Mill Valley, 1994, pp 329-332.
- (7) Alberts, B.; Bray, D.; Lewis, J.; Raff, M.; Roberts, K.; Watson, J. D. *Molecular Biology of the Cell*; Garland Publishing Inc.: New York, 1989, pp 93.
- (8) Stryer, L. *Biochemistry*; 3rd ed.; W.H. Freeman and Co.: New York, 1988.
- (9) Hartkamp, H. *Angew. Chem.* **1959**, *71*, 553.
- (10) Wieghardt, K. *Inorg. Chem.* **1978**, *17*, 57-64.
- (11) Howarth, O. W.; Hunt, J. R. *J. Chem Soc. Dalton trans.* **1979**, 1388-1391.
- (12) Heath, E.; Howarth, O. W. *J. Chem. Soc. Dalton Trans.* **1981**, 1105-1110.
- (13) Howarth, O. *Prog. NMR Spectrosc.* **1990**, *22*, 453-485.
- (14) *Handbook of Biochemistry. Selected Data for Molecular Biology*, 2 ed.; Sober, H. A., Ed.; The Chemical Rubber Co.: Cleveland, 1970.
- (15) Attansio, D.; Suber, L.; Shul'pin, G. B. *Izv. Akad. Nauk. Ser. Khim.* **1992**, *8*, 1918-1921.
- (16) Crans, D. C.; Shin, P. K. *J. Am. Chem. Soc.* **1994**, *116*, 1305-1315.

- (17) Posner, B. I.; Faure, R.; Burgess, J. W.; Bevan, A. P.; Lachance, D.; Zhang-Sun, G.; Fantus, I. G.; Ng, J. B.; Hall, D. A.; Soo Lum, B.; Shaver, A. *J. Biol. Chem.* **1994**, *269*, 4596-4604.
- (18) Unpublished results; Jesse B. Ng, Alan Shaver and Barry Posner.
- (19) Moore, W. J. *Basic Physical Chemistry*; Prentice-Hall Inc.: Englewood Cliffs, 1983, pp 285.
- (20) Lippard, S. J.; Berg, J. M. *Principles of Bioinorganic Chemistry*; University Science Books: Mill Valley, 1994, pp 16.
- (21) Freund, M. S.; Lewis, N. S. *Inorg. Chem.* **1994**, *33*, 1638-1643.
- (22) Bonchio, M.; Conte, V.; Di Furia, F.; Modena, G.; Moro, S.; Carofiglio, T.; Magno, F.; Pastore, P. *Inorg. Chem.* **1993**, *32*, 5797-5799.
- (23) Bard, A. J.; Faulkner, L. R. *Electrochemical Methods. Fundamentals and Applications*; 1st. ed.; John Wiley and Sons: 1980.
- (24) Bockris, J. O.; Reddy, A. K. N. *Modern Electrochemistry*; Plenum Press: New York, 1970; Vol. 1, pp 3-22.
- (25) Butler, I. S.; Harrod, J. F. *Inorganic Chemistry. Principles and Applications*; Benjamin/Cummings Publishing Company Inc.: Redwood City, 1989, pp 624.
- (26) Bonchio, M.; Conte, V.; Di Furia, F.; Modena, G. *J. Org. Chem.* **1989**, *54*, 4368-4371.
- (27) Mimoun, H. *Israel Journal of Chemistry* **1983**, *23*, 451-6.
- (28) Mimoun, H. *Angew. Chem. Int. Ed. Engl.* **1982**, *21*, 734-750.
- (29) Shirom, M.; Stein, G. *J. Chem. Phys.* **1971**, *55*, 3372.
- (30) Shirom, M.; Tomkiewicz, M. *J. Chem. Phys.* **1972**, *56*, 2731-2736.
- (31) Shirom, M.; Stein, G. *J. Chem. Phys.* **1971**, *55*, 3379-3382.
- (32) Vuletic, N.; Djordjevic, C. *J. Chem. Soc. Dalton Trans.* **1973**, 1137-114.
- (33) Quilitzsch, U.; Wieghardt, K. *Inorg. chem.* **1979**, *18*, 869-871.

Chapter 4. The Mechanism of the Inhibition of PTP by Bisperoxovanadium Compounds.

4.1. Introduction

The mechanism by which pV compounds inhibit PTP has not yet been elucidated. An understanding of the mechanism is key to the rational design of new and more potent PTP inhibitors. It is however, reasonable to assume that an interaction in the active site of PTP with pVs is responsible for the inhibition. The presence of a highly conserved cysteine residue in the active site of a number of PTPs suggests an important role for this residue in the enzymatic action of PTPs.¹ The sulfur of the cysteine in the active site of *Yersinia* PTP has a pK_a of 4.7 thus at physiological pH the thiol group is deprotonated.¹ It has been suggested that the thiolate acts as a nucleophile in the hydrolysis of the phosphate-ester bond of phosphotyrosine.¹ Indeed in the crystal structure of a human PTP1B-tungstate complex the Sγ of Cys²¹⁵ is ideally located to act as a nucleophile on a bound phosphotyrosine substrate.¹

Time course studies to determine the reversibility of inhibition of PTP1C by vanadate and peroxovanadates have been carried out.² These studies have shown that after a short incubation period with pV PTP1C remains inhibited even upon removal of pV and/or treatment with biological reducing agents. In the case of vanadate inhibition of PTP1C, nearly full activity can be restored upon removal of the vanadate. This observation points to there being different mechanisms of inhibition of PTPs by vanadate and pV complexes. The irreversibility of inhibition of PTP1C by pV complexes suggests a chemical modification of a catalytically essential element of the enzyme. The interaction of pV compounds with cysteine is therefore of considerable interest and a study has been

undertaken with the goal of elucidating the mechanism of PTP inhibition by pV compounds.

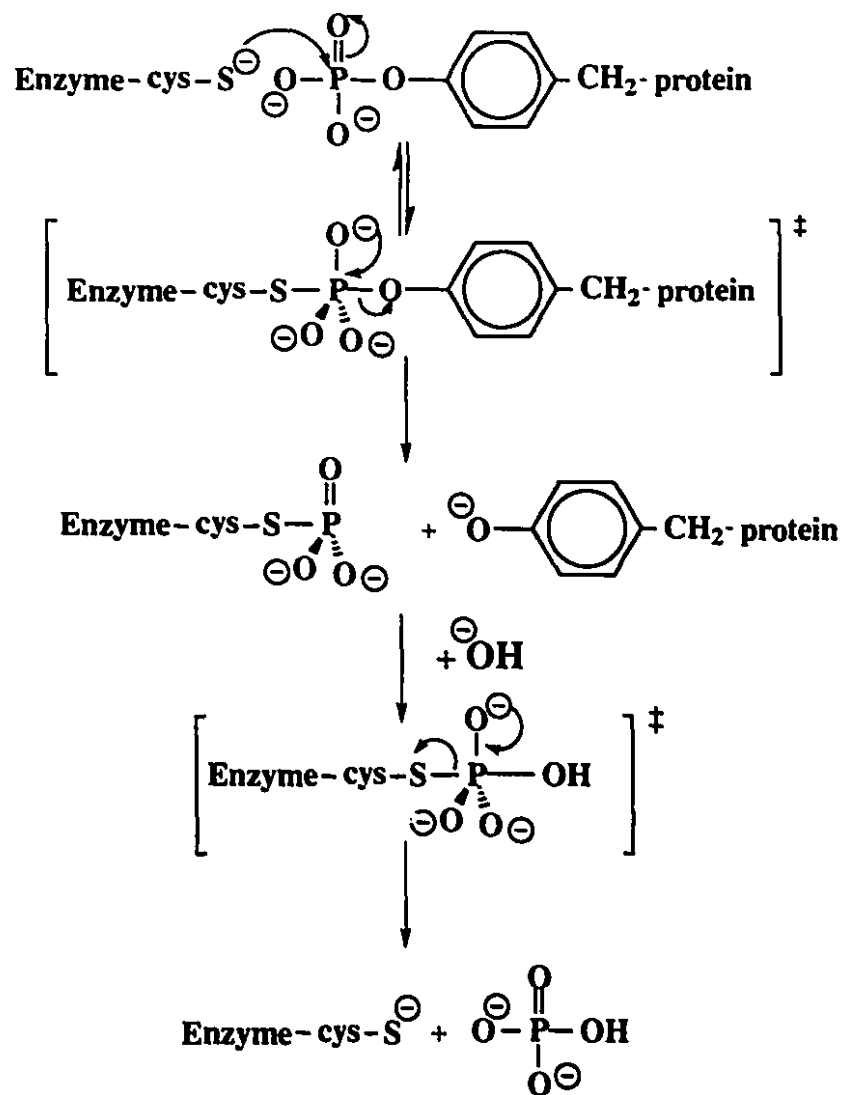


Figure 4.1.1. Putative mechanism for the hydrolysis of phosphate esters by PTP.¹

4.2. Results

4.2.1. Phosphine Oxidations

The reactions of the pV compounds: bpV(OHpic), bpV(2,3-pdc), bpV(2,4-pdc), bpV(2,5-pdc), and bpV(3-acetpic) in water with approximately equimolar amounts of sodium tris(3-sulfonatophenyl)phosphine tetrahydrate were monitored by ^{31}P NMR.³ In all cases after 5 minutes reaction time the phosphine had been completely oxidized to the corresponding oxide, no change was observed in a control solution containing only the phosphine.

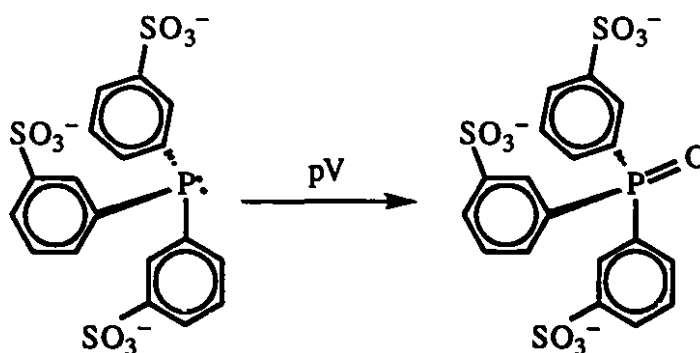


Figure 4.2.1. The oxidation of tris(3-sulfonatophenyl)phosphine by pV compounds.

4.2.2. Cysteine Oxidations, Water Insoluble Products.

Reaction of bpV(pic) and bpV(OH-pic) with cysteine for 4 h, under N_2 , gave a fine white precipitate which was collected and identified as the disulfide cystine by its NMR spectrum. The reactions were conducted with molar ratios of cysteine to bisperoxovanadium complex of 1:1, 2:1, and 4:1, and the conversion to cystine was compared to that observed for a control sample and to that for KVO_3 and H_2O_2 (Table 1). Under the conditions used, the conversion to cystine is negligible for pure cysteine and for

cysteine in the presence of KVO_3 , but the presence of H_2O_2 results in almost complete conversion to cystine.

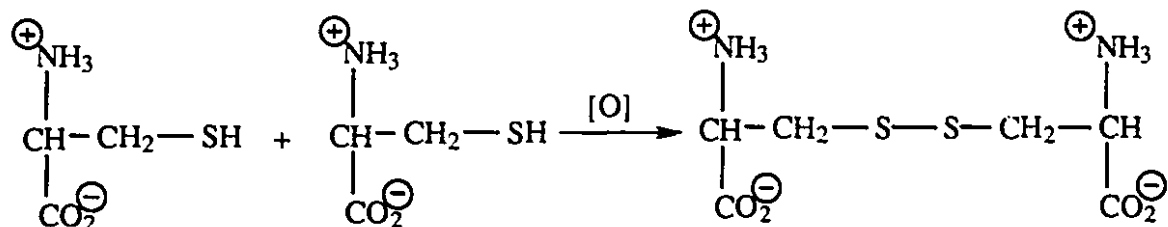


Figure 4.2.2. The oxidative coupling of cysteine to cystine.

Table 4.2.1. Oxidative coupling of cysteine to cystine (% Conversion) by bpV(pic), bpV(OH-pic), KVO_3 , and H_2O_2 after 4 h reaction time (20 h for KVO_3) at room temperature

Ratio	bpV(pic)	bpV(OH-pic)	KVO_3	H_2O_2
1:1	12	44	7.7	96
2:1	47	49	28	92
4:1	38	36	5.9	

Studies of the reactions of bpV(pic) and bpV(OH-pic) with cysteine at a ratio of 1:1 were monitored by ^{51}V NMR spectroscopy. The spectra showed the appearance of peaks due to a number of species in addition to those due to significant amounts of starting material. Some of the new peaks appeared in the region associated with polyvanadates (-548 ppm, mono; -566 ppm, di; -574 ppm, tetra; -582 ppm, penta).^{4,5} For bpV(pic) a peak also appeared at -630 ppm (-626 ppm for bpV(OH-pic)), consistent with the presence of a monoperoxo species.⁶ At molar ratios of cysteine to complex of 2:1 and 4:1 very little of starting bpV(pic) or bpV(OH-pic) remained and only those peaks associated with polyvanadates were observed. The ^{51}V NMR spectra of samples of cysteine and KVO_3 in

the ratios 1:1, 2:1 and 4:1 showed the presence of polyvanadate species (di, tetra, penta), but loss of the signals occurred after 2.5 h in the samples with the 2:1 and 4:1 ratios.

4.2.2. Cysteine Oxidations, Water Soluble Products.

In another experiment the reaction products of bpV(OH-pic) and cysteine were analyzed by HPLC. A mixture of 1:4 cysteine to bpV(OH-pic) along with two control solutions, the first containing only bpV(OH-pic) and the second only cysteine, were prepared in distilled water and allowed to stand for 4 h. The solutions were then passed through anion exchange columns to remove residual bpV(OH-pic). A small aliquot of each of the samples was treated with 9-fluorenylmethylchloroformate which functionalized the cysteine and cysteine oxidation products with a UV-active moiety to facilitate its detection by HPLC.^{7,8} Analysis by HPLC showed a peak corresponding to N-FMOC-cysteinesulfinic acid in the sample containing both cysteine and bpV(OH-pic) that was not present in either of the controls. Confirmation of the identity of the peak was accomplished by spiking the sample with a small amount of pure N-FMOC-cysteinesulfinic acid as is shown in fig. 4.2.4.

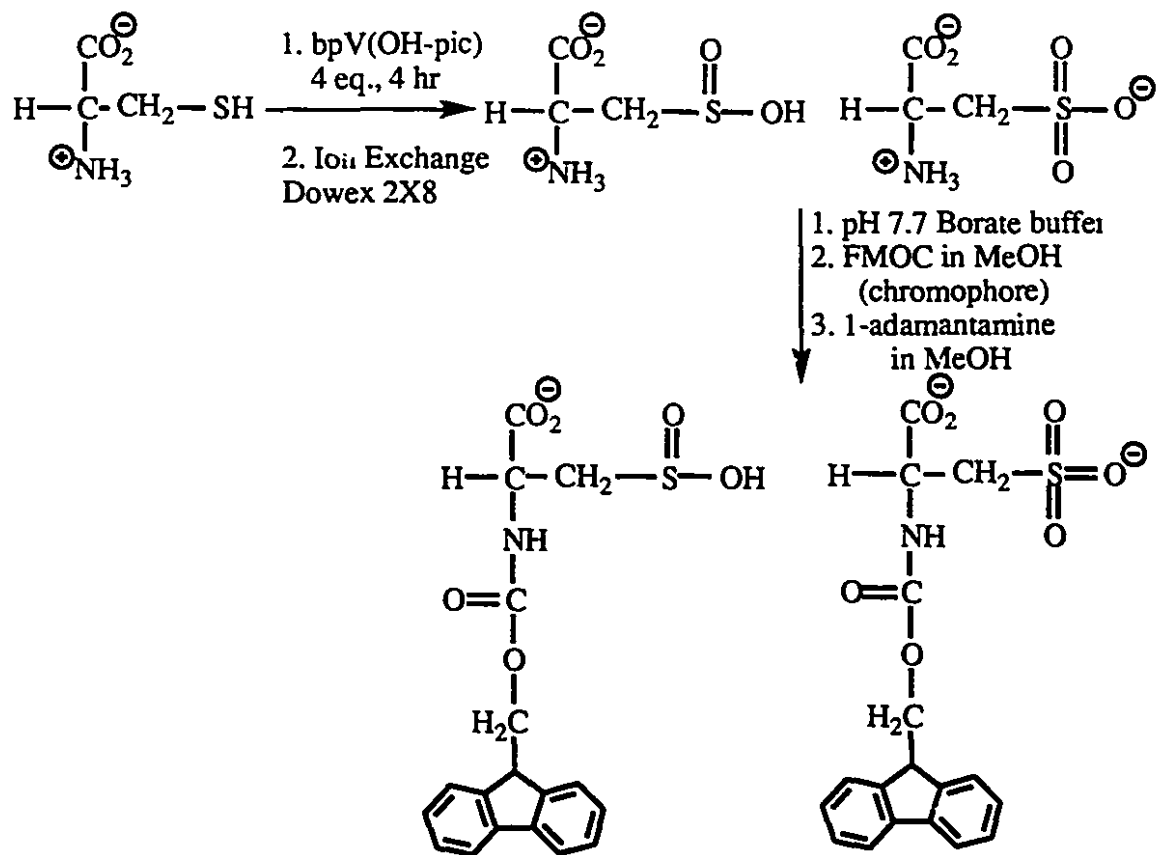


Figure 4.2.3. Scheme illustrating the reaction of bpV(OHpic) with cysteine and the derivatization of the products with Fmoc.

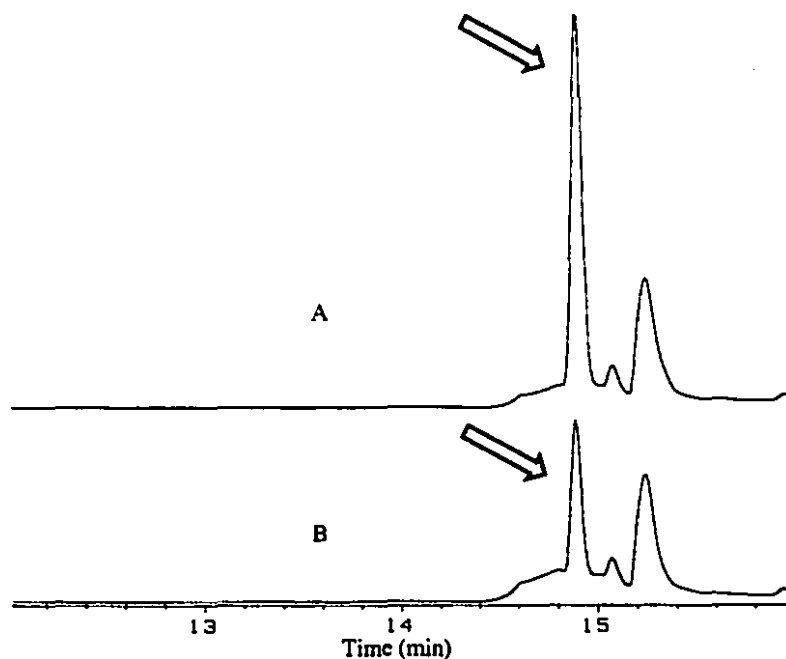


Figure 4.2.4. HPLC spectra of the reaction mixture of L-cysteine and bpV(OHpic) before (B) and after (A) spiking with pure N-FMOC-cysteinesulfinic acid.

4.3. Discussion

The time course inhibition studies of PTP1C by pV compounds are consistent with a chemical modification of a catalytically essential cysteine. The highly oxidative nature of pV compounds⁹ suggests that the most likely modification of a cysteine residue would involve oxidation. Some of the possible oxidation products of cysteine are shown in Figure 4.3.1. Pathway A is generally observed for the aerial or peroxide oxidation of cysteine in solution. The formation of the disulfide requires that two cysteines oxidatively couple, a feat easily accomplished in bulk solution.

It has been shown that pV compounds oxidize cysteine in bulk solution to the disulfide cystine in limited yields. Indeed the maximum conversion observed was approx.

50%, suggesting that other oxidation products were being produced. The observation that the greatest conversion to cystine occurs at a ratio of 2:1 cysteine to bpV complex may be due to competitive reactions. At a ratio of 2:1 cysteine to bpV, the conversion to cystine is favored whereas at other ratios a competing reaction is favoured. Since the oxidative coupling of cysteine to cystine requires two cysteine molecules the ratio of 2:1 cysteine:pV would provide optimum conditions for reaction. Oxidation reactions that involve one molecule of cysteine and one molecule of pV for reaction would be favoured under conditions with higher concentrations of either of the reactants. In this experiment only the water insoluble cystine was collected and identified. Water soluble oxidation products were not identified in this experiment. Both cysteinesulfinic acid and cysteinesulfonic acid are water soluble at neutral pH. If oxygen transfer oxidations occurred and the water soluble cysteinesulfinic and sulfonic acids were produced this would explain the low conversion rates observed.

Cysteine residues that are part of the polypeptide chain of a protein may exist in an environment that is isolated from other cysteine residues. In order to form the disulfide cystine two cysteine residues must be accessible to one another to couple. In order for this coupling to occur intramolecularly a reorganization of the tertiary structure of the protein would be necessary which would present a significant energy barrier. Consequently the chemistry of the active site cysteine in a PTP enzyme is not necessarily the same as that of free cysteine in solution. The rapid oxidation of tris(3-sulfonatophenyl)phosphine by bpV compounds demonstrates the ability of bpV compounds to act as oxygen transfer oxidants as opposed to electron transfer oxidants as is observed for the oxidation of free cysteine. Pathway B as shown in Figure 4.3.1 is therefore more likely for an isolated cysteine residue being oxidized by a bpV complex.

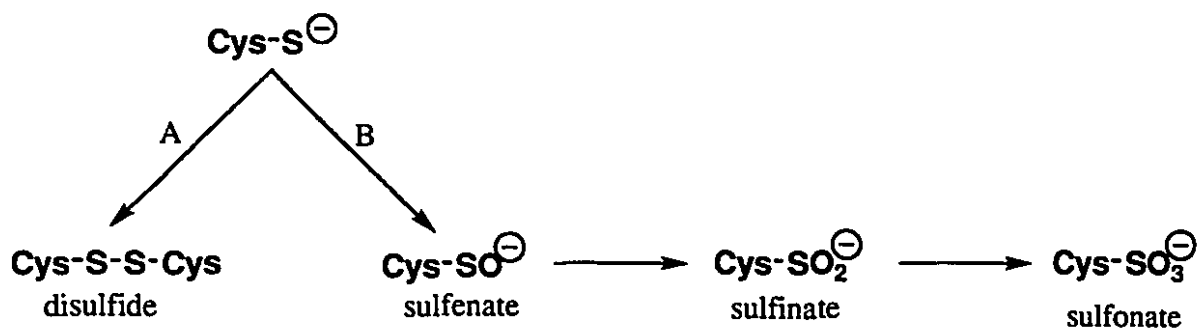
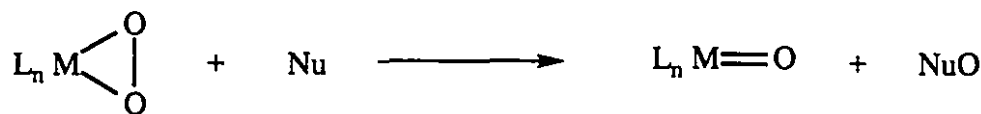


Figure 4.3.1. The oxidative pathways of cysteine thiolate.

Sulfenic acids are generally unstable and immediately undergo further reactions.¹⁰ There are reports of stabilized cysteinesulfenic acids existing in enzymes.¹¹ However due to the instability of these species the evidence for their formation is indirect. Incubation of streptococcal NADH peroxidase with hydrogen peroxide leads to an irreversible inhibition that is presumed to result from further oxidation of the sulfenic acid to either a sulfinic or sulfonic acid.¹¹

The oxidation of cysteine to cysteinesulfinic acid in bulk solution by a pV complex has been demonstrated. In order to favour the formation of oxygen transfer products an excess of pV relative to cysteine was used. The conditions employed in the HPLC analysis were not appropriate for the determination of N-FMOC-cysteinesulfonic acid. Pure samples of this compound run under these conditions were eluted with the solvent front. Consequently the presence of this product cannot be ruled out and indeed seems possible. Nucleophilic attack by sulfides and sulfoxides on the peroxide oxygen of peroxomolybdenum complexes has been reported by Campestrini et al. as shown in Figure 4.3.2.¹² These authors suggest that it is not necessary to coordinate the substrate for oxidation to occur.¹² If oxidation of the sulfur atom of the cysteine in the active site of PTP to either the sulfinic or sulfonic acid were to occur this should irreversibly inhibit the PTP

as neither sulfinic acid nor sulfonic acid is readily reduced in aqueous solution.¹¹ This is consistent with the observation that PTP1C is irreversibly inhibited by pV compounds.



M = Ti(IV), V(V), W(VI), Nu=Nucleophile i.e. sulfides, phosphines

Figure 4.3.2. Nucleophilic attack on a peroxometal compound.¹²

The inhibition of PTP by vanadyl has been modeled using a peptide fragment from the active site of PTP1B.¹³ The interaction was investigated by EPR spectroscopy of the vanadyl ion.¹³ They report the coordination of vanadyl with the cysteine thiolate at basic pH.¹³ A similar interaction might also occur with vanadate. With inert pV compounds it is, however, much more likely that a nucleophilic attack of the cysteine thiolate on a peroxide oxygen atom would occur.¹² This would result in the oxidation of the cysteine to either a sulfinic or sulfonic acid which explains the difference in the reversibility of inhibition by pV versus vanadates.² Thus, the mechanism of inhibition of PTP by pV compounds *in vitro* is likely to occur by this oxidative “suicide inhibition”.

Studies with spontaneously type 1 diabetic rats (BB) have shown that pV compounds are able to replace insulin, these are the first compounds ever to accomplish this feat.¹⁴ In the same study vanadate and vanadyl sulfate were unable to lower blood glucose before inducing acute mortality.¹⁴ This suggests that pV compounds might exert their insulin mimetic effect by a different mechanism than vanadate *in vivo* as well as *in vitro*.¹⁴

4.4. Conclusions

It has been shown that pV compounds can carry out oxidations by both electron and oxygen transfer. Cysteine may undergo oxygen transfer oxidation to cysteine sulfenic, sulfinic or sulfonic acid. Cysteinesulfenic acid is unstable and would undergo further reactions either back to the thiol or undergo further oxidation to sulfinic or sulfonic acid.¹⁰ Reaction of pV complexes with cysteine can produce cysteinesulfinic acid. The presence of cysteinesulfonic acid could neither be confirmed nor ruled out under the conditions of the experiment. The role of pV as oxidants capable of oxygen transfer has been established for cysteine in bulk solution. These reactions should be favoured for cysteine molecules that exist as part of a peptide chain that are unlikely to undergo oxidative coupling as a result of protein conformation. These observations along with the time course inhibition studies² are strongly suggestive of a mechanism for the inhibition of PTP that involves the oxidation of the highly conserved active site cysteine residue to either a cysteinesulfinic or sulfonic acid. Once oxidized the cysteine sulfur would be a poor nucleophile for the cleavage of phosphate esters.

The most promising *in vivo* insulin mimetic effects of pV compounds thus far have been accomplished through intraperitoneal injection¹⁴, clearly this is not an improvement over intramuscular insulin injections. The challenge that remains is the design and synthesis of more potent pV compounds that are readily tolerated and absorbed when given orally or are suitably encapsulated to provide an effective, inexpensive, oral alternative to life-giving insulin injections.

4.5. Experimental

4.5.1. General

^{51}V NMR spectra of solutions of the complexes in D_2O (98% D purity, MSD Isotopes) were obtained at ambient temperature on a Varian XL-300 NMR spectrometer operating at 78.891 MHz. Vanadium-51 chemical shifts were measured in parts per million (± 1 ppm) using VOCl_3 as an external standard at 0.00 ppm, upfield shifts are considered negative. ^{31}P NMR spectra were obtained in a $\text{D}_2\text{O}/\text{H}_2\text{O}$ mixture at ambient temperature on a Varian XL-300 NMR spectrometer operating at 121.4 MHz. Phosphorus-31 chemical shifts were referenced externally to H_3PO_4 (85%) at 0.00 ppm. ^1H NMR spectra of samples in D_2O or CD_3OD (99.9% D, Isotec Inc.) were obtained with a Varian Gemini 200 MHz NMR spectrometer using HOD at 4.63 ppm or residual protons in CD_3OD at 3.30 ppm as references, respectively. ^{13}C NMR spectra of samples in D_2O (99.9% D, Isotec Inc.), using added 1,4-dioxane as a reference at 67.4 ppm, or CD_3OD referenced to 49.0 ppm, were obtained with a Varian Gemini 200 MHz NMR spectrometer operating at 50.289 MHz. Abbreviations for nmr spectra are: s, singlet; m, multiplet; d, doublet; br, broad. All HPLC measurements were performed on a HP 1090m HPLC equipped with a temperature controlled autosampler compartment. A 2.1x100 mm 5 μm ODS Hypersil C18 reverse-phase column maintained at 40 °C was used. Data were collected and integrated using an HP9153c computer. Peaks were observed with a diode array UV detector at 254 nm (Dr J. Chin is thanked for his loan of this equipment). Mass Spectral analysis were carried out by Nadim Saade on a Kratos MS25RFA mass spectrometer under the conditions noted in the text. Elemental analyses were performed by Guelph Chemical Laboratories, Guelph, Ontario, Canada.

4.5.2. Chemicals

Phosphate buffer (pH 7.4, 0.1 M), L-cysteinesulfinic acid, Dowex® 2X8-200 ion exchange resin were purchased from Sigma and used without further purification. Cysteic acid monohydrate (97%) and 9-fluorenylmethyl chloroformate (97%) were purchased from Aldrich and used as received. The compound tris(3-sulfonatophenyl)phosphine tetrahydrate sodium salt (10-15% oxide) was supplied by Strem Chemicals and used as received. Solutions of H₂O₂ (30% by volume) were purchased from ACP Chemicals Inc. All pV compounds were prepared by the method described in Chapter 2 or were prepared by the literature method by either the author or Jesse B. Ng. Distilled water was used in all preparations. All other solvents were ACS reagent grade, from various suppliers

4.5.3. Phosphine Oxidation

Solutions (0.16 M) of the peroxovanadium compounds bpV(OHpic), bpV(2,3-pdc), bpV(2,4-pdc), bpV(2,5-pdc), and bpV(3-acetpic) were prepared in deoxygenated H₂O. A 0.35 mL aliquot of each of these solutions was placed into NMR tubes and to each of these tubes was added 0.35 mL of a solution of sodium tris(3-sulfonatophenyl)phosphine tetrahydrate (0.16M) in deoxygenated D₂O. After approximately 5 minutes reaction time a ³¹P NMR spectrum was obtained for each of the samples. A control sample containing 0.35mL of the phosphine solution and 0.35 mL of D₂O was also prepared and its ³¹P NMR spectrum observed both before and after all other spectra had been obtained to ensure that no aerial oxidation had occurred.

4.5.4. Oxidation of cysteine to cystine with bpV(OHpic), bpV(pic), KVO₃, and H₂O₂.

Stock solutions of L-cysteine (1×10^{-1} M) and the oxidants bpV(OH-pic) (5×10^{-2} M), bpV(pic) (5×10^{-2} M), KVO₃ (5×10^{-2} M), and H₂O₂ (1×10^{-1} M) were prepared in a phosphate buffer solution (pH 7.4) which had been thoroughly deoxygenated by a vigorous stream of N₂. Solutions of cysteine and the oxidants in the molar ratios of 1:1, 2:1, and 4:1 (1:2, 1:1, and 1:2 for H₂O₂) were prepared under N₂ in a three-necked flask by addition of 10 mL of the cysteine stock solution to the appropriate amount of oxidant, followed by dilution with buffer to 30 mL total volume. A control sample (10 mL of cysteine solution plus 20 mL of the buffer) was prepared for each experiment. All the reaction mixtures were stirred for 4 h except those with KVO₃, which were allowed to react for 20 h. Then the samples were filtered through preweighed sintered-glass filters, which were dried under vacuum overnight and reweighed to give the yield of cystine, which was identified in each case by comparison of its ¹H NMR spectrum to that of an authentic sample.

4.5.5. HPLC analysis of the reaction of cysteine with bpV(OHpic).

Stock solutions of bpV(OH-pic) (2×10^{-1} M) and L-cysteine (1×10^{-1} M) were prepared in distilled water. Three solutions: pV only (control), a 1:4 mixture of cysteine to pV, and cysteine only (control), were prepared as summarized in Table 4.5.1.

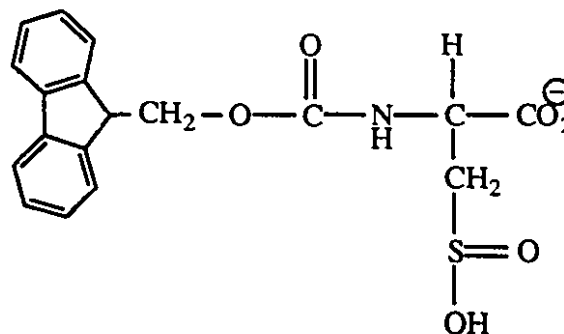
Table 4.5.1. Experimental details of the preparation of samples for reaction and HPLC analysis.

	#1	#2	#3
pV solution	2 mL	2 mL	-
cysteine solution	-	1 mL	1 mL
water	1 mL	-	2 mL

After 4.5 h reaction time the solutions were chromatographed on approximately 4 mL (i.d. 0.6 cm) of Dowex® 2 X 8 400 mesh anion exchange resin (chloride form). Each sample was eluted with 15 mL of distilled water. To a 1 mL aliquot from the effluent of each column was added 1 mL of a 50 mM pH 7.8 borate buffer. Then, 0.5 mL of a 20 mM solution of 9-fluorenylmethyl chloroformate in HPLC grade methanol was added to each sample resulting in the formation of a white precipitate. The solutions were allowed to react 5 minutes before the addition of 0.5 mL of a 40 mM solution of adamantamine hydrochloride in HPLC grade methanol. An additional 3 mL of methanol was added to each of the samples and a 1 mL aliquot of each was taken and to these samples was added 1 mL of HPLC grade methanol. Samples (10 µL) were injected onto the HPLC column and eluted for the first 5 min with NH₄H₂PO₄ (0.2 M at pH 5.5), a 0-40% linear gradient of the ammonium phosphate and 60/40 methanol/water solutions over the next 8 min, a 40-100% gradient over the following 0.5 min, and eluted for a further 12.5 min with 60/40 methanol/water at a flow rate of 0.5 mL/min. A peak was observed in the HPLC spectra at 14.86 minutes consistent with N-FMOC-cysteinesulfinic acid. A small quantity of pure N-FMOC-cysteinesulfinic acid was added to the sample and the HPLC analysis repeated resulting in a substantial increase in the intensity of the peak at 14.86 min.

4.5.6. N-FMOC-cysteinesulfinic acid.

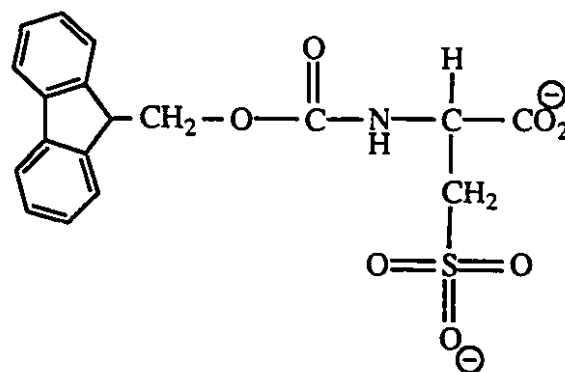
N-FMOC-cysteinesulfinic acid was prepared by modification of a literature technique for the protection of amino acids by 9-fluorenylmethyl chloroformate.¹⁵ L-cysteinesulfinic acid monohydrate (0.66 g, 3.87 mmol) was dissolved in a 10%



solution of K_2CO_3 in distilled water (10 mL). After the solution was cooled in an ice bath 9-fluorenylmethyl chloroformate (1.00g, 3.87 mmol) dissolved in 1,4-dioxane (10 mL) was slowly added while the mixture was stirred. The solution was left stirring overnight in the ice bath allowing it to warm slowly to r.t.. The solution was then added to distilled water (100 mL) and extracted with diethyl ether (2 X 100 mL, 1 X 60 mL). The solution was then concentrated by rotary evaporation to remove any residual diethyl ether and the pH of the solution was lowered to congo red with concentrated HCl resulting in a somewhat viscous solution. After rotary evaporation to 2/3 of its volume the solution was cooled at 5°C overnight. The solution was then filtered and the resulting precipitate dried in vacuo to yield a white powder (1.0 g, 70% yield). 1H NMR (CD_3OD): δ 7.78 (d,2H), 7.66 (d,2H), 7.34 (m, 4H), 4.56 (t, 1H), 4.36(d, 2H), 4.23 (t, 1H), 3.16 (d, 2H). ^{13}C NMR (CD_3OD): δ 173.0, 158.0, 145.1, 142.4, 128.9, 128.3, 126.4, 121.1, 69.1, 61.8, 51.8, 49.2. Melting point: 149-150°C. MS (FAB, NBA/NaCl matrix, 7 kV) [m/z (relative intensity)]: 376 (3.5%), 398 (19%) (Na adduct). Anal. Calc. for $C_{18}H_{17}NO_6S$: C, 57.59; H, 4.56; N, 3.73. Found: C, 57.35; H, 4.46; N, 3.66%.

4.5.7. Potassium N-FMOC-cysteinesulfonate monohydrate.

Potassium N-FMOC-cysteinesulfonate monohydrate was prepared by modification of a literature technique for the protection of amino acids by 9-fluorenylmethyl chloroformate.¹⁵ L-cysteinesulfonic acid monohydrate (0.72 g, 3.87 mmol) was



dissolved in a 10% solution of K_2CO_3 in distilled water (10 mL). After the solution was cooled in an ice bath 9-fluorenylmethyl chloroformate (1.00g, 3.87 mmol) dissolved in 1,4-dioxane (10 mL) was slowly added while the solution was stirred. The solution was left stirring 48 h in the ice bath allowing it to warm slowly to r.t.. The solution was then added to distilled water (200 mL) and extracted with diethyl ether (2 X 100 mL). The solution was then concentrated by rotary evaporated to approx. 1/2 volume and the pH of the solution lowered to congo red with concentrated HCl. The solution was cooled at 5°C for 4 days and filtered to give a white powder that was dried in vacuo (1.16g, 67%). 1H NMR (D_2O): δ 7.67 (d, 2H), 7.45 (t, 2H), 7.29 (m, 4H), 4.46 (t, 2H), 4.30 (d, 1H), 4.05 (t, 1H), 3.28 (m, 2H). ^{13}C NMR (D_2O): δ 173.3, 157.2, 143.6, 140.9, 128.1, 127.6, 125.3, 120.3, 66.9, 66.2, 51.9, 47.7. MS (FAB, NBA/NaCl matrix, 7 kV) [m/z (relative intensity)]: 414 (3.5%) (Na adduct). (FAB, NBA matrix, 7 kV) [m/z (relative intensity)]: 391 (1.7%). Anal. Calc. for $C_{18}H_{17}NO_7SK$: C, 48.42; H, 3.84; N, 3.14. Found: C, 48.20; H, 3.75; N, 3.09%.

4.6. References

- (1) Barford, D.; Flint, A. J.; Tonks, N. K. *Science* **1994**, *263*, 1397-1404.
- (2) Unpublished results; Chang-Ren Yang and Barry Posner.
- (3) Bartik, T.; Berit, B.; Hanson, B. E.; Glass, T.; Bebout, W. *Inorg. Chem.* **1992**, *31*, 2667-2670.
- (4) Butler, A.; Eckert, H. *J. Am. Chem. Soc.* **1989**, *111*, 2802-2809.
- (5) Crans, D. C.; Rithner, C. D.; Thiesen, L. A. *J. Am. Chem. Soc.* **1990**, *112*, 2901-2908.
- (6) Howarth, O. *Prog. NMR Spectrosc.* **1990**, *22*, 453-485.
- (7) Malmer, M. F.; Schroeder, L. A. *J. Chrom.* **1990**, *514*, 227-239.
- (8) Haynes, P. A.; Sheumack, D.; Greig, L. G.; Kibby, J.; Redmond, J. W. *J. Chrom.* **1991**, *588*, 107-1114.
- (9) Butler, A.; Clague, M. J.; Meister, G. E. *Chem. Rev.* **1994**, *94*, 625-638.
- (10) Kühle, E. *The Chemistry of Sulfenic Acids*; Georg Thieme Publishers: Stuttgart, 1973, pp 163.
- (11) Poole, L. B.; Claiborne, A. *J. Biol. Chem.* **1989**, *264*, 12330-12338.
- (12) Campestrini, S.; Conte, V.; Di Furia, F.; Modena, G.; Bortolini, O. *J. Org. Chem.* **1988**, *53*, 5721-5724.
- (13) Cornman, C. R.; Zovinka, E. P.; Meixner, M. H. *Inorg. Chem.* **1995**, *34*, 5099-5100.
- (14) Yale, J.-F.; Lachance, D.; Bevan, A. P.; Vigeant, C.; Shaver, A.; Posner, B. I. *Diabetes* **1995**, *44*, 1274-1279.
- (15) Carpino, L. A.; Han, G. Y. *J. Org. Chem.* **1972**, *37*, 3404-3409.

Contribution to Original Knowledge

Five new insulin-mimetic bpV compounds were synthesized and three representative examples were characterized by single crystal X-ray crystallography. These compounds in addition to a previously reported bpV compound provided two series of compounds that were used to probe structure activity relationships for insulin mimetic peroxovanadium complexes.

The stability of selected peroxovanadium compounds at pHs ranging from 4-7 was determined. The stability data provides the information relevant to the *in vivo* stability of the complexes and their suitability for various routes of administration. The reactivity with various buffers and additives to biological media was also determined. It was shown that HEPES buffer is not suitable for use with pV compounds but that MOPS buffer provided a less reactive alternative. The biological reducing agent DTT was shown to rapidly decompose pV compounds and its use with pV compounds is therefore contraindicated. The chelating agent EDTA reacted only slowly with pV compounds and its use is therefore not strictly contraindicated. It is ineffective as a means to remove pV compounds from solution.

The electron transfer oxidation of cysteine to the disulfide cystine by pV compounds was demonstrated to occur in limited yields. The ability of pV compounds to carry out oxygen transfer oxidations was demonstrated by the oxidation of a water soluble sulfonated triphenylphosphine to the corresponding oxide. The oxidation of cysteine to cysteinesulfinic acid by pV compounds was demonstrated showing the potential for these compounds to carry out oxygen transfer oxidations on cysteine thiols. This reactivity of pV compounds with cysteine was used as a model to propose a mechanism by which this class of compounds could exert their insulin mimetic effect. The oxidation of the

catalytically essential, active site cysteine of PTP would result in an irreversible inhibition of this enzyme. Inhibition of the PTP associated with the insulin receptor kinase would result in a greatly enhanced activity of latter. Increased activity of the insulin receptor kinase would therefore provide a substantial increase in the effects associated with insulin *in vivo*.

Appendices

A.1. Crystallographic Tables and Figures for bpV(OHpic)

Table A.1.1. Crystallographic parameters for bpV(OHpic).

bpV(OHpic)	
	C ₆ H ₄ K ₂ NO ₈ V•3 H ₂ O
fw	401.28
Crystal system	monoclinic
Space group	<i>P2₁/a</i>
Temperature (°C)	20 ± 1
λ (Å)	0.71069
<i>a</i> (Å)	7.078(2)
<i>b</i> (Å)	27.573(6)
<i>c</i> (Å)	7.222(3)
α (°)	
β (°)	105.99(3)
γ (°)	
ρ _{calc} (g cm ⁻³)	1.967
<i>V</i> (Å ³)	1354.8
No. variables	230
No. measured	2594
No. observed ref.	2102
No. unique ref.	2392
Merging R	0.02
<i>Z</i>	4
<i>R</i> ^a	0.023
<i>R</i> _w ^b	0.028
<i>S</i>	1.65
<i>K</i>	0.0001
Secondary Extinction	
μ (mm ⁻¹)	1.38 (Mo Kα)
Transmission range	
Scan (°)	1.5 + 0.30 tan θ
Scan speed (° min ⁻¹) (rescans)	8 (7)
Scan type	ω

$$^a R = \sum ||F_o| - |F_c|| / \sum |F_o|$$

$$^b R_w = \{ \sum w (|F_o| - |F_c|)^2 / \sum w |F_o|^2 \}^{1/2}$$

$$w = 1 / \sigma^2(F_o) + K F_o^2 \quad S = [\sum w (|F_o| - |F_c|)^2 / (n - v)]^{1/2}$$

Table A.1.2. Atomic parameters for bpV(OHpic).

Atomic Parameters x,y,z and Beq, E.S.Ds. refer to the last digit printed.

Atom	x	y	z	Beq
V	0.16670(5)	0.395717(12)	0.21324(5)	1.539(14)
K 1	0.95437(8)	0.441635(19)	0.62766(7)	2.554(22)
K 2	0.51446(8)	0.401212(19)	0.92526(7)	2.660(22)
O 1	0.12720(24)	0.39750 (5)	-0.01661(21)	2.41 (7)
O 2	0.44779(22)	0.38808 (5)	0.28444(21)	2.24 (6)
O 3	0.38518(23)	0.43828 (5)	0.29591(21)	2.47 (7)
O 4	-0.00037(23)	0.44414 (6)	0.26069(21)	2.51 (7)
O 5	-0.09488(23)	0.39658 (6)	0.23767(22)	2.66 (7)
O 6	0.22938(22)	0.37690 (5)	0.53675(19)	1.96 (6)
O 7	0.31469(24)	0.31436 (6)	0.73969(20)	2.70 (8)
O 8	0.2952 (3)	0.22949 (6)	0.61110(25)	3.51 (9)
N	0.16138(25)	0.31837 (6)	0.22920(23)	1.80 (7)
C 1	0.2547 (3)	0.33277 (8)	0.5729 (3)	1.78 (8)
C 2	0.2161 (3)	0.29839 (7)	0.4062 (3)	1.81 (8)
C 3	0.2369 (3)	0.24842 (8)	0.4324 (3)	2.31 (9)
C 4	0.2000 (4)	0.21849 (9)	0.2716 (4)	2.80 (11)
C 5	0.1426 (4)	0.23958 (9)	0.0927 (3)	2.77 (10)
C 6	0.1249 (3)	0.28961 (8)	0.0747 (3)	2.28 (9)
OW1	0.7658 (3)	0.47531 (7)	-0.0891 (3)	3.45 (9)
OW2	0.3149 (3)	0.48489 (8)	0.6342 (3)	3.69 (9)
OW3	0.6938 (3)	0.37108 (7)	0.6502 (3)	2.88 (8)
HO8	0.307 (5)	0.2549 (13)	0.682 (5)	7.0 (10)
H 4	0.216 (3)	0.1849 (9)	0.283 (3)	2.5 (5)
H 5	0.122 (3)	0.2207 (8)	-0.014 (3)	2.6 (5)
H 6	0.083 (3)	0.3048 (8)	-0.046 (3)	2.0 (5)
HOW1A	0.832 (6)	0.4686 (14)	0.024 (5)	7.9 (11)
HOW1B	0.748 (5)	0.5036 (12)	-0.094 (5)	5.7 (9)
HOW2A	0.339 (5)	0.4689 (12)	0.546 (5)	5.7 (9)
HOW2B	0.397 (6)	0.5016 (13)	0.670 (5)	7.1 (12)
HOW3A	0.604 (5)	0.3753 (12)	0.548 (5)	5.7 (9)
HOW3B	0.734 (4)	0.3433 (11)	0.656 (4)	3.8 (7)

Beq is the mean of the principal axes of the thermal ellipsoid for atoms refined anisotropically(non-hydrogens). For hydrogens, Beq = Biso.

Table A.1.3. Thermal factors for bpV(OH-pic).

Anisotropic Thermal factors for bpV(OH-pic). U(i,j) values x 100. E.S.Ds. refer to the last digit printed

Atom	U ₁₁	U ₂₂	U ₃₃	U ₁₂	U ₁₃	U ₂₃
V	2.250(20)	2.082(19)	1.642(19)	0.208(15)	0.750(15)	0.405(14)
K 1	3.40 (3)	3.86 (3)	2.76 (3)	0.180(24)	1.377(22)	0.579(21)
K 2	3.83 (3)	3.85 (3)	2.85 (3)	-0.699(24)	1.639(24)	-0.339(22)
O 1	3.55 (9)	3.72 (9)	1.99 (8)	0.58 (7)	0.95 (7)	0.52 (6)
O 2	2.72 (8)	2.90 (8)	3.02 (8)	0.33 (7)	0.99 (7)	0.38 (7)
O 3	3.27 (9)	2.30 (8)	3.77 (9)	-0.20 (7)	0.90 (7)	0.22 (7)
O 4	3.66 (9)	3.12 (9)	2.95 (8)	0.88 (7)	1.26 (7)	0.39 (7)
O 5	2.68 (9)	4.32 (10)	3.30 (9)	0.03 (8)	1.17 (7)	0.72 (7)
O 6	3.41 (9)	2.10 (8)	2.10 (8)	0.08 (7)	1.03 (7)	-0.03 (6)
O 7	5.15 (11)	3.12 (9)	1.80 (8)	-0.06 (8)	0.64 (7)	0.54 (6)
O 8	7.22 (14)	2.56 (9)	3.05 (9)	-0.28 (9)	0.54 (9)	0.83 (8)
N	2.52 (10)	2.55 (9)	1.90 (9)	-0.29 (8)	0.78 (7)	0.08 (7)
C 1	2.30 (11)	2.54 (11)	2.09 (10)	-0.22 (9)	0.88 (9)	0.09 (9)
C 2	2.36 (11)	2.40 (11)	2.13 (10)	-0.21 (9)	0.67 (9)	0.12 (8)
C 3	3.18 (13)	2.66 (11)	2.88 (11)	-0.28 (10)	0.70 (10)	0.25 (10)
C 4	4.34 (15)	2.16 (12)	4.11 (14)	-0.37 (11)	1.12 (12)	-0.31 (10)
C 5	4.25 (15)	3.33 (13)	2.99 (12)	-0.65 (11)	1.11 (11)	-1.11 (10)
C 6	3.29 (13)	3.32 (13)	2.05 (11)	-0.45 (10)	0.76 (10)	-0.33 (9)
OW1	5.30 (12)	3.10 (11)	4.00 (11)	-0.16 (9)	0.07 (9)	0.81 (8)
OW2	4.12 (12)	4.60 (12)	5.75 (13)	-1.32 (10)	2.09 (10)	-1.94 (10)
OW3	3.65 (11)	3.83 (11)	3.36 (10)	0.24 (9)	0.79 (9)	-0.55 (8)

Anisotropic Temperature Factors are of the form:

$$\text{Temp} = -2\pi^2(h^2U_{11}a^2 + k^2U_{22}b^2 + l^2U_{33}c^2 + 2hkU_{12}ab + 2hlU_{13}ac + 2klU_{23}bc)$$

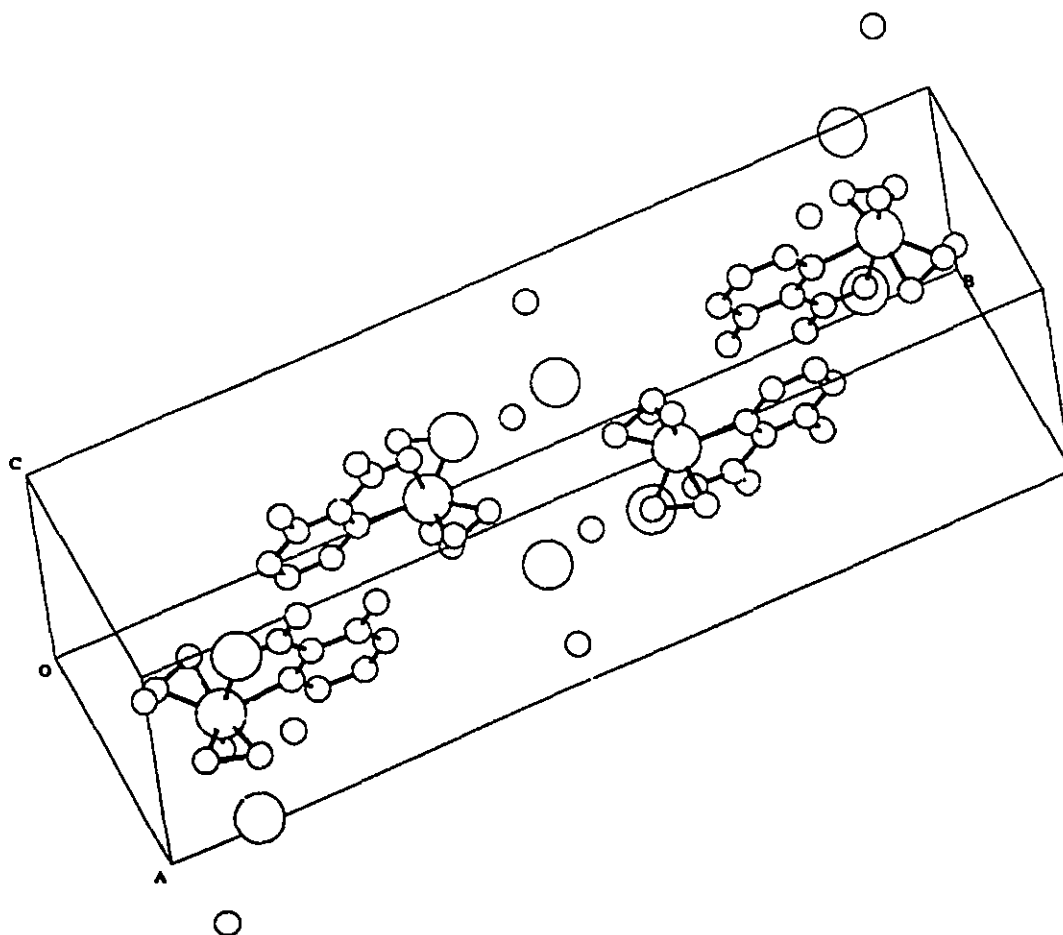
Table A.1.4. Selected bond lengths and angles for bpV(OH-pic).

Selected bond lengths (Å) and angles (°) for bpV(OH-pic). E.S.D.s refer to last digit printed.

Atom	Distance (Å)	Atom	Distance (Å)
V-O(1)	1.6064(16)	O(7)-C(1)	1.2678(24)
V-O(2)	1.9243(17)	O(8)-C(3)	1.347(3)
V-O(3)	1.9016(16)	N-C(2)	1.347(3)
V-O(4)	1.8766(16)	N-C(6)	1.335(3)
V-O(5)	1.9077(17)	C(1)-C(2)	1.497(3)
V-O(6)	2.3138(16)	C(2)-C(3)	1.393(3)
V-N	2.1368(18)	C(3)-C(4)	1.389(3)
O(2)-O(3)	1.4626(21)	C(4)-C(5)	1.373(4)
O(4)-O(5)	1.4607(22)	C(5)-C(6)	1.388(3)
O(6)-C(1)	1.247(3)		

Atom	Angle (°)	Atom	Angle(°)
O(1)-V-O(2)	98.76(8)	V-O(2)-O(3)	66.70(8)
O(1)-V-O(3)	101.56(8)	V-O(3)-O(2)	68.35(9)
O(1)-V-O(4)	103.17(7)	V-O(4)-O(5)	68.42(9)
O(1)-V-O(5)	101.43(8)	V-O(5)-O(4)	66.17(9)
O(1)-V-O(6)	168.73(7)	V-O(6)-C(1)	113.99(12)
O(1)-V-N	94.92(7)	V-N-C(2)	117.03(13)
O(2)-V-O(3)	44.95(7)	V-N-C(6)	123.36(14)
O(2)-V-O(4)	133.33(7)	C(2)-N-C(6)	119.29(19)
O(2)-V-O(5)	159.21(7)	O(6)-C(1)-O(7)	125.49(19)
O(2)-V-O(6)	79.00(6)	O(6)-C(1)-C(2)	117.76(17)
O(2)-V-N	84.76(6)	O(7)-C(1)-C(2)	116.73(18)
O(3)-V-O(4)	90.14(7)	N-C(2)-C(1)	116.44(18)
O(3)-V-O(5)	133.57(7)	N-C(2)-C(3)	121.67(19)
O(3)-V-O(6)	84.74(6)	C(1)-C(2)-C(3)	121.90(18)
O(3)-V-N	128.60(7)	O(8)-C(3)-C(2)	120.40(19)
O(4)-V-O(5)	45.40(7)	O(8)-C(3)-C(4)	120.52(21)
O(4)-V-O(6)	86.00(6)	C(2)-C(3)-C(4)	119.07(20)
O(4)-V-N	132.76(7)	C(3)-C(4)-C(5)	118.28(22)
O(5)-V-O(6)	80.23(7)	C(4)-C(5)-C(6)	120.34(21)
O(5)-V-N	88.59(7)	N-C(6)-C(5)	121.35(21)
O(6)-V-N	73.92(6)		

Figure A.1.1. Packing diagram for bpV(OH-pic).



A.2. Crystallographic Tables and Figures for bpV(2,4pdc)

Table A.2.1. Crystallographic parameters for bpV(2,4-pdc)

bpV(2,4-pdc)	
	$C_7H_3K_3NO_9V \cdot 3.25H_2O$
fw	471.88
Crystal system	monoclinic
Space group	$P2_1$
Temperature ($^{\circ}C$)	20 ± 1
λ (\AA)	1.540 56
a (\AA)	7.1018(12)
b (\AA)	38.187(5)
c (\AA)	11.4088(8)
α ($^{\circ}$)	
β ($^{\circ}$)	90.546(9)
γ ($^{\circ}$)	
ρ_{calc} (g cm^{-3})	2.026
V (\AA^3)	3093.8(7)
No. variables	486 x 2
No. measured	4355
No. observed ref.	3389
No. unique ref.	3978
Merging R	0.03
Z	8
R^a	0.049
R_w^b	0.055
S	1.97
K	0.0001
Secondary Extinction	0.67(4)
μ (mm^{-1})	13.47 (Cu $K\alpha$)
Transmission range	0.095 to 0.199
Scan ($^{\circ}$)	$0.97 + 0.30 \tan \theta$
Scan speed ($^{\circ} \text{min}^{-1}$) (rescans)	8 (7)
Scan type	$\omega/2\theta$

$$^aR = \sum ||F_o| - |F_c|| / \sum |F_o|$$

$$w = 1 / \sigma^2(F_o) + KF_o^2$$

$$^bR_w = \{ \sum w (|F_o| - |F_c|)^2 / \sum w |F_o|^2 \}^{1/2}$$

$$S = [\sum w (|F_o| - |F_c|)^2 / (n - v)]^{1/2}$$

Table A.2.2. Atomic parameters for bpV(2,4-pdc).

Atomic Parameters x, y, z and Biso for bpv(2,4-pdc)

Atom	x	y	z	Biso
VA	0.87408(35)	0.55226(6)	0.48952(20)	2.56(10)
O1A	0.9141(15)	0.5185(2)	0.5690(8)	3.7(5)
O2A	1.1245(14)	0.5634(3)	0.4426(9)	3.8(5)
O3A	1.0185(14)	0.5428(2)	0.3582(8)	3.6(4)
O4A	0.6577(14)	0.5403(2)	0.4072(8)	3.6(4)
O5A	0.6095(13)	0.5571(2)	0.5147(8)	3.1(4)
O6A	0.8270(13)	0.6086(2)	0.4212(7)	3.1(5)
O7A	0.8510(17)	0.6656(2)	0.4760(9)	4.3(6)
O8A	1.0131(17)	0.6890(3)	0.9031(9)	4.5(6)
O9A	1.0327(18)	0.6436(3)	1.0204(9)	4.9(6)
NA	0.9100(16)	0.5870(3)	0.6371(9)	2.4(5)
C1A	0.8590(22)	0.6335(4)	0.4968(12)	3.2(7)
C2A	0.9034(19)	0.6213(3)	0.6200(11)	2.7(6)
C3A	0.9341(21)	0.6453(4)	0.7094(11)	3.0(7)
C4A	0.9635(18)	0.6324(3)	0.8235(11)	2.3(5)
C5A	0.9637(20)	0.5964(4)	0.8395(11)	2.7(6)
C6A	0.9366(22)	0.5746(4)	0.7461(11)	3.2(6)
C7A	1.0067(21)	0.6576(4)	0.9261(13)	3.1(7)
VB	1.14423(31)	0.41281(5)	0.20784(17)	2.33(9)
O1B	1.2111(14)	0.4470(2)	0.2814(7)	2.9(4)
O2B	0.8820(13)	0.4124(2)	0.2438(7)	3.1(4)
O3B	0.9237(13)	0.4288(2)	0.1314(7)	3.0(4)
O4B	1.2719(14)	0.4187(2)	0.0671(7)	3.2(5)
O5B	1.3826(13)	0.3984(2)	0.1504(8)	3.2(4)
O6B	1.0717(12)	0.3577(2)	0.1407(7)	2.2(4)
O7B	1.1041(17)	0.3015(2)	0.1852(8)	4.0(5)
O8B	1.2492(15)	0.2727(2)	0.6113(7)	3.3(5)
O9B	1.2628(18)	0.3171(3)	0.7365(8)	4.5(6)
NB	1.1830(16)	0.3781(3)	0.3542(9)	2.5(5)
C1B	1.1062(19)	0.3324(4)	0.2109(11)	2.7(6)
C2B	1.1599(19)	0.3441(3)	0.3339(11)	2.3(6)
C3B	1.1759(21)	0.3193(3)	0.4238(11)	2.6(6)
C4B	1.2190(20)	0.3311(3)	0.5377(11)	2.6(6)
C5B	1.2420(20)	0.3661(3)	0.5543(11)	2.8(6)
C6B	1.2190(21)	0.3891(3)	0.4606(11)	2.6(6)
C7B	1.2478(20)	0.3049(4)	0.6362(12)	2.7(6)
VC	0.76715(32)	0.40732(5)	0.78005(18)	2.50(9)
O1C	0.7286(13)	0.4432(2)	0.7027(7)	3.2(4)
O3C	0.6257(13)	0.4165(2)	0.9150(7)	3.5(4)
O2C	0.5169(12)	0.3974(2)	0.8274(8)	3.5(4)
O4C	0.9856(12)	0.4189(2)	0.8650(7)	2.9(4)
O5C	1.0305(12)	0.4026(2)	0.7536(7)	2.8(4)
O6C	0.8113(12)	0.3510(2)	0.8463(6)	2.5(4)
O7C	0.7788(14)	0.2959(2)	0.7893(7)	3.6(4)
O8C	0.6279(15)	0.2733(2)	0.3643(7)	4.1(5)
O9C	0.6253(16)	0.3180(3)	0.2398(7)	4.5(5)
NC	0.7300(17)	0.3742(3)	0.6327(9)	3.3(5)
C1C	0.7775(20)	0.3280(3)	0.7713(11)	3.2(6)
C2C	0.7369(17)	0.3396(3)	0.6468(9)	2.1(5)

Table A.2.2. continued.

Atom	x	y	z	Biso
C3C	0.7041(17)	0.3169(3)	0.5548(10)	2.3(5)
C4C	0.6740(20)	0.3296(3)	0.4435(10)	2.8(6)
C5C	0.6766(21)	0.3658(3)	0.4275(10)	3.3(6)
C6C	0.7029(19)	0.3868(3)	0.5231(10)	2.9(6)
C7C	0.6410(19)	0.3054(3)	0.3404(11)	3.3(6)
VD	0.50018(32)	0.54501(0)	1.05914(17)	2.49(9)
O1D	0.4329(13)	0.5111(2)	0.9850(7)	3.2(4)
O3D	0.7216(12)	0.5295(2)	1.1332(7)	3.1(4)
O2D	0.7639(13)	0.5465(2)	1.0202(7)	3.3(4)
O4D	0.3734(12)	0.5391(2)	1.1995(7)	3.2(4)
O5D	0.2619(13)	0.5604(2)	1.1167(7)	3.4(4)
O6D	0.5779(13)	0.5999(2)	1.1246(6)	3.1(4)
O7D	0.5786(17)	0.6569(2)	1.0753(8)	4.8(5)
O8D	0.3780(15)	0.6862(2)	0.6641(8)	4.2(5)
O9D	0.3725(15)	0.6438(2)	0.5305(7)	4.1(5)
ND	0.4603(15)	0.5805(2)	0.9145(8)	2.6(4)
C1D	0.5522(20)	0.6250(3)	1.0505(11)	3.1(6)
C2D	0.4892(17)	0.6144(3)	0.9306(10)	2.4(5)
C3D	0.4693(17)	0.6391(3)	0.8442(11)	2.8(6)
C4D	0.4160(18)	0.6284(3)	0.7319(10)	2.6(5)
C5D	0.3909(19)	0.5930(3)	0.7126(9)	2.9(6)
C6D	0.4135(19)	0.5699(3)	0.8072(10)	2.6(5)
C7D	0.3881(21)	0.6551(3)	0.6324(11)	3.4(6)
K1	0.4481(5)	0.25880(8)	0.8287 (3)	4.07(15)
K2	1.0680(5)	0.50039(8)	0.1339 (3)	3.86(15)
K3	0.9391(4)	0.59332(8)	0.19452(24)	3.35(13)
K4	0.6487(5)	0.72621(8)	0.5546 (3)	3.82(15)
K5	0.7073(4)	0.36593(8)	0.07361(23)	3.01(13)
K6	0.2117(4)	0.36068(7)	0.91418(23)	2.73(12)
K7	0.3207(5)	0.45962(8)	0.8252 (3)	3.59(14)
K8	0.4320(4)	0.59791(7)	0.35092(23)	2.99(13)
K9	0.5768(5)	0.45808(8)	0.1328 (3)	3.64(14)
K10	0.3172(5)	0.50028(8)	0.4414 (3)	3.84(15)
K11	0.3177(6)	0.73498(9)	0.8312 (3)	5.01(18)
K12	0.9670(5)	0.23213(11)	0.6966 (3)	5.21(18)
OW1	0.1310(16)	0.7796 (3)	0.9833 (9)	5.7 (3)
OW2	0.5136(14)	0.5006 (3)	0.6561 (8)	4.31(21)
OW3	0.1742(17)	0.6477 (3)	0.2503 (9)	6.1 (3)
OW4	0.1280(18)	0.2323 (3)	0.9169 (11)	7.1 (3)
OW5	0.1199(14)	0.4591 (3)	0.6091 (8)	4.15(20)
OW6	0.4315(15)	0.3007 (3)	1.0342 (9)	5.14(24)
OW7	1.0655(16)	0.7308 (3)	0.5569 (9)	5.53(25)
OW8	0.3037(15)	0.1874 (3)	0.7237 (9)	5.07(24)
OW9	0.3698(18)	0.7011 (3)	0.3794 (11)	7.1 (3)
OW10	0.7366(16)	0.7335 (3)	0.7926 (9)	5.55(25)
OW11	0.6986(17)	0.4674 (3)	0.3619 (10)	6.0 (3)
OW12	0.9501(16)	0.4936 (3)	-0.0968 (9)	5.36(24)
OW13	0.6776(16)	0.2088 (3)	0.9275 (10)	5.9 (3)

Beq is the mean of the principal axes of the thermal ellipsoid.

Table A.2.2. continued.

Calculated Hydrogen Atom Parameters

Atom	x	y	z	Biso
H3A	0.9281(0)	0.6737(0)	0.6924(0)	3.7(0)
H5A	0.9847(0)	0.5855(0)	0.9273(0)	3.5(0)
H6A	0.9328(0)	0.5464(0)	0.7575(0)	3.9(0)
H3B	1.1642(0)	0.2908(0)	0.4057(0)	3.7(0)
H5B	1.2781(0)	0.3757(0)	0.6419(0)	3.5(0)
H6B	1.2295(0)	0.4175(0)	0.4747(0)	3.4(0)
H3C	0.7013(0)	0.2886(0)	0.5682(0)	3.0(0)
H5C	0.6567(0)	0.3768(0)	0.3385(0)	4.1(0)
H6C	0.7012(0)	0.4154(0)	0.5068(0)	3.6(0)
H3D	0.4963(0)	0.6671(0)	0.8628(0)	3.2(0)
H5D	0.3576(0)	0.5830(0)	0.6242(0)	3.8(0)
H6D	0.3886(0)	0.5421(0)	0.7910(0)	3.0(0)

Hydrogen positions calculated assuming C-H of 1.08Å. Biso(H) is from $U_{iso}(H) = 0.01 + U_{eq}(C)$.

Table A.2.3. Thermal factors for bpV(2,4-pdc).

Anisotropic Thermal factors for bpV(2,4-pdc). U(i,j) values x 100. E.S.Ds. refer to the last digit printed

Atom	u11	u22	u33	u12	u13	u23
VA	3.85(15)	2.87(13)	3.01(13)	0.18(12)	0.29(11)	-0.23(11)
O1A	6.6(7)	3.4(5)	3.8(6)	1.0(5)	-0.4(5)	0.3(5)
O2A	3.9(6)	4.4(6)	5.9(7)	-0.9(5)	0.7(5)	-0.5(5)
O3A	6.0(7)	4.1(6)	3.6(5)	1.5(5)	1.9(5)	-0.8(5)
O4A	5.3(7)	4.1(6)	4.3(6)	-0.6(5)	-0.8(5)	-0.2(5)
O5A	4.3(6)	3.7(5)	3.8(6)	0.6(5)	0.5(5)	0.3(5)
O6A	5.2(6)	3.8(6)	2.6(5)	0.1(5)	0.1(5)	-0.1(4)
O7A	8.2(9)	2.7(6)	5.2(7)	0.8(6)	-0.5(6)	-0.3(5)
O8A	8.5(9)	4.1(7)	4.6(7)	0.0(6)	-0.7(6)	-0.9(5)
O9A	9.8(10)	5.5(7)	3.2(6)	-0.5(7)	-1.0(6)	0.2(6)
NA	4.6(7)	2.1(6)	2.6(6)	-0.1(5)	-0.2(5)	0.2(5)
C1A	5.3(10)	3.7(9)	3.2(8)	0.6(8)	0.6(7)	-0.5(7)
C2A	3.2(8)	3.5(8)	3.6(8)	0.0(7)	1.9(7)	-0.4(6)
C3A	5.4(10)	3.1(8)	3.0(8)	0.2(7)	-0.2(7)	-0.8(7)
C4A	2.6(7)	3.6(8)	2.4(7)	-0.9(6)	0.5(6)	-0.8(6)
C5A	3.9(8)	3.5(8)	2.9(8)	-1.0(7)	0.6(6)	0.5(7)
C6A	5.5(10)	3.5(8)	3.1(8)	-1.1(8)	0.7(7)	0.5(7)
C7A	3.8(9)	3.5(9)	4.3(9)	-0.3(7)	0.3(7)	-0.9(7)
VB	4.06(13)	2.41(11)	2.39(11)	0.24(11)	0.07(10)	0.10(9)
O1B	5.2(6)	2.7(5)	3.2(5)	-0.4(5)	0.1(5)	0.6(4)
O2B	4.3(6)	3.9(6)	3.5(5)	-0.1(5)	1.8(4)	0.4(5)
O3B	4.5(6)	3.3(5)	3.5(5)	0.5(5)	-0.7(5)	0.8(4)
O4B	5.5(7)	3.8(6)	2.9(5)	0.0(5)	0.1(5)	0.2(4)
O5B	3.7(6)	4.7(6)	3.6(5)	0.1(5)	0.4(5)	0.8(5)
O6B	3.4(5)	2.3(5)	2.5(5)	-0.1(4)	-0.1(4)	0.0(4)
O7B	10.1(9)	2.3(6)	2.8(5)	0.4(6)	-1.9(6)	-0.8(4)
O8B	7.1(8)	2.8(6)	2.6(5)	0.2(5)	-0.5(5)	0.0(4)
O9B	11.2(10)	3.8(6)	2.1(5)	1.8(7)	-0.5(6)	0.1(5)
NB	3.6(7)	2.6(6)	3.4(7)	0.1(5)	1.6(5)	-0.6(5)
C1B	2.4(8)	4.4(9)	3.4(8)	0.3(7)	0.6(6)	-0.6(7)
C2B	4.0(8)	2.1(7)	2.6(7)	0.1(6)	-0.3(6)	-1.0(6)
C3B	5.3(9)	2.3(7)	2.2(7)	0.9(7)	-0.4(6)	1.1(6)
C4B	3.9(9)	3.5(8)	2.3(7)	0.4(7)	0.4(6)	-0.5(6)
C5B	4.7(9)	2.6(8)	3.2(8)	0.2(7)	0.1(7)	-0.7(6)
C6B	4.6(9)	2.5(7)	2.9(8)	-0.3(7)	0.4(7)	-0.2(6)
C7B	3.5(8)	3.5(8)	3.2(8)	0.3(7)	-0.1(7)	-0.1(7)
VC	4.07(13)	2.58(11)	2.85(11)	-0.05(11)	0.12(10)	-0.07(9)
O1C	5.1(6)	3.0(5)	3.9(5)	0.7(5)	0.2(5)	0.6(4)
O3C	5.4(6)	4.2(5)	3.8(5)	-0.2(5)	0.9(5)	0.2(4)
O2C	3.7(6)	4.2(5)	5.4(6)	0.0(5)	1.2(5)	0.0(5)
O4C	3.7(5)	3.8(5)	3.4(5)	0.1(4)	0.2(4)	-1.5(4)
O5C	3.9(5)	3.0(5)	3.8(5)	-0.1(4)	0.6(4)	0.1(4)
O6C	4.1(5)	3.4(5)	2.0(4)	-0.3(4)	-0.3(4)	-0.2(4)
O7C	6.7(7)	2.7(5)	4.3(5)	-0.4(5)	-0.7(5)	0.9(4)

Table A.2.3. continued

Atom	u11	u22	u33	u12	u13	u23
O8C	8.6(8)	3.5(5)	3.6(5)	0.6(5)	-0.7(5)	1.8(4)
O9C	9.7(9)	5.3(6)	2.0(5)	-2.1(6)	0.0(5)	-0.2(4)
NC	6.5(8)	2.9(6)	3.2(6)	-0.6(6)	0.4(6)	-0.1(5)
C1C	5.0(9)	3.0(7)	4.1(8)	0.1(7)	0.7(7)	1.1(6)
C2C	3.0(7)	2.6(6)	2.4(6)	0.0(6)	0.5(5)	0.8(5)
C3C	3.9(8)	1.7(6)	3.0(7)	0.2(6)	0.0(6)	-0.5(5)
C4C	5.4(9)	3.2(7)	2.2(6)	0.3(7)	0.9(6)	0.5(5)
C5C	7.2(10)	3.1(7)	2.1(6)	-0.6(7)	0.8(7)	-0.2(5)
C6C	5.2(9)	2.6(7)	3.4(7)	0.3(7)	0.5(7)	0.4(6)
C7C	4.1(8)	4.6(8)	4.0(8)	-0.7(7)	1.7(7)	-0.1(6)
VD	4.11(14)	2.64(11)	2.74(11)	0.14(11)	0.37(10)	0.24(10)
O1D	6.2(7)	2.7(5)	3.1(5)	0.2(5)	-1.0(5)	0.2(4)
O3D	3.8(5)	4.7(5)	3.4(5)	0.7(5)	0.4(4)	0.8(4)
O2D	5.0(6)	3.3(5)	4.2(5)	-0.2(5)	0.4(4)	0.3(4)
O4D	3.3(5)	5.5(6)	3.3(5)	-0.4(5)	0.0(4)	0.5(4)
O5D	4.2(6)	3.6(5)	4.9(6)	0.5(4)	0.7(5)	0.1(4)
O6D	6.0(6)	3.5(5)	2.1(4)	0.7(5)	-0.1(4)	-0.8(4)
O7D	10.4(9)	3.4(5)	4.3(6)	-0.4(6)	-1.6(6)	-0.2(5)
O8D	9.4(8)	2.5(5)	4.2(6)	-0.1(5)	1.1(6)	0.3(4)
O9D	8.8(8)	4.4(6)	2.5(5)	1.2(6)	0.4(5)	-0.6(4)
ND	4.2(7)	2.7(5)	3.0(6)	0.1(5)	-0.3(5)	-0.6(5)
C1D	5.1(9)	2.9(7)	3.8(8)	0.5(7)	-0.3(7)	0.1(6)
C2D	2.9(7)	3.6(7)	2.6(6)	0.1(6)	0.3(6)	-0.6(6)
C3D	2.7(7)	2.9(7)	5.0(8)	0.3(6)	0.9(6)	-0.5(6)
C4D	3.3(7)	3.4(7)	3.0(7)	0.0(6)	-0.6(6)	0.1(6)
C5D	5.3(9)	4.1(8)	1.8(6)	0.6(7)	0.8(6)	-0.8(6)
C6D	4.4(8)	3.1(7)	2.5(6)	0.2(6)	0.5(6)	-0.2(6)
C7D	6.9(10)	2.5(7)	3.6(7)	0.5(7)	1.2(7)	1.0(6)
K1	6.42(23)	3.94(18)	5.09(19)	0.36(17)	-0.49(17)	1.25(15)
K2	4.96(20)	3.27(17)	6.42(22)	0.11(16)	-1.05(17)	0.55(15)
K3	4.61(19)	4.94(18)	3.19(16)	0.52(16)	0.27(14)	0.21(14)
K4	7.10(24)	3.22(16)	4.20(18)	-0.21(17)	0.75(17)	0.35(14)
K5	4.55(18)	3.97(16)	2.91(15)	0.29(15)	0.11(14)	0.22(13)
K6	4.55(18)	3.25(15)	2.58(14)	-0.11(14)	0.49(13)	-0.25(12)
K7	5.72(21)	3.38(16)	4.55(18)	-0.14(16)	-0.35(16)	-0.25(14)
K8	4.86(19)	3.47(16)	3.04(15)	0.16(15)	0.21(14)	-0.08(13)
K9	4.68(20)	3.03(16)	6.11(20)	0.02(15)	-0.53(17)	0.36(15)
K10	6.05(22)	4.06(17)	4.46(19)	-0.28(17)	-0.46(17)	0.02(15)
K11	11.4(3)	4.10(18)	3.54(17)	-0.29(21)	1.84(19)	-0.10(15)
K12	5.93(24)	7.37(24)	6.49(23)	-0.72(21)	-0.31(19)	1.65(20)

Anisotropic Temperature Factors are of the form:

$$\text{Temp} = -2\pi^2(h^2U_{11}a^2 + k^2U_{22}b^2 + \dots + 2hkU_{12}a^*b^* + 2hlU_{13}a^*c^* \dots)$$

Table A.2.4. Selected bond lengths and angles for bpV(2,4-pdc)

Selected bond lengths (Å) and angles (°) for bpV(2,4-pdc). E.S.D.s refer to last digit printed.

Atoms	Distance (Å)	Atoms	Distance (Å)
VA-O(1A)	1.601(9)	VC-O(1C)	1.650(8)
VA-O(2A)	1.910(10)	VC-O(3C)	1.879(8)
VA-O(3A)	1.859(9)	VC-O(2C)	1.901(9)
VA-O(4A)	1.851(10)	VC-O(4C)	1.874(8)
VA-O(5A)	1.913(10)	VC-O(5C)	1.906(8)
VA-O(6A)	2.312(9)	VC-O(6C)	2.298(8)
VA-NA	2.156(10)	VC-NC	2.117(10)
O(2A)-O(3A)	1.448(14)	O(3C)-O(2C)	1.453(13)
O(4A)-O(5A)	1.428(13)	O(4C)-O(5C)	1.454(11)
O(6A)-C(1A)	1.302(17)	O(6C)-C(1C)	1.250(15)
O(7A)-C(1A)	1.248(17)	O(7C)-C(1C)	1.243(15)
O(8A)-C(7A)	1.228(18)	O(8C)-C(7C)	1.258(16)
O(9A)-C(7A)	1.214(19)	O(9C)-C(7C)	1.248(15)
NA-C(2A)	1.328(16)	NC-C(2C)	1.334(15)
NA-C(6A)	1.342(16)	NC-C(6C)	1.351(15)
C(1A)-C(2A)	1.511(20)	C(1C)-C(2C)	1.514(16)
C(2A)-C(3A)	1.386(18)	C(2C)-C(3C)	1.379(15)
C(3A)-C(4A)	1.406(18)	C(3C)-C(4C)	1.374(16)
C(4A)-C(5A)	1.387(19)	C(4C)-C(5C)	1.394(17)
C(4A)-C(7A)	1.544(18)	C(4C)-C(7C)	1.513(18)
C(5A)-C(6A)	1.364(19)	C(5C)-C(6C)	1.363(17)
VB-O(1B)	1.620(9)	VD-O(1D)	1.616(8)
VB-O(2B)	1.911(9)	VD-O(3D)	1.875(8)
VB-O(3B)	1.887(9)	VD-O(2D)	1.930(9)
VB-O(4B)	1.865(9)	VD-O(4D)	1.858(8)
VB-O(5B)	1.903(9)	VD-O(5D)	1.914(9)
VB-O(6B)	2.297(8)	VD-O(6D)	2.291(8)
VB-NB	2.148(11)	VD-ND	2.153(10)
O(2B)-O(3B)	1.460(12)	O(3D)-O(2D)	1.478(11)
O(4B)-O(5B)	1.453(13)	O(4D)-O(5D)	1.472(12)
O(6B)-C(1B)	1.275(16)	O(6D)-C(1D)	1.290(14)
O(7B)-C(1B)	1.217(17)	O(7D)-C(1D)	1.266(15)
O(8B)-C(7B)	1.262(16)	O(8D)-C(7D)	1.242(15)
O(9B)-C(7B)	1.240(16)	O(9D)-C(7D)	1.245(15)
NB-C(2B)	1.326(16)	ND-C(2D)	1.322(15)
NB-C(6B)	1.307(17)	ND-C(6D)	1.330(15)
C(1B)-C(2B)	1.518(18)	C(1D)-C(2D)	1.491(17)
C(2B)-C(3B)	1.402(17)	C(2D)-C(3D)	1.369(17)
C(3B)-C(4B)	1.407(18)	C(3D)-C(4D)	1.394(17)
C(4B)-C(5B)	1.360(18)	C(4D)-C(5D)	1.379(17)
C(4B)-C(7B)	1.518(19)	C(4D)-C(7D)	1.537(17)
C(5B)-C(6B)	1.390(18)	C(5D)-C(6D)	1.403(17)

Table A.2.4. continued

Atoms	Angle (°)	Atoms	Angle (°)
O(1A)-VA-O(2A)	100.2(5)	O(1C)-VC-O(3C)	101.3(4)
O(1A)-VA-O(3A)	101.8(5)	O(1C)-VC-O(2C)	99.6(4)
O(1A)-VA-O(4A)	103.3(5)	O(1C)-VC-O(4C)	102.3(4)
O(1A)-VA-O(5A)	99.3(5)	O(1C)-VC-O(5C)	98.8(4)
O(1A)-VA-O(6A)	164.9(4)	O(1C)-VC-O(6C)	166.6(4)
O(1A)-VA-NA	91.9(4)	O(1C)-VC-NC	93.0(4)
O(2A)-VA-O(3A)	45.2(4)	O(3C)-VC-O(2C)	45.2(4)
O(2A)-VA-O(4A)	133.1(5)	O(3C)-VC-O(4C)	88.8(4)
O(2A)-VA-O(5A)	160.0(4)	O(3C)-VC-O(5C)	132.9(4)
O(2A)-VA-O(6A)	80.3(4)	O(3C)-VC-O(6C)	88.7(3)
O(2A)-VA-NA	88.8(4)	O(3C)-VC-NC	134.3(4)
O(3A)-VA-O(4A)	90.3(5)	O(2C)-VC-O(4C)	132.2(4)
O(3A)-VA-O(5A)	133.6(4)	O(2C)-VC-O(5C)	161.3(4)
O(3A)-VA-O(6A)	89.3(4)	O(2C)-VC-O(6C)	81.0(3)
O(3A)-VA-NA	133.4(5)	O(2C)-VC-NC	89.8(4)
O(4A)-VA-O(5A)	44.6(4)	O(4C)-VC-O(5C)	45.2(3)
O(4A)-VA-O(6A)	86.7(4)	O(4C)-VC-O(6C)	86.6(3)
O(4A)-VA-NA	129.8(5)	O(4C)-VC-NC	130.4(4)
O(5A)-VA-O(6A)	79.7(4)	O(5C)-VC-O(6C)	80.3(3)
O(5A)-VA-NA	86.2(4)	O(5C)-VC-NC	86.1(4)
VA-O(2A)-O(3A)	65.6(5)	VC-O(3C)-O(2C)	68.2(5)
VA-O(3A)-O(2A)	69.3(5)	VC-O(2C)-O(3C)	66.6(5)
VA-O(4A)-O(5A)	70.0(5)	VC-O(4C)-O(5C)	68.5(5)
VA-O(5A)-O(4A)	65.4(5)	VC-O(5C)-O(4C)	66.2(5)
VA-O(6A)-C(1A)	115.6(8)	VC-O(6C)-C(1C)	114.2(7)
VA-NA-C(2A)	119.3(8)	VC-NC-C(2C)	119.5(8)
VA-NA-C(6A)	121.5(8)	VC-NC-C(6C)	122.7(8)
C(2A)-NA-C(6A)	119.2(11)	C(2C)-NC-C(5C)	117.8(10)
O(6A)-C(1A)-O(7A)	125.7(13)	O(6C)-C(1C)-O(7C)	125.6(11)
O(6A)-C(1A)-C(2A)	115.2(12)	O(6C)-C(1C)-C(2C)	118.0(10)
O(7A)-C(1A)-C(2A)	119.2(12)	O(7C)-C(1C)-C(2C)	116.4(11)
NA-C(2A)-C(1A)	116.6(11)	NC-C(2C)-C(1C)	114.2(10)
NA-C(2A)-C(3A)	122.7(12)	NC-C(2C)-C(3C)	121.8(10)
C(1A)-C(2A)-C(3A)	120.7(12)	C(1C)-C(2C)-C(3C)	124.0(10)
C(2A)-C(3A)-C(4A)	118.1(12)	C(2C)-C(3C)-C(4C)	120.3(10)
C(3A)-C(4A)-C(5A)	118.0(11)	C(3C)-C(4C)-C(5C)	118.0(11)
C(3A)-C(4A)-C(7A)	120.7(12)	C(3C)-C(4C)-C(7C)	121.6(11)
C(5A)-C(4A)-C(7A)	121.2(12)	C(5C)-C(4C)-C(7C)	120.4(10)
C(4A)-C(5A)-C(6A)	120.1(12)	C(4C)-C(5C)-C(6C)	118.6(11)
NA-C(6A)-C(5A)	121.9(12)	NC-C(6C)-C(5C)	123.4(11)
O(8A)-C(7A)-O(9A)	127.9(13)	O(8C)-C(7C)-O(9C)	124.7(12)
O(8A)-C(7A)-C(4A)	117.0(13)	O(8C)-C(7C)-C(4C)	115.9(11)
O(9A)-C(7A)-C(4A)	115.1(13)	O(9C)-C(7C)-C(4C)	119.4(11)
O(1B)-VB-O(2B)	100.2(4)	O(1D)-VD-O(3D)	103.0(4)
O(1B)-VB-O(3B)	102.5(4)	O(1D)-VD-O(2D)	100.7(4)
O(1B)-VB-O(4B)	101.9(4)	O(1D)-VD-O(4D)	102.2(4)
O(1B)-VB-O(5B)	98.9(5)	O(1D)-VD-O(5D)	99.7(4)
O(1B)-VB-O(6B)	167.1(4)	O(1D)-VD-O(6D)	166.6(3)
O(1B)-VB-NB	93.5(4)	O(1D)-VD-ND	93.9(4)
O(2B)-VB-O(3B)	45.2(4)	O(3D)-VD-O(2D)	45.7(3)

Table A.2.4. continued

Atoms	Angle (°)	Atoms	Angle (°)
O(2B)-VB-O(4B)	132.0(4)	O(3D)-VD-O(4D)	89.1(4)
O(2B)-VB-O(5B)	160.7(4)	O(3D)-VD-O(5D)	133.1(4)
O(2B)-VB-O(6B)	81.3(4)	O(3D)-VD-O(6D)	86.8(3)
O(2B)-VB-NB	86.9(4)	O(3D)-VD-ND	130.5(4)
O(3B)-VB-O(4B)	88.3(4)	O(2D)-VD-O(4D)	132.9(4)
O(3B)-VB-O(5B)	132.2(4)	O(2D)-VD-O(5D)	158.9(4)
O(3B)-VB-O(6B)	87.7(3)	O(2D)-VD-O(6D)	79.4(3)
O(3B)-VB-NB	131.2(4)	O(2D)-VD-ND	85.7(4)
O(4B)-VB-O(5B)	45.3(4)	O(4D)-VD-O(5D)	45.9(4)
O(4B)-VB-O(6B)	86.2(4)	O(4D)-VD-O(6D)	86.9(3)
O(4B)-VB-NB	133.1(4)	O(4D)-VD-ND	132.5(4)
O(5B)-VB-O(6B)	79.5(4)	O(5D)-VD-O(6D)	79.5(3)
O(5B)-VB-NB	88.9(4)	O(5D)-VD-ND	87.6(4)
VB-O(2B)-O(3B)	66.5(5)	VD-O(3D)-O(2D)	69.1(5)
VB-O(3B)-O(2B)	68.3(5)	VD-O(2D)-O(3D)	65.2(5)
VB-O(4B)-O(5B)	68.7(5)	VD-O(4D)-O(5D)	69.1(5)
VB-O(5B)-O(4B)	66.0(5)	VD-O(5D)-O(4D)	65.0(5)
VB-O(6B)-C(1B)	116.2(8)	VD-O(6D)-C(1D)	115.7(7)
VB-NB-C(2B)	117.6(8)	VD-ND-C(2D)	119.4(7)
VB-NB-C(6B)	123.1(9)	VD-ND-C(6D)	122.9(8)
C(2B)-NB-C(6B)	119.9(11)	C(2D)-ND-C(6D)	117.7(10)
O(6B)-C(1B)-O(7B)	125.4(12)	O(6D)-C(1D)-O(7D)	123.3(11)
O(6B)-C(1B)-C(2B)	113.8(11)	O(6D)-C(1D)-C(2D)	116.2(10)
O(7B)-C(1B)-C(2B)	120.7(12)	O(7D)-C(1D)-C(2D)	120.6(11)
NB-C(2B)-C(1B)	118.5(11)	ND-C(2D)-C(1D)	115.9(10)
NB-C(2B)-C(3B)	121.7(11)	ND-C(2D)-C(3D)	123.9(11)
C(1B)-C(2B)-C(3B)	119.7(11)	C(1D)-C(2D)-C(3D)	120.2(11)
C(2B)-C(3B)-C(4B)	118.3(11)	C(2D)-C(3D)-C(4D)	119.0(11)
C(3B)-C(4B)-C(5B)	117.9(12)	C(3D)-C(4D)-C(5D)	117.8(11)
C(3B)-C(4B)-C(7B)	119.9(11)	C(3D)-C(4D)-C(7D)	121.1(11)
C(5B)-C(4B)-C(7B)	122.1(11)	C(5D)-C(4D)-C(7D)	121.1(10)
C(4B)-C(5B)-C(6B)	120.0(12)	C(4D)-C(5D)-C(6D)	118.8(10)
NB-C(6B)-C(5B)	122.2(11)	ND-C(6D)-C(5D)	122.7(11)
O(8B)-C(7B)-O(9B)	125.1(12)	O(8D)-C(7D)-O(9D)	126.8(11)
O(8B)-C(7B)-C(4B)	118.5(11)	O(8D)-C(7D)-C(4D)	115.2(11)
O(9B)-C(7B)-C(4B)	116.4(12)	O(9D)-C(7D)-C(4D)	118.0(11)

Table A.2.5. Least squares planes for bpV(2,4-pdc)

. Distances(A) to the least-squares planes.

Plane no. 1

Equation of the plane : $7.010(6)X - 0.53(23)Y - 1.93(5)Z = 4.83(14)$

Distances(A) to the plane from the atoms in the plane.

NA	0.012(15)	C2A	-0.020(17)
C3A	0.010(18)	C4A	0.004(16)
C5A	-0.007(17)	C6A	-0.005(19)

Chi squared for this plane 2.670

Distances(A) to the plane from the atoms out of the plane.

O6A	-0.165(23)	O7A	-0.13(3)
O8A	0.168(25)	O9A	0.103(24)
C1A	-0.100(23)	C7A	0.096(23)

Plane no. 2

Equation of the plane : $6.952(9)X - 3.26(23)Y - 2.22(6)Z = 6.20(10)$

Distances(A) to the plane from the atoms in the plane.

NB	0.006(14)	C2B	0.001(17)
C3B	-0.007(18)	C4B	0.001(17)
C5B	0.010(18)	C6B	-0.016(17)

Chi squared for this plane 1.547

Distances(A) to the plane from the atoms out of the plane.

O7B	0.08(3)	O8B	0.238(24)
O9B	-0.09(3)	C1B	-0.061(23)
C7B	0.068(22)		

Table A.2.5. continued

Plane no. 3

Equation of the plane : $7.005(6)X - 0.60(21)Y - 1.98(6)Z = 3.66(8)$

Distances(A) to the plane from the atoms in the plane.

NC	-0.018(15)	C2C	0.023(15)
C3C	-0.011(15)	C4C	-0.010(17)
C5C	0.018(18)	C6C	0.001(17)

Chi squared for this plane 5.995

Distances(A) to the plane from the atoms out of the plane.

O6C	0.143(21)	O7C	0.062(22)
O8C	-0.142(23)	O9C	0.058(24)
C1C	0.068(21)	C7C	-0.023(22)

Plane no. 4

Equation of the plane :- $6.872(10)X + 4.08(20)Y + 2.71(6)Z = 1.68(14)$

Distances(A) to the plane from the atoms in the plane.

ND	0.009(13)	C2D	-0.008(15)
C3D	-0.005(15)	C4D	0.013(16)
C5D	-0.010(17)	C6D	-0.004(16)

Chi squared for this plane 2.066

Distances(A) to the plane from the atoms out of the plane.

O7C	-3.68(6)	O6D	-0.150(21)
O7D	-0.056(23)	O8D	0.326(22)
O9D	-0.171(22)	C7D	0.044(22)

Dihedral angle between planes A and B

A	B	Angle(deg)
1	2	4.4(5)
1	3	0.3(7)
1	4	173.3(4)
2	3	4.2(5)
2	4	177.2(5)
3	4	173.5(4)

Figure A.2.1. Packing diagram for bpV(2,4-pdc).

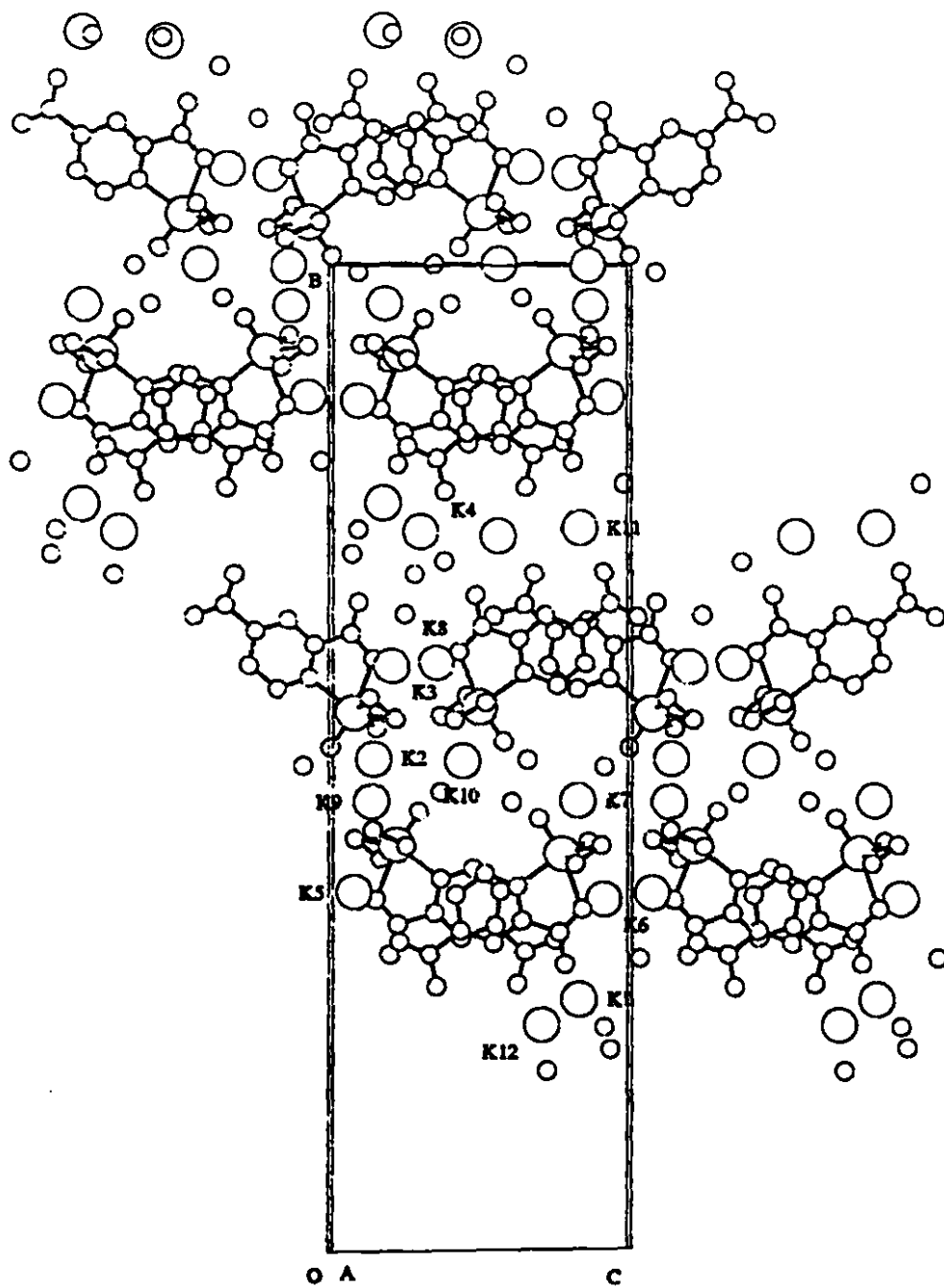
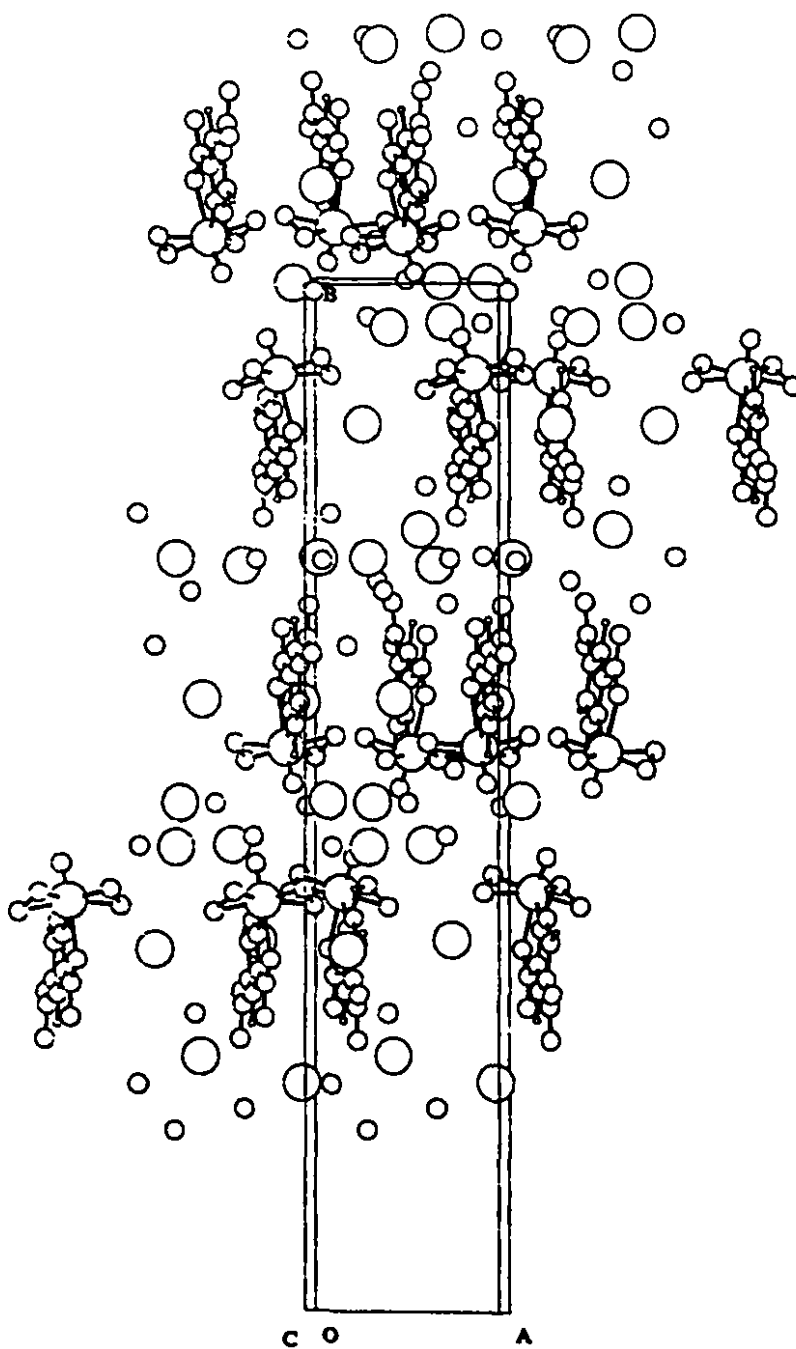


Figure A.2.2. Packing diagram for bpV(2,4-pdc).



A.3. Crystallographic Tables and Figures for bpV(acetpic)

Table A.3.1. Crystallographic parameters for bpV(acetpic).

bpV(acetpic)	
	$C_8H_5K_3NO_{10}V \cdot 2H_2O$
fw	479.39
Crystal system	triclinic
Space group	$P\bar{1}$
Temperature (°C)	20 ± 1
λ (Å)	0.709 30
a (Å)	7.4037(13)
b (Å)	10.709(3)
c (Å)	10.9569(19)
α (°)	110.742(16)
β (°)	95.600(19)
γ (°)	100.195(19)
ρ_{calc} (g cm ⁻³)	2.022
V (Å ³)	787.4(3)
No. variables	263
No. measured	2251
No. observed ref.	1537
No. unique ref.	2060
Merging R	0.02
Z	2
R^a	0.036
R_w^b	0.026
S	1.47
K	0
Secondary Extinction	0.025(7)
μ (mm ⁻¹)	1.47 (Mo K α)
Transmission range	
Scan (°)	$1.5 + 0.30 \tan \theta$
Scan speed (° min ⁻¹) (rescans)	8 (7)
Scan type	$\omega/2\theta$

$$^aR = \frac{\sum ||F_o| - |F_c||}{\sum |F_o|}$$

$$w = 1 / (\sigma(F_o) + KF_o^2)$$

$$^bR_w = \frac{(\sum w (|F_o| - |F_c|)^2 / \sum w |F_o|^2)^{1/2}}{S}$$

$$S = [\sum w (|F_o| - |F_c|)^2 / (n - v)]^{1/2}$$

Table A.3.2. Atomic parameters for bpV(acetpic).

Atomic Parameters x, y, z and Biso for bpV(acetpic)

Atom	x	y	z	B _{eq}
V	0.77355(13)	0.87285(9)	0.27465(8)	1.49(4)
K1	0.50755(18)	0.55017(12)	0.26844(12)	2.19(6)
K2	1.23110(18)	0.87597(12)	0.40930(12)	2.31(6)
K3	0.95528(18)	0.46427(13)	0.24376(12)	2.57(7)
N	0.7224(6)	0.9204(4)	0.0985(4)	1.47(20)
O1	0.9343(5)	1.0116(3)	0.3516(3)	2.15(18)
O2	0.5637(5)	0.9427(3)	0.3352(3)	2.45(20)
O3	0.6335(5)	0.8623(3)	0.4048(3)	2.31(19)
O4	0.8772(5)	0.7321(3)	0.2951(3)	2.51(19)
O5	0.9298(5)	0.7589(3)	0.1784(3)	2.72(21)
O6	0.5472(5)	0.7082(3)	0.1352(3)	2.22(18)
O7	0.3513(5)	0.6286(3)	-0.0552(3)	2.23(18)
O8	0.4634(5)	0.7328(3)	-0.2316(3)	2.38(20)
O9	0.2684(5)	0.5143(3)	-0.4329(3)	2.33(20)
O10	0.2605(5)	0.6291(3)	-0.5679(3)	2.03(19)
C1	0.4896(8)	0.7089(5)	0.0231(5)	1.95(27)
C2	0.6006(7)	0.8250(5)	-0.0063(5)	1.24(25)
C3	0.5788(7)	0.8380(5)	-0.1286(4)	1.48(25)
C4	0.6768(8)	0.9565(5)	-0.1388(5)	2.13(29)
C5	0.7930(7)	1.0552(5)	-0.0282(5)	1.96(28)
C6	0.8153(7)	1.0330(5)	0.0877(5)	1.89(26)
C7	0.4341(8)	0.7478(5)	-0.3566(5)	2.35(30)
C8	0.3080(7)	0.6181(5)	-0.4606(5)	1.73(27)
H 4	0.664(5)	0.962(3)	-0.227(3)	0.5(9)
H 5	0.864(6)	1.127(4)	-0.038(4)	1.7(10)
H 6	0.894(5)	1.095(3)	0.163(3)	0.2(9)
H7A	0.549(6)	0.770(4)	-0.386(4)	3.1(12)
H7B	0.380(6)	0.827(4)	-0.343(4)	2.3(11)
OW1	0.1947(6)	0.4489(4)	0.0685(4)	3.76(25)
OW2	0.0815(7)	0.2859(4)	0.3523(4)	4.89(26)
HW1A	0.177(6)	0.531(4)	0.080(4)	1.6(10)
HW1B	0.207(6)	0.402(4)	-0.034(4)	4.4(15)
HW2A	0.123(7)	0.347(4)	0.415(4)	2.9(12)
HW2B	0.091(9)	0.221(6)	0.364(5)	7.8(19)

B_{eq} is the mean of the principal axes of the thermal ellipsoid.

Table A.3.3. Thermal factors for bpV(acetpic)

Anisotropic Thermal factors for bpV(acetpic). U(i,j) values x 100. E.S.Ds. refer to the last

digit printed

Atom	u11	u22	u33	u12	u13	u23
V	1.85(6)	1.85(5)	1.59(5)	0.15(4)	-0.30(4)	0.51(4)
K1	3.12(8)	2.94(7)	2.59(7)	1.01(6)	0.33(6)	1.32(6)
K2	2.46(8)	2.96(8)	3.00(8)	0.24(6)	-0.23(6)	1.10(6)
K3	2.39(8)	3.87(8)	2.75(7)	0.37(7)	-0.16(6)	0.68(6)
N	1.9(3)	1.4(2)	1.9(2)	0.1(2)	-0.1(2)	0.5(2)
O1	2.7(2)	2.2(2)	2.6(2)	-0.2(2)	-0.7(2)	0.8(2)
O2	3.2(3)	3.5(2)	3.4(2)	1.6(2)	0.8(2)	1.7(2)
O3	3.6(3)	3.0(2)	2.6(2)	1.0(2)	0.6(2)	1.4(2)
O4	3.3(2)	2.5(2)	3.5(2)	0.8(2)	-0.6(2)	1.0(2)
O5	3.2(3)	3.4(2)	3.1(2)	1.0(2)	0.2(2)	0.6(2)
O6	3.2(2)	2.4(2)	2.3(2)	-0.6(2)	-0.5(2)	1.2(2)
O7	2.5(2)	2.6(2)	2.0(2)	-1.2(2)	-1.3(2)	0.5(2)
O8	4.5(3)	2.1(2)	1.7(2)	-0.4(2)	-0.9(2)	0.8(2)
O9	4.1(3)	1.8(2)	2.6(2)	-0.1(2)	-0.6(2)	1.1(2)
O10	3.1(2)	2.9(2)	1.5(2)	0.1(2)	-0.1(2)	1.0(2)
C1	3.0(4)	1.8(3)	2.4(3)	1.1(3)	0.2(3)	0.4(2)
C2	1.2(3)	1.2(3)	2.1(3)	0.2(2)	0.2(2)	0.5(2)
C3	2.3(3)	1.6(3)	1.7(3)	0.4(3)	-0.2(3)	0.6(2)
C4	3.3(4)	3.1(3)	1.9(3)	1.0(3)	0.4(3)	1.1(3)
C5	1.9(3)	2.6(3)	2.9(3)	0.2(3)	0.4(3)	1.2(3)
C6	2.5(3)	1.6(3)	1.8(3)	0.1(3)	-0.4(3)	-0.6(2)
C7	4.7(4)	2.6(3)	1.7(3)	0.5(3)	-0.2(3)	1.2(3)
C8	1.7(3)	2.9(3)	1.7(3)	1.1(3)	-0.1(3)	0.4(3)
OW1	4.0(3)	6.6(3)	3.2(2)	0.7(3)	0.2(2)	1.6(2)
OW2	8.5(4)	3.3(3)	4.1(3)	-0.2(3)	-2.4(3)	-0.2(2)

Anisotropic Temperature Factors are of the form:

$$\text{Temp} = -2\pi^2(h^2U_{11}a^2 + k^2U_{22}b^2 + l^2U_{33}c^2 + 2hkU_{12}ab + 2hlU_{13}ac + 2klU_{23}bc \dots)$$

Table A.3.4. Selected bond lengths and angles bpV(acetpic)

Selected bond lengths (Å) and angles (°) for bpV(acetpic). E.S.D.s refer to last digit

printed.

Atoms	Distance (Å)	Atoms	Distance (Å)
V-N	2.179(4)	O(7)-C(1)	1.233(6)
V-O(1)	1.621(3)	O(8)-C(3)	1.357(6)
V-O(2)	1.917(4)	O(8)-C(7)	1.435(6)
V-O(3)	1.866(4)	O(9)-C(8)	1.247(6)
V-O(5)	1.941(4)	O(10)-C(8)	1.246(6)
V-O(4)	1.878(4)	C(1)-C(2)	1.516(7)
V-O(6)	2.190(3)	C(2)-C(3)	1.393(6)
N-C(2)	1.348(6)	C(3)-C(4)	1.393(7)
N-C(6)	1.328(6)	C(4)-C(5)	1.376(7)
O(2)-O(3)	1.461(5)	C(5)-C(6)	1.373(7)
O(5)-O(4)	1.480(5)	C(7)-C(8)	1.520(7)
O(6)-C(1)	1.264(6)		

Atoms	Angle (°)	Atoms	Angle(°)
N-V-O(1)	93.39(16)	C(2)-N-C(6)	119.7(4)
N-V-O(2)	89.97(15)	V-O(2)-O(3)	65.46(20)
N-V-O(3)	133.67(16)	V-O(3)-O(2)	69.13(19)
N-V-O(5)	85.59(15)	V-O(5)-O(4)	64.99(19)
N-V-O(4)	129.08(15)	V-O(4)-O(5)	69.45(19)
N-V-O(6)	72.76(13)	V-O(6)-C(1)	120.8(3)
O(1)-V-O(2)	98.32(17)	C(3)-O(8)-C(7)	117.9(4)
O(1)-V-O(3)	103.39(17)	O(6)-C(1)-O(7)	124.9(5)
O(1)-V-O(5)	97.78(17)	O(6)-C(1)-C(2)	113.9(4)
O(1)-V-O(4)	104.84(17)	O(7)-C(1)-C(2)	121.2(4)
O(1)-V-O(6)	166.04(15)	N-C(2)-C(1)	114.3(4)
O(2)-V-O(3)	45.41(15)	N-C(2)-C(3)	121.1(4)
O(2)-V-O(5)	163.52(16)	C(1)-C(2)-C(3)	124.5(4)
O(2)-V-O(4)	131.96(16)	O(8)-C(3)-C(2)	117.5(4)
O(2)-V-O(6)	80.34(15)	O(8)-C(3)-C(4)	123.9(4)
O(3)-V-O(5)	132.80(15)	C(2)-C(3)-C(4)	118.6(4)
O(3)-V-O(4)	98.04(16)	C(3)-C(4)-C(5)	118.8(4)
O(3)-V-O(6)	85.66(14)	C(4)-C(5)-C(6)	119.7(4)
O(5)-V-O(4)	45.56(15)	N-C(6)-C(5)	122.0(4)
O(5)-V-O(6)	83.19(15)	O(8)-C(7)-C(8)	110.3(4)
O(4)-V-O(6)	85.85(14)	O(9)-C(8)-O(10)	127.5(4)
V-N-C(2)	117.3(3)	O(9)-C(8)-C(7)	118.8(4)
V-N-C(6)	122.9(3)	O(10)-C(8)-C(7)	113.7(4)

Table A.3.5. Least-squares planes for bpV(acetpic)

Plane no. 1

Equation of the plane: $-6.247 (5) X + 5.808 (10) Y + 2.868 (7) Z = 1.033 (11)$

Distances (A) to the plane from the atoms in the plane.

V	-0.0082 (14)	N	0.082 (4)
O6	0.050 (5)	C1	0.092 (6)
C2	-0.011 (5)	C3	-0.151 (6)
C4	-0.103 (6)	C5	0.0161 (6)
C6	0.125 (6)		

Chi squared for this plane 2147.471

Plane no. 2

Equation of the plane : $-6.838 (17) X + 4.89 (8) Y + 2.19 (5) Z = 0.09 (8)$

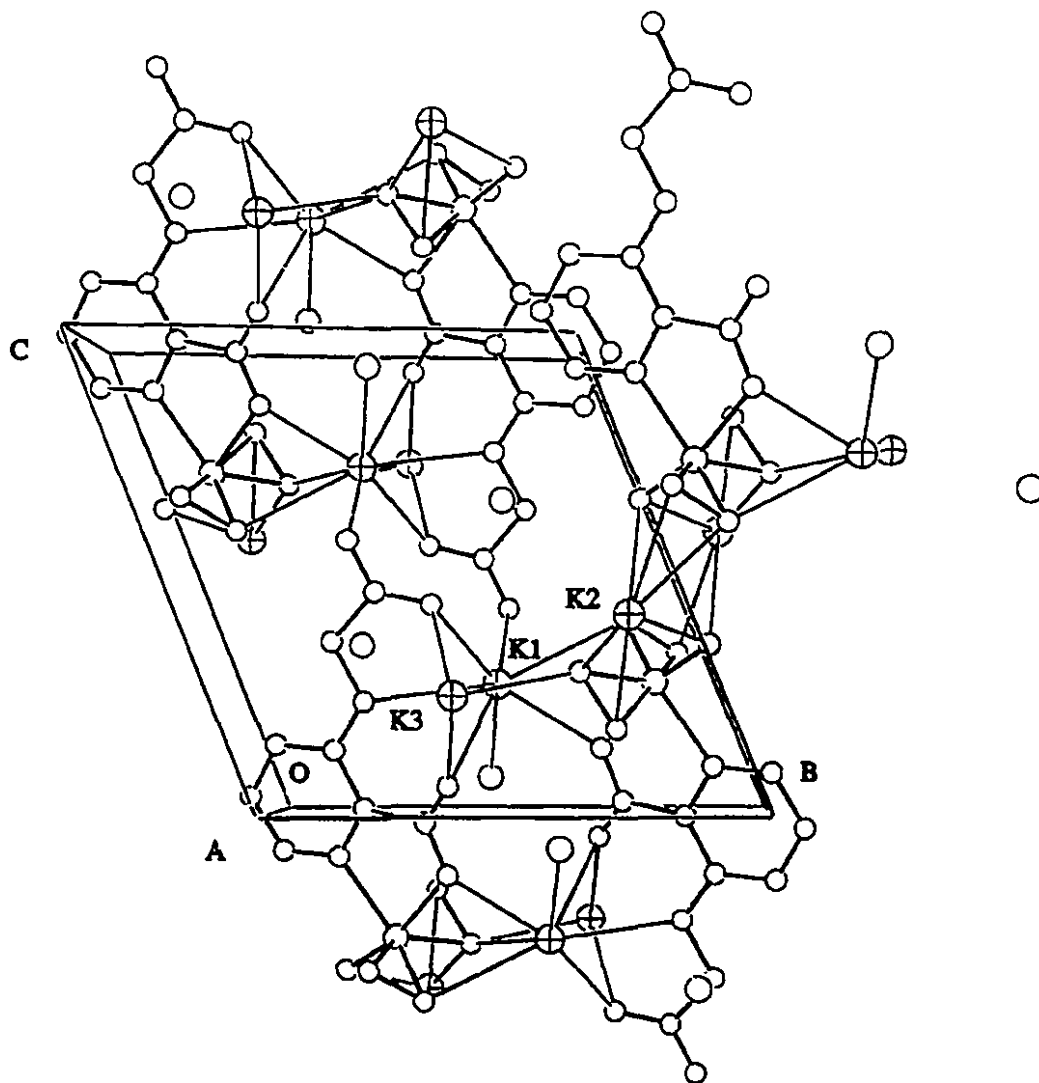
Distances (A) to the plane from the atoms in the plane.

O8	0.000 (5)	C7	0.000 (9)
C8	0.000 (7)		

Dihedral angle between planes A and B

A	B	Angle (deg)
1	2	10.0

Figure A.3.1. Packing diagram for bpV(acetpic)



A.4. Crystallographic Tables and Figures for GmpV(2,6-pdc)

Table A.4.1. Crystallographic parameters for the guanidinium salt of mpV(2,6-pdc).

GmpV(2,6-pdc)	
	$C_8H_{11}NO_8V \cdot H_2O$
fw	360.15
Crystal system	monoclinic
Space group	$P2_1/n$
Temperature ($^{\circ}C$)	20 ± 1
λ (\AA)	0.71069
a (\AA)	10.837(1)
b (\AA)	10.075(1)
c (\AA)	12.440(2)
α ($^{\circ}$)	
β ($^{\circ}$)	103.399(9)
γ ($^{\circ}$)	
ρ_{calc} ($g\ cm^{-3}$)	1.810
V (\AA^3)	1321.3(3)
No. variables	244
No. measured	4896
No. observed ref.	1788
No. unique ref.	2465
Merging R	0.069
Z	4
R^a	0.034
R_w^b	0.043
S	1.27
Secondary Extinction	0.3881×10^{-5}
μ (mm^{-1})	1.38 (Mo $K\alpha$)
Transmission range	0.95-1.00
Scan ($^{\circ}$)	$(0.68 + 0.35 \tan\theta)$
Scan speed ($^{\circ}\ min^{-1}$) (rescans)	8(7)
Scan type	ω -2 θ

$$^aR = \sum ||F_o| - |F_c|| / \sum |F_o|$$

$$^bR_w = \{ \sum w (|F_o| - |F_c|)^2 / \sum w |F_o|^2 \}^{1/2}$$

$$w = 4F_o^2 / \sigma^2(F_o^2) \quad S = [\sum w (|F_o| - |F_c|)^2 / (n - v)]^{1/2}$$

Table A.4.2. Atomic parameters for GmpV(2,6-pdc).

Atomic Parameters x,y,z and Beq, E.S.Ds. refer to the last digit printed.

Atom	x	y	z	B(eq)
V(1)	0.27490(04)	0.04667(05)	0.05230(04)	1.73(2)
O(1)	0.3920(02)	0.1219(02)	0.0231(02)	2.8(1)
O(2)	0.1420(02)	0.1690(02)	0.0134(02)	2.50(9)
O(3)	0.1438(02)	0.0778(02)	-0.0760(02)	2.64(9)
O(4)	0.1271(02)	-0.0808(02)	0.1090(02)	2.6(1)
O(5)	0.2962(02)	-0.1208(02)	-0.0346(02)	2.43(8)
O(6)	0.3783(02)	-0.3233(02)	-0.0323(02)	3.2(1)
O(7)	0.2924(02)	0.1401(02)	0.2007(02)	2.27(8)
O(8)	0.3772(02)	0.1412(02)	0.3820(02)	3.0(1)
O(W)	0.9317(03)	0.1077(03)	0.6629(03)	5.7(1)
N(1)	0.3796(02)	-0.0820(02)	0.1679(02)	1.70(9)
N(2)	0.7547(03)	-0.0113(04)	0.2763(03)	3.8(1)
N(3)	0.6472(03)	0.1860(04)	0.2714(03)	3.6(1)
N(4)	0.7341(04)	0.0859(04)	0.4356(02)	3.4(1)
C(1)	0.3573(03)	0.0884(03)	0.2906(02)	2.0(1)
C(2)	0.4095(03)	-0.0464(03)	0.2751(02)	1.8(1)
C(3)	0.4788(03)	-0.1302(03)	0.3533(03)	2.3(1)
C(4)	0.5147(03)	-0.2518(03)	0.3205(03)	2.7(1)
C(5)	0.4806(03)	-0.2893(04)	0.2105(03)	2.5(1)
C(6)	0.4117(03)	-0.2013(03)	0.1359(02)	2.0(1)
C(7)	0.3609(03)	-0.2208(03)	0.0138(02)	2.2(1)
C(8)	0.7132(03)	0.0867(03)	0.3277(02)	2.3(1)
H(3)	0.497(03)	-0.103(04)	0.427(03)	3.7(8)
H(4)	0.558(03)	-0.312(04)	0.369(03)	3.3(8)
H(5)	0.497(03)	-0.368(04)	0.186(03)	3.3(8)
H(O4)A	0.055(04)	-0.057(04)	0.093(03)	3.2(9)
H(O4)B	0.130(03)	-0.170(04)	0.120(03)	4(1)
H(OW)A*	0.8643	0.0935	0.6570	6.6
H(OW)B*	0.9423	0.1731	0.5942	6.8
H(N2)A	0.740(04)	-0.009(05)	0.206(04)	5(1)
H(N2)B	0.794(04)	-0.072(05)	0.319(04)	5(1)
H(N3)A	0.639(04)	0.185(05)	0.207(04)	5(1)
H(N3)B	0.622(05)	0.251(06)	0.314(04)	9(2)
H(N4)A	0.710(04)	0.141(04)	0.463(03)	3(1)
H(N4)B	0.784(04)	0.025(04)	0.470(03)	3.6(9)

* fixed atom

Table. A.4.3. Thermal factors for GmpV(2.6-pdc).

Anisotropic Thermal factors for bpV(OH-pic). U(i,j) values E.S.Ds. refer to the last digit printed

Atom	U11	U22	U33	U12	U13	U23
V(1)	0.0230(03)	0.0220(03)	0.0207(03)	-0.0021(02)	0.0052(02)	0.0022(02)
O(1)	0.0288(12)	0.0364(14)	0.0439(13)	-0.0059(10)	0.0127(10)	0.0063(11)
O(2)	0.0332(11)	0.0313(13)	0.0292(11)	0.0030(09)	0.0045(09)	0.0043(10)
O(3)	0.0339(12)	0.0392(14)	0.0259(11)	0.0002(10)	0.0043(09)	0.0036(10)
O(4)	0.0266(13)	0.0275(14)	0.0468(14)	-0.0021(10)	0.0126(10)	0.0047(11)
O(5)	0.0349(11)	0.0324(13)	0.0247(11)	-0.0023(10)	0.0065(09)	-0.0039(09)
O(6)	0.0509(14)	0.0352(14)	0.0404(13)	-0.0033(11)	0.0178(11)	-0.0136(12)
O(7)	0.0348(11)	0.0218(11)	0.0272(11)	0.0046(09)	0.0027(09)	-0.0012(09)
O(8)	0.0518(14)	0.0335(13)	0.0268(12)	0.0057(11)	0.0036(10)	-0.0084(10)
O(W)	0.100(02)	0.055(02)	0.064(02)	0.009(02)	0.022(02)	0.009(02)
N(1)	0.0218(12)	0.0187(12)	0.0243(13)	-0.0004(10)	0.0055(09)	-0.0014(10)
N(2)	0.074(02)	0.039(02)	0.037(02)	0.010(02)	0.022(02)	-0.002(02)
N(3)	0.062(02)	0.043(02)	0.034(02)	0.009(02)	0.014(02)	0.010(02)
N(4)	0.066(02)	0.033(02)	0.029(02)	0.009(02)	0.011(02)	-0.0039(14)
C(1)	0.0278(15)	0.022(02)	0.025(02)	-0.0036(12)	0.0062(12)	-0.0011(13)
C(2)	0.0248(14)	0.024(02)	0.0209(14)	-0.0024(12)	0.0067(11)	-0.0021(13)
C(3)	0.029(02)	0.031(02)	0.025(02)	-0.0030(13)	0.0028(12)	0.0042(14)
C(4)	0.030(02)	0.033(02)	0.036(02)	0.0083(14)	0.0021(13)	0.011(02)
C(5)	0.032(02)	0.022(02)	0.044(02)	0.0028(13)	0.0119(14)	-0.0028(15)
C(6)	0.0222(14)	0.025(02)	0.030(02)	-0.0019(12)	0.0092(12)	-0.0032(14)
C(7)	0.0253(15)	0.029(02)	0.034(02)	-0.0053(13)	0.0135(12)	-0.0079(15)
C(8)	0.036(02)	0.024(02)	0.031(02)	-0.0037(13)	0.0138(13)	0.0014(14)
H(3)	0.047(10)					
H(4)	0.042(10)					
H(5)	0.041(10)					
H(O4)A	0.040(11)					
H(O4)B	0.051(12)					
H(OW)A*	0.0840					
H(OW)B*	0.0861					
H(N2)A	0.059(13)					
H(N2)B	0.068(15)					
H(N3)A	0.07(02)					
H(N3)B	0.11(02)					
H(N4)A	0.042(12)					
H(N4)B	0.046(11)					

* fixed atom

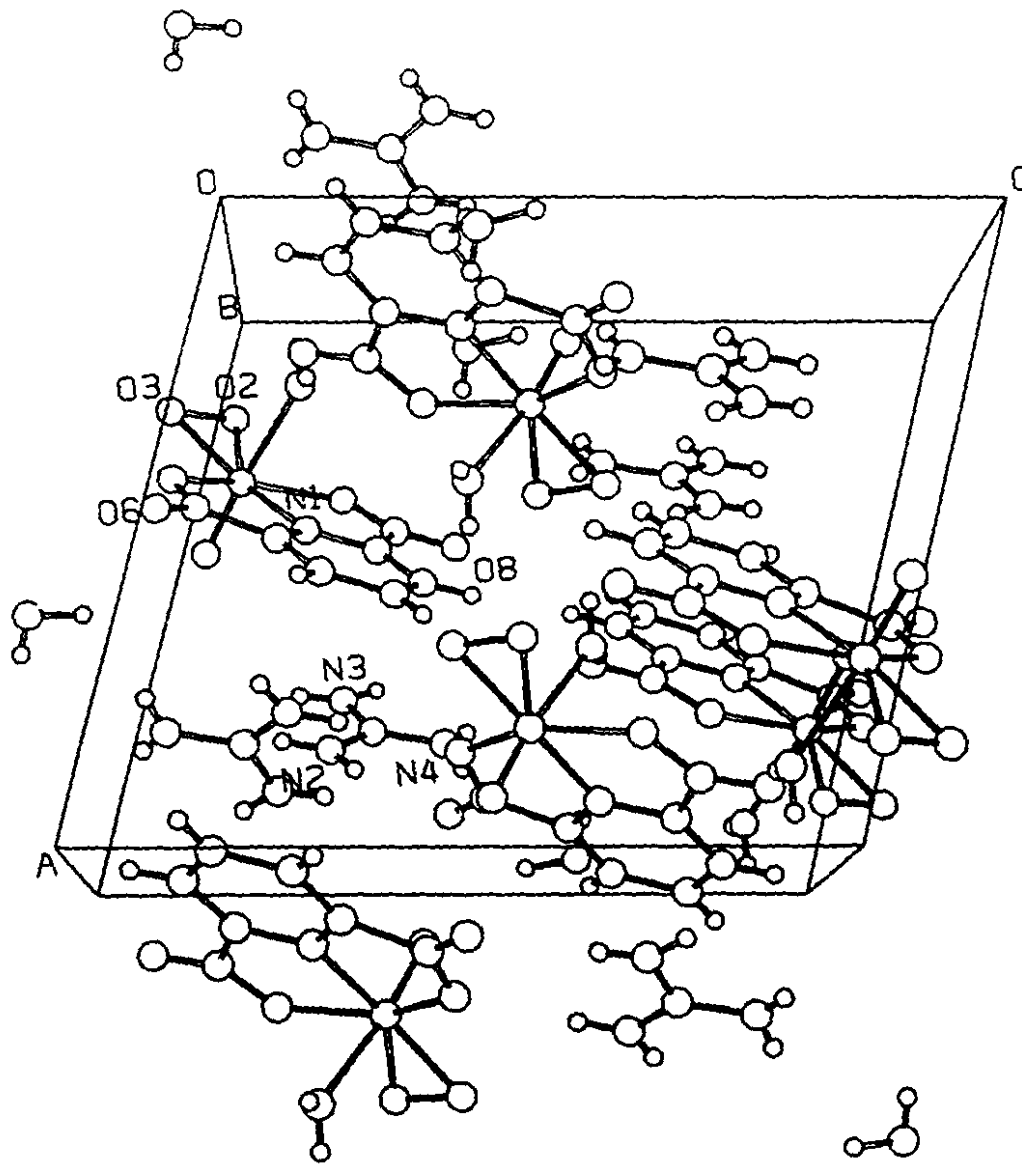
Table A.4.4. Selected bond lengths and angles for GmpV(2,6-pdc).

Selected bond lengths (Å) and angles (°) for GmpV(2,6-pdc). E.S.D.s refer to last digit printed.

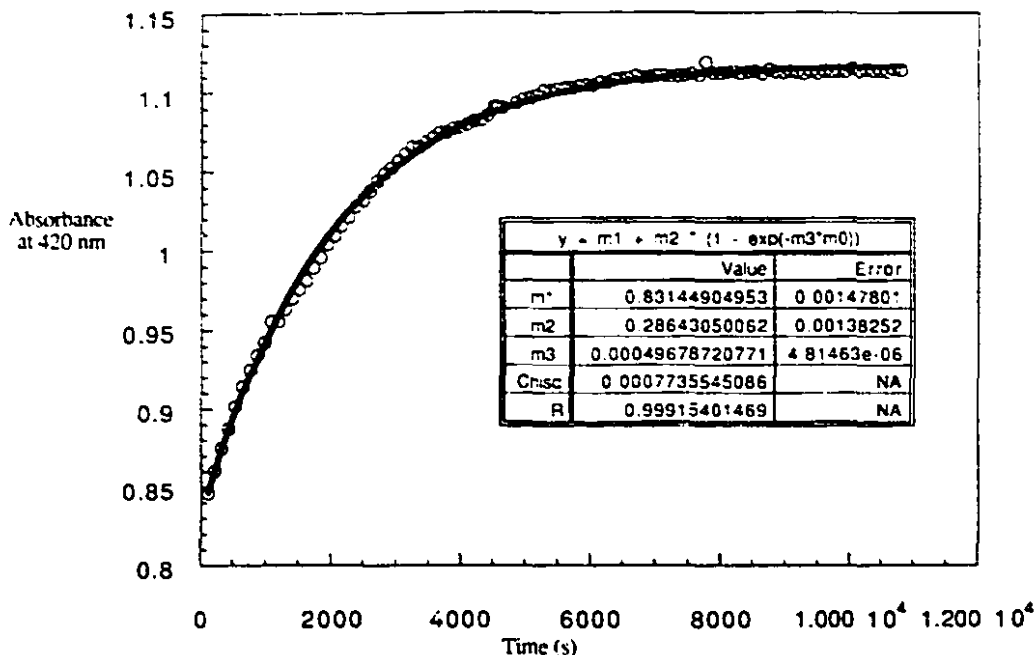
Atom	Atom	Distance	Atom	Atom	Distance
V1	O1	1.590(2)	N1	C2	1.345(3)
V1	O2	1.871(2)	N1	C6	1.338(4)
V1	O3	1.901(2)	N2	C8	1.311(4)
V1	O4	2.289(2)	N3	C8	1.330(5)
V1	O5	2.045(2)	N4	C8	1.308(4)
V1	O7	2.042(2)	C1	C2	1.501(4)
V1	N1	2.069(2)	C2	C3	1.374(4)
O2	O3	1.445(3)	C3	C4	1.376(5)
O5	C7	1.294(4)	C4	C5	1.385(5)
O6	C7	1.217(4)	C5	C6	1.372(4)
O7	C1	1.285(3)	C6	C7	1.504(4)
O8	C1	1.228(4)			

Atom	Atom	Atom	Angle	Atom	Atom	Atom	Angle
O1	V1	O2	103.5(1)	V1	O5	C7	120.8(2)
O1	V1	O3	102.1(1)	V1	O7	C1	121.2(2)
O1	V1	O4	172.0(1)	V1	N1	C2	119.3(2)
O1	V1	O5	94.5(1)	V1	N1	C6	119.6(2)
O1	V1	O7	94.3(1)	C2	N1	C6	121.1(2)
O1	V1	N1	96.9(1)	O7	C1	O8	125.0(3)
O2	V1	O3	45.05(9)	O7	C1	C2	113.6(2)
O2	V1	O4	84.13(9)	O8	C1	C2	121.4(3)
O2	V1	O5	125.50(9)	N1	C2	C1	111.0(2)
O2	V1	O7	80.52(8)	N1	C2	C3	120.3(3)
O2	V1	N1	149.03(9)	C1	C2	C3	128.7(3)
O3	V1	O4	84.91(9)	C2	C3	C4	118.8(3)
O3	V1	O5	81.18(9)	C3	C4	C5	120.5(3)
O3	V1	O7	125.31(9)	C4	C5	C6	118.1(3)
O3	V1	N1	150.5(1)	N1	C6	C5	121.1(3)
O4	V1	O5	82.71(9)	N1	C6	C7	111.1(3)
O4	V1	O7	84.53(9)	C5	C6	C7	127.8(3)
O4	V1	N1	75.17(9)	O5	C7	O6	124.6(3)
O5	V1	O7	149.29(8)	O5	C7	C6	113.6(3)
O5	V1	N1	74.91(9)	O6	C7	C6	121.8(3)
O7	V1	N1	74.86(8)	N2	C8	N3	120.9(3)
V1	O2	O3	68.6(1)	N2	C8	N4	119.8(3)
V1	O3	O2	66.4(1)	N3	C8	N4	119.3(3)

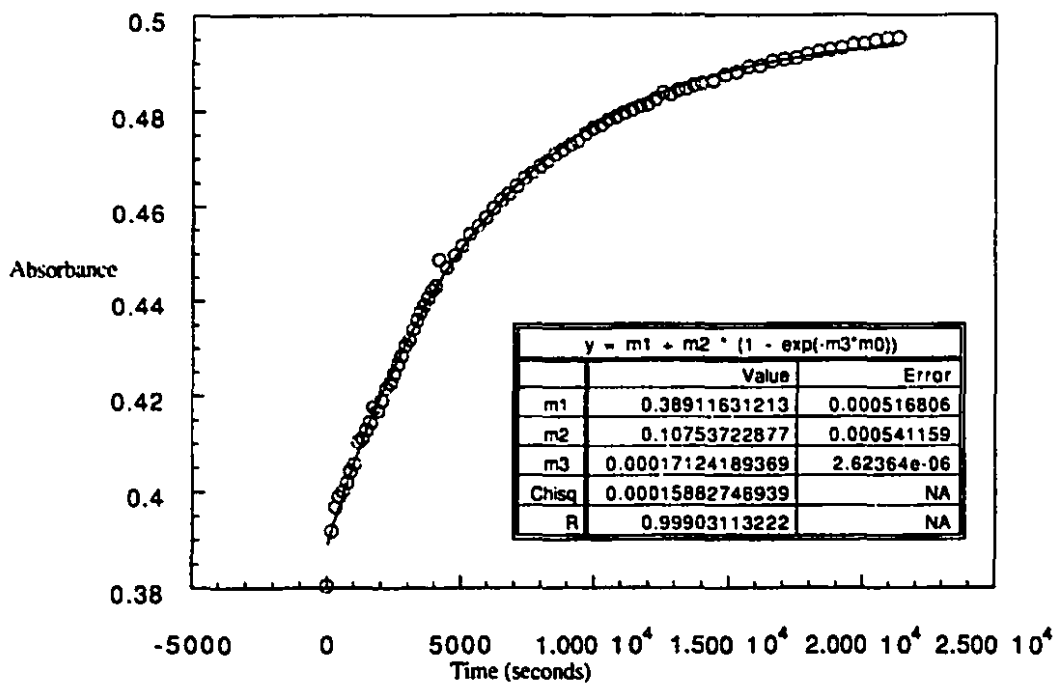
Figure A.4.1. Packing diagram for GmpV(2,6-pdc)



A.5. Kinetic Data for the Reaction of Potassium Ferrocyanide with bpV(OHpic).



Graph A.5.1. Graph showing the absorbance data for sample #2, the reaction of bpV(OHpic) (5.0×10^{-3} M) with potassium ferrocyanide (2.0×10^{-4} M)



Graph A.5.2. Graph showing the absorbance data for sample #1, the reaction of bpV(OHpic) (2.5×10^{-3} M) with potassium ferrocyanide (1.0×10^{-4} M)